

LNCs 12157

Mohamed Jmaiel · Mounir Mokhtari ·
Bessam Abdulrazak · Hamdi Aloulou ·
Slim Kallel (Eds.)

The Impact of Digital Technologies on Public Health in Developed and Developing Countries

18th International Conference, ICOST 2020
Hammamet, Tunisia, June 24–26, 2020
Proceedings



OPEN ACCESS

 Springer

www.dbooks.org

Founding Editors

Gerhard Goos

Karlsruhe Institute of Technology, Karlsruhe, Germany

Juris Hartmanis

Cornell University, Ithaca, NY, USA

Editorial Board Members

Elisa Bertino

Purdue University, West Lafayette, IN, USA

Wen Gao

Peking University, Beijing, China

Bernhard Steffen 

TU Dortmund University, Dortmund, Germany

Gerhard Woeginger 

RWTH Aachen, Aachen, Germany

Moti Yung

Columbia University, New York, NY, USA

More information about this series at <http://www.springer.com/series/7409>

Mohamed Jmaiel · Mounir Mokhtari ·
Bessam Abdulrazak · Hamdi Aloulou ·
Slim Kallel (Eds.)

The Impact of Digital Technologies on Public Health in Developed and Developing Countries

18th International Conference, ICOST 2020
Hammamet, Tunisia, June 24–26, 2020
Proceedings

Editors

Mohamed Jmaiel
Digital Research Centre of Sfax
Sfax, Tunisia

Bessam Abdulrazak
Université de Sherbrooke
Sherbrooke, QC, Canada

Slim Kallel
University of Sfax
Sfax, Tunisia

Mounir Mokhtari
Institut Mines-Télécom, CNRS
Paris, France

Hamdi Aloulou
Digital Research Centre of Sfax
Sfax, Tunisia



ISSN 0302-9743

ISSN 1611-3349 (electronic)

Lecture Notes in Computer Science

ISBN 978-3-030-51516-4

ISBN 978-3-030-51517-1 (eBook)

<https://doi.org/10.1007/978-3-030-51517-1>

LNCS Sublibrary: SL3 – Information Systems and Applications, incl. Internet/Web, and HCI

© The Editor(s) (if applicable) and The Author(s) 2020. This book is an open access publication.

Open Access This book is licensed under the terms of the Creative Commons Attribution 4.0 International License (<http://creativecommons.org/licenses/by/4.0/>), which permits use, sharing, adaptation, distribution and reproduction in any medium or format, as long as you give appropriate credit to the original author(s) and the source, provide a link to the Creative Commons license and indicate if changes were made.

The images or other third party material in this book are included in the book's Creative Commons license, unless indicated otherwise in a credit line to the material. If material is not included in the book's Creative Commons license and your intended use is not permitted by statutory regulation or exceeds the permitted use, you will need to obtain permission directly from the copyright holder.

The use of general descriptive names, registered names, trademarks, service marks, etc. in this publication does not imply, even in the absence of a specific statement, that such names are exempt from the relevant protective laws and regulations and therefore free for general use.

The publisher, the authors and the editors are safe to assume that the advice and information in this book are believed to be true and accurate at the date of publication. Neither the publisher nor the authors or the editors give a warranty, express or implied, with respect to the material contained herein or for any errors or omissions that may have been made. The publisher remains neutral with regard to jurisdictional claims in published maps and institutional affiliations.

This Springer imprint is published by the registered company Springer Nature Switzerland AG
The registered company address is: Gewerbestrasse 11, 6330 Cham, Switzerland

Preface

This year we organized the 18th ICOST conference, an event which has succeeded in bringing together a community from different continents for over a decade and a half and raised awareness about the frail and dependent people's quality of life in our societies.

After 17 very successful conferences held in France (2003, 2009, 2017), Singapore (2004, 2013, 2018), Canada (2005, 2011), Northern Ireland (2006), Japan (2007), the USA (2008, 2014, 2019), South Korea (2010), Italy (2012), Switzerland (2015), and China (2016), we decided to open the conference for the African continent and tackle the digital technologies impact on public health in developed and developing countries. This 18th edition of the International Conference on Smart Living and Public Health (ICOST 2020), was organized by the Digital Research Center (CRNS), Sfax, Tunisia, and the Institut Mines-Télécom (IMT), Paris, France, during June 24–26, 2020. The conference was intended to be hosted in Hammamet, Tunisia, but was finally hosted virtually given the COVID-19 situation faced this year. The theme of the conference was “The Digital Technologies Impact on Public Health in Developed and Developing Countries.”

ICOST 2020 provided a premier venue for the presentation and discussion of research in the design, development, deployment, and evaluation of AI for health, smart urban environments, assistive technologies, chronic disease management, and coaching and health telematics systems. ICOST 2020 aimed to understand and assess the diverse and disparate impact of digital technologies on public health in developing and developed countries. ICOST 2020 brought together stakeholders from health care, public health, academia, and industry along with end users and family caregivers to explore how to utilize technologies to foster health prevention, independent living, and offer an enhanced quality of life. The ICOST 2020 conference featured a dynamic program incorporating a range of oral and poster presentations, along with panel sessions.

ICOST 2020 was proud to extend its hospitality to an international community consisting of researchers from major universities and research centers, representatives from industry, and users from 17 different countries. We would like to thank the authors for submitting their current research work and the Program Committee members for their commitment to reviewing submitted papers. The ICOST proceedings have now reached over 150,000 downloads and are in the top 25% of downloads of Springer LNCS. We are extremely thankful to our sponsors for their commitment and support to the vision and mission of ICOST.

June 2020

Mohamed Jmaiel
Mounir Mokhtari
Bessam Abdulrazak
Hamdi Aloulou
Slim Kallel

Organization

General Chair

Mohamed Jmaiel Digital Research Center, Tunisia

Conference Co-chair

Mounir Mokhtari Institut Mines-Télécom, France, and National
University of Singapore, Singapore

Steering Committee

Mounir Mokhtari	Institut Mines-Télécom, France, and Image & Pervasive Access Lab, Singapore
Sumi Helal	Lancaster University, UK
Bessam Abdulrazak	AmI Lab, University of Sherbrooke, Canada
Hamdi Aloulou	University of Monastir, Digital Research Center, Tunisia, and Institut Mines-Télécom, France
Mohamed Jmaiel	Digital Research Center, Tunisia
Jose Pagan	New York University, New York Academy of Medicine, USA
Maria Fernanda Cabrera	University Politécnica de Madrid, Spain

Scientific Advisory Board

Daqing Zhang	Institut Mines-Télécom, Télécom SudParis, France
Hisato Kobayashi	Hosei University, Japan
Jongbae Kim	Yonsei University, South Korea
Christian Roux	Institut Mines-Télécom, France
Dong Jin Song	National University of Singapore, Singapore, and Griffith University, Australia
Sungyoung Lee	Kyung Hee University, South Korea
Timo Jämsä	EAMBES, University of Oulu, Finland
Daby Sow	IBM Research AI, USA

Program Committee

Chairs

Bessam Abdulrazak	AmI Lab, University of Sherbrooke, Canada
Hamdi Aloulou	University of Monastir, Digital Research Center, Tunisia, and Institut Mines-Télécom, France

Members

Afef Mdhaffar	University of Sfax, Tunisia
Aitor Almeida	University of Deusto, Spain
Bassem Bouaziz	University of Sfax, Tunisia
Belkacem Chikhaoui	University of Quebec, Canada
Boussada Rihab	University of Manouba, Tunisia
Charles Gouin-Vallerand	University of Quebec, Canada
David Menga	EDF R&D, France
Diane Cook	Washington State University, USA
Eric Campo	CNRS, LAAS, France
Franco Mercalli	MultiMed Engineers SRLS, Italy
Fulvio Mastrogiovanni	University of Genoa, Italy
Hisato Kobayashi	Hosei University, Japan
Hongbo Ni	Northwestern Polytechnical University, China
Houssem Aloulou	University of Sfax, Tunisia
Ibrahim Sadek	Institut Mines-Télécom, Image and Pervasive Access Laboratory (IPAL), France
Iyad Abuhadrous	Palestine Technical College, Palestine
Jeffrey Soar	University of Southern Queensland, Australia
Laurent Billonnet	University of Limoges, France
Ludovic Saint-Bauzel	UPMC, France
Lyes Khoukhi	University of Technology of Troyes, France
Manfred Wojciechowski	University of Applied Sciences Dusseldorf, Germany
Meriem Zerkoul	University of Sciences and Technology of Oran, Algeria
Nadine Vigouroux	Institut de Recherche en Informatique de Toulouse, France
Neila Mezghani	University of Quebec, Canada
Salim Hima	ESME, France
Sergio Copelli	MultiMed Engineers SRLS, Italy
Sha Zhao	University of Hangzhou, China
Shafiq Rehman	University of Engineering and Technology, Pakistan
Silvia de Los Rios Perez	University of Madrid, Spain
Slim Kallel	University of Sfax, Tunisia
Sofia Ben Jebara	University of Carthage, COSIM Research Lab, Tunisia
Stefanos Kollias	University of Lincoln, UK
Timo Jamsa	Research Unit of Medical Imaging, Physics and Technology (MIPT), University of Oulu, Finland

Vladimir Urosevic	Belit, Serbia
Wael Sellami	University of Sfax, Tunisia
Yves Demazeau	CNRS, France
Zuraimi Sultan	Berkeley Education Alliance for Research in Singapore (BEARS), Singapore

Organizing Committee

Chair

Slim Kallel	University of Sfax, Tunisia
-------------	-----------------------------

Members

Afef Mdhaffar	University of Sfax, Tunisia
Hamdi Aloulou	Digital Research Center, Tunisia, and Institut Mines-Télécom, France
Ismael Bouassida Rodriguez	University of Sfax, Tunisia
Wael Sellami	University of Sfax, Tunisia

Sponsors

Digital Research Center, Tunisia
Research Laboratory on Development and Control of Distributed Application, Tunisia
National Engineering School of Sfax, Tunisia
Association of Computer Science and Mathematics, Tunisia
Institut Mines-Télécom, France
University of Sherbrooke, Canada

Contents

IoT and AI Solutions for E-Health

Alzheimer's Disease Early Detection Using a Low Cost Three-Dimensional Densenet-121 Architecture	3
<i>Braulio Solano-Rojas, Ricardo Villalón-Fonseca, and Gabriela Marin-Raventós</i>	
Self-adaptative Early Warning Scoring System for Smart Hospital.	16
<i>Imen Ben Ida, Moez Balti, Sondès Chabaane, and Abderrazak Jemai</i>	
Machine Learning Based Rank Attack Detection for Smart [Hospital Infrastructure.	28
<i>Abd Mlak Said, Aymen Yahyaoui, Faicel Yaakoubi, and Takoua Abdellatif</i>	
Remote Health Monitoring Systems Based on Bluetooth Low Energy (BLE) Communication Systems	41
<i>Lamia Chaari Fourati and Sana Said</i>	
Modeling and Specification of Bootstrapping and Registration Design Patterns for IoT Applications	55
<i>Mohamed Hadj Kacem, Imen Tounsi, and Najeh Khalfi</i>	

Biomedical and Health Informatics

EEG-Based Hypo-vigilance Detection Using Convolutional Neural Network	69
<i>Amal Boudaya, Bassem Bouaziz, Siwar Chaabene, Lotfi Chaari, Achraf Ammar, and Anita Hökelmann</i>	
Respiratory Activity Classification Based on Ballistocardiogram Analysis . . .	79
<i>Mohamed Chiheb Ben Nasr, Sofia Ben Jebara, Samuel Otis, Bessam Abdulrazak, and Neila Mezghani</i>	
A Convolutional Neural Network for Lentigo Diagnosis	89
<i>Sana Zorgui, Siwar Chaabene, Bassem Bouaziz, Hadj Batatia, and Lotfi Chaari</i>	
Deep Learning-Based Approach for Atrial Fibrillation Detection.	100
<i>Lazhar Khriji, Marwa Fradi, Mohsen Machhout, and Abdulnasir Hossen</i>	

Unsupervised Method Based on Superpixel Segmentation for Corpus Callosum Parcellation in MRI Scans 114
Amal Jlassi, Khaoula ElBedoui, Walid Barhoumi, and Chokri Maktouf

Behavior and Activity Monitoring

Using Learning Techniques to Observe Elderly’s Behavior Changes over Time in Smart Home. 129
Dorsaf Zekri, Thierry Delot, Mikael Desertot, Sylvain Lecomte, and Marie Thilliez

Personalized and Contextualized Persuasion System for Older Adults’ Physical Activity Promoting 142
Housseem Aloulou, Hamdi Aloulou, Bessam Abdulrazak, and Ahmed Hadj Kacem

Baseline Modelling and Composite Representation of Unobtrusively (IoT) Sensed Behaviour Changes Related to Urban Physical Well-Being 155
Vladimir Urošević, Marina Andrić, and José A. Pagán

Wellbeing Technology

Automatic Daily Activity Schedule Planning for Simulating Smart House with Elderly People Living Alone 171
Can Jiang and Akira Mita

A Novel On-Wrist Fall Detection System Using Supervised Dictionary Learning Technique. 184
Farah Othmen, Mouna Baklouti, André Eugenio Lazzaretti, Marwa Jmal, and Mohamed Abid

Combined Machine Learning and Semantic Modelling for Situation Awareness and Healthcare Decision Support. 197
Amira Henaien, Hadda Ben Elhadj, and Lamia Chaari Fourati

Improving Access and Mental Health for Youth Through Virtual Models of Care 210
Cheryl Forchuk, Sandra Fisman, Jeffrey P. Reiss, Kerry Collins, Julie Eichstedt, Abraham Rudnick, Wanrudee Isaranuwatchai, Jeffrey S. Hoch, Xianbin Wang, Daniel Lizotte, Shona Macpherson, and Richard Booth

Short Contributions: IoT and AI Solutions for E-Health

Study of Middleware for Internet of Healthcare Things and Their Applications.	223
<i>Ghofrane Fersi</i>	
Uncertainty in IoT for Smart Healthcare: Challenges, and Opportunities.	232
<i>Anis Tissaoui and Malak Saidi</i>	
Secure E-Health Platform.	240
<i>Karima Djouadi and Abdelkader Belkhir</i>	
Hybrid and Secure E-Health Data Sharing Architecture in Multi-Clouds Environment.	249
<i>Tayssir Ismail, Haifa Touati, Nasreddine Hajlaoui, and Hassen Hamdi</i>	
Blockchain for Internet of Medical Things: A Technical Review.	259
<i>Fatma Ellouze, Ghofrane Fersi, and Mohamed Jmaiel</i>	
Application of Blockchain Technology in Healthcare: A Comprehensive Study	268
<i>Rim Ben Fekih and Mariam Lahami</i>	
Trust Execution Environment and Multi-party Computation for Blockchain e-Health Systems	277
<i>Feriel Yahmed and Mohamed Abid</i>	
A Fuzzy-Ontology Based Diabetes Monitoring System Using Internet of Things.	287
<i>Sondes Titi, Hadda Ben Elhadj, and Lamia Chaari Fourati</i>	

Short Contributions: Biomedical and Health Informatics

A Hybrid Approach for Heart Disease Diagnosis and Prediction Using Machine Learning Techniques	299
<i>Fatma Zahra Abdeldjouad, Menaouer Brahami, and Nada Matta</i>	
Context-Aware Healthcare Adaptation Model for COPD Diseases.	307
<i>Hamid Mcheick, John Sayegh, and Hicham Ajami</i>	
Study of Healthcare Professionals' Interaction in the Patient Records Based on Annotations	316
<i>Khalil Chehab, Anis Kalboussi, and Ahmed Hadj Kacem</i>	
Multirate ECG Processing and k-Nearest Neighbor Classifier Based Efficient Arrhythmia Diagnosis.	329
<i>Saeed Mian Qaisar, Moez Krichen, and Fatma Jallouli</i>	

Comparative Study of Relevant Methods for MRI/X Brain Image Registration	338
<i>Marwa Abderrahim, Abir Baâzaoui, and Walid Barhoumi</i>	
Machine Learning Classification Models with SPD/ED Dataset: Comparative Study of Abstract Versus Full Article Approach	348
<i>Mayara Khadhraoui, Hatem Bellaaj, Mehdi Ben Ammar, Habib Hamam, and Mohamed Jmaiel</i>	
Evaluation of Stationary Wavelet Transforms in Reconstruction of Pure High Frequency Oscillations (HFOs)	357
<i>Thouraya Guesmi, Abir Hadriche, Nawel Jmail, and Chokri Ben Amar</i>	
Ensuring the Correctness and Well Modeling of Intelligent Healthcare Management Systems	364
<i>Samir Ouchani and Moez Krichen</i>	
Short Contributions: Wellbeing Technology	
An Embedded ANN Raspberry PI for Inertial Sensor Based Human Activity Recognition	375
<i>Achraf Jmal, Rim Barioul, Amel Meddeb Makhlouf, Ahmed Fakhfakh, and Olfa Kanoun</i>	
Human Activities Recognition in Android Smartphone Using WSVM-HMM Classifier	386
<i>M'hamed Bilal Abidine and Belkacem Fergani</i>	
Mobile Assistive Application for Blind People in Indoor Navigation	395
<i>Hanen Jabnoun, Mohammad Abu Hashish, and Faouzi Benzarti</i>	
Older People's Needs and Opportunities for Assistive Technologies	404
<i>Jeffrey Soar, Lei Yu, and Latif Al-Hakim</i>	
Towards a Formal Context-Aware Workflow Model for Ambient Environment.	415
<i>Roumeissa Khennaoui and Nabil Belala</i>	
The PULSE Project: A Case of Use of Big Data Uses Toward a Cohomprehensive Health Vision of City Well Being	423
<i>Domenico Vito, Manuel Ottaviano, Riccardo Bellazzi, Cristiana Larizza, Vittorio Casella, Daniele Pala, and Marica Franzini</i>	

ForeSight - An AI-driven Smart Living Platform, Approach to Add Access Control to openHAB	432
<i>Jochen Bauer, Michael Hechtel, Christoph Konrad, Martin Holzwarth, Hilko Hoffmann, Thomas Feld, Sven Schneider, Ingo Zinnikus, Andreas Mayr, and Jörg Franke</i>	
Author Index	441

IoT and AI Solutions for E-Health



Alzheimer's Disease Early Detection Using a Low Cost Three-Dimensional Densenet-121 Architecture

Braulio Solano-Rojas^(✉), Ricardo Villalón-Fonseca^(✉),
and Gabriela Marín-Raventós^(✉)

CITIC - ECCI, Universidad de Costa Rica, San José, Costa Rica
{braulio.solano,ricardo.villalon,gabriela.marin}@ucr.ac.cr

Abstract. The objective of this work is to detect Alzheimer's disease using Magnetic Resonance Imaging. For this, we use a three-dimensional densenet-121 architecture. With the use of only freely available tools, we obtain good results: a deep neural network showing metrics of 87% accuracy, 87% sensitivity (micro-average), 88% specificity (micro-average), and 92% AUROC (micro-average) for the task of classifying five different classes (disease stages). The use of tools available for free means that this work can be replicated in developing countries.

Keywords: Alzheimer · Deep learning · MRI · Computer-aided detection · Computer-aided diagnosis

1 Introduction

Alzheimer's Disease (AD) is the most common form of dementia among older adults [17]. It is a neurodegenerative disease without a cure. Its early detection is crucial because it allows those people who are going to be affected to prepare for future changes [17]. For example, some medications delay the disease. Also, their relatives can prepare and train for the care that will be necessary [17].

Early detection is not easy. One of the difficulties is the performance of people working at the clinic. People making a diagnosis are affected by several factors such as fatigue, stress, distractions, and inherent cognitive biases to specific conditions of the disease. When radiologists see a medical image, such as a magnetic resonance imaging (MRI), biased reasoning about the conditions of the disease will result in the loss of the opportunity to detect it. Graber et al. [7] found that about 74% of diagnostic errors are attributed to cognitive factors. Lee et al. [14] state that approximately 75% of all medical errors made were due to diagnostic errors by radiologists. A high workload, stress, fatigue, cognitive bias, and an inadequate system are part of the causal factors. Medical errors contrast with the fact that recently artificial intelligence, in particular, deep artificial

Supported by CITIC and ECCI, Universidad de Costa Rica.

© The Author(s) 2020

M. Jmaiel et al. (Eds.): ICOST 2020, LNCS 12157, pp. 3–15, 2020.

https://doi.org/10.1007/978-3-030-51517-1_1

neural networks (DNNs) have shown superhuman abilities in the detection of diseases in medical computer vision, as in the work of Rajpurkar [18]. We can design DNNs to integrate them into computer-aided diagnosis protocols for the detection of many priority diseases. One of these possible diseases is AD.

Currently, there is a body of images of healthy patients and patients with AD that is available through the database Alzheimer Disease Neuroimaging Initiative (ADNI)¹. ADNI launched in 2003 as a public and private initiative. The leadership belongs to the researcher Michael W. Weiner. The main objective of ADNI has been to test whether medical images, other biomarkers, and clinical and neuropsychological evaluation can be combined to measure the progress of AD. The early detection of AD employing software would allow us to strengthen and improve medical protocols by providing what we call Computer-Aided Diagnosis (CAD).

As we commented, DNNs have become increasingly important and useful in recent years. One kind of these type of neural network is Convolutional Neural Networks (CNN). CNNs are inspired by the biological visual cortex and are used in areas as diverse as smart surveillance and monitoring, health and medicine, sports and recreation, robotics, drones, and self-driving cars [12].

This work consists of measuring the accuracy of the detection of Alzheimer's disease of a three-dimensional CNN architecture, specifically a densenet-121, trained using the ADNI MRI images. We also have a low-cost economic objective. We aim to provide a technological artifact that has the potential of being used in the public health and wellbeing of citizens all over the world, in particular, for developing countries that have difficulties in accessing specialized hardware platforms for computation.

Before presenting the results of developing a low-cost densenet for Alzheimer's disease detection, we first provide in Sect. 2 some background definitions to support our work. In Sect. 3 we describe previous work with more detail. Then in the next section, we provide the methodology used to realize this work. We present in Sect. 5 the results of the design chose. Finally, we analyze those results with concluding remarks and future work in Sect. 6.

2 Background

We start with a short review of medical vocabulary used to provide a context for our research. First, we introduce different clinical stages of disease that we want to classify, and later, we describe two types of medical imaging used in the detection and diagnosis of AD.

2.1 Clinical Disease Stages

There are different stages before the clinical diagnosis of AD. These are cognitively normal, significant memory concern, and mild cognitive impairment.

¹ <http://adni.loni.usc.edu>.

Cognitive Normal (CN). CN patients are the control subjects in the ADNI study. They have healthy aging. They show no signs of depression, mild cognitive impairment, or dementia [1].

Significant Memory Concern (SMC). SMC is a self-report significant memory concern from the patient, quantified by using the Cognitive Change Index and the Clinical Dementia Rating (CDR) of zero. Subjective memory concerns are correlated with a higher likelihood of progression, thereby minimizing the stratification of risk among normal controls and addressing the gap between healthy elderly controls and mild cognitive impairment. However, SMC patients score within the normal range for cognition [1].

Mild Cognitive Impairment (MCI). MCI participants have reported a subjective memory concern either autonomously or via an informant or clinician. However, daily living activities are mainly preserved, there are no significant levels of impairment in other cognitive domains, and no signs of dementia exist. Levels of MCI (early or late) are determined using the Wechsler Memory Scale Logical Memory II [1].

Alzheimer’s Disease. AD is the most common cause of dementia, a general term for memory loss and other cognitive abilities severe enough to interfere with daily life. It is a progressive disease, where dementia symptoms gradually worsen over several years. Individuals lose the ability to carry on a conversation and respond to their environment. Current medications cannot stop the disease from progressing, they can temporarily slow the worsening of dementia symptoms and improve quality of life for those with AD and their caregivers [17].

Since we aim to assess if those stages, including AD, are detected on medical imaging, particularly on Magnetic Resonance Imaging, we continue describing two medical imaging techniques.

2.2 Medical Imaging

Medical imaging is the process and technique of creating visual representations of the inner of a human body for clinical analysis and medical intervention. We introduce two types of medical imaging. We are especially interested in the input of Magnetic Resonance Imaging (MRI) on DNN. Moreover, we also mention Positron Emission Tomography (PET) because it is sometimes an input that accompanies MRI. We follow describing what MRI and PET are.

Magnetic Resonance Imaging. MRI is a non-invasive imaging technology that produces three-dimensional detailed anatomical images without the use of radiation that damages human tissues. It is often used for disease detection and diagnosis and treatment monitoring. It is based on sophisticated technology that excites and detects the change in the direction of the rotational axis of protons found in the water that makes up living tissues [15].

Positron Emission Tomography. PET scans use radiopharmaceuticals to create three-dimensional images. These types of scans produce small particles called positrons. A positron is a particle with roughly the same mass as an electron but oppositely charged. Positrons react with electrons in the body, and when these two particles combine, they annihilate each other. This annihilation produces a small amount of energy in the form of two photons that shoot off in opposite directions. The detectors in the PET scanner measure these photons and use this information to create images of internal organs [16].

3 Previous Work

Our literature review assesses how much progress has been made and what can be contributed in the detection of AD using deep learning, in particular with Convolutional Neural Networks (CNN). We only focus on AD however detection of another neurodegenerative disease using DNNs has been investigated [13, 19].

We used IEEE² as the source for Artificial Neural Networks because, according to Journal Rankings³ on the category of Artificial Intelligence, IEEE is the first on both SJR and H-Index sortings. We used the search engines Duck Duck Go, and Google Scholar to find illustrative publications.

We used the search string “deep AND learning AND alzheimer AND mri” in order to assess the use of convolutional deep learning in our application of interest. We ran the query mentioned from 2016 to the present (in 2019) since we are searching about recent advancements in neural networks. We retrieved from IEEE Digital Library 81 records with this query, including conferences, journals, and early access articles.

We screened by title, and if the title was too ambiguous by abstract. We searched for the application of convolutional deep learning and we obtained 32 articles. Notably, we searched for literature that included the design of convolutional deep learning artifacts for computer vision to detect AD in MRI and other modalities. Besides, the literature was restricted to supervised learning. For example, we did not include convolutional autoencoders alone.

For the articles we deemed appropriate, we developed a data extraction spreadsheet to serve for analysis where we collected the following information about each publication: (1) year of the paper, (2) architecture of the neural network, (3) if the MRI images were processed, (5) the modalities (number of inputs), (6) the number of classes used, and the metrics of (7) accuracy, (8) sensitivity, (9) specificity, and finally (9) the Area Under the curve Receiver Operating Characteristics (AUROC).

In this literature review, with our data extraction spreadsheet, we find a severe problem. Almost 50% of papers report accuracy but do not report sensitivity, specificity or AUROC. Accuracy alone can be misleading. A classifier can report a high accuracy and yet have a low capacity of true prediction. We also conclude that the studies are too diverse to allow a meaningful comparison.

² <https://ieeexplore.ieee.org/>.

³ <https://www.scimagojr.com/>.

It seems that there is a race to obtain greater accuracy, although this metric is misleading. In addition, multiclass classification is avoided. Most studies implement one-vs-one classifiers, thus achieving higher accuracy values. When the number of classes increases the accuracy tends to decrease. In fact, we did not find any article with multiclass classification with more than four classes. Nor did we find many articles that used the densenet architecture. Only three papers used densenets, of which two [6,9] are three-dimensional but with shallow densenets and one [11] uses deep densenets but two-dimensional. Finally, the quantitative analysis of the collected items does not generate a great contribution due to these defects. However, in the review of the articles, we find articles of remarkable quality as [2]. We also consider that some of the papers collected are not repeatable.

In contrast to existing studies, we seek to create a multiclass neural network using only tools available for free. Besides, we do not give greater importance to accuracy over other metrics and analysis. Finally, we want our process to be repeatable, and we report it complete along with all the parameters used, as explained in the next sections.

4 Methodology

In this section, we describe how we collect data using the ADNI study and how we preprocess these data. Then, we present the development carried out and how we produced, using the Google Collaboratory tool, an Alzheimer’s prediction model to fulfill the objective of measuring the accuracy of the detection of Alzheimer’s disease using a three-dimensional Densenet-121.

4.1 Data Acquisition

In this work, we used the data from ADNI. We used their beta advanced search functionality with the following criteria. In Projects, we checked ADNI. In Research Group, we checked MCI, EMCI, AD, SMC, and CN. In Modality, we checked MRI. We only chose MRI and did not add PET because of economic restrictions. PET requires radiopharmaceuticals, as mentioned. It is more usual to find MRI in contexts of economic limitations. Continuing with search options, in Image Description, we used MPRAGE. In Acquisition Plane, we used SAGITTAL, and finally, in Weighting, we used T1. The rest of the search fields were left with their default values. With those parameters, we obtained 5556 magnetic resonance images with the following distribution: 1520 Cognitive Normal (CN), 186 Significant Memory Concern (SMC), 1222 Early Mild Cognitive Impairment (EMCI), 1274 Mild Cognitive Impairment (MCI), 636 Late Mild Cognitive Impairment, and 718 Alzheimer’s Disease.

The images obtained from ADNI are in Digital Imaging and Communication On Medicine (DICOM) format. The files are in a zipped archive of 55.5 GB, and the uncompressed files measure 138 GB. We reduce that size with data preprocessing, and we explain how and why in the next section.

4.2 Data Preprocessing

MRI image data are groups of images. Every image is a slice, and the group of slices shapes the MRI. Every image or slice is a matrix of pixels. Each slice has an associated spatial thickness because they represent reality. Also, every pixel in every slice has a spacing, that is the space they represent. Thus, the data is volumetric or, in other words, rectangular cuboids. Taking that into consideration, we do the following transformations to the data. First, we convert all volumetric pixels (voxels) to a spacing of $1 \times 1 \times 1$ mm. This conversion may add or delete slices, or slice pixels. After that, we convert every slice to 256×256 pixels as follows. Some slices are not square. If they are not, we fill in with black pixels. After they are square, if they are not 256×256 , we convert them to that size using interpolation. Concerning the size, we also make the cuboids have 256 slices using interpolation. The result is $256 \times 256 \times 256$ cubes. From these cubes, to keep “see” only the brain as would a human do, we make a cut from slice 40 to slice 214, from row 50 to row 199, and from column 40 to column 239. With that cut, we discard borders full of black pixels and conserve the inner cuboids that have useful information (the brain). Since we made all the MRI the same size, we assume that the cut keeps the brain and we do not have to apply techniques like image segmentation (cutting the brain using pattern recognition). From those cut cuboids, we use only half of the slices and half of the rows and columns of every slice by eliminating one in between for all. The latter reduces the size of the images and the dimensionality of the problem considerably. Last, we normalize the images pixel values to an interval of -1.0 to 1.0 .

Data preprocessing can be done both online or beforehand. We implemented both. However, to maintain a low-cost objective, we use a script to apply the preprocessing previously to the task of neural network training, and we load the MRI data already transformed. The previous transformation may be done on a desktop or laptop computer. Although it will take hours, it is not a task that will take more than a day on current commodity hardware.

After data preprocessing the images occupy only 13.5 GB, we have reduced the size of the images slightly more than ten times. This reduction is beneficial to minimize neural network training time and storage needs of our development explained in the next section.

4.3 Our Development

We chose to use a convolutional DNN of densenet-BC architecture because of our objective to use the least resources possible. This kind of architecture has an excellent performance with fewer parameters to train [10]. We based our development on the implementation of Hara et al. [8]. We used their densenet implementation for the densenet-121 architecture. This implementation, in turn, is based on the two-dimensional implementation available in the Pytorch code. The implementation of Hara et al., however, is not generic. It was made for video and incorporates the variables *sample_size* and *sample_duration* that have to do with the size and duration of video samples. We eliminated that and made the

implementation general. It works with all kinds of cuboids. Also, we added a channels parameter because the implementation always considered 3 channels (usually red, green and blue colors), but the magnetic resonance images are monochromatic.

Using this implementation we configure the training process of the neural network with the following parameters.

Training	We use 75% of the data obtained from ADNI as the training dataset. The data is obtained randomly from the complete data set
Batch size	For the phase of training, we use a batch size of 5 MRI based on experimental results by [2]
Testing	The testing dataset is the remaining 25% of the data
Channels	We send a parameter of 1 to the constructor of the neural network because the images are monochromatic
Classes	Initially, we sent a parameter of 6 to the constructor of the neural network. However, we decided to eliminate the SMC class because it is a subjective class. We consider it training noise. Finally, we use a parameter of 5 classes to classify
Dropout	We use a dropout rate of 0.7 based on observations by [2]. This prevents overfitting
Loss	We use a cross-entropy loss function. It is useful in classification problems that are not binary and, in our case, we have 5 or 6 classes
Optimizer	We use stochastic gradient descent (SGD). This popular optimizer is useful in the case of unbalanced data, which is our case
Learning	In the SGD optimizer, we use a learning rate parameter of 0.1 and a drop in the learning rate in the sixty epoch of 0.1. The latter reduces the learning rate to 0.01 in that epoch
Momentum	Since the SGD optimizer with momentum usually finds flatter local minima, we use a typical momentum of 0.9
Epochs	Since we use the Google Collaboratory platform, we set the maximum number of epochs to 80. It was not possible to exceed above 90 epochs to reach 100 epochs because the platform disconnects us before achieving it

With that parameters, we pushed the limits of the Google Collaboratory platform to produce a state-of-the-art DNN. Although other authors claim that the free-of-charge resources of Google Collaboratory “are far from enough to solve demanding real-world problems and are not scalable” [3], we use it as the platform that provides us Graphics Processing Unit (GPU) computation. This decision has limitations and implications. As explained in [3], there only 12 h of free use of the GPU backend. We have even noticed less sometimes, approximately 10 h. After that time, Google Collaboratory disconnects and deletes the virtual machine provided. If the user reconnects, the new machine supplied only offers 3 h of GPU backend. After that, it is not possible to connect to a backend

with GPU for a determined number of hours. These limitations imply that the training and testing have to be done in one run before the first 12 h end. There are other implications to the restrictions. For instance, it is customary to test or validate neural networks during training; thus the loss and accuracy of the neural networks can be analyzed at each epoch. However, to reduce computation time, testing or validation of the trained DNN is only done at the end. We chose this because a validation cycle of 25% of the data takes approximately 2 or 3 min. In 30 epochs, that would take 1 h or more. This trade-off is not severe, we can save intermediate neural networks states and study them after finishing the training. However, this choice also implies that techniques like early stopping can not be employed. There are also disk size limitations.

Taking all the limitations into account and with the mentioned configuration parameters of our development, we obtained the results that we discuss in the next section.

5 Results and Discussion

The first finding of this work is the characterization of the significant memory concern class as a noisy class for training. This problem may be due to the fact that the class is subjective and is possibly composed of at least two classes: those who will develop the disease and those who will not. Also, those who will develop it may have different levels of progression, being, in turn, a class composed of different classes. Another reason for the class to be problematic is its size. It is the smallest cohort and by far. This makes it difficult to classify during training. In the Fig. 1, we show how this class is not classified after 50 training epochs. As seen, the column of the predicted SMC class is full of zeros. It is also notable that the other classes already have a good level of correct classification. We decided to remove this class from the data set. This reduced the total data set from 5556 MRI to 5370 MRI.

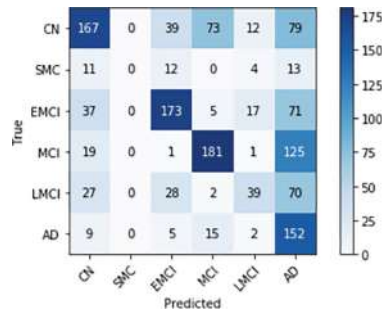


Fig. 1. Confusion matrix with the SMC class at 50 epoch

After eliminating the SMC class and training for 80 epochs, we obtain a neural network with good classification metrics of the five remaining classes.

The results can be seen in Figs. 2a and 2b. In Fig. 2a, the confusion matrix, we can see how most values are kept diagonally. There are a certain amount of incorrect predictions. However, there is an interesting, unexpected feature. These incorrect predictions are mostly pessimistic; that is, there are more errors above the diagonal than under it, and this means that the classifier is making errors that put the prediction on upper disease stages. This is clearly in favor of patients because, in terms of diagnosis of diseases, a false positive is better than a false negative. Figure 2b shows the quality of our classifier for each class and all classes together. As the area under each curve approaches the value 1.0, greater diagnostic ability of the classifier is demonstrated. It is clear that, although our classifier is not perfect, it is a good one.

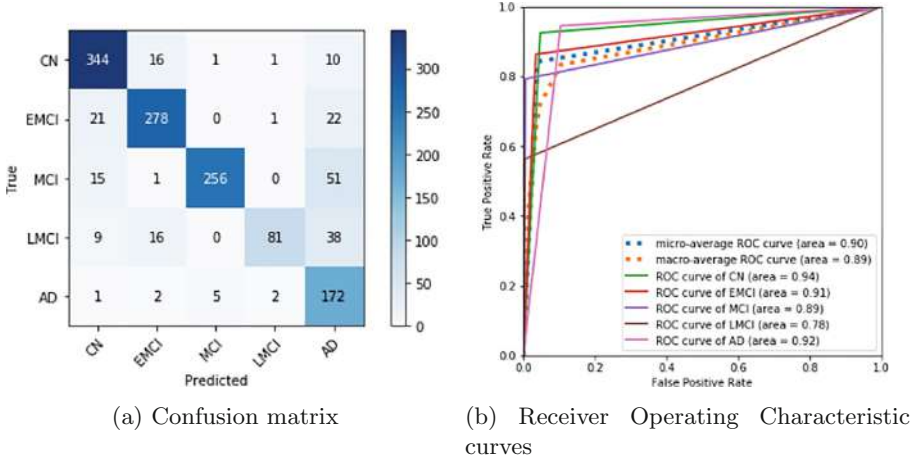


Fig. 2. Metrics of evaluation of the densenet-121 at 80 epochs

Although we obtained an already good predictive model, we wanted to improve it using the same tools we already used. However, because we use Google Colaboratory, we could not repeat the process of training and add a significant number of epochs. Therefore, we saved the model at 80 epochs. Then, after waiting 12 h because of the Google Colaboratory restrictions, we restarted the process of training again from the 80th epoch and pushed it to 110 final epochs. The predictive performance of this new model can be seen in Figs. 3a and 3b.

This new confusion matrix (Fig. 3a) and ROC curve plot (Fig. 3b) show that it is possible to improve the prediction model even under the restrictions of free-of-charge resources like Google Colaboratory. We may notice that as we improve all classes, the Late Mild Cognitive Impairment class gets worse in the prediction. That is, we approach a local minima solution that improves the classes in general but moves away from the correct prediction of the LMCI class. We believe that this effect is due to the lack of balance in the data. LMCI is the class with the least amount of data after we removed Significant Memory Concern. This can

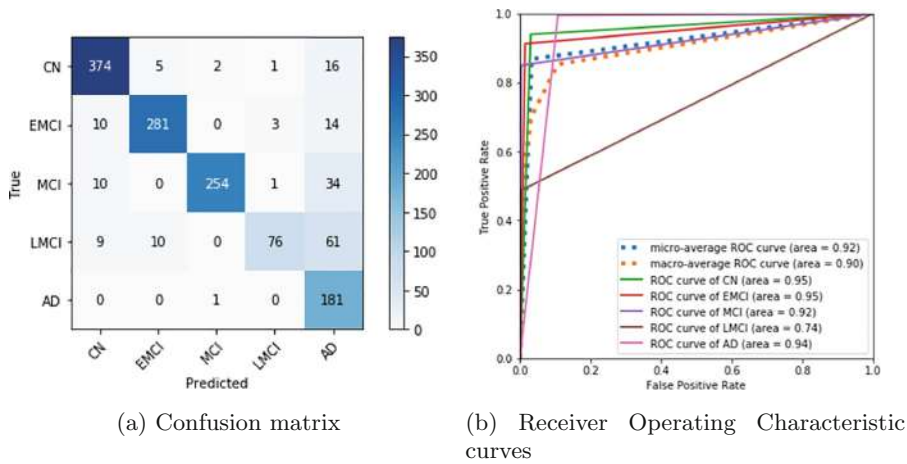


Fig. 3. Metrics of evaluation of the densenet-121 at 110 epochs

be solved with data augmentation as done, for instance, in [4]. However, if we do this, we would reduce the amount of maximum epochs that we can use during training. However, although LMCI does not have the best classification, it is classified pessimistically, then we can accept the commitment of not balancing the data. We include more prediction performance metrics of this last model in Table 1.

Table 1. Metrics of the obtained DNN at 110 epochs

	specificity (precision)	sensitivity (recall)	f1-score	support
Cognitive Normal (CN)	93%	94%	93%	398
Early MCI (EMCI)	95%	91%	93%	308
Mild Cognitive Impairment (MCI)	99%	85%	91%	299
Late MCI (LMCI)	94%	49%	64%	156
Alzheimer's Disease (AD)	59%	99%	74%	182
Macro average	88%	84%	83%	1343
Weighted average	90%	87%	87%	1343

Accuracy	84%
Micro specificity (precision)	84%
Micro sensitivity (recall)	81%

As we can see in Table 1, the worst figures are the specificity of Alzheimer's Disease and the sensitivity of Late Mild Cognitive Impairment. We could also include the sensitivity of Mild Cognitive Impairment in the bad numbers, although the percentage of recall is not poor. The poor specificity of Alzheimer's is acceptable because it reaches almost 100% sensitivity or recall. The number

is bad because other classes are classified as AD, but in a context of pattern recognition that always has risks and costs, it is in favor because it is pessimistic and in medicine that can reduce risk and future costs. In the same manner, the bad number of LMCI is also acceptable because the class is mostly classified as AD. Therefore, considering the economic restrictions, the final figures of 84% accuracy, 84% specificity (micro) and 81% sensitivity (micro) are acceptable. We chose to report final micro-average figures instead of macro-average because in a multi-class classification setup, micro-average is preferable when there is a class imbalance. However, as it can be noticed the macro average and the weighted average are better.

6 Conclusions and Future Work

The use of free-of-charge resources limited this study. With this restriction, we explored a low-cost way to generate a deep artificial neural network that shows good performance metrics. We demonstrate that the model can still be improved. This prediction model can be useful in developing countries if user interface and interpretation are added and it has the potential of being used in remote medicine contexts.

In the future, we want to create a user interface for the diagnosis of AD. We can do this based on the implementation of Chester [5], a computerized chest X-ray disease prediction system that is delivered on the web. With the recent creation of tools such as ONNX and TensorFlow.js, PyTorch-trained models can be converted to work in the browser and compute using WebGL [5]. This interface would have not only prediction but also interpretation or explanation through relevance maps or heat maps.

Last, to contribute to reproducibility and transparency in academic work, we provide the source code of our DNN at <https://github.com/bsolano/Alzheimer-ResNets>.

References

1. Alzheimer's Disease Neuroimaging Initiative: Study Design (2017). <http://adni.loni.usc.edu/study-design/>
2. Bäckström, K., Nazari, M., Gu, I.Y., Jakola, A.S.: An efficient 3D deep convolutional network for Alzheimer's disease diagnosis using MR images. In: 2018 IEEE 15th International Symposium on Biomedical Imaging (ISBI 2018), pp. 149–153, April 2018. <https://doi.org/10.1109/ISBI.2018.8363543>
3. Carneiro, T., Medeiros Da Nóbrega, R.V., Nepomuceno, T., Bian, G., De Albuquerque, V.H.C., Filho, P.P.R.: Performance analysis of Google colab as a tool for accelerating deep learning applications. IEEE Access **6**, 61677–61685 (2018). <https://doi.org/10.1109/ACCESS.2018.2874767>
4. Cheng, D., Liu, M.: CNNs based multi-modality classification for AD diagnosis. In: 2017 10th International Congress on Image and Signal Processing, BioMedical Engineering and Informatics (CISP-BMEI), pp. 1–5, October 2017. <https://doi.org/10.1109/CISP-BMEI.2017.8302281>

5. Cohen, J.P., Bertin, P., Frappier, V.: Chester: A Web Delivered Locally Computed Chest X-Ray Disease Prediction System. [arXiv:1901.11210](https://arxiv.org/abs/1901.11210) (2019)
6. Cui, R., Liu, M.: Hippocampus analysis by combination of 3-D DenseNet and shapes for Alzheimer's disease diagnosis. *IEEE J. Biomed. Health Inform.* **23**(5), 2099–2107 (2019). <https://doi.org/10.1109/JBHI.2018.2882392>
7. Graber, M., Franklin, N.: Diagnostic error in internal medicine. *Arch. Intern. Med.* **165** (2005). <https://doi.org/10.1001/archinte.165.13.1493>
8. Hara, K., Kataoka, H., Satoh, Y.: Can spatiotemporal 3D CNNs retrace the history of 2D CNNs and ImageNet? In: *Proceedings of the IEEE Conference on Computer Vision and Pattern Recognition (CVPR)*, pp. 6546–6555 (2018)
9. He, G., Ping, A., Wang, X., Zhu, Y.: Alzheimer's disease diagnosis model based on three-dimensional full convolutional DenseNet. In: *2019 10th International Conference on Information Technology in Medicine and Education (ITME)*, pp. 13–17, August 2019. <https://doi.org/10.1109/ITME.2019.00014>
10. Huang, G., Liu, Z., Van Der Maaten, L., Weinberger, K.Q.: Densely connected convolutional networks. In: *2017 IEEE Conference on Computer Vision and Pattern Recognition (CVPR)*, Honolulu, HI, pp. 2261–2269 (2017). <https://doi.org/10.1109/CVPR.2017.243>
11. Jabason, E., Ahmad, M.O., Swamy, M.N.S.: Classification of Alzheimer's disease from MRI data using an ensemble of hybrid deep convolutional neural networks. In: *2019 IEEE 62nd International Midwest Symposium on Circuits and Systems (MWSCAS)*, pp. 481–484, August 2019. <https://doi.org/10.1109/MWSCAS.2019.8884939>
12. Khan, S., Rahmani, H., Shah, S., Bennamoun, M.: *A Guide to Convolutional Neural Networks for Computer Vision. Synthesis Lectures on Computer Vision*, No. 1. Morgan & Claypool Publishers (2018). <https://doi.org/10.2200/S00822ED1V01Y201712COV015>
13. Kollias, D., Tagaris, A., Stafylopatis, A., Kollias, S., Tagaris, G.: Deep neural architectures for prediction in healthcare. *Complex Intell. Syst.* **4**(2), 119–131 (2017). <https://doi.org/10.1007/s40747-017-0064-6>
14. Lee, C.S., Nagy, P.G., Weaver, S.J., Newman-Toker, D.E.: Cognitive and system factors contributing to diagnostic errors in radiology. *Am. J. Roentgenol.* **201**(3), 611–617 (2013). <https://doi.org/10.2214/AJR.12.10375>
15. National Institute of Biomedical Imaging and Bioengineering: Magnetic Resonance Imaging (MRI). <https://www.nibib.nih.gov/science-education/science-topics/magnetic-resonance-imaging-mri>
16. National Institute of Biomedical Imaging and Bioengineering: Nuclear Medicine. <https://www.nibib.nih.gov/science-education/science-topics/nuclear-medicine#pid-1001>
17. National Institute on Aging: Alzheimer's Disease Fact Sheet. <https://www.nia.nih.gov/health/alzheimers-disease-fact-sheet>. Accessed 13 May 2018
18. Rajpurkar, P., et al.: CheXNet: radiologist-level pneumonia detection on chest X-rays with deep learning. *CoRR* abs/1711.05225 (2017). <http://arxiv.org/abs/1711.05225>
19. Tagaris, A., Kollias, D., Stafylopatis, A., Tagaris, G., Kollias, S.: Machine learning for neurodegenerative disorder diagnosis — survey of practices and launch of benchmark dataset. *Int. J. Artif. Intell. Tools* **27**(03), 1850011 (2018). <https://doi.org/10.1142/S0218213018500112>

Open Access This chapter is licensed under the terms of the Creative Commons Attribution 4.0 International License (<http://creativecommons.org/licenses/by/4.0/>), which permits use, sharing, adaptation, distribution and reproduction in any medium or format, as long as you give appropriate credit to the original author(s) and the source, provide a link to the Creative Commons license and indicate if changes were made.

The images or other third party material in this chapter are included in the chapter's Creative Commons license, unless indicated otherwise in a credit line to the material. If material is not included in the chapter's Creative Commons license and your intended use is not permitted by statutory regulation or exceeds the permitted use, you will need to obtain permission directly from the copyright holder.





Self-adaptative Early Warning Scoring System for Smart Hospital

Imen Ben Ida^{1(✉)}, Moez Balti^{1,2}, Sondès Chabaane³,
and Abderrazak Jemai^{1,4}

¹ Electronic Systems and Communications Networks Laboratory (SERCOM),
Polytechnic School of Tunisia, Carthage University, Tunis, Tunisia
Imen.benida@gmail.com

² IsetCom, Carthage University, Tunis, Tunisia

³ CNRS UMR 8201 - LAMIH - Laboratory of Automatic Mechanics
and Industrial and Human Informatics, Hauts-de-France Polytechnic University,
59313 Valenciennes, France

⁴ INSAT, Carthage University, Tunis, Tunisia

Abstract. With the advent of the Internet of Things (IoT), various interconnected objects can be used to improve the collection and the process of vital signs with partially or fully automatized methods in smart hospital environment. The vital signs data are used to evaluate patient health status using heuristic approaches, such as the early warning scoring (EWS) approach. Several applications have been proposed based on the early warning scores approach to improve the recognition of patients at risk of deterioration. However, there is a lack of efficient tools that enable a personalized monitoring depending on the patient situations. This paper explores the publish-subscribe pattern to provide a self-adaptative early warning score system in smart hospital context. We propose an adaptative configuration of the vital signs monitoring process depending on the patient health status variation and the medical staff decisions.

Keywords: Computing for healthcare · Early warning scoring system · Internet of Things · Smart hospital

1 Introduction

The smart hospital (SH) is adding the intelligence to traditional hospital system to improve the quality of healthcare services. It is based on the effective use of technology and it covers all the resources and the locations with the patient information. A principal functionality in a smart hospital is the automated and continuous control of the patients during the hospitalization by measuring their vital signs. These observations are important for preventing health deterioration, reducing costs and hospitalization time, and potentially minimizing morbidity and mortality [1]. Several medical approaches are used to evaluate the collected vital signs data. A prevalent example is the Early warning scoring (EWS) approach which has been in use for several years as a tool to predict the risk level of patients [2]. It was proposed for the first time as a paper-based method that need periodical checkups to assign a score based on patient's vital

signs (i.e., heart rate, respiration rate, body temperature, blood pressure). The score of each medical sign depends on the non-respect of a predefined normal interval. The summation of all scores reflects the global patients risk level [2].

By exploring the Internet of Things technologies, the vital signs control solutions are automated based on various medical devices and sensors. Smart medical devices constitute the core part of the smart hospital environment. Their main purpose is to gather vital signs data or other patient physiological conditions. These automated systems reduce the errors of the manual Early Warning Score systems [3] and facilitate the nurses' functions such as constantly gathering and storing the vital signs records.

The emergence of the Internet of Things, the electronic records and the computerized transaction systems have improved the efficiency and effectiveness of EWS systems.

In spite of such advantages using IoT, there are currently two important challenges of early warning scores systems and they need to be considered. The first issue is how to ensure a personalized monitoring of patients' vital signs depending on their situations and the medical experts' requirements especially in case of controlling an important number of patients.

The second issue is the need of timely response of medical staff in case of problem detection.

Our work is motivated by the challenges described above and its main objective is a self-adaptive Early Warning Scoring system that supports the change of the patient control frequency depending on his situation.

This paper is organized as follows: In Sect. 2 we describe the vital signs evaluation with the early warning score systems and we present some related works. Our proposed solution is detailed in Sect. 3. The Implementation and the evaluation are presented and discussed in Sect. 4. The Sect. 5 presents the concluding remarks and future work.

2 Background and Related Works

Early warning systems, also known as 'track-and-trigger' (T&T) systems, consist of evaluating vital signs using scores to recognize patients at risk of deterioration. Since 85% of severe adverse events (SAE) are preceded by abnormal vital signs, the vital signs monitoring based on EWS approach have evolved as a means of alerting health professionals to patient clinical decline [4].

In smart hospitals, particularly in intensive care units, the Early Warning Score (EWS) is a prevalent tool, by which patient's vital signs are periodically recorded and the emergency level is interpreted [3]. To this end, a score (0 for a perfect condition and 3 for the worst condition) is allocated to each vital sign according to its value and the predefined limits. The summation of the obtained scores indicates the degree of health deterioration of the patient (the higher the EWS, the worse the patient's health condition).

Physiological parameter	Score						
	3	2	1	0	1	2	3
Respiration rate (per minute)	≤8		9–11	12–20		21–24	≥25
SpO ₂ Scale 1 (%)	≤91	92–93	94–95	≥96			
SpO ₂ Scale 2 (%)	≤83	84–85	86–87	88–92 ≥93 on air	93–94 on oxygen	95–96 on oxygen	≥97 on oxygen
Air or oxygen?		Oxygen		Air			
Systolic blood pressure (mmHg)	≤90	91–100	101–110	111–219			≥220
Pulse (per minute)	≤40		41–50	51–90	91–110	111–130	≥131
Consciousness				Alert			CVPU
Temperature (°C)	≤35.0		35.1–36.0	36.1–38.0	38.1–39.0	≥39.1	

Fig. 1. The NEWS2 scores chart.

2.1 National Early Warning Scoring (NEWS)2 Approach

NEWS2 chart illustrated in Fig. 1 is a revised version of NEWS chart. The NEWS was created to standardize the process of recording, scoring and responding to changes in routinely measured physiological parameters in acutely ill patients. It was developed to improve the detection of clinical deterioration in patients with acute illness. In [5] NEWS was evaluated against a range of outcomes that are of major importance to patients and staff. It demonstrates a good ability to discriminate patients at risk of the combined outcome of cardiac arrest, unanticipated ICU admission or death within 24 h, which provides ample opportunity for an appropriate clinical intervention to change patient outcome [6].

NEWS2 could be made safer for patients with hypercapnic respiratory failure by having two scoring systems for (saturation pulse oxygen) SpO₂:

- The existing SpO₂ scoring system (Scale 1) that would apply to the majority of patients.
- A dedicated SpO₂ scoring system for patients with hypercapnia respiratory failure (Scale 2). This illness means that the patient doesn't have enough oxygen in his blood and his desired oxygen saturations are set at a lower level (88–92%). The NEWS scoring system is adjusted accordingly.

2.2 Early Warning Score Systems Requirements

Early warning score systems are used to improve the process of recording, scoring and responding to changes in measured vital signs of patients. The following paragraphs present the principal requirements of EWS systems to ensure an efficient detection and response to clinical deterioration:

- Personalization

The patient vital signs data are the key of successful medical decisions. Each patient requires a personalized control depending on his situation [7]. For example a patient with a disease that causes hyperthermia, the temperature is a critical data which must be visualized with more precision; every second. While other non-critical parameters can be calculated only every hour for example.

- Medical staff engagement

The early warning scores systems are highly user-dependent and depend on the appropriate response and actions of the Medical Emergency Teams [4].

- Need for expert's decision

The warning scores cannot replace specialist's decision and the importance on knowing individual patients, they cannot also replace the background to the observations that are recorded [2].

NEWS correlated poorly with the patient's clinical status within the first 24 h post-operatively [2].

2.3 Related Works

In [8], authors present a solution which takes benefits from the concept of Edge computing and fog computing in the context of IoT based Early Warning Scores systems. The solution provides high level services in a Geo-distributed fashion at the edge of the network. The proof of concept is demonstrated with smart e-Health Gateway called UT-GATE implemented for an IoT-based remote health monitoring system. The demonstration includes the data flow processes from data acquisition at sensor nodes to the cloud and the end-users. However, the data has a static interval of acquisition which is defined at the development stage. As a result, the solution does not give the possibility of personalization. The smart e-Health Gateway proposed in [9] provides local storage to perform real-time local data processing and mining. When a patient's vital signal is processed, reliable IoT systems are provided to facilitate fault-tolerant healthcare services. Zhang et al. proposes in [10] a patient-centric cyber-physical system named Health-CPS aiming to ensure convenient Healthcare service. The Health-CPS depends on Cloud computing and data analytics to handle the big data related issues of different healthcare applications. The system is composed of several layers such as data collection layer, data management layer and data-oriented service layer. The system collects data in a unified standard. It supports distributed storage and parallel processing.

The authors present in [11] a low-cost health monitoring system that provides continuous remote monitoring of the ECG and automatic analysis and notification. The system consists of energy-efficient sensor nodes and a fog layer that take full advantage of IoT. The sensor nodes collect and wirelessly transmit ECG, respiration rate, and body temperature to a smart gateway which can be accessed by appropriate care-givers. In addition, the system can represent the collected data in useful ways, perform automatic decision making and provide many advanced services such as real-time notifications for immediate attention.

All the previous proposed solutions require different technology skills to modify or to scale out an existing system in a hospital context. The devices list is predefined at the conception level with fixed parameters of configuration. Added to that, the frequency of collecting and saving data are defined by the developers at the level of implementation without the possibility of modification after the deployment in a real case. As a result of this static configuration, a device collect data with the same parameters defined from the first step of development and it cannot be reused for personalized cases.

However, patient data are different from other collected data in IoT environments as it depends on the no stable situation of the patient health. For example, the frequency of the collected respiration data with a sensor depends on the patient illness. In some cases, an interval of 1 h is sufficient but in other cases 1 min is needed. If the storage operation of data is unique, an important unnecessary information will take place in the memory and demand useless process. In this paper, we propose a health-care system that makes it easy to personalize the vital signs monitoring of a particular patient depending on his health condition.

3 The Proposed Solution

Our proposed solution supports a patient-driven process by giving the possibility to adjust the parameters of vital signs monitoring to a specific health condition or treatment. The following paragraphs describe the solution architecture and the supported communication model.

3.1 Publish-Subscribe Communication Model

Our solution uses the publish/subscribe pattern for the data exchange between the different architecture layers. Publish-subscribe messaging systems support data-centric communication and have been widely used in IoT systems. With the publish-subscribe pattern, the exchange of messages between clients is ensured using a broker that manages topics and sub-topics. A publisher on a given topic can send messages to other clients acting as subscribers to the topic without the need to know about the existence of the receiving clients [5].

To organize the topics and sub-topics in both gateway and server brokers, we define four categories of data:

- **Sensed data:** The collection of time-series data sensed by the medical devices.

- EWS score data: The corresponding score of each sensed data depending on the NEWS2 specification illustrated in Fig. 1.
- Configuration data: The definition of the gateway parameters by the medical staff. For example, the frequency of saving the collected data.

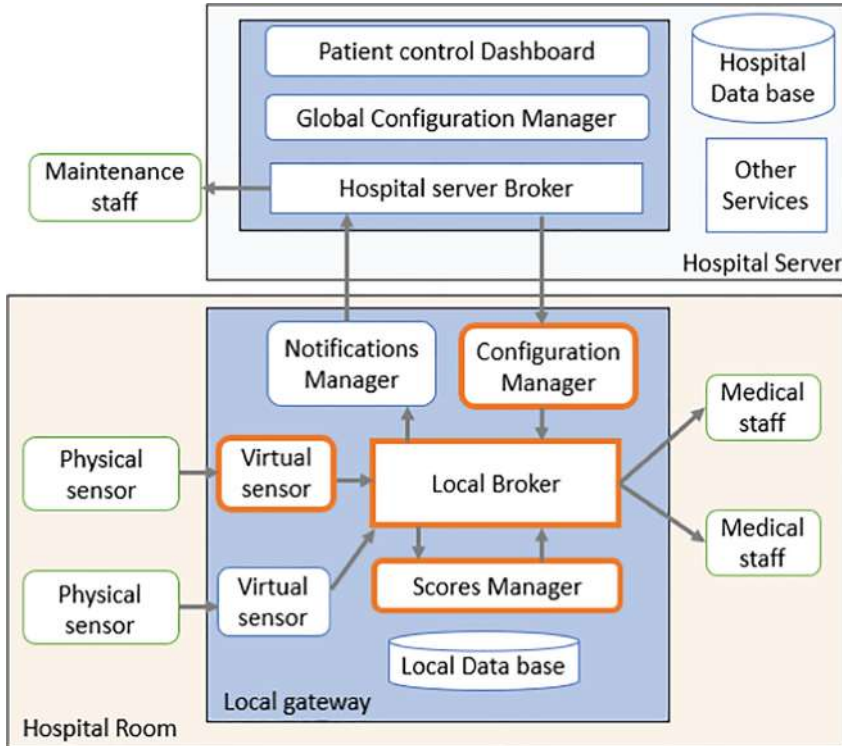


Fig. 2. The solution architecture.

3.2 Gateway Layer Components

We propose the use of a gateway as an edge layer to put the computing at the proximity of data sources. In each hospital room, a smart gateway is used to collect the vital signs of the patients. The main components of the proposed gateway illustrated in Fig. 2 are:

a) Local broker

The Broker server acts as an intermediary for messages sent between the publishers and the subscribers for a specific topic. It routes the messages based on topic rather than the IP address. When a message is sent by the publish client to the broker server, all the subscribe clients interested on the related topic of the message will receive the publication.

Medical devices are considered as data publishers. A topic is the device name and for each device, a subscriber is created to listen to the published data and save it in a local database with the required parameters. The main component of the gateway is an embedded configuration service that provides medical staff with the ability to log into and configure the data process behavior depending on patients' situations. Medical staff can configure publishers and subscribers by providing information such as the ID of the devices, the references of the patients and the corresponding dates of hospitalization.

b) The virtual sensor

It is a software component that has three main roles. First, it saves the received data as significant information in the local database. Second, it calculates the score of the data depending on its type and using the predefined intervals of the NEWS2 approach. In case of problem detection with the calculated score or data interruption, the virtual sensor publishes a notification to the local broker. Added to that, each virtual sensor is subscribed to a configuration topic in order to receive the requested interval of saving data in the local database. To ensure the privacy of the patient information, the virtual sensor does not store the patients' details such as their names or their ages. It stores only the references of patients associated with the devices' numbers and the corresponding range time of data collection.

c) Scores manager

The scores manager is a software component that receive calculated scores from all the virtual sensors. It calculates the global score of each patient and evaluates its risk level. The calculated scores are saved in the local database and they are sent regularly to the hospital server for long term storage. In case of high score detection, the scores manager keep publishing significant notifications to the local broker until it receives a validation of the medical staff intervention.

d) Configuration manager

The configuration manager is in an intermediate position between the hospital server and the virtual sensors. It initializes each new virtual sensor with the corresponding configuration. The configuration manager of each gateway is considered as a subscriber to the corresponding configuration topic defined at the Hospital server.

3.3 Methods

The main objective of our solution is to provide intelligent methods of patient control. Two types of configuration are supported by the configuration manager:

- Devices configuration

The medical staff can submit a configuration request using a web interface, the server broker publish the received request as a configuration message to the concerned gateway. If the request is about adding a new device, a new virtual sensor is created after validation. In case that the medical staff choose to modify some parameters of an existing device, the corresponding virtual sensor checks the different inserted parameters: device identifier, patient reference and the time range of saving data and save the

new configuration. The separation of the virtual sensors as independent subscribers ensures that the modification or the elimination of a device does not affect the whole system.

- Data management configuration

Added to the devices configuration possibility, our system integrates an automation algorithm for the calibration of the data storage and the score calculation frequency.

For each score level, the maximum value is defined as score level limit. The configuration manager reads frequently the calculated score of each vital sign from the local database and compare it with the corresponding predefined limits.

If it captures successive abnormal values, the frequency of the collection of this data is automatically increased to be able to monitor the data concerned with more precision. The new frequency value is saved in the local database and published as a message to the corresponding virtual sensor.

When the measurements become more stable and less than the predefined limits, the administrator can decide to change this frequency.

The values of required frequencies are defined depending on the medical experts' requirements (Fig. 3).

The self-adaptivity process is illustrated in the following algorithm:

Algorithm 1 Self-adaptivity algorithm	
<hr/>	
Inputs: (SC) NEWS2 calculated score, (Freq) Corresponding frequency, (VST) Virtual Sensor Topic	
Variables: (Score0Limit, Score1Limit) NEWS2 scores limits	
Output: NewFreq (new data collection frequency).	
0: begin	
1:	If ((Freq == FreqLevel1) and (SC == 0)) then
2:	Score0Limit = GetScoreLimit (VST, 0)
3:	If (verifEgalityOfLast2Values (VST, SC, Score0Limit)
4:	== false) then
5:	NewFreq = FreqLevel2
6:	End if
7:	Else if ((Freq == 1min) and ((SC == 1) or (SC == 2))) then
8:	Score1Limit = GetScoreLimit (VST, 1)
9:	If (verifEgalityOfLast3Values(VST, SC, Score1Limit)
10:	== false) then
11:	NewFreq = FreqLevel3
12:	End if
13:	End if
14:	Publish (VST, NewFreq)
15:	end

Fig. 3. Self-adaptative configuration algorithm.

4 Implementation and Evaluation

4.1 Materials

The Gateway is a Raspberry Pi 3 which is a small size board with 1 GB of Ram and 1.2 GHz processor [12]. As an Operating System for the gateway, we use Raspbian the pre-compiled Debian OS which is especially optimized for the Raspberry Pi.

We install the InfluxDB database which is an open-source Time Series Database written in Go. At its core is a custom-built storage engine called the Time-Structured Merge (TSM) Tree, which is optimized for time-series data. InfluxDB supports SQL-like query languages named InfluxQL and has the advantage of easy scale-out. It provides support for mathematical and statistical functions across time ranges, also it is developed for custom monitoring, metrics collection and real-time analytics [13].

We use the mosquito implementation as a messages' broker and Node JS clients as subscribers [14].

The messages exchange is ensured by MQ Telemetry Transport (MQTT) protocol [15]. MQTT protocol is a lightweight application layer protocol designed for resource-constrained devices. It runs over TCP/IP, or over other network protocols that provide ordered, lossless and bidirectional connections. It uses the publish/subscribe messaging system combined with the concept of topics to provide one-to-many message distribution. The headers of MQTT messages are small and the connection set up does not require a synchronous handshake which could support a range of 10 to 100 messages per second.

MQTT applies topic-based filtering of messages with a topic being part of each published message. The broker uses the topics to determine whether a subscribing client should receive the message or not. Clients can subscribe to as many topics as they are interested in.

4.2 Evaluation and Results

The evaluation of the presented solution was done from a resource use point of view to analyze whether the self-adaptative algorithm would result in a better performance parameter. The parameters that were taken into account were memory use for stored data and the CPU use of the gateway.

To prove the benefits of the customized use of the gateway, we consider a scenario of controlling the temperature data of one patient with two different scenarios. The first is called fixed case, it is the standard case in which the data are collected with a unique interval of time. In the second case, the interval of data collection changes depending on the patient's score calculation.

In Fig. 4, we illustrate a result of the self-adaptivity configuration. We support 3 levels of data storage frequency depending on the corresponding score. The green signal presents the temperature measurements of a patient. The frequency of saving the sensed data changes when successful augmentation of temperature value is detected. The second signal which does not respect the self-adaptative algorithm contains unnecessary information for the first seven hour and before the increase of patient's temperature.

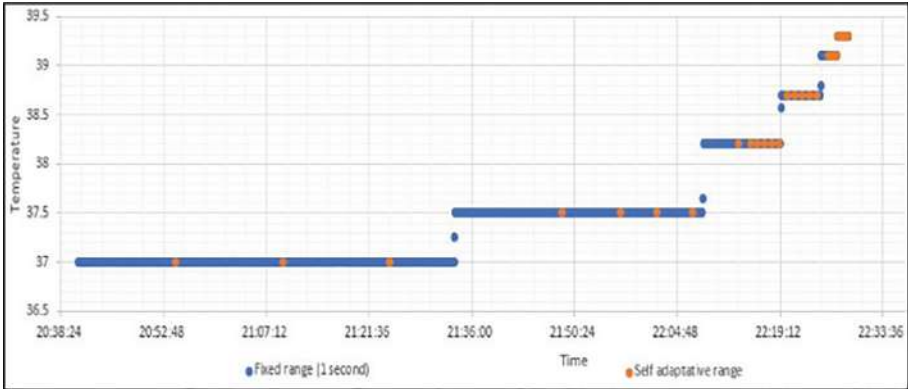


Fig. 4. Self-adaptive configuration example.

We simulate 5 devices that send temperature values using the MQTT protocol. Two scenarios were made for this simulation. The first is to use a temperature interval equal to 1 s for the 5 devices. The second is to vary the sending intervals for each device (10 min, 5 min, 1 h, 30 min, 10 s).

The evaluation results reflected in Fig. 5 and Fig. 6 are obtained using chronograf software which is an administrative tool for InfluxData deployments [16]. It shows that the use of a single data processing strategy in a fixed and non-custom way can result in an unnecessary use of gateway processor and memory which obviously affects performance and the time reaction specially in emergency cases.

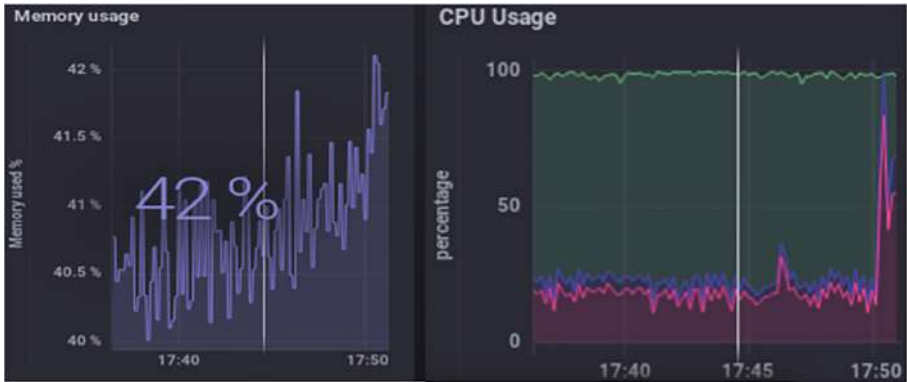


Fig. 5. Evaluation of the fixed scenario

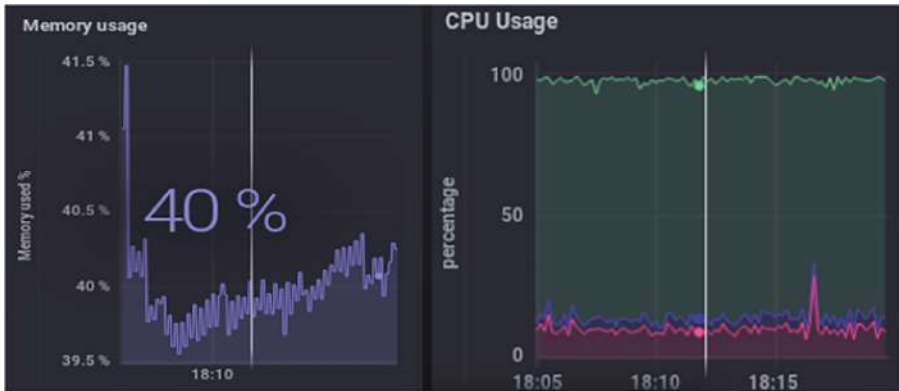


Fig. 6. Evaluation of the self-configuration scenario

5 Conclusion and Future Work

In this paper, we proposed a self-adaptive early warning scores system that respect a risk evaluation approach named NEWS2. It provides a manual and self-adaptive configuration of the vital signs monitoring process depending on the patient health status variation and the medical staff decisions. We aim in our future work to use ontologies for more interpretation of collected data.

References

- Costa, C., Pasluosta, F., Eskofier, B., Silva, D., Righi, R.: Internet of health things: toward intelligent vital signs monitoring in hospital wards. *J. Artif. Intell. Med.* **89**, 61–69 (2018)
- Downey, C.L., Tahir, W., Randell, R., Brown, J.M., Jayne, D.G.: Strengths and limitations of early warning scores: a systematic review and narrative synthesis. *Int. J. Nurs. Stud.* **76**, 106–119 (2017)
- Anzanpour, A., Rahmani, A.-M., Liljeberg, P., Tenhunen, H.: Context-aware early warning system for in-home healthcare using internet-of-things. In: Mandler, B., et al. (eds.) *IoT360 2015*. LNICST, vol. 169, pp. 517–522. Springer, Cham (2016). https://doi.org/10.1007/978-3-319-47063-4_56
- National Early Warning Score (NEWS) 2 (2019) <https://www.rcplondon.ac.uk/projects/outputs/national-early-warning-score-news-2>
- Du, B., Huang, R., Xie, Z., Ma, J., Lv, W.: KID model-driven things-edge-cloud computing paradigm for traffic data as a service. *IEEE Network* **32**(1), 34–41 (2018)
- Mieronkoski, R., et al.: The Internet of Things for basic nursing care—a scoping review. *Int. J. Nursing Stud.* **69**, 78–90 (2017)
- Razzaque, M.A., Milojevic-Jevric, M., Palade, A., Clarke, S.: Middleware for internet of things: a survey. *IEEE Internet Things J.* **3**(1), 70–95 (2016)
- Rahmani, A.M., et al.: Exploiting smart e-Health gateways at the edge of healthcare Internet-of-Things: a fog computing approach *Future Gener. Comput. Syst.* **78**(2), 641–658 (2018)
- Farahani, B., et al.: Towards fog-driven IoT eHealth: Promises and challenges of IoT in medicine and healthcare. *Future Gener. Comput. Syst.* **78**(2), 659–676 (2018)

10. Zhang, Y., Qiu, M., Tsai, C.W., Hassan, M.M., Alamri, A.: Health-CPS: healthcare cyber-physical system assisted by cloud and Big Data. *IEEE Syst. J.* **11**, 88–95 (2017)
11. Gia, N.T., et al.: Low-cost fog-assisted health-care IoT system with energy-efficient sensor nodes. In: 13th International Wireless Communications and Mobile Computing Conference (IWCMC), Valencia, pp. 1765–1770 (2017)
12. Richardson, M., Wallace, S.: *Getting Started with Raspberry PI*. O'Reilly Media, Inc., Sebastopol (2012)
13. Rudolf, C.: SQL, noSQL or newSQL—comparison and applicability for Smart Spaces. *Network Architectures and Services* (2017)
14. Light, R.A.: Mosquitto: server and client implementation of the MQTT protocol. *J. Open Source Softw.* **2**(13), 265 (2017)
15. Banks, A., Gupta, R.: MQTT Version 3.1. 1, OASIS standard, vol. 29 (2014)
16. <https://www.influxdata.com/time-series-platform/chronograf/>

Open Access This chapter is licensed under the terms of the Creative Commons Attribution 4.0 International License (<http://creativecommons.org/licenses/by/4.0/>), which permits use, sharing, adaptation, distribution and reproduction in any medium or format, as long as you give appropriate credit to the original author(s) and the source, provide a link to the Creative Commons license and indicate if changes were made.

The images or other third party material in this chapter are included in the chapter's Creative Commons license, unless indicated otherwise in a credit line to the material. If material is not included in the chapter's Creative Commons license and your intended use is not permitted by statutory regulation or exceeds the permitted use, you will need to obtain permission directly from the copyright holder.





Machine Learning Based Rank Attack Detection for Smart Hospital Infrastructure

Abd Mlak Said^{1(✉)}, Aymen Yahyaoui^{1,2}, Faicel Yaakoubi³,
and Takoua Abdellatif²

¹ Military Academy of Fondouk Jedid, Nabul, Tunisia
maliksaid@outlook.fr

² SERCOM Lab, Polytechnic School of Tunisia, La Marsa, Tunisia

³ Defense Science and Technology Laboratory, Tunis, Tunisia

Abstract. In recent years, many technologies were racing to deliver the best service for human being. Emerging Internet of Things (IoT) technologies made birth to the notion of smart infrastructures such as smart grid, smart factories or smart hospitals. These infrastructures rely on interconnected smart devices collecting real-time data in order to improve existing procedures and systems capabilities. A critical issue in smart infrastructures is the information protection which may be more valuable than physical assets. Therefore, it is extremely important to detect and deter any attacks or breath to the network system for information theft. One of these attacks is the rank attack that is carried out by an intruder node in order to attract legitimate traffic to it, then steal personal data of different persons (both patients and staffs in hospitals). In this paper, we propose an anomaly based rank attack detection system against an IoT network using Support Vector Machines. As a use case, we are interested in the healthcare sector and in particular in smart hospitals which are multifaceted with many challenges such as service resilience, assets interoperability and sensitive information protection. The proposed intrusion detection system (IDS) is implemented and evaluated using Conticki Cooja simulator. Results show a high detection accuracy and low false positive rates.

Keywords: Internet of Things · Smart hospitals · Intrusion detection · Rank attack · Machine learning · RPL

1 Introduction

Nowadays, the deployment of the Internet of Things (IoT) where many objects are connected to the Internet cloud services becomes highly recommended in many applications in various sectors. A highly important concept in the IoT is Wireless Sensor Networks or WSNs where end nodes rely on sensors that can collect data from the environment to ensure tasks such as surveillance or monitoring

for wide areas [7]. This capability made the birth to the notion of smart infrastructures such as smart metering systems, smart grid or smart hospitals. In such infrastructures, end devices collecting data are connected to intermediate nodes that forward data in order to reach border routers using routing protocols. These end nodes are in general limited in terms of computational resources, battery and memory capacities. Also, their number is growing exponentially. Therefore, new protocols are proposed under the IoT paradigm to optimize energy consumption and computations. Two of these protocols are considered the de facto protocols for the Internet of Things (IoT): RPL (Routing Protocol for Low Power Lossy Network) and 6LoWPAN (IPv6 over Low Power Wireless Private Area Network). These protocols are designed for constrained devices in recent IoT applications. Routing is a key part of the IPv6 stack that remains to be specified for 6Low-Pan networks [6]. RPL provides a mechanism whereby multipoint-to-point traffic from devices inside the Low-Power and Lossy-Networks (LLNs) towards a central control point as well as point-to-multipoint traffic from the central control point to the device inside the LLN are supported [8,9]. RPL involves many concepts that make it a flexible protocol, but also rather complex [10]:

- DODAG (Destination Oriented Directed Acyclic Graph): a topology similar to a tree to optimize routes between sink and other nodes for both the collect and distribute data traffics. Each node within the network has an assigned rank, which increases as the nodes move away from the root node. The nodes resend packets using the lowest rank as the route selection criteria.
- DIS (DODAG Information Solicitation): used to solicit a DODAG information object from RPL nodes.
- DIO (DODAG Information Object): used to construct, maintain the DODAG and to periodically refresh the information of the nodes on the topology of the network.
- DAO (DODAG Advertisement Object): used by nodes to propagate destination information upward along the DODAG in order to update the information of their parents.

With the enormous number of devices that are now connected to the Internet, a new solution was proposed: 6LowPan a lightweight protocol that defines how to run IP version 6 (IPv6) over low data rate, low power, small footprint radio networks as typified by the IEEE 802.15.4 radio [11]. In smart infrastructures, the huge amount of sensitive data exchanged among these modules and throughout radio interfaces need to be protected. Therefore, detecting any network or device breach becomes a high priority challenge for researchers due to resource constraints for devices (low processing power, battery power and memory size). Rank attack is one of the most known RPL attacks where the attacker attracts other nodes to establish routes through it by advertising false rank. This way, intruders collect all the data that pass in the network [12].

For this reason, developing specific security solutions for IoT is essential to let users catch all opportunities it offers. One of defense lines designed for detecting attackers is Intrusion Detection Systems [13] (IDS). In this paper, we propose a

centralized anomaly-based IDS for smart infrastructures. We chose O-SVM (One class Support Vector Machines) algorithm for its low energy consuming compared to other machine learning algorithms for Wireless sensor network (WSN) [20].

As a use case, we are interested in smart hospital infrastructures. Such hospitals have a wide range of resources that are essential to maintain their operations, patients, employees and the building itself [1, 2] safety such as follow:

- Remote care assets: medical equipment for tele-monitoring and tele-diagnosis.
- Networked medical devices: wearable mobile devices (heartbeat bracelet, wireless temperature counters, glucose measuring devices...) or an equipment installed to collect health service related data.
- Networking equipment: standards equipment providing connectivity between different equipment (transmission medium, router, gateway...).
- Data: for both clinical and patient data, and staff data, which considered the most critical asset stored in huge datasets or private clouds.
- Building and facilities: the sensors are distributed in the hospital building that monitor the patient safety (temperature sensor for patient room and operation theater, gas sensor are among used sensors).

We target a common IoT architecture that can be considered for smart hospitals. In such architecture, there are mainly three type of components:

Sensing Node: composed of remote care asset, network medical device and different sensors. These sensors will send different type of data and information (patient and staff data, medical equipment status...). They are linked to micro-controllers and radio modules to transmit these data to the processing unit [3].

Edge Router: an edge router or border router is a specialized router residing at the edge or boundary of a network. This node ensures the connectivity of its network with external networks; a wide area network or the Internet. An edge router uses an external border gateway protocol, which is used extensively over the Internet to provide connectivity with remote networks. Instead of providing communication with an internal network, which the core router already manages, a gateway may provide communication with different networks and autonomous systems [4].

Interface Module and Database: this module is the terminal of the network containing all the collected data from different nodes of the network and analyze those information in order to ensure the safety of patient and improve the healthcare system.

Figure 1 [5], presents the typical IoT e-health architecture, where sensors are distributed (medical equipment, room sensors and others) and send data to the IoT gateway. In one hand, this gives the opportunity to medical supervisor to control the patient health status. In the other hand, this data will be saved into databases for more analysis.

The rest of the paper is structured as follows. Section 2 presents the related work. Section 3 presents the Rank attack scenario. Section 4 presents our proposed approach. Section 5 presents our main results and Sect. 6 concludes the paper and presents its perspectives.

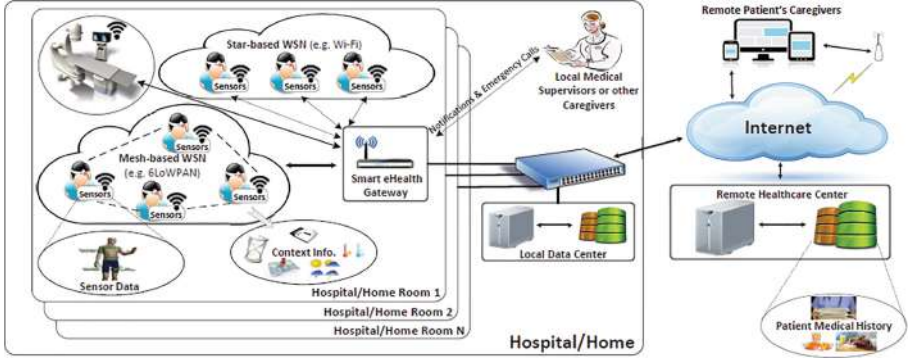


Fig. 1. Smart hospital assets.

2 Related Work

RPL protocol security especially in the healthcare domain is a crucial aspect for preserving personnel data. Nodes rank is an important parameter for an RPL network. It can be used for route optimization, loop prevention, and topology maintenance. In fact, the rank attack can decrease the network performance in terms of packet delivery rate (PDR) to almost 60% [23]. There were different proposed solutions to detect and mitigate RPL attacks such as rank authentication mechanism to avoid false announced ranks by using cryptography technique which was proposed in [24]. However, this technique is not very efficient because of its high computational cost and energy consumption. Authors in [25] propose a monitoring node (MN) based scheme but it is also not efficient because using a large network of MNs causes a communication overhead. In [26], authors propose the IDS called “SVELTE” that can only be used for detection of simple rank attack and has high false alarm rate. A host-based IDS was proposed in [27]. The IDS uses a probabilistic scheme but it is discouraged by RFC6550 for resource constrained networks. Routing Choice “RC” was proposed by Zhag et al. [28]. It is not directly related to the rank attack but it is based on false preferred parent selection. It has a high communication overhead in RPL networks. Trusted platform module (TPM) was proposed by Seeber et al. [29]. It introduces an overlay network of TPM nodes for detection of network attacks. SecureRPL (SRPL) [30] technique prevents RPL network from Rank attack, however it is characterized by a high energy consumption. Therefore, anomaly based solutions using machine learning permit a more efficient detection. Authors of [22] compared several unsupervised machine learning approaches based on local outlier factor, near neighbors, Mahalanobis distance and SVMs for intrusion detection. Their experiments showed that O-SVM is the most appropriate technique to detect selective forwarding and jamming attacks. Actually, we rely on these results in our choice of O-SVM.

3 Rank Attack Scenario

Rank attack is one of well known attacks against the routing protocol for low power and lossy networks (RPL) protocol in the network layer of the Internet of Things. The rank in RPL protocol as shown in Fig. 2 is the physical position of the node with respect to the border router and neighbor nodes [12].

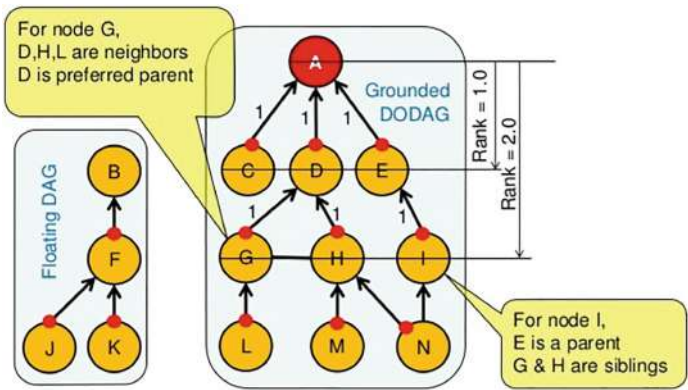


Fig. 2. The rank in IoT network.

Since our network is dynamic due to the mobility of its nodes (sensor moving with patient...), the RPL protocol periodically reformulates the DODAG. As shown in Fig. 3, an attacker may insert a malicious mote into the network to attract other nodes to establish routes through it by advertising false ranks while the reformulation of the DODAG is done [14].

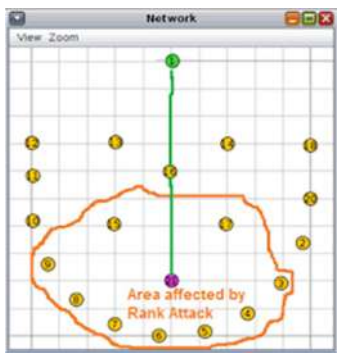


Fig. 3. Rank attack.

By default, RPL has the security mechanisms to mitigate the external attacks but it can not mitigate the internal attacks efficiently. In that case, the rank

attack is considered one of dangerous attacks in dynamic IoT networks since the attacker controls an existing node (being one of the internal attack that can affect the RPL) in the DODAG or he can identify the network and insert his own malicious node and that node will act as the attack node as shown in Fig. 4.

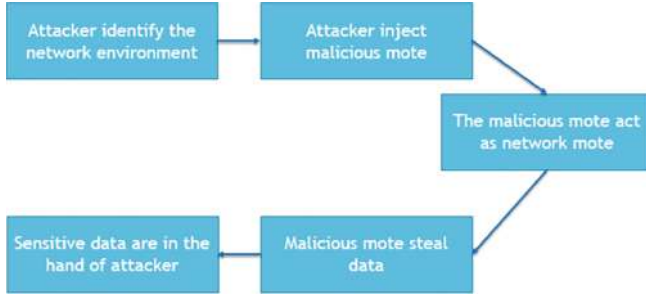


Fig. 4. The rank attack scenario.

4 Proposed Approach

The key features required for our solution are to be adaptive, lightweight, and able to learn from the past. We design an IoT IDS and we implement and evaluate it as authors did in [18,20].

Placement Choice: one of the important decision in intrusion detection is the placement of the IDS in the network. We use a centralized approach by installing the IDS at the border router. Therefore, it can analyze all the packets that pass through it. The choice of the centralized IDS was done to avoid the placement of IDS modules in constrained devices which requires more storage and processing capabilities [15,16]. However, these devices have limited resources.

Detection Method Choice: An intrusion detection system (IDS) is a tool or mechanism to detect attacks against a system or a network by analyzing the activity in the network or in the system itself. Once an attack is detected an IDS may log information about it and/or report an alarm [15,16]. Broadly speaking, we aim to choose the anomaly based detection mechanisms: it tries to detect anomalies in the system by determining the ordinary behavior and using it as baseline. Any deviations from that baseline is considered as an anomaly. This technique have the ability to detect almost any attack and adapt to new environments. We chose Support Vector Machines (SVM) as an anomaly based machine learning technique. It is a discriminating classifier formally defined by a separating hyper-plane. Given labeled training data (supervised learning), the

algorithm outputs an optimal hyper-plane which categorizes new examples. In two dimensional space this hyper-plane is a line dividing a plane in two parts where each class lays in either side. It uses a mathematical function named the kernel to reformulate data. After these transformations, it defines an optimal borderline between the labels. Mainly, it does some extremely complex data transformations to find a solution how to separate the data based on the labels or outputs defined. The concept of SVM learning approach is based on the definition of the optimal separating hyper-plane (Fig. 5) [21] which maximizes the margin of the training data [17,18]. The choice of this machine learning algorithm refers to one important point, it works well with the structured data as tables of values compared to other algorithms.

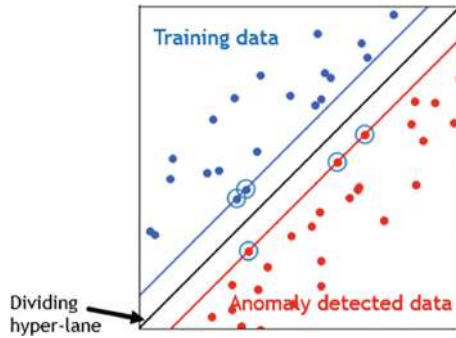


Fig. 5. SVM classification.

We implement the IDS in the smart IoT gateway shown in Fig. 1.

5 IDS Solution and Results

To investigate the effectiveness of our proposed IDS, we implement three scenarios of rank attack using Contiki-Cooja simulator [19]. We assess how our IDS module can detect them. We present next the simulation setup, evaluation metrics, and we discuss the results achieved.

5.1 Simulation Setup

Our simulation scenario consists of a total 11 motes spread across an area of 200×200 m (Simulation of area of hospital where different sensors are placed in every area to control the patient rooms). The topology is shown in Fig. 6 using four scenarios. There is one sink (mote ID:0 with green dot) and 10 senders (yellow motes from ID:1 to ID:10). Every mote sends packet to the sink at the rate of 1 packet every 1 min. We implement the centralized anomaly based IDS at the root mote or the sink and we collect and analyze network data as shown in

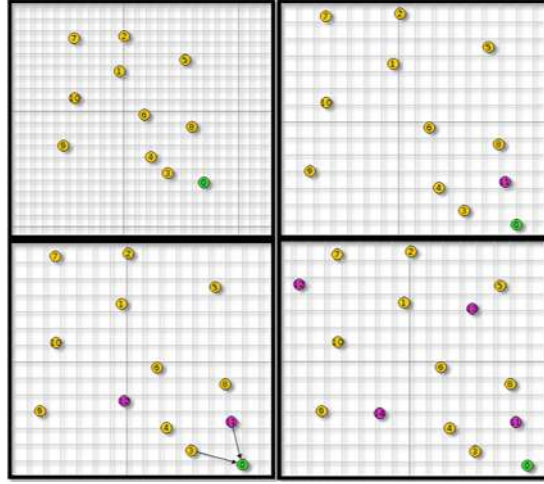


Fig. 6. Simulation topology (Color figure online)

Fig. 6. We inject malicious motes (purple colour) in a random position. Table 1 summarizes the used simulation parameters.

We run four simulation scenarios for 1 h (Fig. 6):

- scenario 1: IoT network without malicious motes.
- scenario 2: IoT network with 1 randomly placed malicious mote.
- scenario 3: IoT network with 2 randomly placed malicious motes.
- scenario 4: IoT network with 4 randomly placed malicious motes.

Table 1. Simulation parameters

Parameter	Value
Platform	Cooja Contiki 3.0
Number of nodes	10 senders, 1 sink
Topology	Star
Area	200 m
Sending rate	1 packet/minute
Simulation run time	1 h
Number of attackers	1, 2 and then 4

5.2 Evaluation Parameter

To evaluate the accuracy of the proposed IDS, we rely on the energy consumption parameter. We collect power tracking data per mote in terms of radio ON energy,

radio transmission TX energy, radio reception RX energy and radio interfered INT energy. In order to calculate this metrics we used the formula [31] (Eq. 1, Table 2) as follow :

$$\begin{aligned}
 Energy(mJ) &= (transmit * 19.5mA + listen * 21.8mA \\
 &\quad + CPU * 1.8mA + LPM * 0.0545mA) \\
 &\quad * 3V / 4096 * 8 \\
 Power(mW) &= \frac{Energy(mJ)}{Time(s)}
 \end{aligned}
 \tag{1}$$

Table 2. Equation parameters description

Variables	Meaning
LPM	Power consumption parameter that indicates the power used when in sleep condition
CPU	Power parameter that indicates the level of node processing
Transmit	Parameter related with node communication while transmitting
Listen	Parameter related with node communication while receiving

5.3 Power Tracking per Mote for Each Simulation

We used data containing 1000 instances of consumed energy values for each node in the network. Figure 7 depicts the evolution of power tracking of each node in the four scenarios:

- scenario 1: when we have a normal behavior in the network, all the sensors show a regular energy consumption in terms of receiving (node 0) and sending (nodes from 1 to 10). We use this simulation to collect the training data for the proposed IDS.
- scenario 2, 3 and 4: for those scenarios, we have a high sending values for the malicious motes. This is explained by the fact that when a malicious mote joins the network, it asks the other motes to recreate the DODAG tree and also to send data that they have, in order to steal as much data as it can. That is why it have a high receiving values too. The other motes do not distinguish that this is a malicious mote, therefore they recreate the DODAG tree, and send their information through the malicious node. We used the first simulation scenario as dataset for our IDS, describing the normal behavior of the network. This 1 h information was enough to detect the malicious activities of the rank attack. Meanwhile, each time we add a malicious mote, the anomaly detection rate increases as shown in Fig. 8.

In each simulation of malicious mote, the proposed IDS indicates the anomaly detection ratio which increases each time while adding another malicious mote. This aims to determine the impact of the number malicious motes compared to normal behavior of the system.

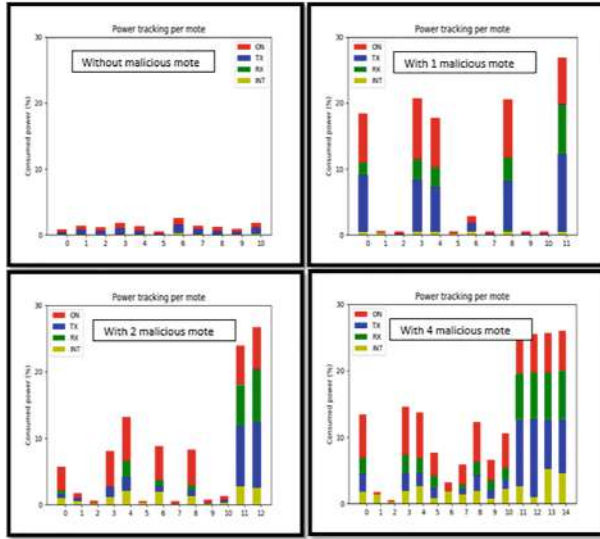


Fig. 7. Power tracking per each mote

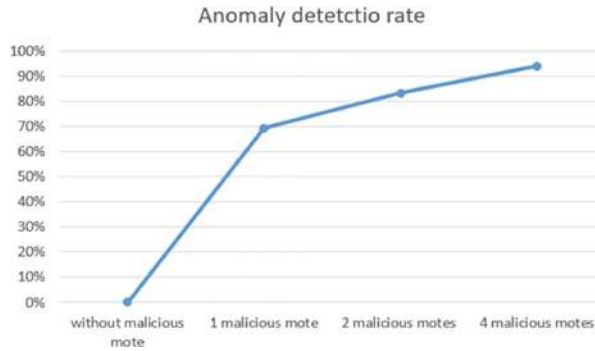


Fig. 8. Evolution of anomaly detection rate

6 Conclusion

In this paper, we propose an intrusion detection system “IDS” for smart hospital infrastructure data protection. The chosen IDS is centralized and anomaly based using a machine learning algorithm OSVM. Simulation results show the efficiency of the approach by a high detection accuracy which is more precise when the number of malicious nodes increases. As future work, we are interested in developing a machine learning based IDS for more RPL attacks detection. Furthermore, we aim to extend this solution to anomaly detection in IoT systems composed not only of WSN networks but also of cloud-based services.

References

1. Yu, L., Lu, Y., Zhu, X.J.: Smart hospital based on Internet of Things. *J. Netw.* **7**(10), 1654 (2012)
2. Attaluri, P., Iqbal, M., Lawrence, C.D.: Smart hospital care system. U.S. Patent Application No. 13/445,299 (2013)
3. Römer, K., Kasten, O., Mattern, F.: Middleware challenges for wireless sensor networks. *Mob. Comput. Commun. Rev.* **6**(4), 59–61 (2002)
4. Kuang, X., Shao, H.: Study of the gateway of wireless sensor networks. *Jisuanji Gongcheng/Comput. Eng.* **33**(6), 228–230 (2007)
5. Rahmani, A.M., et al.: Smart e-health gateway: bringing intelligence to internet-of-things based ubiquitous healthcare systems. In: 2015 12th Annual IEEE Consumer Communications and Networking Conference (CCNC), pp. 826–834. IEEE, January 2015
6. Gaddour, O., Koubâa, A.: RPL in a nutshell: a survey. *Comput. Netw.* **56**(14), 3163–3178 (2012)
7. Zhang, T., Li, X.: Evaluating and analyzing the performance of RPL in contiki. In: Proceedings of the First International Workshop on Mobile Sensing, Computing and Communication, pp. 19–24, August 2014
8. Winter, T., Thubert, P., Brandt, A., et al.: RPL: IPv6 routing protocol for low-power and lossy networks. In: RFC 6550, March 2012
9. Garcia-Morchon, O., Hummen, R., Kumar, S.S., Struik, R., Keoh, S.L.: Security Considerations in the IP-based Internet of Things, March 2012
10. Perazzo, P., Vallati, C., Arena, A., Anastasi, G., Dini, G.: An implementation and evaluation of the security features of RPL. In: Puliafito, A., Bruneo, D., Distefano, S., Longo, F. (eds.) ADHOC-NOW 2017. LNCS, vol. 10517, pp. 63–76. Springer, Cham (2017). https://doi.org/10.1007/978-3-319-67910-5_6
11. Kushalnagar, T., Montenegro, G., Schumacher, C.: IPv6 over low-power wireless personal area networks (6LoWPANs): overview, assumptions, problem statement, and goals. In: RFC, vol. 4919 (2007)
12. Rehman, A., et al.: Rank attack using objective function in RPL for low power and lossy networks. In: 2016 International Conference on Industrial Informatics and Computer Systems (CIICS). IEEE (2016)
13. Farooqi, A.H., Khan, F.A.: Intrusion detection systems for wireless sensor networks: a survey. In: Ślęzak, D., Kim, T., Chang, A.C.-C., Vasilakos, T., Li, M.C., Sakurai, K. (eds.) FGCN 2009. CCIS, vol. 56, pp. 234–241. Springer, Heidelberg (2009). https://doi.org/10.1007/978-3-642-10844-0_29
14. Wallgren, L., Raza, S., Voigt, T.: Routing attacks and countermeasures in the RPL-based Internet of Things. *Int. J. Distrib. Sens. Netw.* **9**(8), 794326 (2013)
15. Zarpelão, B.B., Miani, R.S., Kawakani, C.T., de Alvarenga, S.C.: A survey of intrusion detection in Internet of Things. *J. Netw. Comput. Appl.* **84**, 25–37 (2017)
16. Yang, K., Ren, J., Zhu, Y., Zhang, W.: Active learning for wireless IoT intrusion detection. *IEEE Wirel. Commun.* **25**(6), 19–25 (2018)
17. Kim, D.S., Nguyen, H.N., Park, J.S.: Genetic algorithm to improve SVM based network intrusion detection system. In: 19th International Conference on Advanced Information Networking and Applications (AINA 2005), Volume 1 (AINA papers), vol. 2, pp. 155–158. IEEE, March 2005
18. Wang, J., Hong, X., Ren, R.R., Li, T.H.: A real-time intrusion detection system based on PSO-SVM. In: Proceedings The 2009 International Workshop on Information Security and Application (IWISA 2009), p. 319. Academy Publisher (2009)

19. Bagula, B.A., Erasmus, Z.: IoT emulation with cooja. In: ICTP-IoT Workshop, March 2015
20. Yahyaoui, A., Abdellatif, T., Attia, R.: READ: reliable event and anomaly detection system in wireless sensor networks. In: 2018 IEEE 27th International Conference on Enabling Technologies: Infrastructure for Collaborative Enterprises (WET-ICE), pp. 193–198. IEEE (2018)
21. Wang, J., Chen, Q., Chen, Y.: RBF kernel based support vector machine with universal approximation and its application. In: Yin, F.-L., Wang, J., Guo, C. (eds.) ISBN 2004. LNCS, vol. 3173, pp. 512–517. Springer, Heidelberg (2004). https://doi.org/10.1007/978-3-540-28647-9_85
22. Garcia-font, V., Garrigues, C., Rifà-pous, H.: A comparative study of anomaly detection techniques for smart city wireless sensor networks. *Sensors* **16**(6), 868 (2016)
23. Le, A., Loo, J., Luo, Y., Lasebae, A.: The impacts of internal threats towards routing protocol for low power and lossy network performance. In: IEEE Symposium Computer and Communications (ISCC), pp 789–794 (2013)
24. Dvir, A., Holczer, T., Buttyan, L.: VeRA-version number and rank authentication in RPL. In: 2011 IEEE 8th International Conference on Mobile Ad hoc and sensor systems (MASS). IEEE (2011)
25. Anhtuan, L., et al.: Specification-based IDS for securing RPL from topology attacks. In: 2011 IFIP Wireless Days (WD), pp. 4–6. IEEE (2011)
26. Raza, S., Shahid, L.W., Voigt, T.: SVELTE: real-time intrusion detection in the Internet of Things. *Ad Hoc Netw.* **11**(8), 2661–2674 (2013)
27. Iuchi, K., et al.: Secure parent node selection scheme in route construction to exclude attacking nodes from RPL network. *IEICE Commun. Express* **4**(11), 340–345 (2015)
28. Zhang, L., Feng, G., Qin, S.: Intrusion detection system for RPL from routing choice intrusion. In: 2015 IEEE International Conference on Communication Workshop (ICCW), pp. 2652–2658. IEEE (2015)
29. Sebastian, S., et al.: Towards a trust computing architecture for RPL in cyber physical systems. In: 2013 9th International Conference on Network and service management (CNSM), pp. 134–137. IEEE (2013)
30. Glissa, G., Rachedi, A., Meddeb, A.: A secure routing protocol based on RPL for Internet of Things. In: 2016 IEEE Global Communications Conference (GLOBECOM). IEEE (2016)
31. Hassani, A.E., Sahel, A., Badri, A.: Impact of RPL objective functions on energy consumption in Ipv6 based wireless sensor networks, June 2019


Open Access This chapter is licensed under the terms of the Creative Commons Attribution 4.0 International License (<http://creativecommons.org/licenses/by/4.0/>), which permits use, sharing, adaptation, distribution and reproduction in any medium or format, as long as you give appropriate credit to the original author(s) and the source, provide a link to the Creative Commons license and indicate if changes were made.

The images or other third party material in this chapter are included in the chapter's Creative Commons license, unless indicated otherwise in a credit line to the material. If material is not included in the chapter's Creative Commons license and your intended use is not permitted by statutory regulation or exceeds the permitted use, you will need to obtain permission directly from the copyright holder.





Remote Health Monitoring Systems Based on Bluetooth Low Energy (BLE) Communication Systems

Lamia Chaari Fourati^(✉)  and Sana Said

Digital Research Center of Sfax (CRNS), Laboratory of Technologies and Smart
Systems (LT2S), University of Sfax, Sfax, Tunisia
lamiachaari1@gmail.com

Abstract. Nowadays, remote healthcare monitoring systems (RHMS) are attracting patients, doctors and caregivers. RHMS reduces the number of unessential hospitalizations by providing the required healthcare services for patients at home. Furthermore, continuous health monitoring using RHMS is a hopeful solution for elderly people suffering from chronic diseases. RHMS is in general three tiers architecture where the first tier uses intelligent wearable sensors to gather physiological signs. The majority of wearable sensors constructors commercialized sensing devices with Bluetooth Low Energy (BLE) communication interfaces, which lead to the development of diverse RHMS deploying BLE communication interfaces for physiological patient data gathering. In this paper, we introduce the basic concepts related to RHMS design and development. Besides that, we focus our investigation on the BLE communication protocol used in the healthcare context and its configuration to sense several physiological data. Also, we highlight the different steps enabling reading sensed data on mobile application.

Keywords: Remote health monitoring system · Bluetooth Low Energy · Healthcare services

1 Introduction

1.1 General Context

Healthcare is one of the fastest-growing business fields and an important market for most countries and healthcare services are the most needed and consumed service by elderly people in the world. Providing healthcare services for every citizen everywhere becoming possible thanks to remote healthcare monitoring systems (RHMS), which allow long-term management of health conditions, diseases prevention and detection of emergencies. RHMS is based on the deployment of Wireless Body Area Network (WBAN) using wearable and/or implantable sensors in or around the human body. The sensed physiological data are forwarded

Supported by SFAX Digital Research Center: CRNS.

© The Author(s) 2020

M. Jmaiel et al. (Eds.): ICOST 2020, LNCS 12157, pp. 41–54, 2020.

https://doi.org/10.1007/978-3-030-51517-1_4

to collecting node known as data collector or a gateway or a coordinator (smart-phone or PDA: Personal Data Assistant) which is connected to the remote server (for data processing and storage) through the internet network (via WiFi) or the cellular networks (4G or 5G) [1]. RHMS could be based on three or four tiers architectures [2]. In this work, we focus our investigation on the first tier. Therefore, different communication technologies were suggested for the data exchange between the body sensors nodes and the coordinator(the first tier). Among the most deployed communication technologies in the first tier, we can highlight the following:

IEEE 802.15.4 [3–6].

IEEE 802.15.6 [7–12].

Bluetooth Low Energy [13–15].

The IEEE 802.15.6 [7] is the dedicated standards for the communication between the sensors and the coordinator. Nowadays, sensing devices with 802.15.6 modules are not available enough for the commercial usage in the market and they are more expensive than wearable sensors with Bluetooth Low Energy (BLE) which are widely commercialized by many sensors constructors such as libelium, mindwave.... For this reason, in this paper, our investigation is related to RHMS using sensors with BLE interfaces.

1.2 Contributions and Paper Organisation

The goal of this article is to study and analyze the most significant efforts related to RHMS integrating BLE communication modules. Accordingly, this paper provides a rich bibliography in the domain that can support future reading in this emerging field and pinpoints the technical issues related to the design and development of the BLE based RHMS. Furthermore, this investigation selects and considers several pioneering studies that can act as a roadmap of this wide-ranging research area. Although there is a lot of research works recently proposed that focused on RHMS, to the best of our knowledge, there is no thorough study that cogitates all BLE based RHMS design and development issues. The main contributions of this paper summarized as follows:

- (1) state-of-the-art analysis related to BLE based RHMS for mono and multi physiological data sensing;
- (2) comprehensive study and roadmap related to the design and the development of BLE based RHMS;
- (3) BLE Processing and computation issues of sensed physiological data.

The rest of this paper is organized as follows: the second section describes the basic architecture of RHMS and analyses some related works about BLE based systems for single or multiple sensors. The third section overviews the basic concepts of communication systems based on BLE. The fourth section describes BLE Processing and computation of sensed physiological data such as ECG, SpO2, EMG, HR, etc... and highlights BLE service characteristics data related to each sensor. Finally, the fifth section concludes the paper and draws our future directions.

2 BLE Based RHMS

This section illustrates and explains the general architecture of the RHMS. Then, it studies and analyzes related works focusing on RHMS that integrate BLE communication interfaces between the physiological sensors and the PDA.

2.1 RHMS Basic Architecture

Generally, RHMS can be structured into three or four tiers [2]. In the following, we highlight the basic elements related to RHMS that are based on the three tiers architecture. The first tier involves the wearable sensors attached to the human body and the gateway or the coordinator. In this paper, the selected communication technology between the sensors and the PDA is BLE. Therefore the first tier which is the WBAN is composed by wearable sensors that sense the body vital signs (e.g. body temperature, heart rate, ECG, etc.) through the sensor nodes and sent them to the smartphone via BLE communication interfaces. The second tier that includes the networking infrastructure provides the connectivity between (1) the PDA and the remote medical servers, (2) between the PDA and the cloud. The third tier includes the medical web servers for data visualisation and the cloud (private: for security issues) for the data storage and processing. Figure 1 illustrates the RHMS three tiers architecture incorporating BLE communication interfaces.

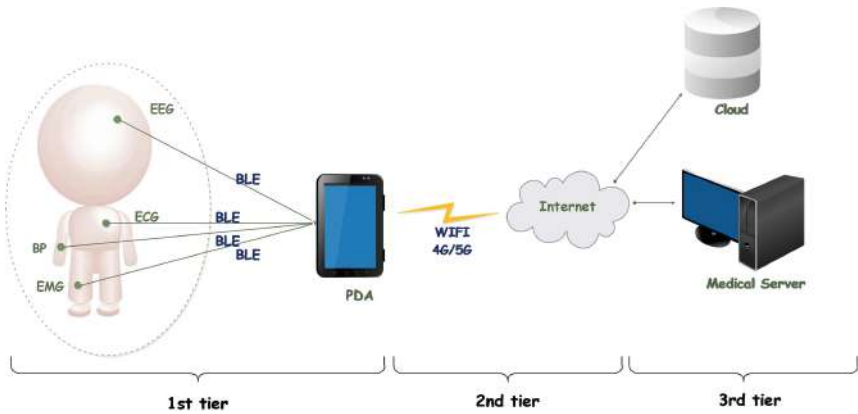


Fig. 1. Remote healthcare monitoring system integrating BLE communication interfaces.

2.2 Related Works About RHMS Using BLE

Several communication technologies could be used in the first tier (as we mentioned in the introduction). In this section, we will focus only on the RHMS

related works that are based on the BLE protocol for data gathering. We classified the studied contributions into two categories. The first category corresponds to RHMS that control or sense one physiological patient data. The second category resembles the RHMS using multiple sensors to sense several physiological data.

Mono-Sensing RHMS. In this subsection, we will analyze related works about RHMS that sense and collect physiological information from a single sensor.

- ***Wearable Noncontact Armband for Mobile ECG Monitoring System:*** Rachim and all. [16] proposed to implement a mobile ECG monitoring system using a wearable noncontact armband ECG signal. The proposed system solved the problem of the previous healthcare heart devices which do not provide patient's information such as heartbeat, heart disease, and heart conditions. The proposed system consists of capacitive-coupled electrodes fixed in an armband which is more convenient (smaller) than systems with ECG sensors strapped to the chest. The capacitive-coupled electrodes can sense bio-signals through the clothes. According to the experimental results carried by the authors, the developed system can still function with different clothing thicknesses between the sensors and the skin and when the user carries out various daily living activities. Furthermore, the authors developed an Android application showing in real-time the evolution of the ECG signal on a graph and analyze the sensed data for first notifications making.

- ***Wireless Ring-Type Pulse Oximeter with Multi-detectors:*** The authors of [17] conceived and developed a wireless finger ring-type pulse oximeter with multi-detectors to monitor the blood oxygen saturation (SpO₂). The developed system contains (1) three optical probes to provide the light source and receive the penetrated light that passes through the human tissue; (2) a wireless data acquisition module containing a microprocessor (MSP430), a LED driving circuit, PD amplifier circuits and a wireless transmission unit. PD amplifier circuits amplify and filter the received penetrated light. Therefore, the digitized penetrated light signal will be sent to the host system (that receive, display, store and analyze the penetrated light signal) using a wireless transmission unit including a Bluetooth v2.0 module and a printed circuit board (PCB) antenna. The monitoring program built in the host system will.

- ***Wireless Scale Based on the Bluetooth 4.0 Low-Energy:*** Huang and all. [18] realized a low power and smart Bluetooth scale with a sensor chip CC2540 monitored through a mobile application. The weight sensors produce deformation and change their shapes when a patient ascend on the scale this lead to a variation of the driven voltage. Therefore, these signals are amplified and transmitted to an A/D converter.

- ***Muscle Activity Monitoring:*** Several systems integrating EMG sensors to measure the electrical muscle activity and a BLE communication module to transmit gathered data to a mobile phone. In this context, authors in [19]

designed a fabric stretch sensor embedded system for muscle activity monitoring. The strain sensor resistance varies sensitively with body movements. The designed system includes an application that shows muscle activity data and highlights the features such as muscle movement distribution. To avoid sports injuries during exercise, authors in [20] designed an EMG patch to supervise the muscle fatigue conditions during isotonic contraction. The developed system deploys two electrodes to measure the sEMG signal. A microcontroller unit in the EMG patch is used to measure in real-time the median frequency of an EMG signal. When the muscle is tired, the median frequency will shift to a low value. The sensed values are sent via BLE to a mobile phone running an APP that displays the muscle fatigue levels and the user riding information.

- **Brain Activity Monitoring:** Sullivan and all. [21] proposed a brain activity monitoring system using the non-invasive electroencephalogram EEG sensor that measures the neural electrical activity of the brain from the scalp surface. The developed EEG monitoring system assisted by deep learning mechanism provides information about neonatal brain health to help clinicians in neonatal EEG abnormalities diagnosing. The proposed system uses a low-cost -low-power EEG acquisition system including BLE interface for communication. Besides that, the authors developed an Android app visualizing single-channel EEG and the neonatal seizure presence. A deep convolutional neural network and an algorithm for EEG sonification used to perceive EEG morphology changes.

- **Breath Rate Monitoring:** Authors in [22] developed a new system to supervise in real-time the respiratory signal. The developed system includes three parts: smart belts, a display unit, and an online storage unit. A textile-based pressure fabric attached to a belt converting the stomach movement into an electrical signal that is transmitted via BLE to a remote station where it is displayed in real-time and uploaded to an online repository for future analysis. The authors tested the performance of the system when individuals performed activities like talking and walking. In [23] authors developed a system detecting sleep disorders such as respiratory flow repetitive cessations during sleep using a magnetometer sensor placed onto the body detecting millimetre night-time breathing movements by measuring the change in the magnetic vectors. The developed system includes a noninvasive wearable sensor, a wireless BLE module and a low-power microcontroller.

Table 1 gives a summary of all mono-sensing RHMS based BLE system.

Multi-sensing RHMS. This subsection analyzes related works about RHMS that sense and collect physiological informations from more than one physiological sensor.

- **Cardiovascular RHMS Using Multi-sensing:** Authors in [30] designed an epidermal patch, which is called Chem-Phys that offers simultaneous real-time monitoring of a biochemical (lactate) and an electrophysiological signal (electrocardiogram) for fitness monitoring. Besides that, for monitoring the cardiovascular disease authors in [31] designed wearable devices such as ECG and heart

Table 1. Recapitulative table related to monosensing RHMS based BLE.

Ref and date	Sensors	Placement	Applications
[16] 2016	ECG	Arm	Wearable Noncontact Armband for Mobile ECG Monitoring System
[17] 2014	SpO2	Finger	Oxygenated hemoglobin in the blood
[18] 2015	Weight	Outside the body	Low power and smart Bluetooth scale for weight monitoring.
[19] 2017	Strain	Fabric stretch sensor attached to the clothes	-Muscle activity Monitoring and body motion recognition
[20] 2019	EMG	Lower leg, the gastrocnemius muscle	Real time monitoring of muscle attached to the clothes
[21] 2018	EEG	Scalp	Brain activity Monitoring
[22] 2018	PPG	Stomach movement	Respiratory rate monitoring

rate that can be integrated into clothes or attached directly to the human body. In addition, Li Jinming and all. [26] proposed a multi-parameter cardiac remote monitoring system based on ECG, pulse rate and heart sound sensed data. This system is composed of a multi-channel physiological parameter acquisition unit, an Android terminal, a cloud server and a Bluetooth Low Energy BLE protocol for data communication. Besides that, [29] introduced heart-monitoring system evaluating the heart conditions based on sensed data from several wearable devices such as heart rate, blood pressure, body and skin temperature. The sensed patient information are transmitted to a smartphone (running an Android application) by the low energy protocol BLE and then will be visualized on the Web application. According the authors, evaluation of the developed monitoring system under expert's supervision for 40 individuals (aged between 18 and 66 years) showed that the proposed system is convenient and reliable generating warning messages to the doctor and patient under critical circumstances.

- *Diabete Chronic Condition Monitoring Using Multi-sensing:* Muhammad Syafrudin and all. [27] developed a healthcare monitoring system wich utilizing BLE based sensors to control the personal vital signs data such as heart rate, blood glucose, and blood pressure to support diabetic patients to manage individually their chronic condition. The BLE used in this system to transmit patient's health information from sensors to the smartphone, while to manage the sensor data by utilizing the real-time data processing, which used the Apache Kafka as a platform and MongoDB as a database for storing the patient's informations.

- *A Wearable Human Healthcare Monitoring System:* proposed by [19] supervising personal's information such as body temperature, heart rate, and blood oxygen saturation. The sensing node is wearable, miniaturized and based on the microchip CC2538 and Contiki OS. The sensed data are transmitted via a BLE communication interface to a mobile application. These data are stored on cloud server using the MQTT protocol and analyzed via the data

mining approaches to diagnose user's health status. In addition, authors in [28] designed a low-cost healthcare monitoring IoT-based system with the Fog layer sensing vital signs such as ECG, body temperature, and the respiration rate and contextual data (i.e. humidity and environment temperature).

- **Chronic Respiratory Monitoring Using Multi-sensing:** James and all. [22] developed BLE-based RHMS to monitor chronic respiratory disease that sense multi-parameters. The system comprises a chest patch and a wristband. The chest patch sensors corresponds to ECG, PPG, motion and acoustic signal. The wristband sensors track ozone exposure, ambient relative humidity, ambient temperature, PPG and motion. The data from each sensor is transferring by BLE communication interface to the server for storage.

3 BLE Communication Protocols

3.1 Basic Concepts

Bluetooth v4.0 known as Bluetooth Low Energy is ideal for applications requiring sporadic or periodic transfer of small amounts of data. Thus, BLE is well suited for sensors, actuators and other small devices requiring low power consumption. BLE works well with high numbers of communication nodes with limited latency requirements, very low power consumption and short connection times and wake-up. BLE aims to provide the same communication range as classic Bluetooth while consuming less power. The most significant differences between BLE and Classic Bluetooth are (1) the BLE has a lower data rate, (2) BLE use just 40 channels (37 for data and 3 for advertising) instead of 79, (3) no support for audio and (4) simplified state machines. Both BLE and Classic Bluetooth, operates in the 2.4 GHz ISM (industrial scientific and medical) frequency band, precisely BLE frequency band range from 2.402 GHz to 2.480 GHz. To minimize the overlapping with other IEEE 802.11 channels, the three advertisement channels (37, 38, and 39) centered on 2,402 GHz, 2,426 GHz and 2,480 GHz. Advertising is a process required for devices to find each other. At the link layer BLE device, function as a state machine with four states: standby, scanning (master procedure), advertising (slave procedure), initiating and connection. Furthermore, BLE operates in piconets wit a star topology. The central node is the master and all other nodes in the piconet are slaves. BLE has an architecture client/server which the client can be the Master such as smartphone, gateway, etc and the server is the peripheral such as sensors.

The connection establishment occurs after sending connection request packet which handle connection parameters (connection interval, slave latency and supervision timeout).

- **Connection interval:** corresponds to the time elapsed between two connection events. BLE devices are communicating only in connection events to save energy. So bigger interval between those events will save more energy but decrease data rate. No matter if device has data to send, it has to wait until next connection event. The interval can be set from 7.5 ms to 4 s.

- **Slave latency:** is the number of connection events, that sensor node can skip to save energy without the risk of disconnected.

- **Connection supervision timeout:** specifies the maximum time between two valid data received before a connection is lost.

The master coordinates the MAC using a TDMA scheme, determines the instants in which slaves are required to listen, and provides them with the map of data channels to be used.

3.2 BLE Protocols Stack

BLE protocol stack involves two main elements: the controller and the Host. The Controller includes the physical layer and the link layer. Both implemented on a single chip with an integrated radio interface. The Host runs on an application processor. It covers five upper layer functionalities (the Logical Link Control and Adaptation Protocol (L2CAP), the Attribute Protocol (ATT), the Generic Attribute Profile (GATT), the Security Manager Protocol (SMP) and the Generic Access Profile (GAP). The standardized Host Controller Interface (HCI) provides the exchange between the Host and the Controller. An application layer can be developed on the top of the Host.

- **L2CAP:** acts as an interface between the link layer and the Upper layer protocols (ATT, SMP and Link Layer control signaling). It multiplexes, segments, reassembles data packets and offers support quality of service management.

- **ATT:** is a client/server stateless protocol based on attributes presented by a device. Each server holds data organized in the form of attribute managed by the GATT. Universally unique identifier (UUID), a set of permissions and a value identify each attribute (see Fig. 2).

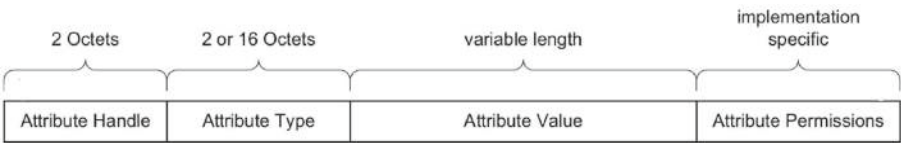


Fig. 2. Attribute representation.

- **SMP:** offers security services for protecting the information exchange between two connected peers. It allows the generation and the exchange of security keys and it hide the public Bluetooth Address if required.

- **GATT:** defines the GATT server and the GATT client and specifies the framework and operations for data transfer procedures over a BLE connection. A GATT client requests and receives data from a GATT server, whose makes the

data available to the GATT client. Data is structured in sections called services that assembles related pieces of user data known as characteristics.

- **GAP:** outlines rules and concepts to standardize the low-level operation of devices. It defines how devices perform control procedures such as device discovery, security establishment and connection...to guarantee interoperability between devices from different vendors.

4 Reading Sensed Physiological Signs with BLE

The most difficult task confronted during mobile healthcare application development is sensed data reading. In this paper, we use BLE to get data from sensors and forward them to the PDA. In general, we develop an application for Android device (PDA: mobile phone) to get data from sensors. The complexity resides in the diversity of health devices (thermometer, heart-rate monitor, blood pressure monitor, scale . . .), where each device has a specific profile, services, UUID, characteristics, and descriptors. Therefore, to read measured data from sensors, we need to develop a specific application for each profile. In this paper, we describe two health devices equipped with the BLE corresponding respectively to Health Thermometer and Blood Pressure Monitor.

4.1 Example of Services and Characteristics of HDP

In order to standardize the way medical data is transmitted over BLE technology, the Bluetooth Special Interest Group (SIG) released in 2008 the Health Device Profile (HDP) that utilizes the IEEE 11073-20601 Data Exchange Protocol as the transport content. Below the specification of the service and characteristic of the studied health devices which according to the SIG group.

Thermometer:

(1) *Health Thermometer Service:* (UUID = 0x1809; Definition: This service exposes temperature and other data from a Health Thermometer Sensor;

Type = org.bluetooth.service.health-thermometer),

(2) *Temperature Measurement Characteristic* (UUID = 0x2A1C; Definition: This characteristic is used to send a temperature measurement;

Type: org.bluetooth.characteristic.temperature measurement).

SPO2:

(1) *Health PulseOximeter Service:* (UUID = 0x1822; Definition: This Service exposes pulse oximetry data related to a non-invasive pulse oximetry sensor for consumer healthcare applications; Type = org.bluetooth.service.pulse-oximeter),

(2) *PLX Continuous-Measurement* (UUID = 0x2A5F; Definition: This characteristic is used to send a PulseOximetre measurement;

Type: type = org.bluetooth.characteristic.plx-continuous-measurement).

Developers can obtain the services and characteristics of any BLE health device from the main Bluetooth webpage [24].

4.2 Steps for Reading Sensed Data on Mobile App

The development of a Mobile App able to read BLE sensed data can be resumed by the following steps:

Step 1: Declaring permission on a manifest file is required to use BLE features and to perform BLE communication toward requesting or accepting connection or reading the different measurements.

Step 2: Assigning UUID for service and characteristic as declared in the previous subsection.

Step 3: Checking that BLE is supported on the PDA and enable it.

Step 4: Turning On the Bluetooth and displaying dialogue box on the PDA that asking for permission from the user to turn on Bluetooth.

Step 5: Scanning and visualizing nearby BLE health devices and their addresses on the PDA.

Step 6: Connecting to a GATT server on health device to manage the connection and to send data using the `connectGatt()` method that requires as parameters (a Context object, `autoConnect` and a reference to a `BluetoothGattCallback`). The `BluetoothGattCallback` is used to deliver GATT client operations to the client (Mobile App on the PDA).

Step 7: Discovering, reading and displaying GATT services and characteristics by controlling the device activity (`DeviceControlActivity`).

Step 8: Reading Sensed Data (for example: temperature). Thus, we set notification or indication value on Temperature Measurement Characteristic then write to the descriptor to set the right value for characteristics. The updates from the health device on characteristics value will be posted on the next callback using `onCharacteristicChanged`.

Developers can get detailed description and example of codes from the main android (section Bluetooth connectivity) webpage [25].

We recapitulate the different steps required for enabling a mobile App to get sensed data from health devices in Fig. 3.

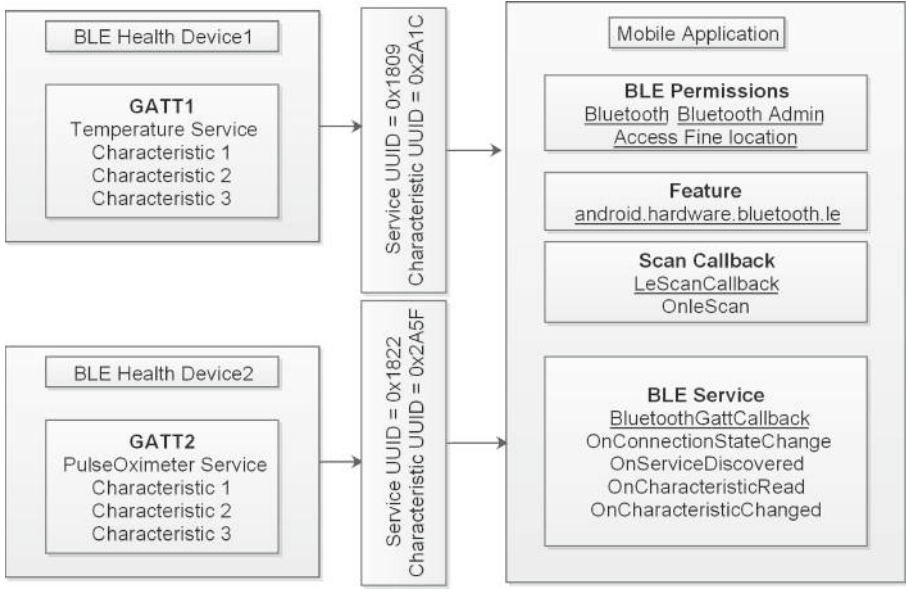


Fig. 3. Required components for android BLE communication.

5 Conclusion

In this paper, we provided a detailed study related to RHMS based on BLE communication. We notice that several RHMS based BLE was developed and tested for different physiological signs, accordingly, in this paper, we studied and highlighted different mono and multi-sensing RHMS using BLE communication interfaces for physiological signs sensing. Besides that, we overviewed BLE communication in a comprehensive way to help readers and mobile app developers to understand the basic concepts of BLE communication. Furthermore, we detailed the different steps required for enabling sensor-side control and BLE communication on an android system as the mobile platform for the health sensor's client application. We limited our investigation to sensed data reading. In an extended version of this work, we will provide a whole prototype that could be tested beyond the development environment and providing several vital signs monitoring (remote control, data visualization graphically) and decision making through the processing of sensed vital signs.

References

1. Movassaghi, S., Abolhasan, M., Lipman, J., Smith, D., Jamalipour, A.: Wireless body area networks: a survey. *IEEE Commun. Surv. Tutorials* **16**(3), 1658–1686 (2014)

2. Manirabona, A., Fourati, L.C.: A 4-tiers architecture for mobile WBAN based health remote monitoring system. *Wireless Netw.* **24**(6), 2179–2190 (2017). <https://doi.org/10.1007/s11276-017-1456-7>
3. Fourati, H., Khssibi, S., Val, T., Idoudi, H., Van den Bossche, A., Saidane, L.A.: Comparative study of IEEE 802.15. 4 and IEEE 802.15. 6 for WBAN-based CANet, November 2015
4. Iova, O., Theoleyre, F., Watteyne, T., Noel, T.: The love-hate relationship between IEEE 802.15. 4 and RPL. *IEEE Commun. Mag.* **55**(1), 188–194 (2016)
5. Ahmed, N., Rahman, H., Hussain, M.I.: A comparison of 802.11 ah and 802.15. 4 for IoT. *ICT Express* **2**(3), 100–102 (2016)
6. Tennina, S., Gaddour, O., Koubâa, A., Royo, F., Alves, M., Abid, M.: Z-monitor: a protocol analyzer for IEEE 802.15. 4-based low-power wireless networks. *Comput. Netw.* **95**, 77–96 (2016)
7. Astrin, A.: IEEE Standard for Local and metropolitan area networks part 15.6: Wireless Body Area Networks. *IEEE Std 802.15. 6* (2012)
8. Mile, A., Okeyo, G., Kibe, A.: Hybrid IEEE 802.15. 6 wireless body area networks interference mitigation model for high mobility interference scenarios. *Wireless Eng. Technol.* **9**(02), 34 (2018)
9. Zhao, B., Lian, Y., Niknejad, A.M., Heng, C.H.: A low-power compact IEEE 802.15. 6 compatible human body communication transceiver with digital sigma-delta IIR mask shaping. *IEEE J. Solid-State Circ.* **54**(2), 346–357 (2018)
10. Sarkar, S., Misra, S., Bandyopadhyay, B., Chakraborty, C., Obaidat, M.S.: Performance analysis of IEEE 802.15. 6 MAC protocol under non-ideal channel conditions and saturated traffic regime. *IEEE Trans. Comput.* **64**(10), 2912–2925 (2015)
11. Salehi, S.A., Razzaque, M.A., Tomeo-Reyes, I., Hussain, N.: IEEE 802.15. 6 standard in wireless body area networks from a healthcare point of view. In: *IEEE, 22nd Asia-Pacific Conference on Communications (APCC)*, pp. 523–528, August 2016
12. Liu, H., et al.: Performance assessment of IR-UWB body area network (BAN) based on IEEE 802.15. 6 standard. *IEEE Antennas Wirel. Propag. Lett.* **15**, 1645–1648 (2016)
13. Sherratt, R.S., Janko, B., Hui, T., Harwin, W., Diaz-Sanchez, D.: Dictionary memory based software architecture for distributed bluetooth low energy host controllers enabling high coverage in consumer residential healthcare environments. In: *2017 IEEE International Conference on Consumer Electronics (ICCE)*, pp. 406–407. IEEE, January 2017
14. Şişman, C., Sağır, S., Kaya, İ., Ünal, S., Baltacı, Y.: Coding and diversity gains of low power radio communications: BLE and ZigBee. In: *2018 41st International Conference on Telecommunications and Signal Processing (TSP)*, pp. 1–4. IEEE, July 2018
15. Santos, D.F., Gorgônio, K.C., Perkusich, A., Almeida, H.O.: A standard-based and context-aware architecture for personal healthcare smart gateways. *J. Med. Syst.* **40**(10), 224(2016)
16. Rachim, V.P., Chung, W.Y.: Wearable noncontact armband for mobile ECG monitoring system. *IEEE Trans. Biomed. Circuits Syst.* **10**(6), 1112–1118 (2016)
17. Huang, C.Y., Chan, M.C., Chen, C.Y., Lin, B.S.: Novel wearable and wireless ring-type pulse oximeter with multi-detectors. *Sensors* **14**(9), 17586–17599 (2014)
18. Huang, Q., Chen, K.: The implementation of wireless scale based on the Bluetooth 4.0 low-energy. In: *2015 International Industrial Informatics and Computer Engineering Conference*. Atlantis Press, March 2015

19. Vu, C., Kim, J.: Muscle activity monitoring with fabric stretch sensors. *Fibers Polym.* **18**(10), 1931–1937 (2017). <https://doi.org/10.1007/s12221-017-7042-x>
20. Liu, S.H., Lin, C.B., Chen, Y., Chen, W., Huang, T.S., Hsu, C.Y.: An EMG patch for the real-time monitoring of muscle-fatigue conditions during exercise. *Sensors* **19**(14), 3108 (2019)
21. O'Sullivan, M., et al.: Neonatal EEG interpretation and decision support framework for mobile platforms. In: 2018 40th Annual International Conference of the IEEE Engineering in Medicine and Biology Society (EMBC), pp. 4881–4884. IEEE, July 2018
22. Mukhopadhyay, B., Sharma, O., Kar, S.: IoT based wearable knitted fabric respiratory monitoring system. In: 2018 IEEE SENSORS, pp. 1–4. IEEE, October 2018
23. Milici, S., Lázaro, A., Villarino, R., Girbau, D., Magnarosa, M.: Wireless wearable magnetometer-based sensor for sleep quality monitoring. *IEEE Sens. J.* **18**(5), 2145–2152 (2018)
24. Bluetooth Homepage. <https://www.bluetooth.com/specifications/gatt/characteristics/>. Accessed 09 Feb 2020
25. Android Homepage. <https://developer.android.com/guide/topics/connectivity/bluetooth-le/>. Accessed 09 Feb 2020
26. Jinming, L., Cheng, Z., Yinlong, L., Yihe, W.: Multi-parameter cardiac remote monitoring system based on Android. *J. Excellence Comput. Sci. Eng.* **2**(2), 18–24 (2016)
27. Alfian, G., Syafrudin, M., Ijaz, M.F., Syaekhoni, M.A., Fitriyani, N.L., Rhee, J.: A personalized healthcare monitoring system for diabetic patients by utilizing BLE-based sensors and real-time data processing. *Sensors* **18**(7), 2183 (2018)
28. Gia, T.N., Jiang, M., Sarker, V.K., Rahmani, A.M., Westerlund, T., Liljeberg, P., Tenhunen, H.: Low-cost fog-assisted health-care IoT system with energy-efficient sensor nodes. In: 2017 13th International Wireless Communications and Mobile Computing Conference (IWCMC), pp. 1765–1770. IEEE, June 2017
29. Kakria, P., Tripathi, N.K., Kitipawang, P.: A real-time human-health monitoring system for remote cardiac patients using smartphone and wearable sensors. *Int. J. Telemed. Appl.* **2015** (2015)
30. Imani, S., et al.: A wearable chemical–electrophysiological hybrid biosensing system for real-time health and fitness monitoring. *Nat. Commun.* **7**(1), 1–7 (2016)
31. Pigini, L., et al.: Pilot test of a new personal health system integrating environmental and wearable sensors for telemonitoring and care of elderly people at home (SMARTA project). *Gerontology* **63**(3), 281–286 (2017)

Open Access This chapter is licensed under the terms of the Creative Commons Attribution 4.0 International License (<http://creativecommons.org/licenses/by/4.0/>), which permits use, sharing, adaptation, distribution and reproduction in any medium or format, as long as you give appropriate credit to the original author(s) and the source, provide a link to the Creative Commons license and indicate if changes were made.

The images or other third party material in this chapter are included in the chapter's Creative Commons license, unless indicated otherwise in a credit line to the material. If material is not included in the chapter's Creative Commons license and your intended use is not permitted by statutory regulation or exceeds the permitted use, you will need to obtain permission directly from the copyright holder.





Modeling and Specification of Bootstrapping and Registration Design Patterns for IoT Applications

Mohamed Hadj Kacem^(✉), Imen Tounsi, and Najeh Khalfi

ReDCAD laboratory, University of Sfax, Sfax, Tunisia
mohamed.hadjkacem@isimsf.rnu.tn, imen.tounsi@redcad.org
<http://www.redcad.org/members/hadjkacem/>,
<http://www.redcad.org/members/imen.tounsi/>

Abstract. The architectures of software systems are becoming more complex, large, and dynamic. The design of these architectures allows architects to master building complex software systems. But, their informal description, may give rise to ambiguity, their understanding becomes more and more difficult and leads to the incorrect implementation of these software systems. There are many solutions allowing software architecture design. In this paper, we use software design patterns as a solution. This is due to their reusable software elements. Our principal objective is to propose other alternatives to the informal visual description of software architectures. In past work, we have studied Service Oriented Architectures. We used SOA design patterns with standard formal notations. This work is a continuation to the past one. We apply our approach on design patterns for the Internet of Things. We introduce a refinement-based approach for modeling IoT design patterns. It takes advantage of graphical modeling and formal method. It is organized around two main axes. The first axis is to provide modeling solutions in conformance with the UML standard language. The second axis covers the general specification of design pattern models with the Event-B method. As a result, we propose a design support tool for IoT architectures based on IoT design patterns. It allows modeling of correct-by-design software systems.

Keywords: Design patterns · UML modeling · Event-B method · Pattern modeling · Formal specification

1 Introduction

The Internet of Things (IoT) is a complex domain of application that allows objects to exist on the Internet. Creating systems in this domain is a challenge because it involves both software and hardware, sensing and actuating devices, a communication infrastructure, in addition to storage constraints. For this, a variety of IoT design patterns have been proposed in various categories to address variety of issues [7]. They propose solutions for common and recurring

problems to architects and designers in the IoT domain. Most of these patterns are presented visually and informally, there is no formal semantics associated with them. Hence, their meanings may be imprecise. They can lead to their misunderstanding and misuse.

To remedy this problem, we propose an approach that allows to model and specify these patterns with a formal notation that allows to reuse them correctly. Our objective is to prove the relevance of these patterns. We illustrate our approach with different pattern examples. We propose a graphical modeling of these patterns in order to describe both their structural and behavioral features. Then, we propose a generic formal specification of these patterns using the formal Event-B method. Finally, we develop a graphical editor describing our approach using the Eclipse modeling platform.

The rest of this paper is organized as follows. Section 2 focuses on the structural modeling of IoT design patterns and Sect. 3 focuses on the behavioral modeling. In Sect. 4, we present an application to a case study of our approach. Section 5 describes how to formally specify IoT design patterns with the Event-B method. In Sect. 6, we present our tool, which implements the proposed approach. Section 7 discusses related work. Section 8 concludes and gives future work directions.

2 Structural Patterns Modeling

We provide a modeling solution for describing IoT design patterns using a visual notation based on the graphical UML language in order to give readable models. We first describe a meta-model, then we present a model instance of the design pattern. The metamodel extends the component diagram of UML 2.0 (Unified Modeling Language). The use of UML is motivated by four distinct rationales: (i) It is a standard modeling language defined by OMG. (ii) It is used to describe software architectures. (iii) Component diagrams of UML allow us to represent structural features of patterns. (iv) Sequence diagrams of UML allow us to represent behavioral features of patterns.

Structural features of patterns are generally specified by the types of entities. The configuration of the entities is also described in terms of static relationships between them [16]. We model structural features of design patterns with the extended *Component* diagram. In the following, we present the proposed meta-model. An example of a corresponding model is presented and illustrated with case studies as follows.

2.1 Metamodel

The extended *Component* diagram describes, by a set of concepts, the structure of an IoT architecture. We use it to describe the architecture of IoT design patterns. More specifically, it is to define the entities that can be involved in the pattern, their types and their dependencies (connections). The metamodel presented in Fig. 1 extends the metamodel of the component diagram of UML

2.0. In this metamodel, we concentrate on two categories of design patterns; “Bootstrapping Design Patterns” and “Registration Design Patterns”.

“Bootstrapping Design Patterns” allow configuring new devices. They are composed of “Medium Based Bootstrap Pattern” and “Remote Bootstrap Pattern”. “Medium Based Bootstrap Pattern” allows to configure a new device on-site through a removable storage medium inserted in the device. This support contains the necessary information for configuration. “Remote Bootstrap Pattern” is a configuration pattern used in case that a device is placed far away and is difficult to reach. The configuration in this case is done by downloading configuration information from a bootstrap server.

“Registration Design Patterns” allow to register the attributes and the features of a new device on the Back-end server. The registration is used to facilitate the communication and the interrogation with other connected objects. There are many registration patterns. In this work, we present two patterns. So “Registration Design Patterns” are composed of “Automatic Client Driven Registration Pattern” and “Server Driven Model Pattern”. The “Automatic Client Driven Registration Pattern” allows the device to register on the Back-end server via an API call. The “Server Driven Model Pattern” is used to create a device model that includes its description and functionality.

The basic elements of the metamodel are:

Component and Object: Entities, that make up the architecture of an IoT design pattern, can be either *Components* or *Objects*. All objects are components, but not all components are necessarily objects. An object can be connected to the internet, it can receive and send data.

Port: Entities can have *Ports* that constitute interaction points with their environment. These *Ports* are related to one or more *provided* or *required Interfaces*.

Interface: The interfaces are the points of communication that allow interaction with the environment. For an entity, there are two types of interfaces. The *Provided Interfaces* describe the services provided by the component. The *Required Interfaces* describe the required services that other components must provide for the good functioning of component. These interfaces are specified via the ports.

Connector: The communication path between Entities within an architecture is called a *Connector*. It ensures the link between a *Provided* port and a *Required* port to form a complete and coherent system.

Device: A device is an Object. It is the entry point of the physical environment, it is used to process sensor data and to control actuators.

2.2 General Pattern Model

In this section, we present two general pattern models as instances of the proposed metamodel. We have used different notations that can be used as a graphical description of the entities presented in the model. We are based on the work of Reinfurt et al. [8].

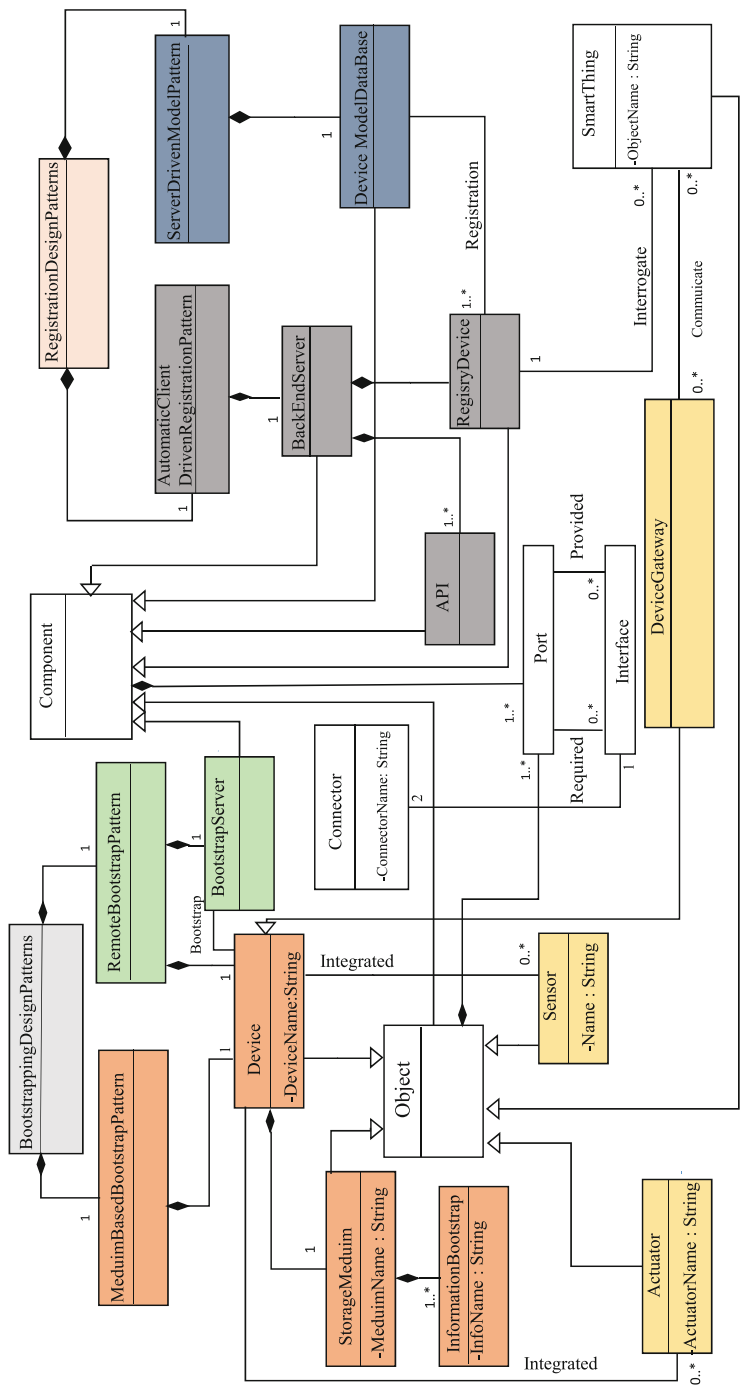


Fig. 1. Metamodel of IoT design patterns

There are two possible general models depending on the location of the device. If the device is placed locally, we use the “Medium Based Bootstrap Pattern” as a solution to configure the new device. If it is placed at a distance, we use the “Remote Bootstrap Pattern” as a solution. In Fig. 2, we represent the general pattern model of the “Medium Based Bootstrap Pattern”. The solution proposed by this pattern to configure a new local device is to use an object of type *Storage Medium* containing information configuration. In Fig. 3, we represent the general pattern model of the “Remote Bootstrap Pattern”. The solution proposed by this pattern to configure a new remote device is to use a component of type *BootstrapServer* allowing the upload of the configuration information using the *PushBD* connector.

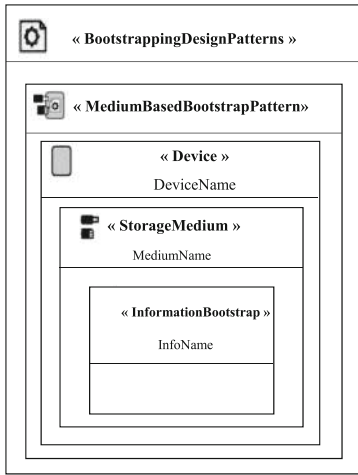


Fig. 2. General pattern model of the Medium Based Bootstrap Pattern

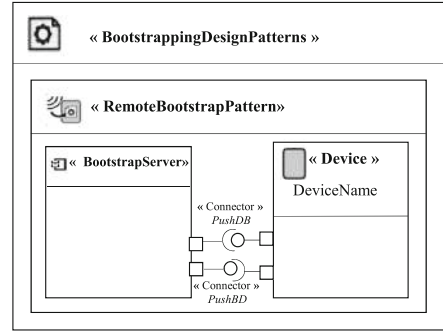


Fig. 3. General pattern model of the Remote Bootstrap Pattern

In Fig. 4, we represent the general pattern model of the “Registration Design Pattern”. The solution proposed by this pattern to register a new device. The device is related to the *BackEndServer* with a connector named *PushDA* in order to be registered on it via an *API* call. Meta-data entered by the device are recorded in the *RegistryDevice* through the *PushAR* connector. The *RegistryDevice* component has a connector named *PushRDM* to store a device template in a database component named *Device Model DataBase* of the “Server Driven Model pattern”. A device can integrate an object of type *Sensor* or an *Actuator*. All objects of the patterns have ports to communicate with others.

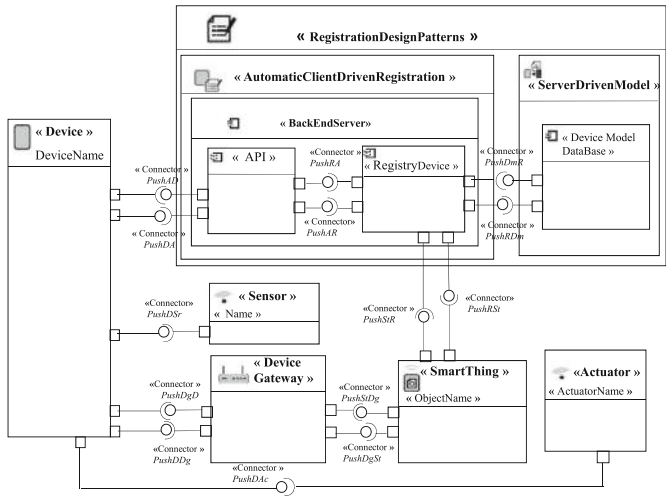


Fig. 4. General pattern model of the Registration Design Pattern

3 Behavioral Patterns Modeling

To model behavioral features of the design patterns, we use the UML 2.3 sequence diagram. We describe through this diagram successive interactions between the different entities of the IoT application in order to represent the two categories of the design patterns. Figure 5 represent the sequence diagram that illustrates this behavior. We grouped the interactions into two phases.

- **Configuration phase:**
 - **Local configuration:** In the configuration phase and at the “Medium Based Bootstrap Pattern” level, the configuration is done by cutting the storage medium configuration information (*Storage Medium*) to the device.
 - **Remote configuration:** The configuration at the “Remote Bootstrap Pattern” is done by downloading information from a *Bootstrap Server* to the device.
- **Registration phase:** In the registration phase, the device triggers a registration process on the *Back-end Server*. After the registration, the metadata provided by the device are registered in the *RegistryDevice*. Subsequently, an instance of the model of this device is stored in a *Device Model Database*.

If the device, go through the configuration and the registration phases, it becomes able to create communication links with other connected objects. The exchange of messages between them is done through a communication intermediary (*Device Gateway*). A connected object (smart thing) can interact directly with the *RegistryDevice* to retrieve information about a device if it is offline.

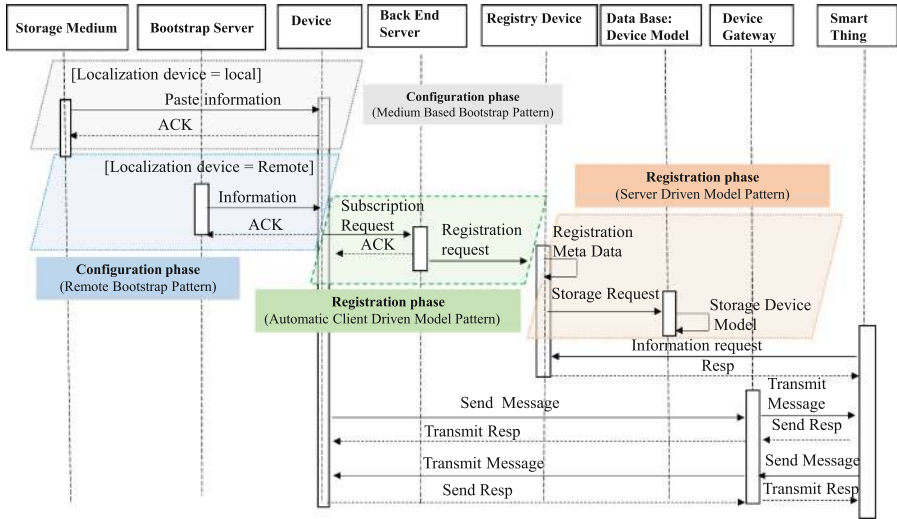


Fig. 5. Sequence diagram of the used IoT patterns

4 Case Study: Smart Home

To validate our approach, we chose to apply a case study in the IoT application domain called “Smart Home”.

A smart home is usually made up of remote-controlled automated components which can be doors, windows, lamps, etc. It can include several other components that can be monitored and controlled remotely. Most of these components can be controlled by a mobile device or a computer. In our case study, we add a new device (a camera) to a smart home. This device makes it possible to control the various rooms of the house. For example, if a door or a window left open, the camera informs the user immediately through a notification sent to their smartphone. It can also send alerts when it detects unknown faces.

First, the camera is added without any information to initiate its first connection. We then apply the Meduim Based Bootstrap design pattern to have its configuration information. This information is inserted into the device through a memory card. Second, we go through the registration procedure on the main server (BackEndServer). This procedure is done through the use of the two patterns of the Registration Design Patterns category which are the automatic client driven registration pattern and the server driven model pattern which allow registering the device on the main server. Finally, the camera became able to communicate and create connection links with its communication partners. The camera communicates with the user's smartphone to notify him of what is happening in real-time.

We model this application through the use of the model shown in Fig. 6. The camera is associated with an object of type “Device”, the memory card is defined as an object of type “Storage Medium” and the Smart phone is associated as

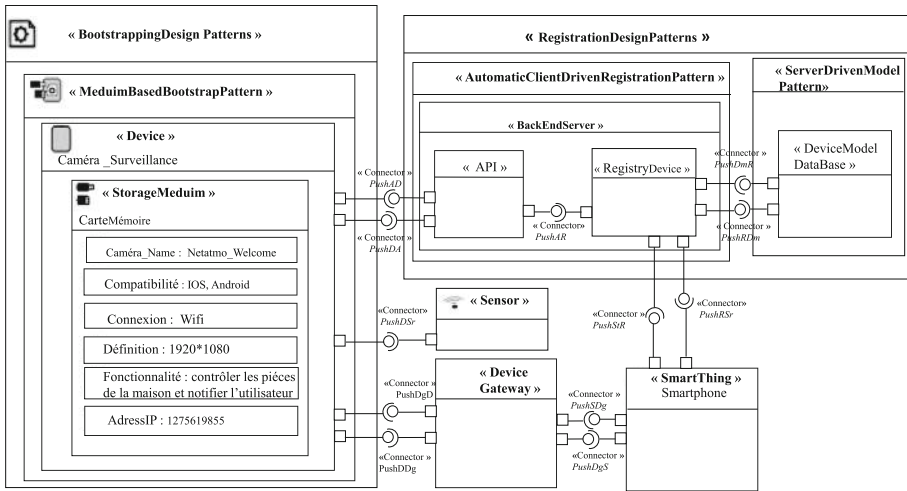


Fig. 6. Smart home case study

an object of type “SmartThing”. The propagation of events between objects is done through a *DeviceGateway*.

5 Patterns Specification

UML, as semi-formal language offers several benefits to the definition of IoT design patterns, such as visual and standard notation. This graphical aspect is certainly interesting and useful to an architect, in the sense that graphic design is easy. However, the fact that UML lack a precise semantics is a serious drawback because this language did not allow checks which we must carry. So, pattern models generated at the modeling approach can be ambiguous and imprecise. In addition, during the modeling phase, the architect can easily fall into the error. This is due to the absence of a precise formal semantics of UML that do not provide rigorous tools for verification and proof. However, any error or any bad modeling of a design pattern can cause serious problems that generate bad consequences.

Thus, ensuring the reliability and the correctness of IoT design patterns is a goal that we have fixed. For this, we propose an approach to formally specify design patterns by using the formal method Event-B that is well suited to our needs and goals. Thus, each diagram graphically modeled will be accompanied by a formal semantics. This approach allows the validation of the modeling part and ensure the verification of the relevant properties of design patterns.

Event-B method is well-suited for specifying IoT design patterns: (i) The primary concept in doing formal developments in Event-B is that of a model. It is made of several components of two kinds: machines and contexts. Machines contain the dynamic parts of a model, whereas contexts contain the static parts

of a model [1]. Thanks to this classification, Event-B allows the specification of structural and behavioral features of design patterns. (ii) Refinement techniques proposed by this method allow us to build patterns gradually and at different abstraction levels. (iii) Mathematical proofs allow verifying model consistency and consistency between refinement levels. (iv) The most important reason to use Event-B method is the availability of a supporting tool called the Rodin platform [2]. It is an Eclipse-based tool set that provides effective support for modeling and automated proof. The platform is open source and is further extendable with plug-ins. A range of plug-ins have already been developed including ones that support animation and model checking like the Prob plug-in [5] that we used.

Extended *Component* diagram that model structural features of design patterns are transformed to a context in the Event-B method in which we specify entities of the architecture and their relations. The *Sequence* diagram is transformed into a machine in Event-B in which we specify events made between entities of the patterns. This transformation is proposed in order to attribute formal notations to IoT design patterns for the purpose of checking their design correctness in a second step. We explicitly defined a refinement strategy to follow. This strategy is interesting because it defines the pattern development process and improves the quality of the obtained models, and therefore the success of the formal development process. We defined specification levels by using a step-wise development approach.

6 Tool Support

We developed a graphical modeling tool that implements our approach; it ensures an easy and efficient modeling way for users. With our tool, we aim to make concrete the aforementioned concepts. The architect can model the solution of the IoT design patterns using an Eclipse plug-in that we propose. The tool, in its development, is based on EMF¹ (*Eclipse Modeling Framework*) [10]. This was chosen since we use models, which are basic building units, to develop our approach (Fig. 7).

7 Related Work

Research connected to design patterns in the field of software architecture, are mainly classified into four branches of work according to their architectural style. The first is about design patterns for Object-Oriented Architectures, the second is about design patterns for Enterprise Application Integration (EAI), the third is for Service Oriented Architectures (SOA) and the fourth one is for connected object architectures.

Most of the proposed design patterns are described with a combination of a text description and a graphical representation sometimes using a proprietary notation in the aim of making them easy to understand. However,

¹ https://wiki.eclipse.org/Eclipse_Modeling_Framework.

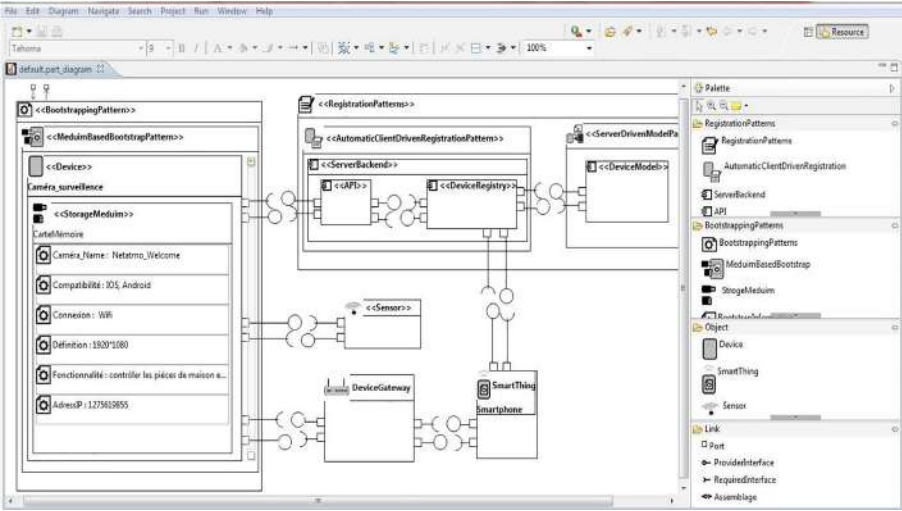


Fig. 7. The tool editor

these descriptions make patterns ambiguous and may lack details. Some work so have proposed the semi-formal representations of these patterns using modeling languages [4]. Some other works use or provide formal languages based on mathematical notation for a precise pattern specification [16]. However, these approaches require knowledge of mathematics and first order logic to use them. Some research has chosen to combine the semi-formal and formal representations of patterns. This representation ensures a better understanding and precision of patterns. Generally speaking, there is a consensus on the elements that make up and define a design pattern. However, there is no consensus on the specification of the patterns.

In past work [11,13] we focused on both the modeling, the formal specification and the composition of SOA design patterns [12,14] and established the link between them with an automatic transformation [15]. We used the SoaML language for the pattern modeling that ease the understanding of pattern models. For the pattern specification, we used the Event-B formal method in order to attribute formal notations to SOA design patterns for the purpose of checking their design correctness.

In this work, we are interested with the IoT design patterns. In this context we find several researchers who proposed a set of IoT design patterns in various categories. Eloranta et al. [3] proposed patterns for the construction of distributed control systems. Qanbari et al. [6] presented four patterns for the supply, deployment, orchestration and monitoring shipboard applications. Reinfurt et al. [7,9] have published patterns for device power supply, operation and communication modes and a number of IoT design models. All these patterns are described with a visual and informal notation. There is no formal

semantics associated. There is no research work that deals with the modeling of IoT patterns. In this paper, we present the modeling of IoT design patterns proposed by Reinfurt et al. [7].

8 Conclusions

In this paper, we presented an approach that allows to model and specify connected object architecture design patterns. In particular modeling the “Bootstrapping Design Patterns” category and the “Registration Design Patterns” category. The modeling phase consists of presenting models of the design patterns in order to present a meta-model that presents an abstract view of a model of the patterns. Subsequently, we described the structural and behavioral features of the pattern. Then, we formally specified these design patterns using the formal Event-B method. Finally, we developed a plug-in under the Eclipse Modeling platform that offers a graphical editor for modeling IoT design patterns. Currently, the transition from the SoaML modeling to the formal specification is achieved manually, we are working on automating this phase by implementing transformation rules.

References

1. Abrial, J.R.: Modeling in Event-B: System and Software Engineering, 1st edn. Cambridge University Press, New York (2010)
2. Abrial, J.R., Butler, M., Hallerstede, S., Hoang, T., Mehta, F., Voisin, L.: Rodin: an open toolset for modelling and reasoning in event-B. *Int. J. Softw. Tools Technol. Transf.* **12**(6), 447–466 (2010)
3. Chandra, G.S.: Pattern language for IoT applications. In: PLoP Conference, USA (2016)
4. Dong, J., Alencar, P., Cowan, D.D., Sheng, Y.: Composing pattern-based components and verifying correctness. *J. Syst. Softw.* **80**, 1755–1769 (2007)
5. Leuschel, M., Butler, M.: ProB: a model checker for B. In: Araki, K., Gnesi, S., Mandrioli, D. (eds.) FME 2003. LNCS, vol. 2805, pp. 855–874. Springer, Heidelberg (2003). https://doi.org/10.1007/978-3-540-45236-2_46
6. Qanbari, S., et al.: IoT design patterns: computational constructs to design, build and engineer edge applications. In: 2016 IEEE First International Conference on Internet-of-Things Design and Implementation (IoTDI), pp. 277–282 (2016)
7. Reinfurt, L., Breitenbücher, U., Falkenthal, M., Leymann, F., Riegg, A.: Internet of things patterns for device bootstrapping and registration. In: Proceedings of the 22Nd European Conference on Pattern Languages of Programs, EuroPLoP 2017, pp. 15:1–15:27. ACM, New York (2017)
8. Reinfurt, L., Breitenbücher, U., Falkenthal, M., Leymann, F., Riegg, A.: Internet of things patterns for devices. In: Proceedings of the Ninth International Conferences on Pervasive Patterns and Applications (PATTERNS), pp. 117–126 (2017)
9. Reinfurt, L., Falkenthal, M., Breitenbücher, U., Leymann, F.: Applying IoT patterns to smart factory systems. Advanced Summer School on Service Oriented Computing, Summer SOC (2017)

10. Steinberg, D., Budinsky, F., Paternostro, M., Merks, E.: *EMF: Eclipse Modeling Framework 2.0*, 2nd edn. Addison-Wesley Professional (2009)
11. Tounsi, I., Hadj Kacem, M., Hadj Kacem, A.: An approach for modeling and formalizing SOA design patterns. In: *Proceedings of the 22nd IEEE International Conference on Enabling Technologies: Infrastructure for Collaborative Enterprises, WETICE 2013*, pp. 330–335. IEEE Computer Society, Hammamet, June 2013
12. Tounsi, I., Hadj Kacem, M., Hadj Kacem, A., Drira, K.: An approach for SOA design patterns composition. In: *Proceedings of the IEEE 8th International Conference on Service-Oriented Computing and Applications, (SOCA 2015)*, pp. 219–226. IEEE Computer Society, Rome, Italy, October 2015
13. Tounsi, I., Hadj Kacem, M., Hadj Kacem, A., Drira, K.: A refinement-based approach for building valid SOA design patterns. *IJCC, Int. J. Cloud Comput.* **4**(1), 78–104 (2015). <https://doi.org/10.1504/IJCC.2015.067705>
14. Tounsi, I., Hadj Kacem, M., Hadj Kacem, A., Drira, K.: Transformation of compound SOA design patterns. In: *The 8th International Conference on Ambient Systems, Networks and Technologies (ANT 2017)/The 7th International Conference on Sustainable Energy Information Technology (SEIT 2017)*, 16–19 May 2017, Madeira, Portugal, pp. 408–415 (2017)
15. Tounsi, I., Hrichi, Z., Hadj Kacem, M., Hadj Kacem, A., Drira, K.: Using SoaML models and Event-B specifications for modeling SOA design patterns. In: *Proceedings of the 15th International Conference on Enterprise Information Systems, ICEIS 2013*, Angers, France, pp. 294–301, July 2013
16. Zhu, H., Bayley, I.: Laws of pattern composition. In: Dong, J.S., Zhu, H. (eds.) *ICFEM 2010. LNCS*, vol. 6447, pp. 630–645. Springer, Heidelberg (2010). https://doi.org/10.1007/978-3-642-16901-4_41

Open Access This chapter is licensed under the terms of the Creative Commons Attribution 4.0 International License (<http://creativecommons.org/licenses/by/4.0/>), which permits use, sharing, adaptation, distribution and reproduction in any medium or format, as long as you give appropriate credit to the original author(s) and the source, provide a link to the Creative Commons license and indicate if changes were made.

The images or other third party material in this chapter are included in the chapter's Creative Commons license, unless indicated otherwise in a credit line to the material. If material is not included in the chapter's Creative Commons license and your intended use is not permitted by statutory regulation or exceeds the permitted use, you will need to obtain permission directly from the copyright holder.



Biomedical and Health Informatics



EEG-Based Hypo-vigilance Detection Using Convolutional Neural Network

Amal Boudaya^{1,2(✉)}, Bassem Bouaziz^{1,2(✉)}, Siwar Chaabene^{1,2}, Lotfi Chaari³, Achraf Ammar⁴, and Anita Hökelmann⁴

¹ Multimedia Information Systems and Advanced Computing Laboratory (MIRACL), University of Sfax, 3021 Sfax, Tunisia
amalboudaya71@gmail.com, Bassem.Bouaziz@isims.usf.tn, siwarchaabene@gmail.com

² Digital Research Center of Sfax, B.P. 275, 3021 Sakiet Ez Zit, Sfax, Tunisia

³ University of Toulouse, IRIT-ENSEEIH, Toulouse, France
lotfi.chaari@toulouse-inp.fr

⁴ Institute of Sport Science, Otto-von-Guericke University Magdeburg, 39104 Magdeburg, Germany
ammar.achraf@gmail.com, anita.hoekelmann@ovgu.de

Abstract. Hypo-vigilance detection is becoming an important active research areas in the biomedical signal processing field. For this purpose, electroencephalogram (EEG) is one of the most common modalities in drowsiness and awakesness detection. In this context, we propose a new EEG classification method for detecting fatigue state. Our method makes use of a and awakesness detection. In this context, we propose a new EEG classification method for detecting fatigue state. Our method makes use of a Convolutional Neural Network (CNN) architecture. We define an experimental protocol using the Emotiv EPOC+ headset. After that, we evaluate our proposed method on a recorded and annotated dataset. The reported results demonstrate high detection accuracy (93%) and indicate that the proposed method is an efficient alternative for hypo-vigilance detection as compared with other methods.

Keywords: Hypo-vigilance detection · EEG · CNN

1 Introduction

Hypo-vigilance has been one of the major causes of accidents in many areas such as driving [1], aviation [2] and military sector [3]. Hence, the drowsiness problem has gained great interest from researchers. This is today a real up to date problem within the current Covid-19 [4] pandemic where medical stuff is generally overlooked. In fact, the drowsy condition is expressed predominantly by the emergence of various behavioral signs such as heaviness in terms of reaction, reflex reduction, occurrences of yawning, heaviness of the eyelids and/or the difficulty of keeping the head in the frontal position relative to the field of

vision. Many studies [5–8] have been proposed to detect hypo-vigilance based on biomedical signals such as electroencephalogram (EEG), electrocardiogram (ECG), electromyogram (EMG), and electrooculogram (EOG). Given, its high temporal resolution, portability and reasonable cost, the present work focus on hypo-vigilance detection by analyzing EEG signal of various brain’s functionalities using fourteen electrodes placed on the participant’s scalp. On the other hand, deep learning networks offer great potential for biomedical signals analysis through the simplification of raw input signals (i.e., through various steps including feature extraction, denoising and feature selection) and the improvement of the classification results.

In this paper, we focus on the EEG signal study recorded by fourteen electrodes for hypo-vigilance detection by analyzing the various functionalities of the brain from the electrodes placed on the participant’s scalp.

Various deep learning architectures [9] exist such as Convolutional Neural Network (CNN), Recurrent CNN (R-CNN), Auto-Encoder (AE), Deep Belief Network (DBN), including Long Short-Term Memory (LSTM) and Gated Recurrent Units (GRU). As in [10], the CNN architecture is the most used to biomedical signals analysis providing a high classification accuracy. Previous related work [11] proposes a hypo-vigilance detection method using CNN by facial features. This method showed a classification accuracy of 92.33%. Likewise [12], introduces an adaptive conditional representation learning system for driver drowsiness detection based on a 3D-CNN. The proposed system consists of four steps (spatio-temporal representation, data preprocessing, features combination and somnolence detection). The experimental results show a detection accuracy equal to 92.04%. In this paper, we propose a CNN hypo-vigilance detection method using EEG data in order to classify drowsiness and awakeness states. Accordingly, the proposed approach including used equipment are presented in Sect. 2. Section 3 describes the experimental results and the evaluation of the employed method. Finally, a conclusion and future work are drawn in Sect. 4.

2 Proposed Approach

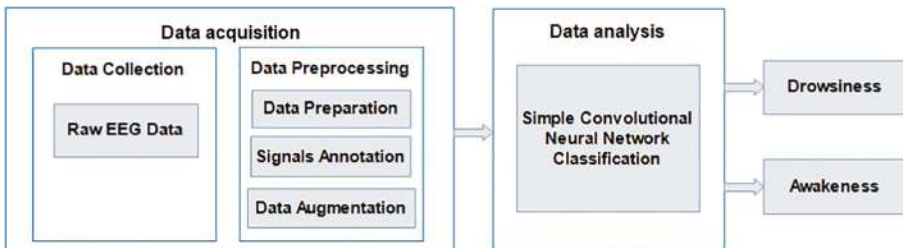


Fig. 1. Pipeline for the proposed approach.

As shown in Fig. 1, the realization of the proposed approach is suggested by two primary procedures: data acquisition and data analysis. The following subsections provide a detailed explanation of each procedure.

2.1 Data Acquisition

The EEG data acquisition procedure is made up of two main steps which are data collection and data preprocessing.

Data Collection: To collect the raw EEG data from participants, we use an Emotiv EPOC+ headset as shown in Fig. 2[a] for the data acquisition process. The key feature of this headset is a non-invasive Brain computer Interface (BCI) tool designed for the development of human brain and contextual research [13].

The Emotiv EPOC + helmet contains fourteen active electrodes with two reference electrodes (DRL and CMS), as shown in Fig. 2[b]. The electrodes are placed around the participant’s head in the structures of the following zones: frontal and anterior parietal (AF3, AF4, F3, F4, F7, F8, FC5, FC6), temporal (T7, T8) and occipital-parietal (O1, O2, P7, P8).



Fig. 2. (a) Emotiv EPOC+ helmet, (b) Location of the Emotiv EPOC+ helmet electrodes (10–20 International Standard).

Data Preprocessing: The specific preprocessing steps of the data revolve around the following points which are data preparation, data annotation and data augmentation.

– Data Preparation

During data acquisition, our raw EEG signals may be influenced by various sources of artifacts and noise such as endogenous electrical properties, specific fabrics physical structure, dipolar size variation, muscle shifts and Blinks. Hence, data processing is a preliminary step to denoising the raw signals. We suggest using an infinite impulse response (IIR) filter that manages an impulsive signal within time and frequency domains. Other sophisticated denoising approaches could be considered at the expense of higher computational complexity [14, 15].

– Signals Annotation

To evaluate each individual's state of exhaustion, we concentrate on the brain areas that are responsible for hypo-vigilance detection. In this regard, different brain waves are targeted such as [16]:

- **Delta waves** refer to consciousness, sleep or deep sleep states. These waves were found in the temporal and occipital conditions with low frequency (less than 4 Hz) and high amplitude.
- **Theta waves** design the relaxation and hypnosis states with a range of frequency between 4 and 8 Hz. Theta waves are extracted from the temporal zone and are produced during the first phase of slow sleep or in deep relaxation state.
- **Alpha waves** refer to waking but relaxed states. These waves are captured in the posterior part, precisely the occipital region, with a frequency interval between 8 and 12 Hz and a low amplitude interval between 20 and 60 μV .
- **Beta waves** relate to alertness states. These waves are captured from the temporal and occipital lobes of the brain. They are characterized by high frequency interval of 12 to 30 Hz with a low amplitude interval of 10 to 30 μV .
- **Gamma waves** refer to hypervigilance states with a frequency interval between 30 to 80 Hz.

In the data annotation step, we only use the O1 and O2 electrodes of occipital zone which are responsible for drowsiness sensation.

As an annotation example, Fig. 3 indicates the amplitudes of the alpha and theta signals from the two O1 and O2 electrodes reported for a participant in three periods of the day. The relaxation state has been indicated by alpha waves which have a frequency interval between 8 to 12 Hz and an amplitude interval between 20 to 60 μV . The somnolence state has been indicated by theta waves which have a frequency interval between 4 to 8 Hz and an amplitude interval between 50 and 75 μV .

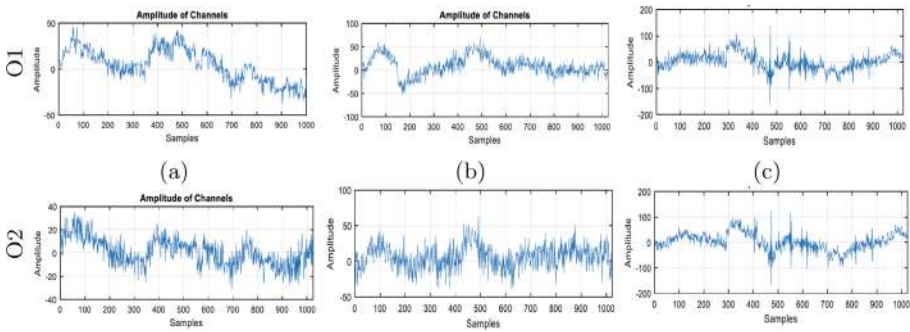


Fig. 3. The monitoring of O1 and O2 electrodes in the mornings (a), afternoons (b) and evenings (c).

– **Data augmentation**

In order to reduce overfitting and increase testing accuracy, we use the data augmentation technique [17] which consists of increasing the training set by label-retaining data transformations. The purpose procedure is to extend the data by doubling the vectors from (5850, 2) to (59053, 2) where 5850 (resp. 59053) represents the vector size and 2 represents the class number.

2.2 Data Analysis: Simple CNN Classification

The diagram of the neural network simple CNN used in our EEG drowsiness detection approach is represented in Fig. 4. The proposed simple CNN model is composed of the following six main layers:

- **The convolutional layers** allow the filter application and the features extraction characteristics of the input signals.
- **The sample-based discretization max-pooling-1D blocks** is used to sub-sample each input layer by reducing its dimensionality using a decrease in the number of the parameters to learn, there by reducing calculation costs.
- **The flatten layer** is used to flatten out multidimensional data.
- **The dropout layers** help to reduce the loss accuracy by regularizing and enhancing the overfitting of neural networks during the classification process.
- **The BatchNormalization layers** are used to scale and speed up learning of all activations. These layers normalize the previous activation layer output by subtracting the batches average and dividing it by the standard deviation to improve a neural network’s stability.
- **The dense layers** allow to done a connectivity function between the next and intermediate neurons layer.

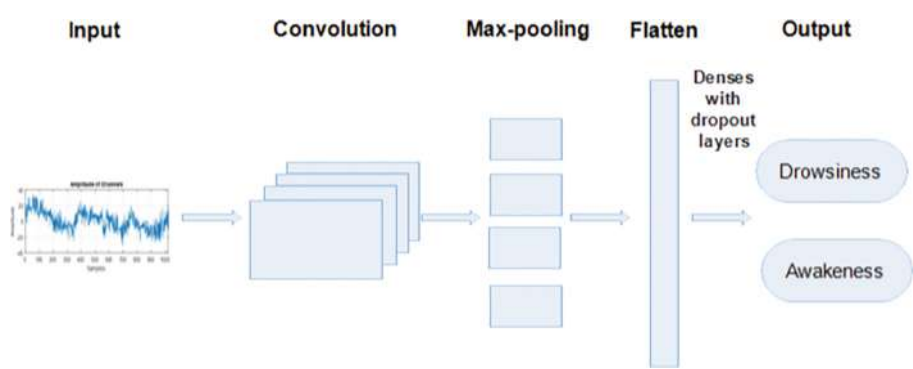


Fig. 4. The diagram of the simple CNN used in the proposed approach.

3 Experimental Evaluation

Our protocol revolves around the following axes: eight volunteers in which four women and four men aged twenty six and fifty eight with normal mental health. For each participant, we make three recordings of sixteen minutes divided over three day periods (morning, afternoon and evening). To fully understand the condition of the participants, we split the signal into windows to accurately identify these different states.

In the proposed simple CNN architecture for EEG signals classification, we use the Keras deep learning library. The different parameters as filters, kernel-size, padding, kernel-initializer, and activation of the four convolutional layers have the same values respectively 512, 32, same, normal and relu. The parameter values of the remaining layers are detailed in the following:

- the dropout layer value equal to 0.2 (respect. 0.5) is used to inactivate 20% (respect. 50%) of neurons in order to prevent overfitting.
- the Max-Pooling 1D layer is used with a filter size of 128.
- The multi-dimensional data output flattening using 1D flatten layer.
- For better classification results, two dropout layers are used. The first hidden layer takes a value of 128 neurons. Since a binary classification problem, the second layer takes a value of 1.

The choice of the optimization algorithm makes the difference between good results in minutes, hours or even days. There are various optimizers like Adam [18], SGD [19] and RMS pop optimizer [20]. In our model, we use the SGD optimizer which is more popular [21]. The method of this optimizer is simple and effective for finding optimal values in a neural network. Table 1 presents the hyperparameters choice of our model.

Table 1. Hyperparameters choices.

Parameters	Value
Optimization algorithm	SGD
Momentum	0.5
Batch size	64
Activation function	Sigmoid

For selecting the best accuracy rate of the proposed method, we propose to compare different results recorded by different numbers of electrodes. In [22, 23], the authors discover that the prefrontal and occipital cortex are the most important channels to better diagnose the hypo-vigilance state. In this regard, we choose the following recorded data:

- Recorded data by 2 electrodes (O1 and O2) electrodes from the occipital area.

- Recorded data by 4 electrodes (T7, T8, O1 and O2) from temporal and occipital areas.
- Recorded data by 7 electrodes (AF3, F7, F3, T7, O2, P8, F8) from prefrontal and occipital areas.
- Recorded data by 14 electrodes.

For the distribution of our data, we choose 70% for the train part and 30% for the test. Table 2 presents the reported testing and training accuracy respectively with two, four, seven and fourteen electrodes. After convergence the optimum number of test epochs for all the different electrodes results establish a value equal to 80. The best results are given by the recording of 2 electrodes from the occipital area. The curves of testing and training results for recorded data by O1 and O2 electrodes are represented in Fig. 5.

Table 2. Training and testing results of the different numbers of electrodes with data augmentation.

Number of electrodes	2	4	7	14
Accuracy train	98.18%	98.28%	98.99%	98.99 %
Accuracy test	93.94%	65.58%	76.43%	77.43 %

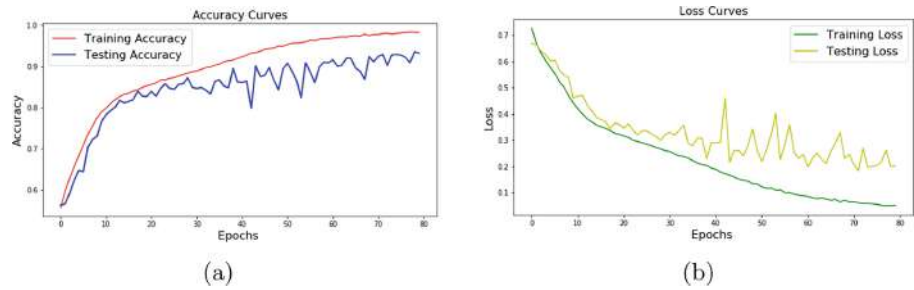


Fig. 5. (a) Accuracy graph, (b) Loss graph.

According to results obtained in Fig. 5, we note that the test accuracy increases after a certain number of epochs and the test loss decreases. To test our system’s efficiency we measured the precision, recall and F1-score. Table 3 shows these different measures in our experimental configuration.

For comparison purposes, we compare the proposed method with recent drowsiness methodology [24] where the authors propose a driver hypovigilance detection using the Emotiv EPOC+ helmet. The Common Spatial Pattern (CSP) algorithm is used for optimization accuracy of Extreme Learning Machine (ELM). The reported values in Table 4 indicate that our method gives the optimum accuracy value classification.

Table 3. Accuracy, precision, recall and F1-score of our experimental configuration

Accuracy	Precision	Recall	F1 score
93.94%	87.29%	99.79%	93.12%

Table 4. Accuracy comparison with related works.

Drowsiness detection methodology	Accuracy	Classification method
R. Osmalina et al. [24]	91.67%	CSP algorithm
Proposed method	93.94 %	CNNs

4 Conclusion

The present work proposes a CNN based approach for Hypo-vigilance detection. In order to create a EEG dataset, we recorded raw EEG data using Epoc+ headset. The suggested system achieves an average classification accuracy to 93.94% by testing it on a real dataset of eight participants. In future work, we will focus to improve classification accuracy with large datasets. Additionally, fusion with other biomedical signals should be also considered to improve the classification accuracy.

References

1. Hu, J., Wang, P.: Noise robustness analysis of performance for EEG-based driver fatigue detection using different entropy feature sets. *Entropy* **19**, 385 (2017)
2. Thomas, L.C., Gast, C., Grube, R., Craig, K.: Fatigue detection in commercial flight operations: results using physiological measures. *Procedia Manuf.* **3**, 2357–2364 (2015)
3. Neri, D.F., Shappell, S.A., DeJohn, C.A.: Simulated sustained flight operations and performance, part 1: effects of fatigue. *Mil. Psychol.* **4**, 137–155 (1992)
4. Chaari, L., Golubnitschaja, O.: Covid-19 pandemic by the “real-time” monitoring: the Tunisian case and lessons for global epidemics in the context of 3PM strategies. *EPMA J.* (2020)
5. Sahayadhas, A., Sundaraj, K., Murugappan, M.: Electromyogram signal based hypovigilance detection. *Biomed. Res. (India)* **25**, 281–288 (2014)
6. Wang, F., Wang, H., Fu, R.: Real-time ECG-based detection of fatigue driving using sample entropy. *Entropy* **20**(3), 196 (2018)
7. Ahn, S., Nguyen, T., Jang, H., Kim, J.G., Jun, S.C.: Exploring neuro-physiological correlates of drivers’ mental fatigue caused by sleep deprivation using simultaneous EEG, ECG, and fNIRS data. *Front. Hum. Neurosci.* **10**, 219 (2016)
8. Basri, C., et al.: Muscle fatigue detections during arm movement using EMG signal. *IOP Conf. Ser. Mater. Sci. Eng.* **557**, 012004 (2019)
9. Alom, M.Z., et al.: A state-of-the-art survey on deep learning theory and architectures. *Electronics* **8**(3), 292 (2019)

10. Kiranyaz, S., Ince, T., Abdeljaber, O., Avci, O., Gabbouj, M.: 1-D convolutional neural networks for signal processing applications. In: ICASSP, IEEE International Conference on Acoustics, Speech and Signal Processing - Proceedings, pp. 8360–8364, May 2019
11. Dwivedi, K., Biswaranjan, K., Sethi, A.: Drowsy driver detection using representation learning. In: IEEE International Advance Computing Conference, IACC, pp. 995–999, February 2014
12. Yu, J., Park, S., Lee, S., Jeon, M.: Driver drowsiness detection using condition-adaptive representation learning framework. *IEEE Trans. Intell. Transp. Syst.* **20**, 4206–4218 (2018)
13. Strmiska, M., Koudelkova, Z.: Analysis of performance metrics using Emotiv EPOC+. *MATEC Web Conf.* **210**, 4–7 (2018)
14. Laruelo, A., et al.: Hybrid sparse regularization for magnetic resonance spectroscopy. In: IEEE International Conference of Engineering in Medicine and Biology Society (EMBC), pp. 3–7, July 2013
15. Chaari, L., Tourneret, J.-Y., Chaux, C.: Sparse signal recovery using a Bernoulli generalized gaussian prior. In: European Signal Processing Conference (EUSIPCO), Nice, France, 31 August–4 September 2015 (2015)
16. Surangsrirat, D., Intarapanich, A.: Analysis of the meditation brainwave from consumer EEG device. In: IEEE SOUTHEASTCON, pp. 1–6, June 2015
17. Solé-Casals, J., et al.: A novel deep learning approach with data augmentation to classify motor imagery signals. *IEEE Access* **7**, 15945–15954 (2019)
18. Jung, J.J., Youn, Y.C., Camacho, D., Li, G., Lee, C.H.: Deep learning for EEG data analytics: a survey. *Concurr. Comput.* (2019)
19. Shaf, A., Ali, T., Farooq, W., Javaid, S., Draz, U., Yasin, S.: Two classes classification using different optimizers in convolutional neural network. In: International Multi-topic Conference (INMIC), pp. 1–6 (2018)
20. Tafast, A., Ferroudji, K., Hadjili, M.L., Bouakaz, A., Benoudjit, N.: Automatic microemboli characterization using convolutional neural networks and radio frequency signals. In: 2018 International Conference on Communications and Electrical Engineering (ICCEE), pp. 1–4, December 2018
21. Reddy, S.V.G., Reddy, K.T., ValliKumari, V.: Optimization of deep learning using various optimizers, loss functions and dropout. *Int. J. Innov. Technol. Explor. Eng*
22. Nugraha, B.T., Sarno, R., Asfani, D.A., Igasaki, T., Munawar, M.N.: Classification of driver fatigue state based on EEG using Emotiv EPOC+. *J. Theor. Appl. Inf. Technol.* **86**, 347–359 (2016)
23. Sarno, R., Nugraha, B.T., Munawar, M.N.: Real time fatigue-driver detection from electroencephalography using Emotiv EPOC+. *Int. Rev. Comput. Softw. (IRECOS)* **11**, 214 (2016)
24. Osmalina, R., Rahmatillah, A.: Drowsiness analysis using common spatial pattern and extreme learning machine based on electroencephalogram signal. *J. Med. Signals Sens.* **9**(2), 130–136 (2019)

Open Access This chapter is licensed under the terms of the Creative Commons Attribution 4.0 International License (<http://creativecommons.org/licenses/by/4.0/>), which permits use, sharing, adaptation, distribution and reproduction in any medium or format, as long as you give appropriate credit to the original author(s) and the source, provide a link to the Creative Commons license and indicate if changes were made.

The images or other third party material in this chapter are included in the chapter's Creative Commons license, unless indicated otherwise in a credit line to the material. If material is not included in the chapter's Creative Commons license and your intended use is not permitted by statutory regulation or exceeds the permitted use, you will need to obtain permission directly from the copyright holder.





Respiratory Activity Classification Based on Ballistocardiogram Analysis

Mohamed Chiheb Ben Nasr^{1(✉)}, Sofia Ben Jebara¹, Samuel Otis²,
Bessam Abdulrazak⁴, and Neila Mezghani^{2,3}

¹ Higher School of Communication of Tunis, Carthage University, Aryanah, Tunisia
{mohamedchiheb.bennaser, sofia.benjebara}@supcom.tn

² Laboratoire de recherche en imagerie et en orthopédie, CRCHUM,
Montreal, Canada

samuel.otis.1@ens.etsmtl.ca

³ LICEF Institute, TELUQ University, Montreal, Canada
neila.mezghani@teluq.ca

⁴ Department of Computer Science, Sherbrooke University, Sherbrooke, Canada
Bessam.Abdulrazak@usherbrooke.ca

Abstract. Ballistocardiogram signals describe the mechanical activity of the heart. It can be measured by an intelligent mattress in a totally unobtrusive way during periods of rest in bed or sitting on a chair. The BCG signals are highly vulnerable to artefacts such as noise and movement making useful information like respiratory activities difficult to extract. The purpose of this study is to investigate a classification method to distinguish between seven types of respiratory activities such as normal breathing, cough and hold breath. We propose a feature selection method based on a spectral analysis namely spectral flatness measure (SFM) and spectral centroid (SC). The classification is carried out using the nearest neighbor classifier. The proposed method is able to discriminate between the seven classes with the accuracy of 94% which shows its usefulness in context of Telemedicine.

Keywords: Ballistocardiogram · Machine learning · Biomedical signal processing · Spectral analysis

1 Introduction

The development of connected object for personalized services, especially for monitoring purposes, have significantly increased worldwide over the last few years [1]. More specifically those that deals with the monitoring of respiratory and cardiac diseases. Indeed these diseases are among the leading cause of death and disability in the world. One of these respiratory diseases is the Chronic Obstructive Pulmonary Disease COPD [2] a progressive life threatening lung disease. According to the World Health Organization [3], COPD affects more than 250 million cases globally, a staggering 3.17 million deaths per year and

is associated with a huge economic burden. In fact, numbers published by the Global initiative for Chronic Obstructive Lung Disease [4] shows that the direct costs of respiratory disease in the European Union are estimated to be about 6% of the total annual healthcare budget with COPD accounting for 56% (38.6 billion Euros) of the cost of respiratory disease. These numbers are further amplified by the ever-growing healthcare costs, the aging of the population and the widespread of such diseases. The monitoring of respiratory activities plays an important role in the current management of patients with acute respiratory failure [5]. As a consequence, it is recommended to have continuous monitoring of the vital signs to ensure an optimal diagnosis of a patient's state [6]. Moreover, monitoring of respiratory activity is useful for detecting respiratory disorders, such as the sleep apnea, cessation of breathing in infants, shortness of breath in patients with heart failure, and so on. Hence, it is important to monitor respiratory activities such as normal breathing, cough, hold breath expiration.

A new generation of sensor-based mattress is able to unobtrusively monitor vital signs such as the Heart rate Beat Rate (HBR) and the Respiratory Rate (RR). Indeed, this study considered an Optical Fiber based Sensor (FOS) [7] for the unobstructed monitoring of the Ballistocardiogram (BCG) signal. Due to the ejection of the blood during the systole, the body's mechanical reaction is measured hence the BCG signal. Our aim is to investigate a classification method to distinguish between several types of respiratory activities such as normal breathing, cough and hold breath using the BCG signal.

This paper is organized as follows. Section 2 is dedicated to describe the material and method. It describes the data collection, BCG signal analysis and feature extraction and classification. Section 3 provides information about the experimental results mainly feature illustration and classifier evaluation. Finally, Sect. 4 concludes the study and gives perspectives.

2 Material and Method

2.1 Data Collection

The system used for collecting data includes a small FOS mattress and a module to gather optical data coming from the mattress [8, 9]. The FOS mattress was fixed on the back of a regular office chair. The raw data is sampled at 50 Hz by the module.

The BCG signals were acquired on 6 healthy participants: 3 male and 3 female aged between 21 and 32 years. The participants were asked to perform a certain experimental protocol. A part of normal breathing, other human body activities that commonly occur are introduced in this protocol. It is composed of the following steps by following activities: normal breathing (C1), cough (C2), Normal breathing after cough (C3), hold breath (C4), expiration (C5), movement (C6). We also consider a class other to regroup all other activities (C7). Figure 1 illustrates an example of the BCG signal. The different human body activities are plotted in different colors. The objective is to highlight the differences in the BCG signal according to the activity.

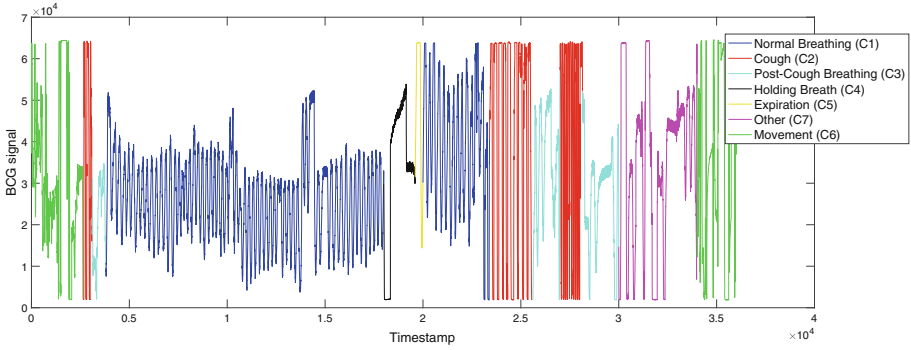


Fig. 1. Illustration of the BCG signal during the experimental protocol activities. (Color figure online)

2.2 BCG Signal Analysis

In this subsection we inspect the effect of different activities in the BCG signal. Figure 2 illustrates five different activities. In the plot illustrating Normal respiration (C1), we can easily extract both the HBR and RR, the big period corresponds to the movements of the thoracic cage. By extracting the distance between two consecutive peaks of this waveform, we can extract the RR. The small period appearing in the BCG signal represents the heart beats. The extraction of these little fluctuations results in the extraction of the HBR.

The signals corresponding to the cough (C2) and movement (C6) are very similar. Both signals attain the upper limit of the acquisition equipment which is explained by the broad peaks in the BCG signals. We believe however that these broad peaks have different explanations. The peaks in the movement signal comes from the acceleration of the subject's body and the peaks during the cough comes from the reaction of the body after coughing.

The post-cough normal breathing is corrupted and we can hardly find the peaks of the respiratory activity. The peaks are broader and that results in a lack of precision of HBR and RR.

The holding breath BCG contains only cardiac information. The periodicity is clearly noticed which was not obvious in other activities.

This analysis of the BCG signal's content motivates the use of an approach based on the characterization of the useful frames. This particular problem is complex and thus is demanding when it comes to the choice of the features with physical significance. In the next subsections, we will define the features and try to highlight the intuition behind each one of them.

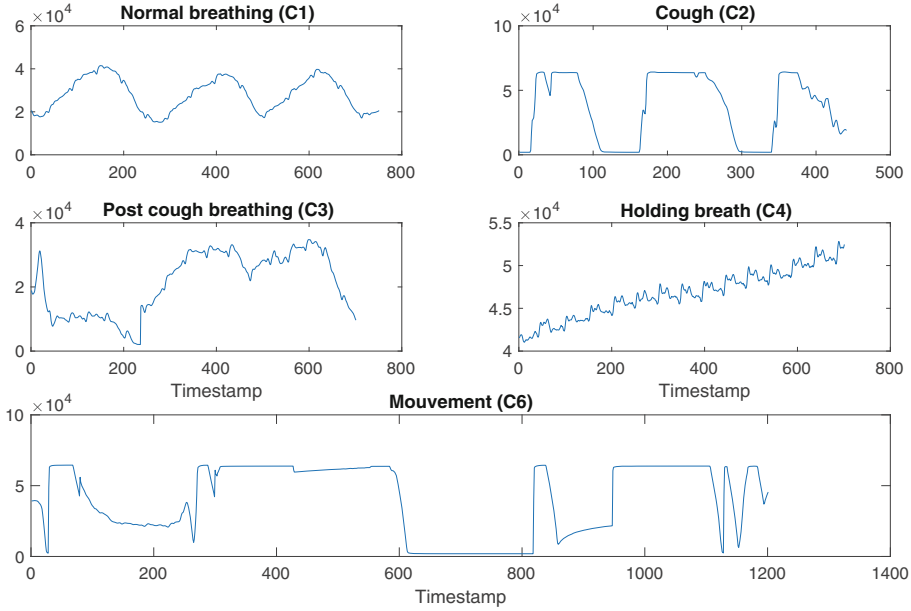


Fig. 2. Illustration of the BCG signal of the different activities of the subjects.

2.3 BCG Signal Feature Extraction

A periodic signal can be represented as a sum of sine waves and thus the Fourier transformation of this particular signal will be spiky. This statement motivated the idea of using the following two features: Spectral Flatness Measure (*SFM*) and Spectral Centroid (*SC*).

Let $x(n)$ be a BCG signal. The later is decomposed into frames of short duration. These frames should be long enough to carry information about the activity but not too long to avoid an overlap of two or more different activities. In the frequency domain, the short-term Fourier transform is calculated and its amplitude is extracted. It is denoted $|X(m, k)|$, where m is the frame index and k is the discrete frequency.

Spectral Flatness Measure (SFM): The SFM, also known as Wiener entropy, is a signal processing measure used to describe the flatness of the spectrum of the signal [10, 11]. The *SFM* is defined as the ratio of the geometric mean and arithmetic mean of the Fourier transforms. When the spectrum is flat (white noise signal), the resulting measure is close to 1.

$$SFM(m) = \frac{\sqrt[N]{\prod_{k=1}^N |X(m, k)|}}{\frac{\sum_{k=1}^N |X(m, k)|}{N}}, \quad (1)$$

where k is the frequency bin index and N is the number of frequency bins.

Spectral Centroid (SC): The SC indicates where the center of mass of the spectrum is located.

$$SC(m) = \frac{\sum_{k=1}^N (|X(m, k)| * f(k))}{\sum_{k=1}^N |X(m, k)|}, \quad (2)$$

where $f(k)$ is the frequency in Hz of the bin k .

BCG Feature Engineering: The SFM and SC measures have been evaluated on each frame of the BCG signal. However, in order to avoid complexity that comes with it (overlap noise propagation, presence of different labels in the same frame, frames too small to be representative...), we propose to create a time-series out of the SFM and SC values in each frame.

- Signal decomposition: the original BCG signal is decomposed into frames of length 1024 with an overlap of 960 samples. Hence we used a windowing function. In this work we used a *Hamming* window with an increment of 64 samples.
- The feature vector $F(m) = [SFM(m), SC(m)]^T$ is extracted from each frame.
- Each feature of raw data $SFM = [sfm(1), sfm(2)...sfm(L)]^T$ (L is the number of frames) is transformed into a time-series (equivalent to a signal) by overlapping and adding the sfm of each frame. Note that the latter is a constant vector, whose value is sfm and whose length is the frame size.

The sfm_{signal} and sc_{signal} are then used for the purpose of classification.

2.4 Activities Classification

Respiratory activities classification has been performed using a K-nearest neighbors classifier. It is a non-parametric classification method which classifies a sample based on a plurality vote of its neighbors. The sample is assigned to the class most common among its K nearest neighbors (K is a positive integer) in terms of minimal distance. The algorithm adopted is Fine KNN which is the finest variation of KNN since it labels the new input with the same label as only one of its nearest neighbour $K = 1$. The evaluation of the algorithm as well as the classification results were conducted using k-fold cross validation with $k = 5$.

2.5 Classification Evaluation

The classification performance is evaluated in terms of true positive rate and positive predicted value.

True Positive Rate: The performance of our model will mainly be measured using the confusion matrix [12]. Specifically TPR measures the proportion of

detected positives from the actual positive in other terms TPR measures how sensitive your model is to the positive class.

$$TPR^i = \frac{true\ positives}{true\ positives + false\ negatives}, \quad (3)$$

where i corresponds to the class (activity) of the subject ($i = 1..7$). The terms of the confusion matrix presented in Fig. 4 are defined as follows:

$$Conf_{tp}(i, j) = \frac{M_{ij}}{\sum_{j=1}^C M_{ij}}, \quad (4)$$

where C is the number of classes, M_{ij} is the number of predictions of class i that actually belongs to class j it is usually measured by comparing the test results to the ground truth.

Positive Predictive Value: The proportion of the predictions made that are actually true and happened. PPV Highlights mostly how refined our model is and how frequent we have false alerts.

$$PPV^i = \frac{true\ positives}{true\ positives + false\ positives}. \quad (5)$$

The terms of the confusion matrix presented in Fig. 5 are defined as follows:

$$Conf_{ppv}(i, j) = \frac{M_{ij}}{\sum_{i=1}^C M_{ij}}, \quad (6)$$

3 Experimental Results

3.1 Feature Illustration

This section illustrates the feature analysis and interpretation by providing the means of the SFM and SC for each activity.

The BCG signal we are working with is the same displayed on Fig. 1. The mean values are given in Table 1. We note that the normal breathing mean value of the SFM is the lowest which confirms the periodicity hypothesis. The values of SFM and SC taken during the coughing portion (C2) as well as the movement portion (C6) are relatively high which further confirms the non-periodicity in the corresponding portions.

For the post-cough breathing, we notice that, unlike the portion of normal breathing, the values of the descriptors are high and close to those during the movement and coughing activities which supports our choice to isolate these portions.

The closest values of the descriptors to the ideal ones (those of the normal breathing) are the values recorded during the holding breath, this is due to the fact that the portions of holding breath are periodic and carry only the heart rhythm information.

Table 1. Mean value of *SFM* and *SC* during each activity.

Activities	<i>SFM</i>	<i>SC</i>
Normal respiration (C1)	0.02	0.807
Cough (C2)	0.1582	2.3591
Post cough breathing (C3)	0.14	1.2638
Holding breath (C4)	0.102	0.7662
Movement	0.2293	1.4844

Figure 3 show the *sfm_{signal}* of some activities. In the top right, the normal respiration phase is considered. The values of *SFM* are low as expected to be. This fact is due to the clear periodicity in that activity. The *SFM* of holding breath (down left plot) is pretty low and that is as well an expected result since there's the cardiac information in the holding breath activity. Both cough and movement activities (right plots) manifest big fluctuations in their respective *sfm_{signal}*, this is due to the absence of periodicity in these signals.

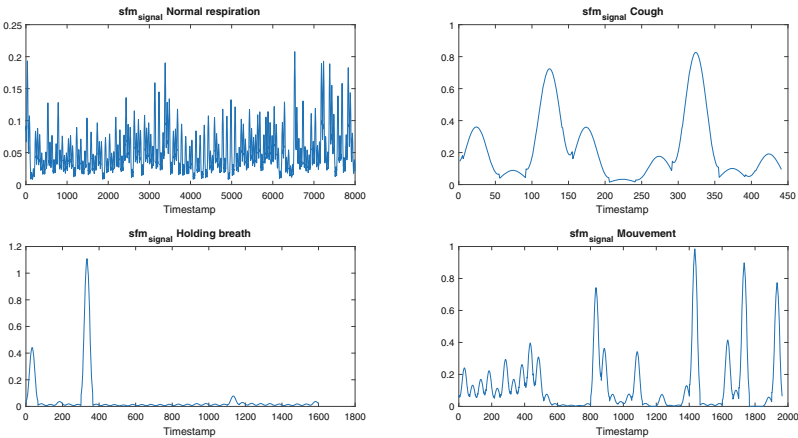


Fig. 3. Variation of *sfm* signal of the sample for each activity.

3.2 Classifier Evaluation

Using the sfm_{signal} and sc_{signal} we obtained a classification rate of 94%. Figure 4 shows the TPR confusion matrix. We can observe that our model performs very well overall. The TPR value appears in the diagonal of the confusion matrix. Most of the errors are detected in the class $C4$, where 31% of the latter (corresponds to the class: holding breath) is predicted as normal respiration. This result is expected since the periodicity in the holding breath portions is present due to the cardiac activity. We observe as well a high confusion between the class cough (C2) and the class movement (C6). This is due to the fact that our predictors are well equipped to detect the existence of the periodicity in the portions.

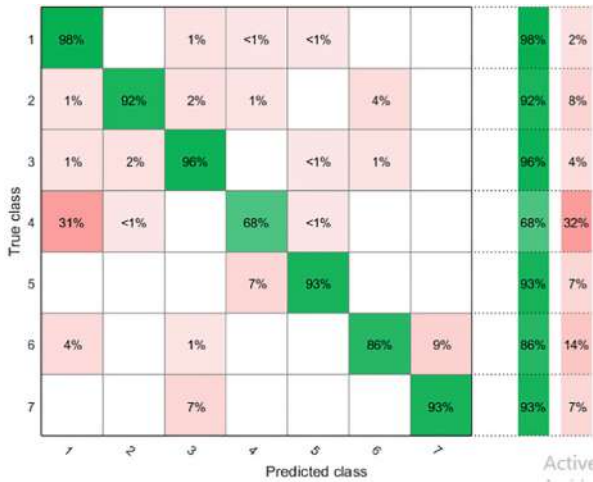


Fig. 4. TPR confusion matrix

Figure 5 shows the PPV confusion matrix. We can observe the confusion between the classes C1 and C4 (7%) in terms of PPV this corresponds to a high false-alert rate (the majority of false alerts in the class: Normal respiration are recorded as Holding breath) which further confirms the similar periodicity hypothesis mentioned in the previous paragraph we can also pinpoint an alarming 13% with the class C5 which is due to the lack of the adopted features when it comes to differentiating between the highly non-periodic portions.



Fig. 5. PPV Confusion matrix

4 Conclusion

In this study we investigated the respiratory activity classification based on the BCG signal. We used a reconstructed time-series signal from the spectral flatness measure (SFM) and spectral centroid (SC) of the raw data. We obtained a classification rate of 94% which show the effectiveness of the proposed method. The supervised classification process, however, is demanding when it comes to data and computation. Treating the feature extraction process by generating a time series is a novelty which motivates the use of more sophisticated deep-learning algorithms such as the Long Short Term Memory LSTM as one of the most used Recurrent Neural Network RNN architectures in time series related problems.

References

1. Wearable Monitoring System for Chronic Cardio-Respiratory Diseases. In: 30th Annual International IEEE EMBS Conference Vancouver, British Columbia, Canada, 20–24 August 2008
2. Forum of International Respiratory Societies: The Global Impact of Respiratory Disease, 2nd edn. European Respiratory Society, Sheffield (2017)
3. Who.int. Chronic respiratory diseases (2020). <https://www.who.int/health-topics/chronic-respiratory-diseases>. Accessed 18 Feb 2020
4. Global strategy for the diagnosis, Management and prevention of Chronic Obstructive Pulmonary Disease 2020 report
5. Clinical review: Respiratory monitoring in the ICU - a consensus of 16. Crit Care. 16(2), 219 (2012). <https://doi.org/10.1186/cc11146>. PMID: 22546221

6. Liu, J., Wang, Y., Chen, Y., Yang, J., Chen, X., Cheng, J.: Tracking vital signs during sleep leveraging off-the-shelf WiFi. In: Proceedings of the 16th ACM International Symposium on Mobile Ad Hoc Networking and Computing, MobiHoc 2015, New York, NY, USA, pp. 267–276. ACM (2015)
7. Sadek, I., Biswas, J., Abdulrazak, B.: Ballistocardiogram signal processing: a review. *Health Inf. Sci. Syst.* **7**(1), 1–23 (2019). <https://doi.org/10.1007/s13755-019-0071-7>
8. Ramakrishnan, M., Rajan, G., Semenova, Y., Farrell, G.: Overview of fiber optic sensor technologies for strain/temperature sensing applications in composite materials. *Sensors* **16**(1), 99 (2016)
9. Otis, S., Mezghani, N., Abdulrazak, B.: Comparative Study of Heart Rate Extraction Methods for a Novel Intelligent Mattress. In: IEEE International Symposium on Signal Image, Video and Communications (ISIVC), pp. 27–29, Rabat, Morocco (2018)
10. Dubnov, S.: Generalization of spectral flatness measure for non-gaussian linear processes. *IEEE Sig. Process. Lett.* **11**(8), 698–701 (2004)
11. Madhu, N.: Note on measures for spectral flatness. *Electron. Lett.* **45**, 1195–1196 (2009). <https://doi.org/10.1049/el.2009.1977>
12. Stehman, S.: Selecting and interpreting measures of thematic classification accuracy. *Remote Sens. Environ.* **62**(1), 77–89 (1997)

Open Access This chapter is licensed under the terms of the Creative Commons Attribution 4.0 International License (<http://creativecommons.org/licenses/by/4.0/>), which permits use, sharing, adaptation, distribution and reproduction in any medium or format, as long as you give appropriate credit to the original author(s) and the source, provide a link to the Creative Commons license and indicate if changes were made.

The images or other third party material in this chapter are included in the chapter's Creative Commons license, unless indicated otherwise in a credit line to the material. If material is not included in the chapter's Creative Commons license and your intended use is not permitted by statutory regulation or exceeds the permitted use, you will need to obtain permission directly from the copyright holder.





A Convolutional Neural Network for Lentigo Diagnosis

Sana Zorgui^{1(✉)}, Siwar Chaabene^{1(✉)}, Bassem Bouaziz^{1(✉)}, Hadj Batatia^{2(✉)},
and Lotfi Chaari^{2(✉)}

¹ MIRACL and CRNS, University of Sfax, Sfax, Tunisia
sanazorgui@gmail.com, siwarchaabene@gmail.com,
bassem.bouaziz@isims.usf.tn

² University of Toulouse, IRT - INP-ENSEEIH, Toulouse, France
{hadj.batatia,lotfi.chaari}@toulouse-inp.fr

Abstract. Using Reflectance Confocal Microscopy (RCM) for lentigo diagnosis is today considered essential. Indeed, RCM allows fast data acquisition with a high spatial resolution of the skin. In this paper, we use a deep convolutional neural network (CNN) to perform RCM image classification in order to detect lentigo. The proposed method relies on an InceptionV3 architecture combined with data augmentation and transfer learning. The method is validated on RCM data and shows very efficient detection performance with more than 98% of accuracy.

Keywords: Reflectance Confocal Microscopy · Lentigo · CNN
classification · InceptionV3

1 Introduction

Reflectance Confocal Microscopy (RCM) [1] is a modality increasingly used in medical imaging like MRI (Magnetic Resonance Imaging) [2–4] or X-ray imaging [5]. In vivo RCM technique is easy to use during the patient examination and acquires high resolution skin images in a short time. This modality can be used to help dermatologists diagnose different skin diseases. However, it takes a long time for dermatologists to make full use of the possibilities of this technique for diagnostic purposes. Our work aims to develop a new tool to automate certain diagnostic steps required using deep learning [6]. On the other side, the lentigos are age spots that mainly appear on the hand or on the areas most frequently exposed to the sunlight. On the surface, they appear as a darker spot. Inside the skin layers, it is mainly at the level of the dermis-epidermis junction that the differences can be visible [7]. Therefore, the distinction of lentigos can be made using the RCM images. Several deep learning architectures, especially convolutional neural network (CNN) [5,8] show great potential in medical imaging classification. In this paper, we propose a new 3D RCM image (2D + depth) classification method for lentigo detection. The method is based on a CNN on InceptionV3 architecture [9].

© The Author(s) 2020

M. Jmaiel et al. (Eds.): ICOST 2020, LNCS 12157, pp. 89–99, 2020.

https://doi.org/10.1007/978-3-030-51517-1_8

Until now, little works have been proposed for lentigo/healthy classification of RCM images. In [10], the authors perform a two-dimensional wavelet decomposition. Then a generalized Gaussian distribution was applied to the wavelet coefficients in order to perform a quantitative analysis assisted by a support vector machine (SVM) to classify RCM images obtaining an accuracy of 84.4%. Another approach in [11] explores a new unsupervised Bayesian algorithm for the joint reconstruction and classification of RCM images. The resulting algorithm for healthy and lentigo classification reached an accuracy percentage of 97%. Beside, the paper [12] automatically diagnosed lentigo by using three separate feature extraction methods like Wavelets, Haralick and CNN by Transfer Learning. The healthy/lentigo classification results reached an accuracy of 76%.

The present paper is organized as follows. Section 2 presents the problem formulation of lentigo diagnosis. Section 3 detailed the proposed lentigo detection method. Section 4 presents the experiment validation of our method. Finally, conclusion and some perspectives are drawn in Sect. 5.

2 Related Work

2.1 Lentigo Detection

Lentigo is a lesion that occurs in the dermal epidermal junction between the dermis and the epidermis involving a high concentration of melanocytes in the dermal papillae walls. Most forms of lentigo are benign [13] like lentigo simplex as Fig. 1(a) and solar lentigo as Fig. 1(b). They are usually removed for cosmetic purposes. However, certain types such as lentigo maligna [14] as Fig. 1(c) may be harmful and must be removed.



Fig. 1. Lentigo simplex (a), Solar lentigo (b) and Lentigo maligna (c).

Usually, lentigo is diagnosed using dermatoscopy [15]. Sadly, non-pigmented melanocytes with this modality can go completely unnoticed leading to complications in identifying the lesion contours with precision. Histopathology [16] is also used to confirm the diagnosis, but it can be inconvenient due to the fact that it is an in vitro technique involving performing a biopsy from the pigmented areas. For these reasons, the RCM modality emerged to solve the problems encountered before. Therefore, this modality allows the expert to carry out a real-time 3D

data acquisition and to facilitate the full observation of the biological structures in deformation over time. Due to all of these reasons, our approach is based on images acquired thanks to this modality. In [10,11], the authors propose two RCM lentigo detection methods based on the statistical and Bayesian models [17] respectively. The methods have proved complicated and hard to implement. They require manual procedures like feature selection and data preparation. To this regard, we propose here a method for RCM image classification using a CNN architecture. Indeed, CNNs have proven their capacity to efficiently solve several complex problems in medical imaging.

2.2 Convolutional Neural Networks

The CNN [8] is a deep learning architecture that is primarily used for image classification and object detection. Figure 2 displays a general CNN architecture, where one can easily identify the following layers:

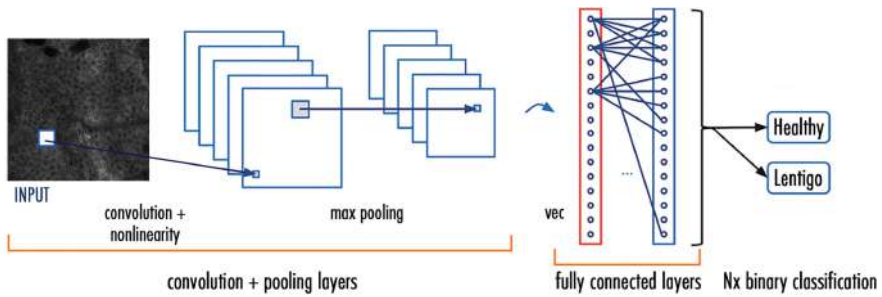


Fig. 2. The CNN architecture model.

- The convolutional layers: a key component of a CNN architecture, used for automatic feature extraction.
- The rectified linear units (ReLU): used after each convolutional layer. Each layer combines nonlinear layers and rectification layers to add nonlinearity to the system.
- The pooling layers: used for feature selection by maximum or/and average pooling.
- The fully connected layers: also known as dense layers receiving the flattened (1D) feature map. Usually, the final fully connected layer has the same number of output nodes as the class numbers.
- The Softmax function: calculates the probabilities of each target class over all possible classes. This function helps determine the target class for the given inputs.

3 Proposed Method for Lentigo Detection

The proposed method consists of classifying RCM images into healthy/lentigo classes using an InceptionV3 architecture. Our lentigo detection method combines the InceptionV3 model with other known deep learning techniques like transfer learning [18] and data augmentation [19]. Figure 3 presents the different steps used in the proposed lentigo detection method. The following subsections give detailed descriptions of each step.

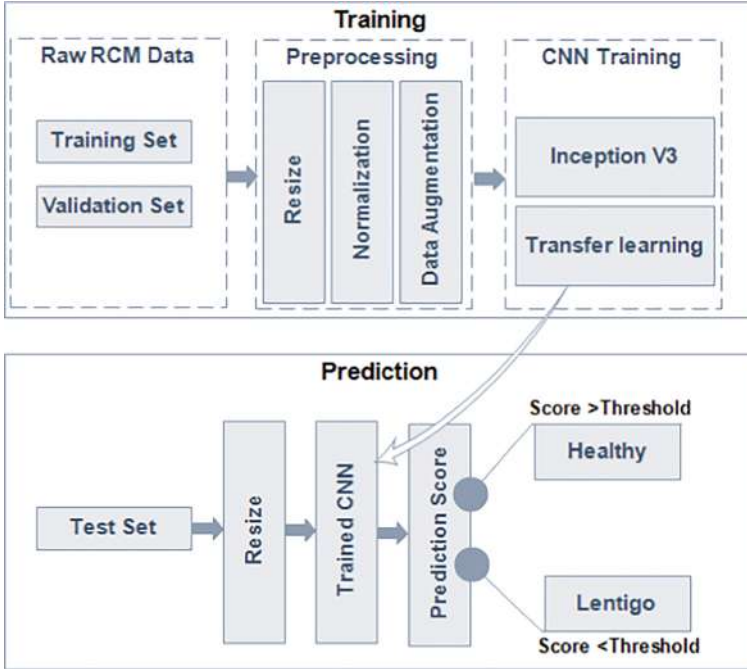


Fig. 3. Pipeline of the proposed method.

3.1 Data Preparation

The input RCM images for the training procedure combines two sets such as a 73% training set and a 14% validation set. The remaining 13% is dedicated to the prediction phase. In order to avoid overfitting, a validation set is added to our training phase because the non linear InceptionV3 model will possibly achieve 100% training accuracy and overfit.

3.2 Data Preprocessing

In the first step of the preprocessing procedure, the RCM images of the training set are resized to fit in the InceptionV3 network. A normalization step is added to help the CNN better process the input images, in order that all feature values have the same range and the system needs only one global learning rate multiplier. Afterwards, the data augmentation step is proposed to improve our classification results. This step prevents accuracy decay and overfitting. In [20] the authors demonstrate the importance of data augmentation as a regularizer in the CNN classification model.

3.3 InceptionV3 Model

The InceptionV3 model is a complex heavily engineered network that considered a major breakthrough in CNN's [9]. Before the current model, many common CNN's claimed that stacking layers after layers is the only way to increase accuracy. However, this network suggested some solutions to improve accuracy and speed without piling many layers. As shown in Fig. 4, the InceptionV3 model consists of a combination of three main modules.

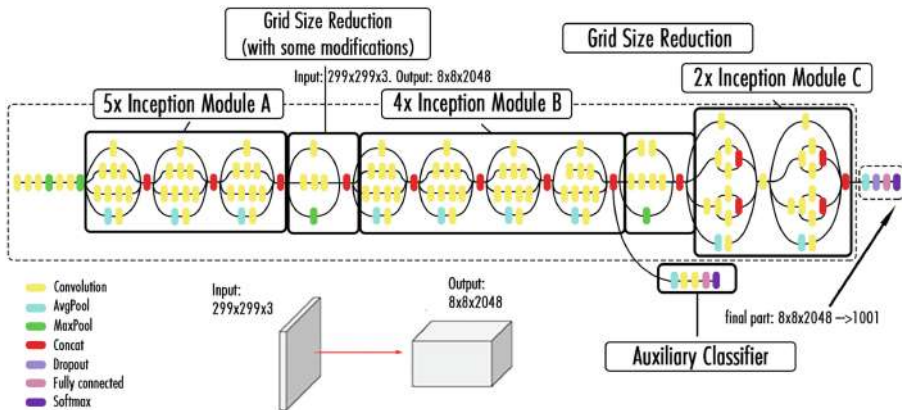


Fig. 4. Architecture of the InceptionV3 model.

The first one (Module A) uses two smaller convolution layers (3×3) to decrease the computational cost by reducing the number of parameters to improve performance. Module B divides each convolution layer of $n \times n$ size to two layers of $1 \times n$ and $n \times 1$ dimensions to have a less complex network. Finally, Module C reduces the representational bottleneck by expanding the filters in order to evade information loss. More upgrades are also proposed by the InceptionV3 network other than the smart factorization methods such as:

- RMSProp optimizer allows a faster convergence of the model thus allowing a higher learning rate.

- BatchNorm reduces the covariance shift and allows each network layer to learn a little independently of the others.
- Label Smoothing is a regularizing component applied to the loss formula to prevent overfitting.

The InceptionV3 network is 42 layers deep. Therefore, the computational cost is just around 2.5 higher than GoogLeNet’s [21]. In addition, the inception modules are a novel and popular concept due to their smaller convolutions, which explains the reduction in the number of parameters. The InceptionV3 model gathers more information without impacting the computational speed thanks to its depth and the various kernel sizes used in the convolution operations.

3.4 Transfer Learning

As shown in Fig. 3, transfer learning [22] is proposed in order to ensure better performance of the model. The model needs lots of labeled images to be capable of solving complex problems. This has proved to be challenging especially when the available dataset is small. Transfer learning is a deep learning method, in which a model developed for a task is reused for a second task. This technique uses pre-trained models as a starting point for other medical imaging tasks given the vast computational and time resources required to develop CNN models on these problems.

3.5 Prediction Model

In the prediction phase, the RCM images test set are resized and provided to the trained CNN. Our system calculates a prediction score for each test image after resizing it and compares it with the threshold T equal to 0.5. The threshold value is chosen that way due to the fact that we are performing a binary classification. The classification condition is as follows: if the predicted score (PS) value of the image test is lower than T then this RCM image is classified as lentigo and conversely.

4 Experimental Validation

This section evaluates the validation of the proposed lentigo detection method on real RCM data. In our work, the dataset is provided from Lab. Pierre Fabre. In this experiment, the data include 428 RCM images which high spatial resolutions and annotation on each image into two healthy and lentigo classes. The images were acquired with a Vivascope 1500 apparatus. Each RCM image shows a field of view of $500 \times 500 \mu\text{m}$ with 1000×1000 pixels. A selection of 45 women aged 60 years were recruited. All participants have offered their informed consent to the RCM skin test. We split these data into three main sets:

- A 314 images training set divided into two classes of 160 healthy images and 154 lentigo images.

- A validation set of 60 images, divided equally between two classes of lentigo and healthy. The validation set has been added to evaluate our training procedure. The main objective is to prevent over-fitting.
- A 54 RCM images testing set divided equally for healthy and lentigo classes.

Our classification method based on the InceptionV3 network is build using the Keras library. The InceptionV3 model is configured to accept the greyscale RCM images. As initialization, all RCM images were resized into new dimensions of 299×299 pixels and rescaled to help CNN processing. The parameter values of data augmentation step are presented in Table 1. The shear, zoom and translation ranges vary from 0 to 1. We choose the value of 0.2 for each to enrich the dataset without altering the image main features and confusing the system. The rotation range varies to 0° from 180° and a small rotation angle was proposed for the same reasons.

Table 1. Data augmentation parameters.

Parameter	value
Shear	0.2
Zoom	0.2
Rotation degree	20°
Horizontal translation	0.2
Vertical translation	0.2

Figure 5 displays the accuracy curves of the training and validation sets, as well as the training loss. The accuracy curves suggest that our system converged after 40 epochs. The system reached an accuracy value of 94% for training and 69% for validation. Hence, the reported values indicate that our system learns well without over- or under-fitting.

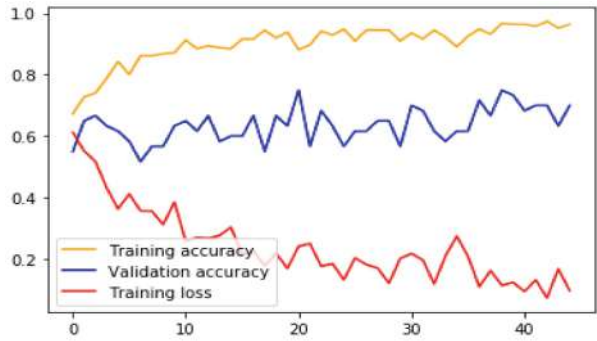


Fig. 5. Proposed method accuracy graph and loss graph for training and validation sets after each epoch.

The performance of the proposed method is indicated by the test set according to the ability to correctly diagnose the provided skin tissues. The reported values in Table 2 indicate the performance of our classification method. Therefore, 53 out of 54 images test set were correctly classified with an accuracy of **98,14%**.

Table 2. Confusion matrix.

	Lentigo	Sane
Lentigo	27/27 = 100% (TP)	1/27 = 3,7% (FN)
Sane	0/27 = 0% (FP)	26/27 = 96,3% (TN)

In Table 2, TP, TN, FP and FN represent respectively true positives, true negatives, false positives and false negatives. Based on the confusion matrix, Accuracy, Precision, Specificity, Recall and F-score values are reported in Table 3. All the mentioned measures indicate a good performance of the proposed method with values equal or very close to one.

Table 3. Quantitative evaluation of the proposed method performance.

Accuracy	$(TP + TN)/(TP + TN + FP + FN)$	0.98
Precision (P)	$TP/(TP + FP)$	1
Specificity	$TN/(FP + TN)$	1
Recall (R)	$TP/(TP + FN)$	0.96
F-score	$(2 \times P \times R)/(P + R)$	0.97

Figure 6 presents four correct classification examples of RCM images from the test set. The reported values shown with each test image indicate the prediction score (PS). The displayed images correspond to different PS ranges. We can notice that the model performs well both for images with PS close to 0 or 1, but also for images with PS close to 0.5 (images (b) and (d)).

Figure 7 shows the only image wrongly classified using our proposed method. This image shows some type of skin deformation similar to the changes the skin undergoes due to lentigo. Hence, the network interpreted it as a lentigo lesion. For the sake of further evaluation, we compare the accuracy of the test with related works that used the same dataset. The reported values in Table 4 show that our model outperforms in comparison with the other methods. Specifically, we compare our results with those reported in [10] where the authors used a Statistical model combined with an SVM classifier and [11] where the authors use an unsupervised Bayesian approach.

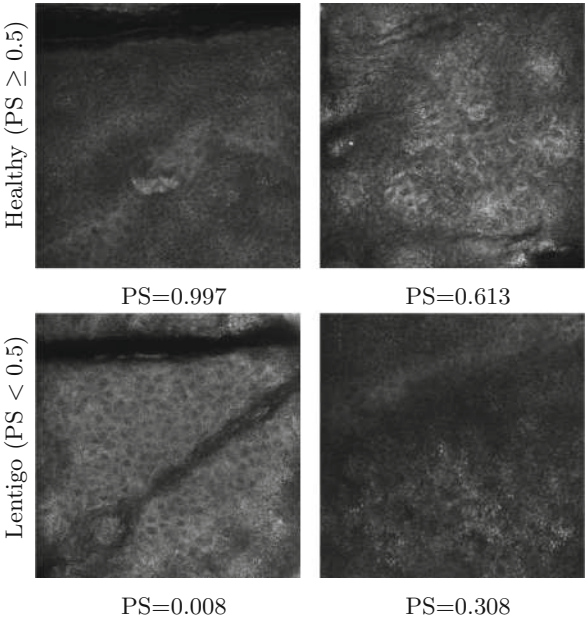


Fig. 6. Correct classification examples of RCM images for Healthy and Lentigo patients classified by the proposed method.

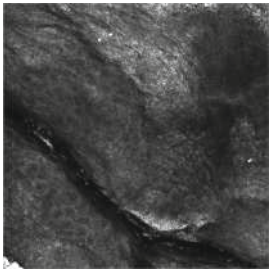


Fig. 7. The only false classification (PS = 0.0005).

Table 4. Comparison performance with state of the art methods.

Lentigo detection method	Accuracy
Halimi et al. 2017 [10]	84.4%
Halimi et al. 2017 [11]	97.7%
Proposed method	98,14%

5 Conclusion

In this paper, we proposed a new method to classify RCM images into healthy and lentigo skins. This method is based on the InceptionV3 CNN architecture. The network was trained with a dataset of 374 images and tested on 54 images of different stacks and depths. The suggested CNN method shows huge potential and very promising results. In future work, we will focus on applying the proposed approach to larger datasets and comparisons to other deep architectures.

Acknowledgements. The authors would like to thank Gwendal JOSSE et Jimmy Le Digabel from Lab. Pierre Fabre for providing data.

References

1. Rajadhyaksha, M., Grossman, M., Esterowitz, D., Webb, R.H., Anderson, R.R.: In vivo confocal scanning laser microscopy of human skin: melanin provides strong contrast. *J. Invest. Dermatol.* **104**, 946–952 (1995)
2. Laruelo, A., et al.: Hybrid sparse regularization for magnetic resonance spectroscopy. In: IEEE International Conference of Engineering in Medicine and Biology Society (EMBC), Osaka, Japan, 3–7 July 2013, pp. 6768–6771 (2013)
3. Albughdadi, M., Chaari, L., Tourneret, J.Y., Forbes, F., Ciuciu, P.: A Bayesian non-parametric hidden Markov random model for hemodynamic brain parcellation. *Sig. Process.* **135**(10223), 132–146 (2017)
4. Chaabene, S., Chaari, L., Kallel, A.: Bayesian sparse regularization for parallel MRI reconstruction using complex Bernoulli–Laplace mixture priors. *SIViP* **14**(3), 445–453 (2019). <https://doi.org/10.1007/s11760-019-01567-5>
5. Fakhfakh, M., Bouaziz, B., Gargouri, F., Chaari, L.: 1ProgNet: Covid-19 prognosis using recurrent and convolutional neural networks. *IEEE Trans. Artif. Intell.* (2020, submitted)
6. Geert, L., et al.: A survey on deep learning in medical image analysis. *Med. Image Anal.* **42**, 60–88 (2017)
7. Calzavara-Pinton, P., Longo, C., Venturini, M., Sala, R., Pellacani, G.: Reflectance confocal microscopy for in vivo skin imaging. *Photochem. Photobiol.* **84**, 1421–1430 (2008)
8. Yamashita, R., Nishio, M., Do, R.K.G., Togashi, K.: Convolutional neural networks: an overview and application in radiology. *Insights Imaging* **9**(4), 611–629 (2018). <https://doi.org/10.1007/s13244-018-0639-9>
9. Szegedy, C., Vanhoucke, V., Ioffe, S., Shlens, J., Wojna, Z.: Rethinking the inception architecture for computer vision. *Computing Research Repository (CoRR)* (2015)
10. Halimi, A., Batatia, H., Digabel, J., Josse, G., Tourneret, J.Y.: Statistical modeling and classification of reflectance confocal microscopy images. In: *Computational Advances in Multi-Sensor Adaptive Processing (CAMSAP)*, pp. 1–5, December 2017
11. Halimi, A., Batatia, H., Digabel, J., Josse, G., Tourneret, J.Y.: An unsupervised Bayesian approach for the joint reconstruction and classification of cutaneous reflectance confocal microscopy images. In: *European Signal Processing Conference EUSIPCO*, pp. 241–245, August 2017

12. Cendre, R., Mansouri, A., Benezeth, Y., Marzani, F., Jean, P., Cinotti, E.: Two schemes for automated diagnosis of lentigo on confocal microscopy images. In: International Conference on Signal and Image Processing (ICSIP), pp. 143–147, July 2019
13. Ève, O.: Les produits dépigmentants: le point en 2011, p. 78, September 2011
14. Cohen, L.M.: Lentigo maligna and lentigo maligna melanoma. *J. Am. Acad. Dermatol.* **33**(6), 923–936 (1995)
15. Bollea-Garlatti, L.A., Galimberti, G.N., Galimberti, R.L.: Lentigo maligna: keys to dermoscopic diagnosis. *Actas Dermo-Sifiliográficas (English Edition)* **107**(6), 489–497 (2016)
16. Andersen, W.K., Labadie, R.R., Bhawan, J.: Histopathology of solar lentigines of the face: a quantitative study. *J. Am. Acad. Dermatol.* **36**(3), 444–447 (1997)
17. Chaari, L.: A Bayesian grouplet transform. *SIViP* **13**(5), 871–878 (2019). <https://doi.org/10.1007/s11760-019-01423-6>
18. Ribani, R., Marengoni, M.: A survey of transfer learning for convolutional neural networks. In: Conference on Graphics, Patterns and Images Tutorials, pp. 47–57 (2019)
19. Shorten, C., Khoshgoftaar, T.M.: A survey on image data augmentation for deep learning. *J. Big Data* **6**(1), 1–48 (2019). <https://doi.org/10.1186/s40537-019-0197-0>
20. García, A.H., König, P.: Further advantages of data augmentation on convolutional neural networks. In: Kůrková, V., Manolopoulos, Y., Hammer, B., Iliadis, L., Maglogiannis, I. (eds.) ICANN 2018. LNCS, vol. 11139, pp. 95–103. Springer, Cham (2018). https://doi.org/10.1007/978-3-030-01418-6_10
21. Szegedy, C., et al.: Going deeper with convolutions. In: IEEE Conference on Computer Vision and Pattern Recognition (CVPR), pp. 1–9, June 2015
22. Yosinski, J., Clune, J., Bengio, Y., Lipson, H.: How transferable are features in deep neural networks? Computing Research Repository (CoRR), pp. 3320–3328 (2014)

Open Access This chapter is licensed under the terms of the Creative Commons Attribution 4.0 International License (<http://creativecommons.org/licenses/by/4.0/>), which permits use, sharing, adaptation, distribution and reproduction in any medium or format, as long as you give appropriate credit to the original author(s) and the source, provide a link to the Creative Commons license and indicate if changes were made.

The images or other third party material in this chapter are included in the chapter's Creative Commons license, unless indicated otherwise in a credit line to the material. If material is not included in the chapter's Creative Commons license and your intended use is not permitted by statutory regulation or exceeds the permitted use, you will need to obtain permission directly from the copyright holder.





Deep Learning-Based Approach for Atrial Fibrillation Detection

Lazhar Khriji^{1,2(✉)}, Marwa Fradi², Mohsen Machhout²,
and Abdulnasir Hossen¹

¹ College of Engineering, Sultan Qaboos University, Muscat, Oman
{lazhar, abhossen}@squ.edu.om

² Faculty of Sciences of Monastir, Monastir University, Monastir, Tunisia
marwafradi32@gmail.com, machhout@yahoo.fr

Abstract. Atrial Fibrillation (AF) is a health-threatening condition, which is a violation of the heart rhythm that can lead to heart-related complications. Remarkable interest has been given to ECG signals analysis for AF detection in an early stage. In this context, we propose an artificial neural network ANN application to classify ECG signals into three classes, the first presents Normal Sinus Rhythm NSR, the second depicts abnormal signal with Atrial Fibrillation (AF) and the third shows noisy ECG signals. Accordingly, we achieve 93.1% accuracy classification results, 95.1% of sensitivity, 90.5% of specificity and 98%. Furthermore, we yield a value of zero error and a low value of cross entropy, which prove the robustness of the proposed ANN model architecture. Thus, we outperform the state of the art by achieving high accuracy classification without pre-processing step and without high level of feature extraction, and then we enable clinicians to determine automatically the class of each patient ECG signal.

Keywords: ECG-classification · AF detection · Confusion matrix · ROC · ANN · Histogram error

1 Introduction

ECG signals classification is a crucial step to determine given the importance to assign to each patient its ECG class. Indeed, heart diseases have known a big spread in the last recent years. Such as arrhythmia cardiac problems like Atrial Fibrillation (AFIB). The prevalence of arterial fibrillation (AF) is increasing during the last few years and presenting the most common health problem in many countries [1]. AF presents a very critical health issue, which affects the quality of life of persons and leading to many risks such as cardiac stroke. An analysis of AF is based on a clinical evaluation and requires electrocardiogram (ECG) documentation during the arrhythmia. During the last few years, deep learning (DL) revolutionized the medical area as the deep neural networks presented the state of the art results in many applications such as computer vision, image processing, robotics, medical imaging, etc. The high performance obtained by the deep neural network is based on the use of powerful graphic processing units (GPUs) which allowed these implementations to outperform the classic ones.

Because of the outstanding development in DL, its application in medical field (using biomedical signals) is of huge interest. Accordingly, many works were developed using DL models for ECG classification. In this context, our work in this paper presents a new contribution using artificial neural network (ANN) architecture, to classify MIT-BIH dataset signal into normal and AFIB ECG signals.

The rest of this work is divided into 4 sections. Section 2 summarizes the state of the art. Section 3 presents the propounded neural network model and experimental results. Discussions and conclusion are depicted in Sects. 4 and 5, respectively.

2 State of the Art

In [2], Rahal et al. proposed a new approach for active classification of electrocardiogram ECG signals based on deep neural networks (DNN). Electrocardiogram ECG classification plays an essential role in clinical diagnosis of cardiac insufficiency. Zubair et al. in [3] proposed an ECG beat classification system based on convolutional neural network (CNN). This model is divided into two main parts, one for features extraction and the second for classification. Electrocardiogram ECG interpretation plays an important role in clinical ECG workflow. Rajpurkar et al. [4] developed a new method based on deep convolutional neural network to classify ECG signals belonging to fourteen different classes. Acharya et al. [5] did another study where they designed a novel deep CNN for ECG signals classification. Another work was proposed in [6] based on deep belief Net used for classifying heartbeats into four classes. A new method is presented in [7], which presents a new deep learning approach used for detecting atrial fibrillation in real time. In this work, authors used an end-to-end neural network combining a convolutional with a recurrent neural network (CNN, RNN) in order to extract high-level features from the input signals.

This hybrid model was trained and tested under three different datasets containing a total number of 85 classes. This model presents a particular performance by its ability of analyzing 24 h of ECG recordings in less than one second. This algorithm was tested on the three datasets in order to test its robustness and achieved the following results: 98.96% of specificity and 86.4% for sensitivity. Figure 1 presents a classic architecture of a Convolutional neural network (CNN).

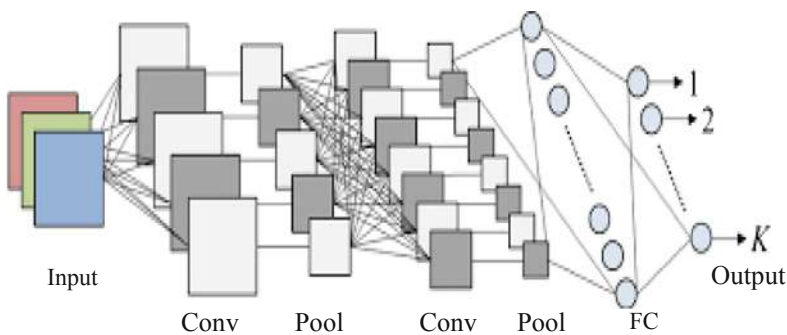


Fig. 1. A CNN classical architecture

There are many different approaches to the task of arrhythmia classification of ECG signals in terms of which method is used, which arrhythmias are classified, which data set is used, which features are extracted and whether individual beats or longer intervals are classified. For example, Rajpurkar et al. [4] uses a deep convolutional neural network trained on 30-s intervals of raw ECG signal data to classify 14 different classes, including normal sinus rhythm, noise, atrial fibrillation and atrial flutter.

Atrial fibrillation presents a very complex input data for a neural network. Deep neural networks have shown a big performance in learning non-linear input data. As deep neural network is able to learn complex pattern presenting AF in ECG signal, these techniques can widely help researchers on finding parts that are more important on the ECG to focus on during the training set. Indeed, using a CNN results accuracy overcome 95% [8, 10]. Accordingly, in [13], authors introduce a 2-channels neural network in order to address the problem of AF presence in the ECG signals. This new neural network is named “ECGNet”. By using this model, authors achieved very encouraging results coming up to 99.4% as detection accuracy in MIT-BIH atrial fibrillation dataset with 5-s ECG segments. Figure 2 presents the architecture of the proposed ECGNet neural network. This DL technique has shown its ability to detect FA in a short time process. In addition, the Attention Network has achieved 99.8 of accuracy.

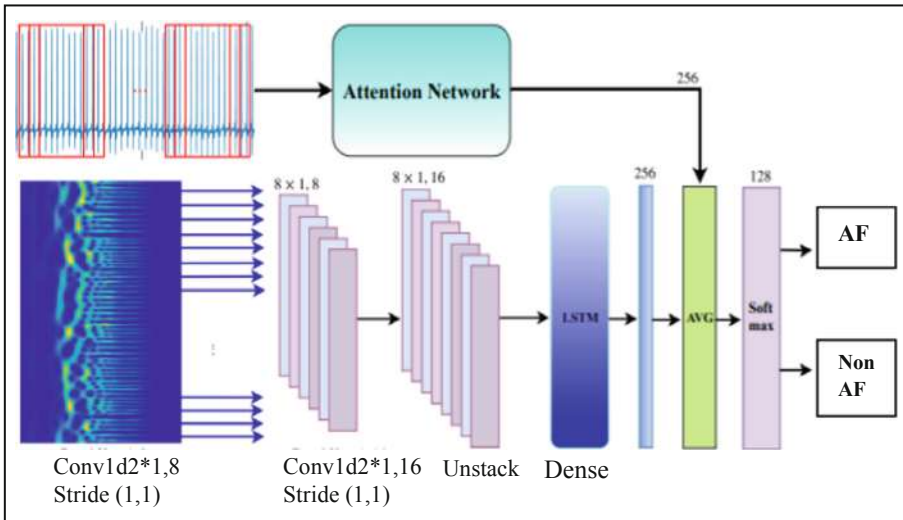


Fig. 2. ECG-Net architecture

3 Method and Results

3.1 Method

3.1.1 Dataset

The MIT-BIH dataset is known by its popularity as it has served for a long time as an interesting reference to be useful for ECG signals classification and diagnosis detection. In this context, we use three types of records from MIT-BIT dataset such as 100 samples of Normal sinus rhythm NSR, 40 samples of Atrial Fibrillation ATFIB and finally 60 samples of Noisy ECG signals. Each sample constitutes of a matrix with a size of $3600 * 1$, reaching a total of $202 * 3600$ for the input ECG data. Records as depicted in Table 1 recognize each type of signals. For each record, an atrial fibrillation should be classified similarly as a specialist would, the annotated parameters have been labelled by specialist for a long time.

Table 1. MIT-BIH dataset

Records	Samples	Matrix-size of samples	Annotations
100,101,105,109,112,113,114,115,116,117	100	$3600 * 1$	NSR
201, 202, 203, 210, 219	42	$3600 * 1$	AFIB
205, 223, 207	60	$3600 * 1$	Noisy-ECG

Each record consisted of 3600 samples, with a frequency of sampling of $1/360$ s. Figures 3, 4 and 5 represent an ECG signal of record 201, 203 and 100, respectively, with 3600 samples for each record.

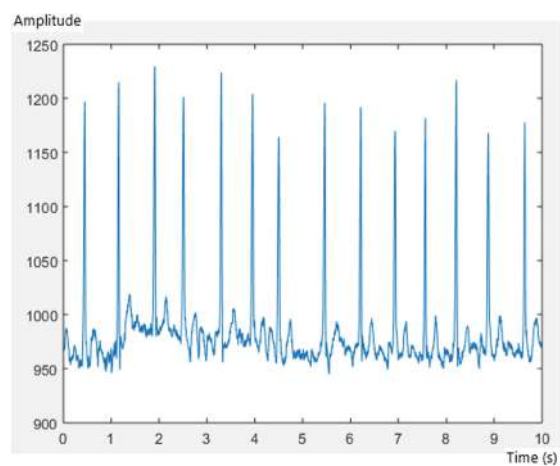


Fig. 3. AFIB ECG of record 201

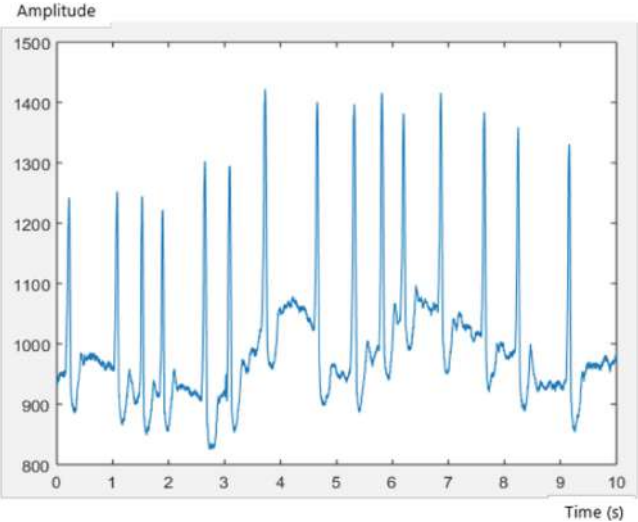


Fig. 4. AFIB ECG of record 203

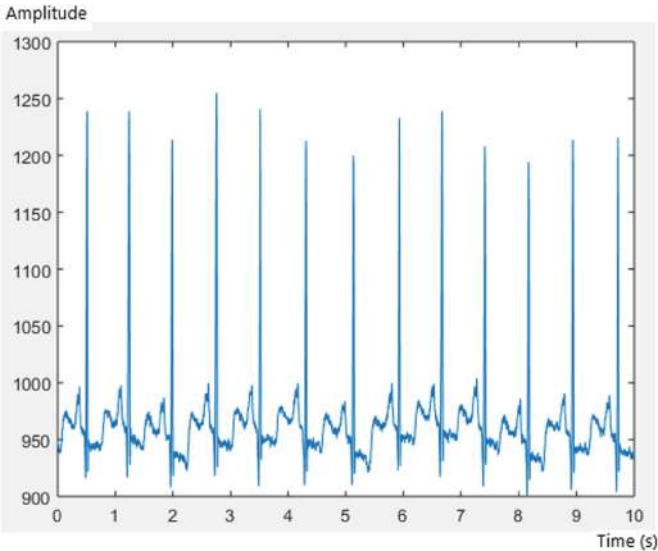


Fig. 5. SNR ECG of record 100

3.1.2 Artificial Neural Network (ANN)

The Propounded ANN Architecture

The idea of creating an artificial neural network architecture was inspired by the biological neural system [12]. Indeed, our proposed artificial neural network consists on the input layer, which contains 202 samples of ECG signals, each sample consists of a matrix sized 3600 * 1; the input dataset is a 202 samples of vectors, constituting a matrix of 3600 * 202 of ECG signals. Then, a sigmoid activation function is applied, creating a respectful numbers of parameters, which present the feature maps of the ECG signals, passing through 10 hidden layer, and 10 neurons per layer, having 100 parameters, with a sigmoid activation function as depicted by the Eq. (1). Then a softmax function, presented by the Eq. (2), is applied to classify signals into three classes the first present an AFIB signal however, the second presents a SNR signal and the third depicts noisy ECG-signals. The suggested ANN architecture is depicted in Fig. 6 and Fig. 7 (a, b and c). The latter shows the used architecture when the number of Hidden Layers (HL) is 10, 2, and 20, respectively.

$$y = \frac{1}{1 + e^{-x}} \tag{1}$$

$$Softmax(x_i) = \frac{e^{x_i}}{\sum_j e^{x_j}} \tag{2}$$

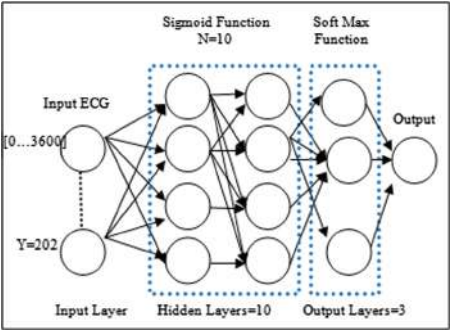


Fig. 6. Synoptic flow of the proposed ANN architecture

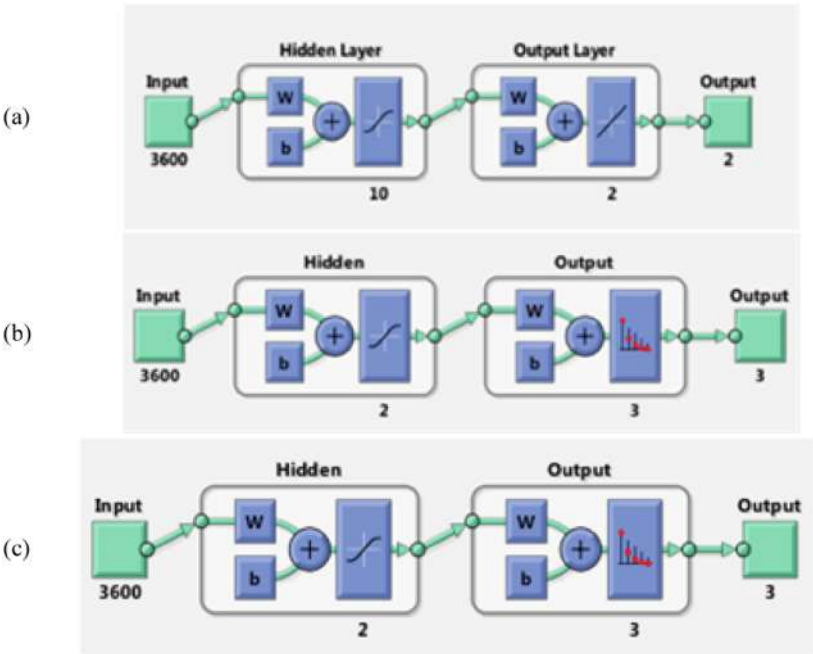


Fig. 7. ANN trained architecture: (a) ANN with HL = 10, (b) ANN with HL = 2, (c) ANN with HL = 20.

Training Data Parameters

Training parameters have a crucial role to obtain excellent accuracy. For this fact, the number of parameters should be done with the exact precision to get high accuracy, sensitivity and specificity results and to yield the best values. In fact, For ANN1, we use 10 hidden layer with 10 neurons for each layer. Thus, we obtain a number of 100 parameters, presenting the feature maps extracted from ECG signals. However, for ANN2 and ANN3, the number of hidden layers is 2 and 20 respectively. Thus,

Table 2. Training data parameters

Training parameters	ANN1	ANN2	ANN3
Iterations	1000	1000	1000
Activation function	Sigmoid	Sigmoid	Sigmoid
Classifier function	Soft-max	Soft-max	Soft-max
Hidden layers	10	2	20
Parameters numbers	100	20	200
Train-samples	142	142	142
Validation-samples	30	30	30
Test-images	30	30	30
Error-rate	0.001	0.001	0.001
Batch	3600 samples	3600 samples	3600 samples

accuracy results will be discussed in the next section. Then, more the number of iterations is increasing; more classification results are going higher. Table 2 depicts all used parameters for the ECG classification process.

3.2 ECG Classification Results

The propounded artificial neural network is presented with the confusion matrix, the histogram error, and the curve ROC and training performance results.

3.2.1 Confusion Matrix

A confusion matrix is a crucial method to determine the performance classification of a system since it divides the results into four classes such as True Positive (TP), True Negative (TN), False Positive (FP) and False Negative (FN). Accordingly, in Fig. 8, FP results are shown in the confusion matrix in the last row and the FN are depicted in the last column. It summarizes the prediction results on a classification issue. Therefore, it answers the problem of determination of the class of each signal. Indeed, it is depicted by a size of $n \times n$ associated with a classifier showing the predicted and actual classification, where n is the number of different classes. Table 1 shows a confusion matrix for $n = 3$. It gives us a sight not only into the errors being made by a classifier but more importantly the types of errors that are being made. The classification accuracy alone can be misleading where we have an unequal number of observations in each class or in case of having more than two classes in the dataset. Calculating a confusion matrix gives a better idea of what a classification model is getting right and what types of errors it is making. Indeed, performance results are calculated by the following equations presenting the sensitivity, the specificity and the accuracy.

$$\text{Sensitivity (True positive rate)} = \frac{TP}{TP + FN} \quad (3)$$

$$\text{Specificity (False positive rate)} = \frac{TN}{TN + FP} \quad (4)$$

$$\text{Accuracy (percent of all samples correctly classified)} = \frac{TN + TP}{TN + TP + FN + FP} \quad (5)$$

The prediction results (Fig. 8) show an accuracy of 100% for the training process, 80% for the validation process and 73.3% for the testing process. These results presented a high precision of classification, which proves the robustness of the used artificial neural network architecture. Indeed, there are no misclassified signals in the training confusion matrix. However, in the validation confusion matrix in all confusion matrix a value of 0% for misclassified signal is achieved. The green colour in the confusion matrix represents the true positive classified ECG signals; however, the red colour depicts the misclassified signals. The first class presents the atrial fibrillation

ECG signal, the second-class presents the SNR classified ECG signals. We used 142 records in the training process, where 69 records are classified as SNR signals, 28 records are classified as AFIB signals and 45 records are classified as noisy ECG signals, yielding a value of 100% of sensitivity and specificity. Moreover, for the validation stage, we used 30 records where 24 records are well-classified achieving accuracy value of 80%. Accordingly, test process achieved also a value of 73.3, where 22 records with 3600 samples for each record are well assigned to the right class, and 8 records are misclassified (3 records for the first class, 2 records for the second class and 3 records for the third class). These results are achieved due to the proposed architecture with 10 hidden layers, 10 neurons for each layer, with a sigmoid activation function and finally Softmax classifier proves its ability not seen before by the system. However, using a small number of hidden layers, the accuracy classification is with 82.6% and 87% using a high number of layers. Thus, the choice of a precision number of hidden layers for getting precise number of parameters shows its worth in the ECG-classification process.

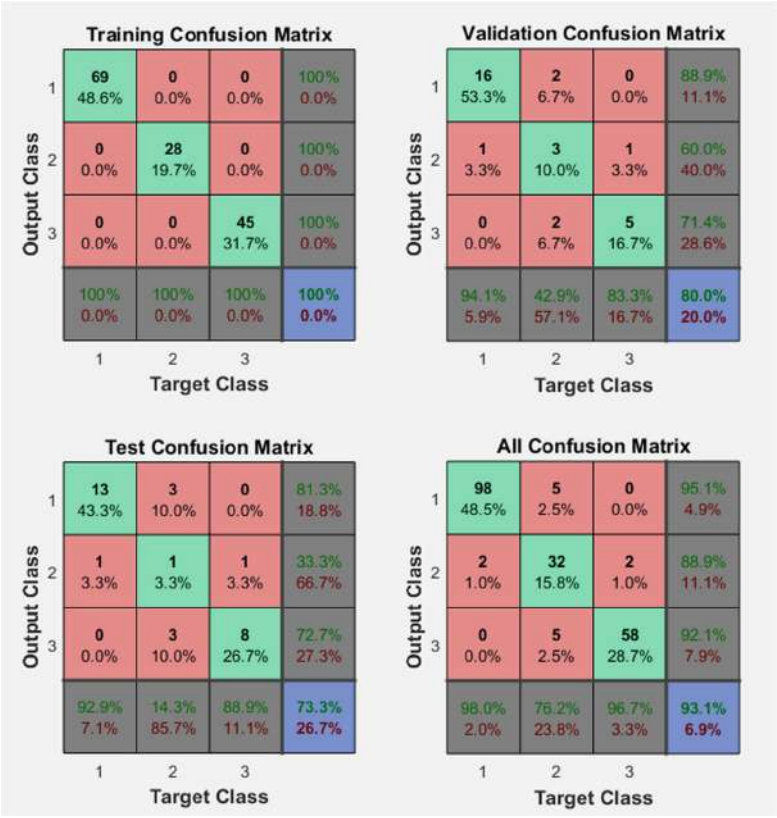


Fig. 8. Confusion Matrix: training, validation and testing results with ANN1

3.2.2 Histogram Error

The histogram error determines the rate of the existent error in classifying the signals used for training, for validation and for testing. The precision shows whether the classification is well done or not (i.e. with errors). Indeed, in our ECG signals classification results yield roughly 0.07% errors as depicted in Fig. 9 where the data fitting errors are presented within a reasonably good range close to zero.

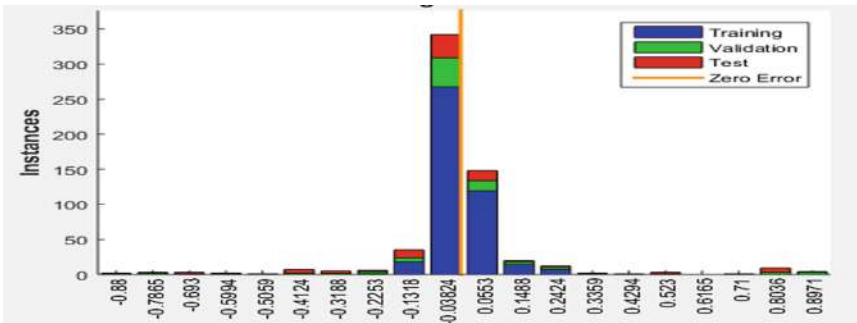


Fig. 9. Histogram error results where Errors = Targets–Outputs

3.2.3 Receiver-Operating Curve (ROC)

The ROC curve (Fig. 10) is a graphical tool allowing presenting the capacity of a test to discriminate between different classes. It plays a huge role to depict TP rate against FP

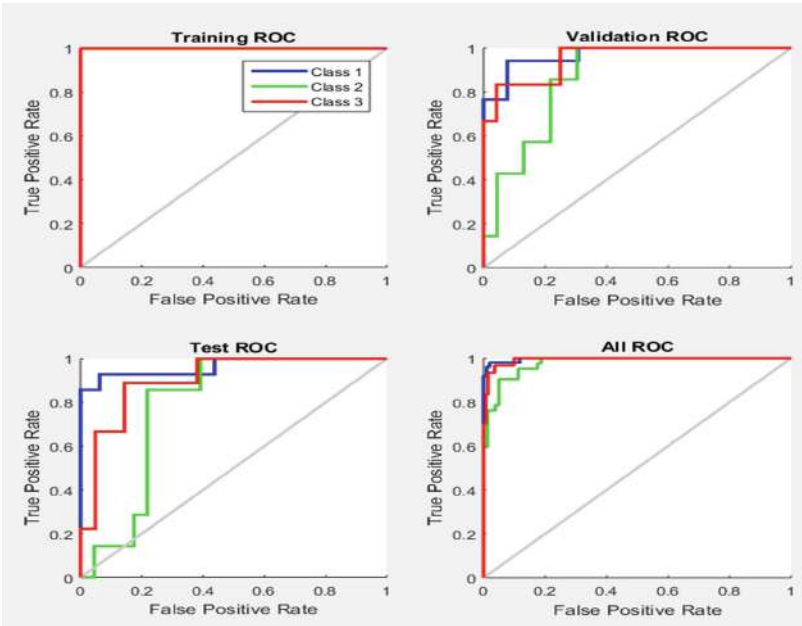


Fig. 10. ROC results

rate in medical statistics and more specifically in the field of ECG signals classification. Indeed, within our proposed ANN, we have an excellent rate of classification as seen in the ROC and a perfect prediction would yield an AUC of 0.93, presenting a value close to 1 for the training process, blue coloured in the curve. Similarly, test and validation process present high accuracy rate according to the curve.

3.2.4 Cross Entropy Results

Table 3 shows the cross entropy and errors result through the training, the validation and the testing neural network process. Indeed, it is important to have low values of cross entropy to achieve good classification results. As presented in Fig. 11, the cross entropy value is roughly low which proves the efficiency of our model. Accordingly, Percent error indicates the fraction of samples, which are misclassified. A value of 0 means no misclassifications, 100 indicates maximum misclassifications.

Table 3. Cross-entropy and error results

Process	Numbers of records	Length of each record	Cross-entropy	Error
Training	142	10-s	$5.91e^{-1}$	0
Validation	30	10-s	$1.94e^0$	20
Testing	30	10-s	$1.95e^0$	26.7

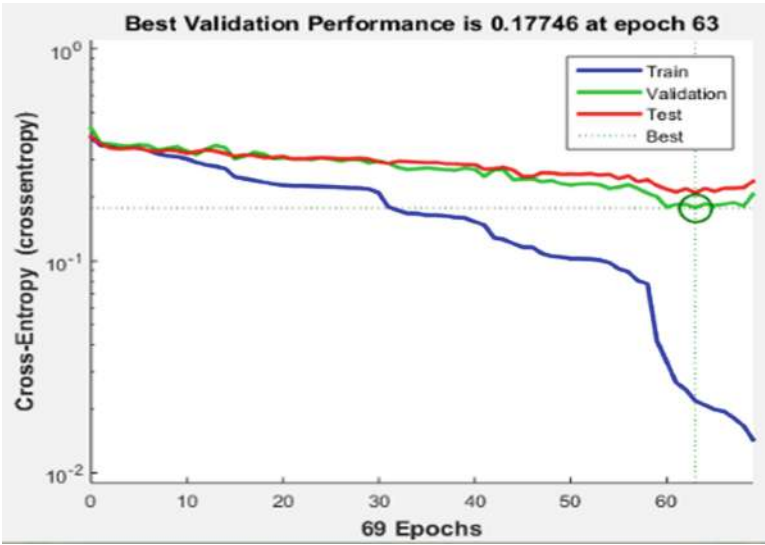


Fig. 11. Best performance results

3.2.5 Processing Time

Experimental results obtained from using the MIT-BIH Arrhythmia Database showed that the processing time efficiency of our system can be highly increased by implementing the algorithm on GPU instead of the actual CPU. By using CPU, our algorithm took 2.052 s to make the real time classification of an ECG signal. Nevertheless, further improvement can be done on this method to achieve higher accuracy with less processing time.

4 Discussions

The ANN application for ECG signals classification demonstrates greater accuracy compared to the state of the art, which proves that the ANN system is able to get more and more advanced results. Indeed, the state to have 100% of accuracy and 0% of error is hard to achieve. Despite this problem, ANN achieves high accuracy in comparison with related works. In [2], authors achieved 86% of accuracy. Accordingly, our ANN method overcomes results depicted in [2] with 7% of accuracy for ECG signals classifications. Indeed more, we are going deeper through layers, more accuracy results are better. We have achieved the top accuracy for MIT-BIH-ECG signal classification using the artificial neural network model by a value of 93.1% of accuracy where CNN comes with the third top accuracy with 92.7%. In Fact, we overcome [9], where authors proposed an Echo state neural network, with 92.7% of accuracy. Moreover, we surpass the state of the art in [11] with more than 3% of accuracy, and we have an error close to zero in histogram error detection with a low value of cross entropy, which proves the robustness of our classifier model. To conclude, the achieved results as depicted in Table 4 are comparable with the state of the art in fully automatic ECG classifiers and even outperform other ECG classifiers that follow more complex feature-selection approaches. Indeed, as presented in Table 4, we achieved encouraging results coming up to 93%, close to ECG –Net that is very complex and time consuming (it is using a huge amount of parameters and samples leading to increase the network complexity). Thus, there is no doubt to say that we succeed to better compromise between the testing accuracy and the network parameters complexity.

Table 4. Comparative study with the state of the art

Method	Best accuracy	Time process
Our work: ANN1	93.1%	2.052 s
CNN + FCN layers [2]	86%	–
DenseNet [11]	89.5%	–
SVM [3]	87.5%
Echo state networks [9]	92.7%
ECG-Net [13]	94.0%

5 Conclusion

In this paper, we have achieved the top accuracy of MIT-BIH-ECG signal classification using the artificial neural network model by a value of 93.3% of test-accuracy, of sensitivity and of precision. Accordingly, the ROC shows an excellent curve of rate classification results. Accordingly, the histogram presents 0.07% error, which overcomes the state of the art without a huge number of feature extraction and without pre-processing stage. Our method is promising and can help clinicians to determine the class of each ECG patient. Indeed, for going faster, the next step will be dedicated to our application implementation on GPU and then on an FPGA.

Acknowledgment. The authors would like to thank OMANTEL and Sultan Qaboos University for their financial support, grant number “EG/SQU-OT/18/01”.

References

1. Visa, S., Ramsay, B., Ralescu, A.L., Van Der Knaap, E.: Confusion matrix-based feature selection. *MAICS* **710**, 120–127 (2011)
2. Pyakillya, B., Kazachenko, N., Mikhailovsky, N.: Deep learning for ECG classification. In: *Journal of Physics Conference Series*, vol. 913, no. 1, p. 012004. IOP Publishing (2017)
3. Celin, S., Vasanth, K.: ECG signal classification using various machine learning techniques. *J. Med. Syst.* **42**(12), 241 (2018)
4. Rajpurkar, P., Hannun, A.Y., Haghpanahi, M., Bourn, C., Ng, A.Y.: Cardiologist-level arrhythmia detection with convolutional neural networks (2017). ArXiv e-prints, arXiv: 1707.01836
5. Acharya, U.R., et al.: A deep convolutional neural network model to classify heartbeats. *Comput. Biol. Med.* **89**, 389–396 (2017)
6. Wu, Z., et al.: A novel features learning method for ECG arrhythmias using deep belief networks. In: 2016 6th International Conference on Digital Home (ICDH), pp. 192–196. IEEE (2016)
7. Andersen, R.S., Peimankar, A., Puthusserypady, S.: A deep learning approach for real-time detection of atrial fibrillation. *Exp. Syst. Appl.* **115**, 465–473 (2019)
8. Kachuee, M., Fazeli, S., Sarrafzadeh, M.: Ecg heartbeat classification: a deep transferable representation. In: 2018 IEEE International Conference on Healthcare Informatics (ICHI), pp. 443–444. IEEE (2018)
9. Alfaras, M., Soriano, M.C., Ortín, S.: A fast machine learning model for ECG-based heartbeat classification and arrhythmia detection. *Front. Phys.* **7**, 103 (2019)
10. Ji, Y., Zhang, S., Xiao, W.: Electrocardiogram classification based on faster regions with convolutional neural network. *Sensors* **19**(11), 2558 (2019)
11. Guo, L., Sim, G., Matuszewski, B.: Inter-patient ECG classification with convolutional and recurrent neural networks. *Biocybern. Biomed. Eng.* **39**(3), 868–879 (2019)

12. Bouallegue, K.: A new class of neural networks and its applications. *Neurocomputing* **249**, 28–47 (2017)
13. Mousavi, S., Afghah, F., Razi, A., et al.: ECGNET: learning where to attend for detection of atrial fibrillation with deep visual attention. In: 2019 IEEE EMBS International Conference on Biomedical & Health Informatics (BHI), pp. 1–8. IEEE (2019)

Open Access This chapter is licensed under the terms of the Creative Commons Attribution 4.0 International License (<http://creativecommons.org/licenses/by/4.0/>), which permits use, sharing, adaptation, distribution and reproduction in any medium or format, as long as you give appropriate credit to the original author(s) and the source, provide a link to the Creative Commons license and indicate if changes were made.

The images or other third party material in this chapter are included in the chapter's Creative Commons license, unless indicated otherwise in a credit line to the material. If material is not included in the chapter's Creative Commons license and your intended use is not permitted by statutory regulation or exceeds the permitted use, you will need to obtain permission directly from the copyright holder.





Unsupervised Method Based on Superpixel Segmentation for Corpus Callosum Parcellation in MRI Scans

Amal Jlassi^{1(✉)}, Khaoula ElBedoui^{1,2}, Walid Barhoumi^{1,2},
and Chokri Maktouf³

¹ Institut Supérieur d'Informatique, Research Team on Intelligent Systems in Imaging and Artificial Vision (SIIVA), LR16ES06 Laboratoire de recherche en Informatique, Modélisation et Traitement de l'Information et de la Connaissance (LIMTIC), Université de Tunis El Manar, Tunis, Tunisia
amal.jlassi1991@hotmail.com

² Université de Carthage, Ecole Nationale d'Ingénieurs de Carthage, Tunis, Tunisia
{khaoula.elbedoui,walid.barhoumi}@enicarthage.rnu.tn

³ Nuclear Medicine Department, Pasteur Institute of Tunis, Tunis, Tunisia

Abstract. In this paper, we introduce an unsupervised method for the parcellation of the Corpus Callosum (CC) from MRI images. Since there are no visible landmarks within the structure that explicit its parcels, non-geometric CC parcellation is a challenging task especially that almost of proposed methods are geometric or data-based. In fact, in order to subdivide the CC from brain sagittal MRI scans, we adopt the probabilistic neural network as a clustering technique. Then, we use a cluster validity measure based on the maximum entropy (Vmep) to obtain the optimal number of classes. After that, we obtain the isolated CC that we parcel automatically using SLIC (Simple Linear Iterative Clustering) as superpixel segmentation technique. The obtained results on two challenging public datasets prove the performance of the proposed method against geometric methods from the state of the art. Indeed, as best as we know, it is the first work that investigates the validation of a CC parcellation method on ground-truth datasets using many objective metrics.

Keywords: Corpus callosum · MRI · Parcellation · Superpixel

1 Introduction

Thanks to advances in magnetic resonance imaging, neuroscientists and clinicians can study in depth the Corpus Callosum (CC) and mainly the correlation between the CC's dimensions and some neurological diseases. The CC, which is the largest white matter structure and the biggest fiber tract connecting corresponding regions of the cerebral cortex in the two cerebral hemispheres, integrates motor, sensory, and cognitive functions of the brain [1]. Anatomically,

more than half of the axons composing the CC are surrounded by myelin, which gives this structure its remarkable appearance in midsagittal T1-weighted MRI images. However, in many sagittal brain MRI slices, the fornix appears in the neighborhood of the CC with a similar intensity (Fig. 1) [2]. The CC is usually divided into smaller regions such as rostrum, genu, body, and splenium. This subdivision of the CC is called parcellation and it is proving to be very useful for an effective analysis of the CC [2,3]. In fact, the CC shape may be the cause of many neurodegenerative diseases such as epilepsy, alzheimer, autism, depression and other types of psychosis [4]. The CC analysis is also important for studying aging, gender differences and laterality [5]. Hence, various studies have evaluated shape or volume variation of the CC parcels. They revealed a correlation between CC's abnormalities and many diseases. For instance, [6] shows that the rate of change in CC or one of its sub-regions is more closely associated with the progression of Alzheimer's disease. Moreover, the CC parcelling can be an appropriate group biomarker for an objective evaluation of treatments aimed at slowing the progression of Alzheimer [7]. Furthermore, several works have identified volume alterations of the CC and its sub-regions in subjects with Autism Spectrum Disorders (ASD). In this context, a study of the CC volume of 40 pre-schoolers, with different sex and age, suffering from ASD was made by applying the "FreeSurfer" automated parcellation software. This study demonstrated that the total volume of the CC and its sub-regions is correlated with autism severity [8]. Another study conducted on 75 participants with Parkinson Disease (PD) and 24 Healthy Control (HC) confirms that CC sub-regions abnormalities might be the cause of Parkinson disease. Indeed, participants with PD showed an increase in the 3 anterior callosal segments compared to HC [9].

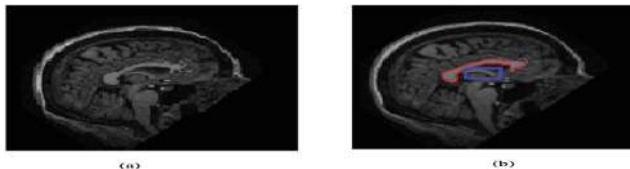


Fig. 1. Example of sagittal brain MRI slices from the OASIS dataset: (a) The input MRI. (b) Delineation of the CC, where the fornix (framed in blue) appears in the neighborhood of the CC while being of similar appearance. (Color figure online)

Generally, the CC parcellation into callosal regions allows for a precise differentiation of motor connectivity and the structural integrity of these tracts in the CC [10]. Thus, the CC parcellation should be so helpful to better understand inter-hemispherical callosal connectivity in patients or healthy subjects [11]. In particular, MRI takes advantage of the macroscopic geometrical arrangement of white matter bundles that it makes capable of generating good CC visualization from the sagittal plane. In any way, the parcellation of the CC stills an important task for radiologic assessment despite there are no real or visible borders

to allow this subdivision. Nevertheless, the visual inspection of CC structures in MRI scans suffers from both inter- and intra-specialist variability. On the one hand, the manual CC segmentation methods require strongly visual effort, specialized training skill, and are time-consuming processes. On the other hand, several geometrical methods for the CC parcellation have been proposed such as Witelson and Hofer methods [12]. However, these methods cannot be satisfactorily validated due to the lack of qualitative parameters and reference standards. Although all these difficulties, the development of an automatic CC parcellation method is an inescapable need to ensure a reliable diagnosis. Such parcellation is so independent from the operator skills and may be extended to other brain structures parcellation. Thus, since there are no visible landmarks indicating where the CC should be subdivided, the development of a fully automatic CC parcellation method is highly challenging, even for specialists. To deal with this issue, we propose to automatically parcel the CC within MRI images. By validating it, for the first time, on large and public datasets, the proposed method records promising results. In fact, the contribution of this work is twofold:

- As best as we know, we adopt for the first time the superpixel segmentation algorithm called Simple Linear Iterative Clustering (SLIC) for the CC parcellation [13]. Despite its simplicity, SLIC has been demonstrated to be effective in various computer vision applications [14].
- The subdivision process of the proposed method is fully automatic and it is the second study that proposed a non-geometric analysis for the CC parcels, to the best of our knowledge [15]. Although it is based only on the MRI data of each analyzed subject, with no parameter adjusting, the proposed method proved quantitatively its superiority over state-of-the-art methods.

The rest of this paper is organized as follows. In Sect. 2, we briefly review existing methods for the CC parcellation. Section 3 presents the proposed method based on SLIC. Experimental results are discussed in Sect. 4. The last section concludes the paper and points some directions for future work.

2 Related Work

Few CC parcellation methods were proposed. However, most of these methods have not surmounted all the challenges encountered. In fact, the CC parcellation is a challenging task given that a normal shape of the CC might not clearly highlight all parcels, what can increase the diagnosis complexity. In addition, many internal abnormalities might include bumps which are hard to detect. Existing CC parcellation methods can be divided into two main classes: geometric methods and non-geometric ones. On the one hand, since there are no real or visible boundaries allowing the CC parcellation, several geometrical methods were presented to perform this task. Among these methods, two particular ones are widely adopted. The first was proposed by Witelson and it is based on postmortem connectivity analysis in primates and humans [16]. This method divides the CC into five regions ranging from anterior dimension to the posterior

dimension. The CC subdivision is done into an anterior third, the middle of the anterior and posterior midbody, a posterior third and the posterior one-fifth. The rostrum, genu, and rostral body presenting the regions of the anterior third illustrate the prefrontal, premotor, and supplementary motor cortical areas. However, the posterior midbody is crossed by the somaesthetic and posterior parietal fiber bundles. The sub-regions of the posterior third, containing the isthmus and splenium, are allocated to temporal, parietal, and occipital cortical regions. Thus, this parcellation method, and as any geometric methods, neither reflects the real texture nor the internal organization of the CC. In addition, the CC parcellation is strongly dependent on the brain conservation process, since it is based on post-mortem data. Differently, Hofer proposed the only work based on tractography of DTI (Diffusion Tensor Imaging) by subdividing the CC into five regions from an average behavior observed via tractography in a specific population of 8 subjects [1]. As already proposed by Witelson, the geometric baseline in the midsagittal section of the CC is defining the anterior and posterior points of the structure. The first region, which represents the first sixth, contains fibers projected in the prefrontal region. The remainder of the anterior half CC illustrates the second region containing the fibers that form the motor and motor areas of the cerebral cortex. In fact, these fibers form together the largest CC region and are placed in the back section of the structure. The third region presents the posterior half minus the posterior third. It contains fibers responsible for the primary motor cortex. However, this part of the parcellation scheme is in conflict with Witelson's method. The fourth region forms third minus the posterior quarter, presenting the primary sensory fibers. The last and the fifth region represents the CC posterior quarter crossed by the parietal, temporal and visual fibers. Figure 2 shows a comparison between the geometric schemes proposed by Witelson and Hofer. We notice that geometric methods allow only to divide the CC into the same regions among all subjects without considering the human and individual brain features between different subjects. On the second hand, differently to geometric parcellation methods, Rittner proposed a data-driven method based on the Watershed technique [15]. This method is composed of four steps. The first step consists in the weighting of the fractional anisotropy. The second step performs the selection of the brain midsagittal plane, followed by the third and the last step which are the CC segmentation using the Watershed technique, and its parcellation with fixed markers. Nevertheless, this method suffers from sensitivity to parameters selection. In order to overcome its limitations, Cover extended the Rittner method with some important changes [12]. Practically, the author replaced all steps except the first step in order to lead to a more robust data-driven method. Indeed, the parcellation is improved by applying the K-means algorithm after defining the CC centerline. When comparing this method to that of Rittner, and although both are based on Watershed, it is confirmed that this method had a better generalization ability using no fixed markers to execute the Watershed transform. However, due to the lack of quantitative metrics and reference standards, these methods cannot be correctly validated.

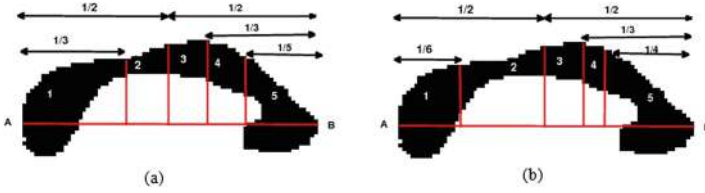


Fig. 2. CC geometric parcellation with divisions presenting the five regions (on an MRI scan from the OASIS dataset) using the method of: (a) Witelson. (b) Hofer.

3 Proposed Method

Differently to existing methods, we propose a subdivision scheme that considers only the MRI data [14]. Using the SLIC superpixel segmentation technique, the method is composed of two main steps: CC segmentation and CC parcellation. This comes from that the SLIC presents one of the most popular images over segmentations that is commonly used as supporting regions for primitives to reduce computations in various computer vision tasks.

3.1 CC Segmentation of the Midsagittal Slice

We adopt herein our previous method [17] for the automatic CC segmentation of MRI sagittal section. It includes three main steps: image preprocessing using the Anisotropic Diffusion Filtering (ADF), classification based on the unsupervised Probabilistic Neural Network (PNN) classifier, and CC isolation using a spatial filtering (Fig. 3). In fact, the first step aims to enhance the signal-to-noise ratio by eliminating unwanted parts in the background and smoothing the internal part of the region while preserving its borders. In fact, ADF allows to unblock high-frequency noise while preserving the main edges of structures [18]. Then, the classification step permits to define the target classes using K-means, before classifying them by the PNN [17]. Thereafter, the Vmep index, which is based on the maximum entropy principle as an evaluation method that is called the cluster validity, is applied in order to determine the optimal number of clusters. The optimal number of classes is obtained when the Vmep validity index reaches its maximum value. This number is adopted for the PNN classification process to obtain the final cluster map. Once the CC class is identified, the CC region will be isolated by a spatial-based filtering. Finally, we defined the CC contour by applying a follow-up algorithm on the border pixels of the CC region that are characterized by a maximum of the spatial gradient [19].

3.2 CC Parcellation

We propose a CC parcellation method based on SLIC, which is non-geometric and fully automatic superpixel segmentation technique. It works with no parameter adjusting and with no instantaneous training, leading to a more robust technique. Thus, in order to segment the CC into a set of superpixels, which refer

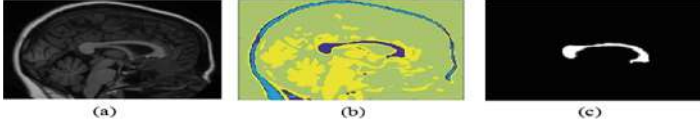


Fig. 3. CC segmentation: (a) Input sagittal MRI. (b) Cluster Map. (c) Isolated CC.

to groups of pixels that represent perceptually significant small defined regions, we adopt the SLIC technique. It is an arrangement of K-means for superpixel generation in order to be faster than existing methods, more memory efficient while improving significantly the segmentation accuracy. It allows two important directions [14]. Firstly, it reduces greatly the number of distance calculations by restricting the search space to a region corresponding to the superpixel size. Therefore, a reduction in the complexity of being linear is achieved in the pixels' number N and superpixels' number K that is independent and user-defined. In our case, N and K are equal to 256 and 200, respectively. Secondly, a combination of color and spatial proximity is reached by a weighted distance measure that allows both controls over the size and compactness of the superpixels. Thus, each slice of the input MRI image is partitioned into different size regions. In fact, the initial grid size is defined as S (1). From the geometric center, the center superpixel of each region is computed. This geometrical center of each region is recursively updated in each iteration.

$$S = \sqrt{\frac{N}{K}}. \quad (1)$$

In order to regroup the pixel, both spatial and intensity distances are used. The spatial distance between the pixels i and j is defined as follows (2):

$$S_d = \sqrt{(p_j - p_i)^2 + (q_j - q_i)^2}, \quad (2)$$

where the coordinate values of pixel i and j are represented by p and q . The Eq. 3 calculates the intensity distance.

$$I_d = \sqrt{N_j + N_i}, \quad (3)$$

where N_j and N_i represent the normalized intensity of pixel j and i , respectively. Equation 4 defines the combined distance measure C_d of spatial and intensity.

$$C_d = \sqrt{I_d^2 \cdot \left(\frac{S_d}{S}\right)^2 + e^2}, \quad (4)$$

where e denotes the compactness coefficient. In fact, larger value of e illustrates more compact segments, whereas lower value of e represents flexible boundaries. The compactness coefficient is fixed in the range of $[0, 1]$. The superpixel computation of the proposed method is shown in Fig. 4.

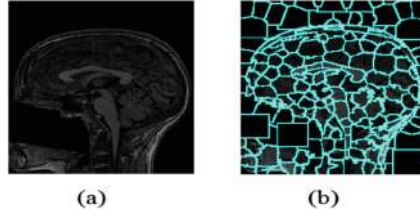


Fig. 4. SLIC-based parcellation: (a) The input MRI. (b) Result of the SLIC method.

4 Experimental Results

For the evaluation of the proposed parcellation method, we are the only study that used brain MRI scans from two public datasets. On the one hand, we used the Open Access Series of Imaging Studies (OASIS) dataset, which is freely available on www.oasis-brains.org. It is created by Washington University Alzheimer’s disease Research Centre. This MRI dataset included a longitudinal collection of 416 subjects aged between 18 and 96 years, men and women, including 100 individuals with very mild to moderate Alzheimer’s disease (AD). All images were acquired on the same scanner using the same sequences. Each subject was scanned on two or more visits, separated by at least one year for a total of 373 imaging sessions. Each MR image within this dataset is composed of 128 slices with a resolution of 256×256 ($1 \times 1mm$). In this work, we selected 1806 sagittal images that are qualified by a quality control according to severe artifacts. On the other hand, Autism Brain Imaging Data Exchange (ABIDE) is also investigated. In order to accelerate understanding of the neural bases of autism, the ABIDE dataset has supplied functional and structural brain imaging data collected from laboratories around the world. This dataset is composed of two large-scale collections called ABIDE-I and ABIDE-II. Each collection was collected independently across more than 24 international brain imaging laboratories. Thus, we generate a total of 2200 sagittal images with a resolution of 256×256 . It is worthy noting that we have a challenging heterogeneous set of images of normal subjects and individuals with Autism and Alzheimer.

4.1 Qualitative Evaluation

For each subject, the proposed parcellation method gives an apparent variation in the positioning of the CC parcels. This is because this method is purely automatic and does not follow any atlas or any prior knowledge (Fig. 5). The geometric methods of Hofer and Witelson do not present the variation of their proportion of CC parcels and consequently, the same behavior can be observed on the results of all the subjects. Figure 5 shows that the proposed CC parcellation method is more similar to the Hofer parcellation than the Rittne one. This can be explained by the fact that Hofer subdivisions are based on the connections of the cortical fibers to find the CC parcels. The largest differences between

the proposed parcellation and that of Witelson are observed in the parcels 1 and 4. In fact, according to our collaborator clinician expert, the CC shape and parcellation are well defined and the delineated CC area shows closely the five anatomical subdivisions of the CC, especially the critical ones: the rostrum and the splenium. The fornix is correctly removed from the CC area and the obtained CC parcellation shows a precise subdivision of CC into five regions within brain MRI scans, without penetrating the irrelevant neighboring structures. Note that, within the selected sample of MRI brain scans, the CC is extracted and parcelled both on female (column 1 and 3) and male (column 2 and 4) subjects. In fact, we applied the proposed method on subjects from the ABIDE dataset (column 1 and 2) as well as from the OASIS dataset (column 3 and 4).

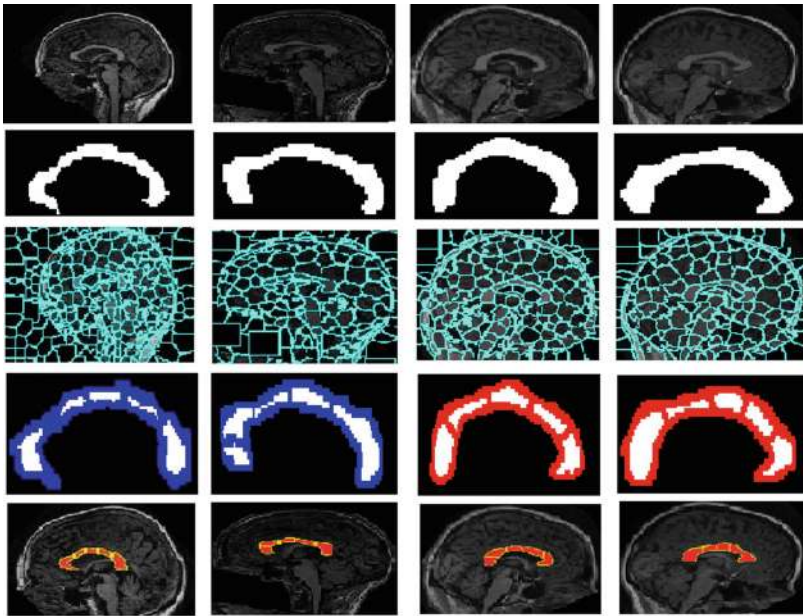


Fig. 5. Experimental results: 1st line: Input image. 2nd line: Isolated CC. 3rd line: Brain parcellation. 4th line: Proposed CC parcellation. 5th line: Ground-truth.

4.2 Quantitative Evaluation

In order to evaluate the performance of the proposed method, we used the following commonly used metrics: Dice, accuracy, sensitivity, specificity and precision.

- The Dice coefficient (5) is a statistical measure that is used for comparing the similarity of two sample sets.
- The accuracy (6) is defined as the rate of correctly classified items.
- The sensitivity (7) is the proportion of positive items correctly classified.
- The specificity (8) is the rate of negative items rightly identified.

- The precision (9) is the ratio of correctly predicted positive samples to the total predicted positive samples.

$$Dice = \frac{2 \times TP}{2 \times TP + FN + FP} \quad (5)$$

$$Accuracy = \frac{(TP + TN)}{(TP + FN + TN + FP)} \quad (6)$$

$$Sensitivity = \frac{TP}{(TP + FN)} \quad (7)$$

$$Specificity = \frac{TN}{(TN + FP)} \quad (8)$$

$$Precision = \frac{TP}{(TP + FP)} \quad (9)$$

TP refers to the True Positive (region correctly parcelled as the concerned parcel), TN refers to the True Negative (region correctly classified as background), FP refers to the False Positive (region which is parcelled as the concerned parcel) and FN refers to the False Negative (region which is incorrectly classified as background). We notice that we produce five parcels, and for each parcel we measure the five metrics. It is worthy noting that for the first time, a very useful ground-truth for CC segmentation and parcellation within the challenging widely used OASIS and ABIDE datasets is used. Therefore, we are the only work that is compared to a such ground-truth. However, the Rittner method is evaluated only on the agreement between the results achieved by different CC parcellation methods. In fact, a professional neurologist from Pasteur Institute of Tunis and a junior doctor have been charged with manually preparing the CC regions and parcels from all images belonging to the OASIS and the ABIDE datasets. Besides, we applied post-processing in order to exclusively extract the CC area and parcels. Table 1 shows the recorded results comparatively to the ground-truth. It is clear that the Proposed Method (PM) records the higher Dice coefficient score (> 0.84) in the parcels 1, 2, and 5, and a sufficient Dice coefficient score (> 0.75) in parcels 3 and 4 comparatively to the ground-truth. Evenly, it reaches a higher accuracy, specificity and sensitivity scores with values > 0.90 . The decline of the proposed method performance according to the precision metric can be explained by the cause of the ground-truth which is manually drawing and the processing applied to do the evaluation in each parcel. Furthermore, for the two datasets and for each CC parcel, the Dice coefficient was computed pairwise for the methods of the state of the art (Table 2) as it is used in the Rittner work. Therefore, the previous analyzes allow only verifying the similarity between the resulting CC parcels, or which present statistical differences between methods of the literature since this is a problem without a gold standard (Table 2). Hence, it is now possible to know the correct CC parcellation by producing ground-truth for both Witelson and Hofer methods. Since the Hofer and Witelson CC parcellation methods are based on geometric CC parcellation,

their results did not vary among different subjects throughout the experimented dataset. This explains this overlap measurement obtained which would have maximum value if any of the methods was the same. The most pertinent difference between these CC parcellation methods was related to the automatic and non-geometric behavior defined by our proposed parcellation. Table 2 presents different results between methods while recording interesting similarities in some cases. The proposed CC parcellation method demonstrates to be nearby to the Hofer method, mainly on parcels 1, 2 and 3, while the Witelson method presents significant statistical difference on the parcels 4 and 5.

Table 1. Evaluation of the proposed method.

	Dice	Accuracy	Sensitivity	Specificity	Precision
Parcel 1	0.9401	0.9986	0.9992	0.9986	0.7246
Parcel 2	0.8488	0.9927	0.9935	0.9927	0.4817
Parcel 3	0.7583	0.9944	0.9959	0.9944	0.5496
Parcel 4	0.7707	0.9960	0.9972	0.9960	0.6280
Parcel 5	0.8473	0.9889	0.9845	0.9890	0.3790
Mean±std	0.8330 ± 0.050	0.9941 ± 0.003	0.9941 ± 0.001	0.9941 ± 0.013	0.5526 ± 0.363

Table 2. Dice coefficient for the two datasets (best value are in bold).

	Witelson vs PM	Hofer vs. PM	PM vs. GT	Witelson vs. GT	Hofer vs. GT
Parcel 1	0.8512	0.9100	0.9401	0.6125	0.7013
Parcel 2	0.6001	0.7589	0.8488	0.2822	0.1624
Parcel 3	0.8845	0.8700	0.7583	0.4760	0.47163
Parcel 4	0.5113	0.5236	0.7707	0.4909	0.5120
Parcel 5	0.5112	0.4958	0.8473	0.6868	0.8014

5 Conclusion

CC is the biggest fiber tract within the human brain that allows the communication between the two cerebral hemispheres. The CC form and sub-regions might cause some diseases. The CC parcellation from MRI images can predict future cases of diseases or progress neurological patterns in the development of different diseases. This paper presented a fully automatic non-geometric CC parcellation based on the SLIC supervoxel algorithm, with no parameter adjusting and instantaneous training. Since there is no gold standard used to evaluate the existing methods, we produced for the first time a ground-truth led to evaluate quantitatively CC parcellation methods. Extensive experiments and quantitative comparisons with relevant CC parcellation methods, proved the accuracy of the proposed method on two challenging standard datasets. Indeed, the proposed method achieves higher performance values for each parcel. As future work, we aim to propose a super voxel method based on the SLIC algorithm, from not only MRI scans but also from functional magnetic resonance imaging.

References

1. Hofer, S., Frahm, J.: Topography of the human corpus callosum revisited—comprehensive fiber tractography using diffusion tensor magnetic resonance imaging. *Neuroimage* **32**(3), 989–994 (2006)
2. Lacerda, A., Brambilla, P., Sassi, R., Nicoletti, M.: Anatomical MRI study of corpus callosum in unipolar depression. *J. Psychiatr. Res.* **39**(4), 347–354 (2005)
3. Witelson, S., Goldsmith, C.: The relationship of hand preference to anatomy of the corpus callosum in men. *Brain Res.* **545**(1–2), 175–182 (1991)
4. El-Baz, A., Elnakib, A., Casanova, M.: Accurate automated detection of autism related corpus callosum abnormalities. *J. Med. Syst.* **35**(5), 929–939 (2011)
5. Johnson, S., Farnworth, T., Pinkston, J.: Corpus callosum surface area across the human adult life span: effect of age and gender. *Brain Res. Bull.* **35**(4), 373–377 (1994)
6. Van Schependom, J., Niemantsverdriet, E.: Callosal circularity as an early marker for Alzheimer’s disease. *NeuroImage Clin.* **19**(1), 516–526 (2018)
7. Bachman, A., Lee, S., Sidtis, J.: Corpus callosum shape and size changes in early Alzheimer’s disease: a longitudinal MRI study using the OASIS brain database. *J. Alzheimers Dis.* **39**(1), 71–78 (2014)
8. Giuliano, A., Saviozzi, I., Brambilla, P.: The effect of age, sex and clinical features on the volume of Corpus Callosum in pre-schoolers with Autism Spectrum Disorder: a case-control study. *Eur. J. Neurosci.* **47**(6), 568–578 (2018)
9. Bledsoe, I., Stebbins, G.: White matter abnormalities in the corpus callosum with cognitive impairment in Parkinson disease. *Neurology* **91**(24), e2244–e2255 (2018)
10. Domin, M., Lotze, M.: Parcellation of motor cortex-associated regions in the human corpus callosum on the basis of Human Connectome Project data. *Brain Struct. Funct.* **224**(4), 1447–1455 (2019). <https://doi.org/10.1007/s00429-019-01849-1>
11. Anand, C., Brandmaier, A., Arshad, M.: White-matter microstructural properties of the corpus callosum: test-retest and repositioning effects in two parcellation schemes. *Brain Struct. Funct.* **224**(9), 3373–3385 (2019)
12. Cover, G., Pereira, M., Bento, M.: Data-driven corpus callosum parcellation method through diffusion tensor imaging. *IEEE Access* **5**(1), 22421–22432 (2017)
13. Cover, G., Herrera, W., Bento, M.: Computational methods for corpus callosum segmentation on MRI: a systematic literature review. *Comput. Methods Programs Biomed.* **154**(1), 25–35 (2018)
14. Achanta, R., Shaji, A.: SLIC superpixels compared to state-of-the-art superpixel methods. *IEEE Trans. Pattern Anal. Mach. Intell.* **34**(11), 2274–2282 (2012)
15. Rittner, L., Freitas, P.: Automatic DTI-based parcellation of the corpus callosum through the watershed transform. *Revista Brasileira de Engenharia Biomedica* **30**(2), 132–143 (2014)
16. Witelson, S.: Hand and sex differences in the isthmus and genu of the human corpus callosum: a postmortem morphological study. *Brain* **112**(3), 799–835 (1989)
17. Jlassi, A., ElBedoui, K., Barhoumi, W., Maktouf, C.H.: Unsupervised method based on probabilistic neural network for the segmentation of corpus callosum in MRI scans. the 14th International Joint Conference on Computer Vision, Imaging and Computer Graphics Theory and Applications, no. 4, pp. 790–798 (2019)

18. Baâzaoui, A., Berrabah, M., Barhoumi, W., Zagrouba, E.: Multimodal registration of PET/MR brain images based on adaptive mutual information. In: Blanc-Talon, J., Distant, C., Philips, W., Popescu, D., Scheunders, P. (eds.) ACIVS 2016. LNCS, vol. 10016, pp. 361–372. Springer, Cham (2016). https://doi.org/10.1007/978-3-319-48680-2_32
19. Barhoumi, W., Zagrouba, E.: Boundaries detection based on polygonal approximation by genetic algorithms. *Frontiers Artif. Intell. Appl.*, 1529–1533 (2002)

Open Access This chapter is licensed under the terms of the Creative Commons Attribution 4.0 International License (<http://creativecommons.org/licenses/by/4.0/>), which permits use, sharing, adaptation, distribution and reproduction in any medium or format, as long as you give appropriate credit to the original author(s) and the source, provide a link to the Creative Commons license and indicate if changes were made.

The images or other third party material in this chapter are included in the chapter's Creative Commons license, unless indicated otherwise in a credit line to the material. If material is not included in the chapter's Creative Commons license and your intended use is not permitted by statutory regulation or exceeds the permitted use, you will need to obtain permission directly from the copyright holder.



Behavior and Activity Monitoring



Using Learning Techniques to Observe Elderly's Behavior Changes over Time in Smart Home

Dorsaf Zekri^{1,2(✉)}, Thierry Delot^{1(✉)}, Mikael Desertot^{1(✉)},
Sylvain Lecomte^{1(✉)}, and Marie Thilliez^{1(✉)}

¹ Université Polytechnique Hauts-de-France, LAMIH UMR CNRS 8201,
Hauts-de-France, France

{Dorsaf.Zekri2,Thierry.Delot,Mikael.Desertot,Sylvain.Lecomte,
Marie.Thilliez}@uphf.fr

² ReDCAD Laboratory, University of Sfax, B.P. 1173 Sfax, Tunisia

Abstract. Smart environments and technology used for elder care, increases independent living time and cuts long-term care costs. A key requirement for these systems consists in detecting and informing about abnormal behavior in users' routines. In this paper, our objective is to automatically observe the elderly behavior over time and detect anomalies that may occur on the long term. Therefore, we propose a learning method to formalize a normal behavior pattern for each elderly people related to his Activities of Daily Living (ADL). We also adopt a temporal similarity score between activities that allows to detect behavior changes over time. In change behavior period we focus on each activity to detect anomalies. A use case with real datasets are promising.

Keywords: Behavior change observation · Elderly people · Smart home · Activities of Daily Living

1 Introduction

With the growing elderly population, research in elderly living and well-being has been aimed toward medical analysis and supporting independent living of elderly people. Elderly people are often disabled by several interacting problems, such as loss of function and social and environmental factors. All these factors, separately or together, determine the elderly person's level of independence and influence his/her quality of life.

In this context, most researchers aim to improve the living of elderly people with medical issues, such as diabetes and cognitive disabilities, by analyzing the behavior of residents within sensor-based environments. The progress of technology (wearable sensors, smart phones and other mobile devices, wireless communications, etc.) enables the development of effective solutions to help older people to live independently in their homes.

The smart home concept includes homes equipped with simple environmental sensors and more complex systems including audio, video and biometric systems. The raw information captured by the sensors can obviously not be shared as such with the medical staff or used directly to detect changes in behavior automatically. On the contrary, extracted knowledge could be used to enrich the information displayed to the medical staff and improve the precision of early detections. There is evidence that opportunistic home surveillance prevents in some cases hospitalization.

In this paper, we focus on the problem of learning from smart home sensor data describing elderly's activities. Our objective in this work is to propose an approach to identify periods of time when behavior changes occur and detect anomalies in this period (e.g., the elderly sleep less and less every month). Our contributions in this paper can be summarized as follows.

1. We model a behavior pattern using training dataset, defined as the user's usual activities in his/her daily routine.
2. We calculate a daily score by comparing activity patterns. This daily score variation provides a global vision of the behavior of the elderly person over a period of time.
3. We detect anomalies related to every activity in the period of behavioral deviation.

The rest of this paper is organized as follows. In Sect. 2, we discuss related works. In Sect. 3 we present our approach. In Sect. 4 we report the experimentation of our proposal on real datasets. In Sect. 5 we present our conclusions and some research directions.

2 Related Works

With the use of smart homes, the daily activities and behavioral patterns of residents can now be monitored through sensors embedded within various areas in the home. This allows elderly people to be more independent while providing assistance to their family and caregivers. In this section, we describe some research works regarding the analysis of behavior and health monitoring for elderly people in the smart home context.

Works in [1] use anomaly detections on wearable sensors to provide an intelligent living environment for elderly residents. The detection of anomalies is based on several parameters: location, time, duration, type of activity and transitions between activities. The experiments provided consist in a semi-supervised learning approach.

[2] and [3] study elderly residents diagnosed with dementia living independently in real home environments. They applied respectively neural networks and clustering algorithms to predict sensor activity. When an error is detected, timely audio or visual prompts are sent to the dementia patients.

Gjoreski et al. [4] have proposed a system to monitor users' daily activity by combining accelerometers with an electrocardiogram (ECG) sensor. Measured

acceleration data can thus be analyzed in conjunction with the ECG signals to detect anomalies in the user's behavior and heart-related problems.

Another detection strategy was proposed by Sprint et al. [5]. First, sensor data are labeled to correspond to activity "to sleep". Features are then extracted and used as inputs to change detection algorithms such as RuLSIF, virtual classifier, and sw-PCAR to detect and analyze behavior changes that accompany health events. If the change is significant, change analysis is performed to explain the source of change. Use cases studied in this context concern older adults who experienced major health events, including cancer treatment and insomnia.

Anomaly detection systems for detecting abnormal behavior has been surveyed and reviewed in [6–8] implicitly rely of representation of the human activity in a spatiotemporal context highlighting various techniques/methods (classification, clustering, nearest neighbor, statistical).

Previous works describe existing research regarding the analysis of behavior and health monitoring from a smart home. A set of these works [1,4] only use wearable sensors to monitor vital signs. Works in [2,3,5–8] consider home sensors to monitor daily activities but do not analyze all activities of the elderly person at the same time. For example, [5] studied the behavior change related to sleeping only. All the solutions mentioned previously have been developed to quickly detect and react as soon as possible when a sudden behavior change occurs, especially "the fall" of the monitored person. Our objective in this work is, not only to detect sudden changes, but also to analyze the possible evolution of the behavior over a long period of time.

3 Our Approach

The overall objective of this study is to analyze the daily behavior of elderly people in their apartment through ambient sensors. In the following, we introduce our model to characterize the normal behavior pattern for elderly people. This normal behavior pattern can then be used to detect behavior changes over time by comparing the current behavioral data of an elderly with her/his usual behavior pattern.

3.1 Activities and Daily Behavior Pattern

Activities of Daily Living (ADLs) is a term used by healthcare professionals to refer to the basic self-care tasks an individual does on a day-to-day basis. These fundamental activities are crucial for maintaining independence. They are used by health professionals as a way of measuring an individual's functional status, especially for elderly people.

The importance of this issue has led to the development of numerous solutions that can monitor activities (e.g., [9]). Basic ADLs are self-care activities routinely performed which include, but are not limited to seven activities: sleeping, getting dressed, eating (three times per day), going to the toilet, hygiene activities (to take shower and/or bathing) and going outside.

Our notion of activity comprises two key criteria used also in [10] that are at the basis of our verification process:

1. Location: the specific place where an activity occurs, for example, “eating” takes place in the kitchen.
2. Time: the duration and occurring time of an activity. The user may perform a same activity at different times (e.g., going to the toilet) but some activities only occur at specific times of the day (e.g., eating breakfast). The start time and duration of each activity instance may be logged by the user, or better detected by an activity recognition system based on in-home sensors.

Let $A = \{a_1; a_2; \dots; a_n\}$ the set of activities labels. An activity pattern represents when and where an activity usually occurs. It is defined as a tuple:

$$P_a = (a_i, S_a(t), D_a(t))$$

where:

- $a_i \in A$ is an activity label
- $S_a(t)$ is a time interval representing the usual start time of activity a_i
- $D_a(t)$ is a time interval representing the usual duration of activity a_i

The daily behavior pattern involves several activity patterns. It defines order constraints on them and introduces eventual temporal delays. The daily behavior pattern describes how the user performs her/his activities at different times and models links between them. The daily behavior pattern is represented by a sequence of usual activities. It can be built from data derived from sensors in a smart home.

$$B = (P_{a1}, P_{a2}, P_{a3}) \text{ Where } P_{ai} \text{ is an activity pattern}$$

For each day of the week D_i we built a behavior pattern B_i which is a set of segments P_{ai} , where each segment P_{ai} is a sequence of tuples $a_i, S_a(t), D_a(t)$ related to each activity. In this pattern we consider three activities: “sleeping”, “eating”, “taking a shower”, which occur at specific times of the day. “Going to the toilet” may occur at many times during the day. It will be studied separately as we will see later.

3.2 Normal Behavior Pattern for the Elderly

The first step of any behavior anomaly detection system is to characterize the normal behavior, also called *routine behavior* or *regular behavior*, based on training data to model regularities in every individual activity. The normal behavior consists of the list of activities that a resident performs in her/his house, with time of the day and the duration. Thus, it captures the repetitive daily routines and deviations from the normal behavior may indicate changes of lifestyle or loss of capacity.

To build the routine behavior model, we follow the following steps:

1. We first use training data collected during the previous period which was treated as a baseline behavior period. We then follow an unsupervised learning approach: clustering to find point anomalies. To address this, we cluster instances of each activity based on start time and duration without considering the day of the week. For clustering, we use the DBSCAN algorithm [11] which is a density based clustering algorithm. The major advantage of DBSCAN, compared with other clustering algorithms like K-means, is that we do not need to specify how many clusters should be identified. After clustering, DBSCAN marks each point as belonging to a cluster or as noise(anomaly).
2. We eliminate point anomaly and we calculate the average start time and duration for each activity in training data.

The activity “going to the toilets” that occurs several times a day is treated separately. There are usually regular schedules for this activity. It is not essential to be very precise on the realization time of this activity. We then choose to study its frequency rather than the occurring time. Using the same training data to model regularities in the three studied activities, we calculate the frequency, per n hours, of the activity “going to the toilets”.

3.3 Elderly's Behavior Change Detection

Once computed, the normal behavior pattern can be used to detect anomalies by comparing the current behavioral data of an elderly with her/his normal behavior pattern. The basic idea of our behavioral deviation detection system is to estimate the similarity between both patterns using a score. We therefore consider three criteria for the activities: the time, duration and chronological order of the activities in the sequence.

Behavior Modeling Using a Daily Activity Score: Intuitively, a particular activity is similar to a pattern if its start time, duration and location are similar to the ones defined by the pattern. The similarity of the time and duration for each activity is estimated by a score.

The similarity score of an activity a in a day d is calculated by the formula (1). It is given as a percentage and represents the temporal intersection of the normal behavior pattern and one observed day pattern, for the same activity. We note that S_{ad} is the start time of activity a_d , D_{ad} is the duration of activity a_d and $E_{ad} = S_{ad} + D_{ad}$ is the end time of activity a_d

$$\text{Similarity score} = \frac{(\inf(E_{an}, E_{ad}), \sup(S_{an}, S_{ad})) * 100}{D_{an}} \quad (1)$$

The similarity score for one day is the average of similarity scores for all activities occurring in this day.

The duration score is calculated by the formula (2). It is a percentage of the duration of an activity in an observed day compared to the duration of the same activity in the normal behavior pattern.

$$Duration\ score = \frac{D_{ad} * 100}{D_{an}} \quad (2)$$

The duration score for one day is the average of duration scores for all activities occurring on this day. The duration score can exceed 100% if the duration of an activity at the observed day is greater than the expected duration in the normal behavior pattern. This simply means that the elderly takes longer to achieve the activity which may be caused by a loss of autonomy if this is observed regularly.

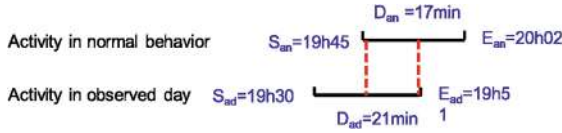


Fig. 1. Illustration of the similarity and duration scores for the activity “eating lunch”

In the example presented in Fig. 1, the similarity score is 35.29%. It represents the temporal intersection for the activity “to eat lunch” in one observed day pattern compared to the same activity in the normal behavior pattern. The duration score (80.95% in our example) is the percentage of the duration of the activity “to eat lunch” in an observed day compared to the duration of the same activity in the normal behavior pattern.

The variation of these scores over time, represents the evolution of the elderly’s life pace. These scores thus give us an indication of the variation with an elderly’s usual behavior for a particular activity. A large decrease in these scores over a long period (from a few days to a few weeks) may be an initial signal of decline and should generate a notification to the caregivers or the family members.

For regular activities, occurring several times a day, we compare the frequency between a routine day and an observed day. By simply plotting the daily score along time, it is possible to identify certain days with unusual activities (i.e., with lower scores), or trends of evolution that indicate deviations from the previous activity routine.

A subsequent work detailed in Sect. 3.3 consists in studying in details the activities related to the behavior change period to discover the deviation cause(s).

Anomaly Detection in Behavior Change Period: In this section, we investigate the accuracy of anomaly detection: per day and per hour of the day, in the

behavior change period. Activities in this period has been mapped and compared with normal life pattern.

In the domain of at-home activities, anomalies can be classified as point, collective and contextual anomalies. The *point anomaly* [12–14] considers each activity independently and decides whether it is normal or not with respect to the normal behavior. The *collective anomaly* [15] considers groups of activity instances together to determine whether the group is normal or not. The *contextual anomaly* [16, 17] considers activities under a particular context (e.g., day of week, person under medication, etc.). In our work, we focus on detecting *point anomaly* (i.e., missing activity or activity with an unusually long/short duration).

For the activity “going to the toilet” which occurs several times per day, we model and compare frequencies between a routine day and the observed day in the behavior change period. A frequency is provided by the normal behavior pattern. This will be illustrated in the following section.

4 Use Case

In this section, we present in 4.1 the dataset used as use case. We detail in 4.2 the learning steps for building the normal behavior pattern. By plotting the daily score along time in 4.3, we exhibit the period when the score changes over time and then identify daily anomalous activities found in the behavior change period.

4.1 Dataset

The dataset used for our analysis is provided by Washington State University's CASAS program¹ [18]. CASAS (Center for Advanced Studies in Adaptive Systems) aims to provide aid to residents using smart home technology. They therefore collect and use real-time data from sensors to analyze and monitor residents' health and behavior to improve future smart home living.

We use one public data set (named HH120) [18] which was used in other works like [19]. It includes one unique subject, covering a total of 63 days. All data used in this paper was handled in an anonymized way. The set of activities includes “sleeping”, “eating meals”, “taking a shower”, “going outside” and “going to the toilet”. The data sets do not provide any medical information. For training the normal behavior model, we use the first month while the rest of the available data is used to test the effectiveness of our proposals.

4.2 Learning for Building the Normal Behavior Pattern

For building the normal behavior pattern from the training data set, we follow the different learning steps presented in the Sect. 3.2. We then apply the

¹ <http://casas.wsu.edu/>.

DBSCAN algorithm on the training dataset for clustering and eliminate activities out of the identified clusters and marked as noise. DBSCAN has two parameters; one is *min_pts* which is the minimum number of points in a cluster, and the other is *Eps* which is the maximum distance between two data points for them to be considered in the same cluster. While learning, data out of *Eps* would be considered out of clusters so marked anomalous. Trained results are depicted in Fig. 2.

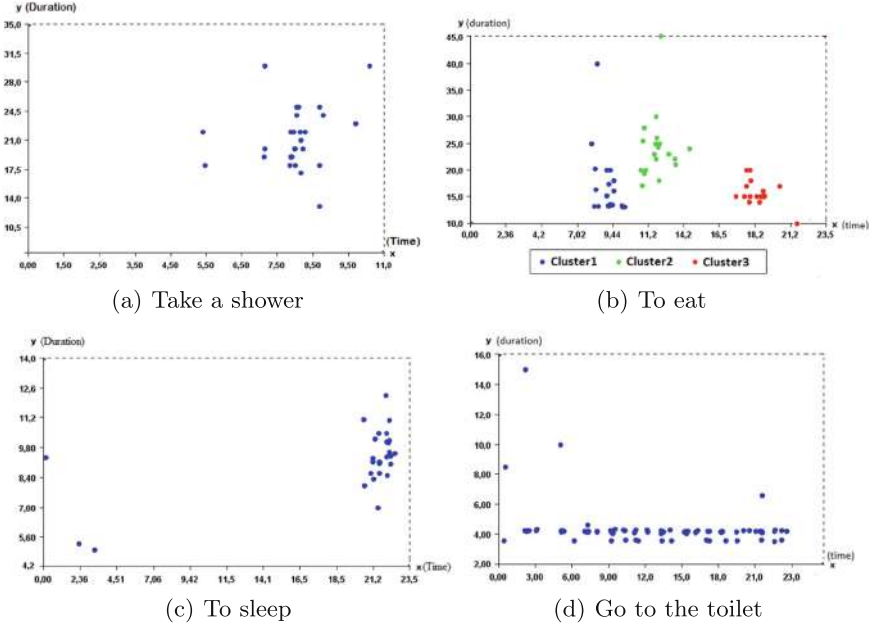


Fig. 2. DBSCAN Clustering for detecting anomalies

Figure 2(b) illustrate 3 clusters which represent 3 daily meals. The elderly person is habituated to have her breakfast at 9:44 AM for maximum 25 min. Figure 2(b) shows that this person can have her breakfast for 40 min which is abnormal behavior depicted by the point outside the middle cluster.

We then eliminate point anomalies and calculate, for every activity in the training data set representing one month of collected data, the average start time and average duration. Figure 3 illustrates the daily behavioral model thus generated using the previous learning step.

4.3 Behavior Change Period and Anomalous Activities

In the first stage of our experiments, we computed the daily scores introduced in Sect. 3.3. By plotting scores, we can observe the behavior evolution day by



Fig. 3. Normal behavior pattern

day to follow the evolution of elderly’s life pace. Thus, it is possible to identify trends in the daily evolution scores as shown in Fig. 4 where we can observe a decrease compared to the previous routine activity.

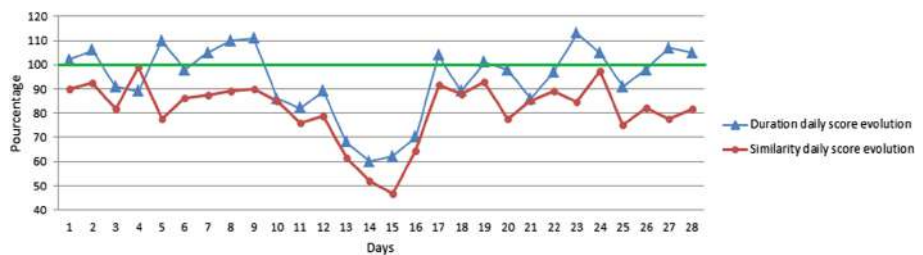


Fig. 4. Daily scores evolution

In the second stage of our experiment, we focus on the deviation period (days with decreasing/increasing scores) to detect point anomalies due to a missing activity or activities with unusually long/short durations. To do this, we plot in Figs. 5 and 6 duration and start time respectively for 3 activities (to sleep, to eat (breakfast, lunch, dinner) and take a shower). In these figures, the average start time and the average duration in normal behavior pattern are represented for each activity by an horizontal line.

At days 13 and 14, Figs. 5 and 6 reveal unusual sleep times, shorter than usual, as well as later times to go to bed (2:00 AM and 4:00 AM). The results also indicate that day 15 is a day with unusual activity because the elderly skipped a lunch. At the same day, the elderly performs more times than usual the activity “taking a shower” and “sleeping”. During these 3 days we detect 2 types of anomaly: point anomaly due to missing activity and activities in unusually long/short durations.

As mentioned previously, the activity “going to the toilet” that occurs several times a day is treated separately. As for the other activities, anomalies related to duration are eliminated using DBSCAN as illustrated in Fig. 2. To analyze the elderly’s behavior, we focus both on the frequency per 2 h and the duration. Figure 7 shows that both these parameters increase in the deviation period compared to the normal behavior (represented with the horizontal line).

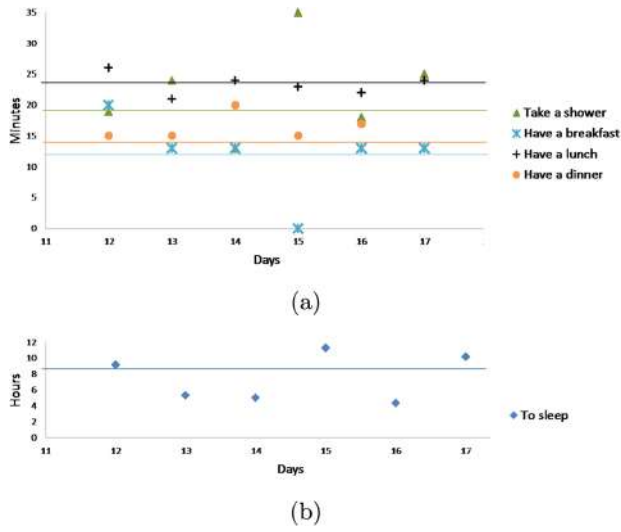


Fig. 5. (a) Activities durations in observed days (b) sleeping duration

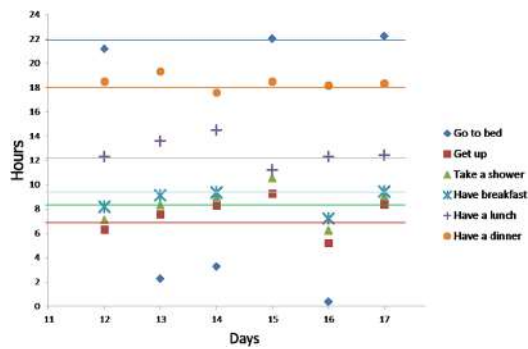


Fig. 6. Activities start time in observed days

All these anomalies may be a signal of sickness (urinary tract infection, gastrointestinal problem, etc.) so our system may send an alert message to inform remote caregivers.

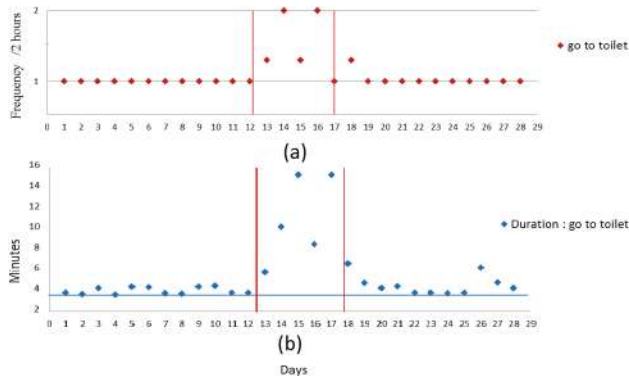


Fig. 7. (a) Frequency “go to the toilet” (b) Duration “go to the toilet”

5 Conclusion

In this article, we presented our research work to detect behavioral changes in the elderly's usual behavior. Our solution relies on the construction of a behavior model. Thanks to this scheme and based on the detection of anomalies, we are able to detect changes in the elderly behavior, not only sudden changes such as a fall or a temporary illness, but also changes over time. For example, the elderly sleep less and less every month, which can be worrying and cause many problems. In the future, we would like to integrate other activities into our model, such as “going outside”, which are an important aspect for characterizing the elderly's health. This information should also be coupled with contextual elements such as weather conditions. Other information on health conditions can also be used to refine our detection of behavioral changes. Finally, when our system detects changes in behavior, it must make a decision on the appropriate solution: for example, if it is a sudden and persistent change, it may be an emergency solution and if it is a degradation of the subject's daily routine, a visit from the caregiver would be necessary. It is difficult to make the “best” decision so we plan at this point to talk to healthcare professionals to configure our decision support system.

Acknowledgements. This work has been sponsored by the ELSAT2020 project co-financed by the European Union with the European Regional Development Fund, the French state and the Hauts de France Region Council.

References

1. Zhu, C., Sheng, W., Liu, M.: Wearable sensor-based behavioral anomaly detection in smart assisted living systems. *IEEE Trans. Autom. Sci. Eng.* **12**(4), 1225–1234 (2015)
2. Ord, F.J., de Toledo, P., Sanchis, A.: Sensor-based bayesian detection of anomalous living patterns in a home setting. *Pers. Ubiquit. Comput.* **19**, 259–270 (2015)

3. Lotfi, A., Langensiepen, C., Mahmoud, S.M., Akhlaghinia, M.J.: Smart homes for the elderly dementia sufferers: identification and prediction of abnormal behaviour. *J. Ambient Intell. Hum. Comput.* **3**(3), 205–218 (2012)
4. Gjoreski, H., Rashkovska, A., Kozina, S., Lustrek, M., Gams, M.: Telehealth using ECG sensor and accelerometer. In: *Proceedings of the 37th International Convention on Information and Communication Technology, Electronics and Microelectronics (MIPRO)*, pp. 270–274 (2014)
5. Sprint, G., Cook, D., Fritz, R.: Schmitter-Edgecombe, M.: Detecting health and behavior change by analyzing smart home sensor data. In: *IEEE International Conference on Smart Computing (SMARTCOMP)*, pp. 1–3 (2016)
6. Bakar, U.A.B.U.A., Ghayvat, H., Hasanm, S.F., Mukhopadhyay, S.C.: Activity and anomaly detection in smart home: a survey. In: Mukhopadhyay, S.C. (ed.) *Next Generation Sensors and Systems. SSMI*, vol. 16, pp. 191–220. Springer, Cham (2016). https://doi.org/10.1007/978-3-319-21671-3_9
7. Dhiman, C., Vishwakarma, D.K.: A review of state-of-the-art techniques for abnormal human activity recognition. *Eng. Appl. Artif. Intell.* **77**, 21–45 (2019)
8. Essghaier F., Delcroix V., Marcal de Oliveira K., Puisieux F., Gaxatte C., Pudlo P.: Towards a fall prevention system design by using ontology. *Francophone Days of Knowledge Engineering (IC)* (2019)
9. Hossain, M.A.: Perspectives of human factors in designing elderly monitoring system. *Comput. Hum. Behav.* **63–68**, 33 (2014)
10. Kaddachi, F., et al.: Technological approach for behavior change detection toward better adaptation of services for elderly people. In: *HEALTHINF*, pp. 96–105 (2017)
11. Ester, M., Kriegel, H., Sander, J., Xu, X.: A density-based algorithm for discovering clusters in large spatial databases with noise. In: *Proceedings of the Second International Conference on Knowledge Discovery and Data Mining, KDD 1996*, pp. 226–231 (1996)
12. Riboni, D., Bettini, C., Civitares, G., Janjua, Z.H.: SmartFABER: recognizing fine-grained abnormal behaviors for early detection of mild cognitive impairment. *Artif. Intell. Med.* **67**, 57–64 (2016)
13. Janjua, Z.H., Riboni, D., Bettini, C.: Towards automatic induction of abnormal behavioral patterns for recognizing mild cognitive impairment. In: *Proceedings of the 31st Annual ACM Symposium on Applied Computing, SAC 2016*, pp 143–148 (2016)
14. Riboni, D., Bettini, C., Civitarese, G., Janjua, Z.H., Helaoui, R.: Fine-grained recognition of abnormal behaviors for early detection of mild cognitive impairment. In: *IEEE International Conference on Pervasive Computing and Communications (PerCom)*, pp. 149–154 (2015)
15. Anderson, D.T., Ros, M., Keller, J.M., Cuellar, M.P., Popescu, M., Delgado, M.: Similarity measure for anomaly detection and comparing human behaviors. *Int. J. Intell. Syst.* **27**(8), 733–756 (2012)
16. Hoque, E., Dickerson, R.F., Preum, S.M., Hanson, M., Barth, A., Stankovic, J.A.: Holmes: a comprehensive anomaly detection system for daily in-home activities. In: *International Conference on Distributed Computing in Sensor Systems, Fortaleza*, pp. 40–51 (2015)
17. Hayes, M.A., Capretz, M.A.M.: Contextual anomaly detection framework for big sensor data. *J. Big Data* **2**(1), 1–22 (2015). <https://doi.org/10.1186/s40537-014-0011-y>

18. Cook, D.J., Crandall, A.S., Thomas, B.L., Krishnan, N.C.: CASAS : a smart home in a box. *IEEE Comput.* **46**(7), 62–69 (2013)
19. Lago, P., Jimz-Guar, C., Roncancio, C.: Contextualized behavior patterns for change reasoning in ambient assisted living: a formal model. *Exp. Syst.* **34**(2), e12163 (2017)

Open Access This chapter is licensed under the terms of the Creative Commons Attribution 4.0 International License (<http://creativecommons.org/licenses/by/4.0/>), which permits use, sharing, adaptation, distribution and reproduction in any medium or format, as long as you give appropriate credit to the original author(s) and the source, provide a link to the Creative Commons license and indicate if changes were made.

The images or other third party material in this chapter are included in the chapter's Creative Commons license, unless indicated otherwise in a credit line to the material. If material is not included in the chapter's Creative Commons license and your intended use is not permitted by statutory regulation or exceeds the permitted use, you will need to obtain permission directly from the copyright holder.





Personalized and Contextualized Persuasion System for Older Adults' Physical Activity Promoting

Houssem Aloulou^{1(✉)}, Hamdi Aloulou^{2(✉)}, Bessam Abdulrazak^{3(✉)},
and Ahmed Hadj Kacem^{1(✉)}

¹ ReDCAD, University of Sfax, Sfax, Tunisia
Houssem.aloulou@gmail.com,
ahmed.hadjkacem@fsegs.usf.tn

² ReDCAD, Digital Research Centre of Sfax, Sfax, Tunisia
hamdi.aloulou@redcad.tn

³ University of Sherbrooke, Quebec, Canada
Bessam.Abdulrazak@usherbrooke.ca

Abstract. Aging often involves a significant change in roles and social positions. The greatest health risk for seniors is the adoption of a sedentary lifestyle that causes isolation, depression, and many diseases. However, convincing an older adult to regularly do physical activities is not generally a simple mission.

This paper proposes a personalized and contextualized persuasion system to promote physical activities for older adults. In fact, our approach considers the personal and health profile of the older adult. It also considers different context parameters (context-awareness). This intelligence is guaranteed thanks to the use of the semantic modeling and reasoning, which from different types of information would be able to decide the best moment to trigger notifications from our persuasive system to the participating older adults.

Keywords: Persuasion strategy · Captology · Physical activities · Older adults · Context-awareness · Semantic modeling · Semantic reasoning · Pervasive technology

1 Introduction

Nowadays, information technology has a growing influence around the world and brings new opportunities to solve many of society's problems. One of the most irritating problem is the sedentary lifestyle of older adults. In fact, the lack of physical activities accelerates the transition of people to the age of dependency.

The best way to thwart the sedentary lifestyle among the older adults is to promote physical activities [1]. Generally, older adult trend to limit their physical activities as they often consider them difficult to do. Hence, they must be motivated to change their behavior. Motivation is a set of dynamic factors that guide the action of a person toward a given purpose, which determine his behavior and cause him to behave in a given way or modify his actual behavior [1].

There exist several behaviors change techniques which use persuasion methods to convince subjects to change behaviors. These techniques are inspired by social and cognitive psychology and models associated with them.

We have based our methodology on the output of these technics' analysis. We have also taken into consideration the older adults' profiles and contextual information to increase the probability of success of our persuasion technique. Persuasion technics, profiles and contextual information were modeled and realized using the semantic modeling while persuasion strategies were guaranteed using the semantic reasoning.

Following, Sect. 2 presents a detailed state of the art of behavior change persuasion theories and existing systems for promoting physical activities. Section 3 expound our proposed persuasion technique. In Sect. 4, we introduce the used architecture. Then in Sect. 5, we present our first prototype. To validate our persuasive approach and decision-making platform, we propose a first textbook case. Finally, we conclude this article.

2 State of the Art

2.1 Behavior Change Persuasion Theories

There are several theories that presents methods that aim to persuade people to change their behavior. Bandura presented a comprehensive theory of human motivation and action called the "Social Cognitive Theory" as an extension of his theory of social learning [2, 3]. In this theory, people are not motivated by internal forces, but by external factors. He emphasizes reciprocal causation through the interplay of cognitive (personal) factors, behavioral factors, and environmental factors. These prominent factors are guided by several variables that intervene in the process of behavior change: self-efficacy, outcome expectations, self-control, reinforcements, emotional coping, and observational learning.

Fogg has identified many principles of persuasion that new technologies can use to influence the behavior of their users. He called this concept the "Captology" (Computers As Persuasive Technology) [4]. He described it as the region where technology and persuasion overlap. For him, behavior change must be voluntary and by conviction. Fogg has also emphasized computer efficacy to persuade users to change behavior through a functional triad. He asserted that, from a user's point of view, there is three fundamental roles that a computer can play: as tool, as social actor and as media. Each role of the triad is divided into several strategies. For a computer system to be persuasive, it must apply all or most of these strategies.

Additionally, Fogg also demonstrated in his behavior model FBM [5] that 3 conditions must converge at the same time for a behavior to be realized: sufficient "motivation" and "capacity" to do the requested behavior and a well-chosen moment to "trigger" the behavior (physical location, emotions, availability, proximity, etc.) when the person is most open to persuasion (Kairos factor) and thanks to the availability and portability of mobile devices (convenience factor).

For the motivation, Fogg created a framework with three basic motivators formed by tuples in [5]: Sensation (Pleasure/Pain), Anticipation (Hope/Fear) and Belonging (Social acceptance/Social rejection).

Oinas-Kukkonen et al. were inspired by Fogg's works when proposing the process of "Persuasive System Design" (PSD) [6] that aims to facilitate design and evaluation of persuasive system. The framework is based on seven (7) hypotheses to understand the problems of persuasive systems. The context of persuasion is then analyzed by designers to have a deepening understanding of changes using three (3) major elements: Intention, Event and Strategy. Outcomes are then used to design system's qualities by meeting several criteria: primary tasks support, dialogue, credibility, and social support.

Later, Oinas-Kukkonen presented the "Behavior Change Support Systems" (BCSS) as an extension of the PSD process [7]. BCSS uses persuasive technology which allows to create, reinforce, and change behaviors. It is based on a design matrix to determine the nature of the behavior change. Rows of the matrix contain types of outcome (formation, altering or reinforcing) and columns contain types of changes (complying, behavior, or attitude).

To help designers in matching target behaviors with solutions for achieving them, Fogg and Hreha proposed the "behavior Wizard" based on the "behavior Grid" [8]. The latter consists of three (3) rows to present the duration of the target behavior and five (5) columns to present the nature of the target behavior. The intersection of a row and a column presents a behavior changing strategy.

Tracking behaviors change of a person involves following the steps of changing actions from the current unwanted behavior to the requested or desired behavior. In this research, we will apply the most important elements of behavior change theories to motivate seniors to adopt a healthy lifestyle. The biggest challenge remaining now is how to adapt the persuasion to the complexity and versatility of every older adult to maximize persuasive effectiveness.

2.2 Existing Systems for Promoting Physical Activity

There are several systems that apply persuasive technology in different domains like health care, leisure, e-commerce, education, etc. Many of these applications were created to promote physical activities. In [9], authors identified 64 apps to promote physical activity among adults. They rated them based on the taxonomy of behavior change techniques. For instance, in [10] research was to understand motivators of changing behavior and sharing results on tweeter by the users of RunKeeper App. It takes the theory of planned behavior as a starting point for their conceptual model. There model consider the influence of altruism, reputation building, community identification, social norms, getting feedback and information sharing. Strava [11] is a persuasive app created for runners and cyclists to track adults activities and offer analysis on their performance. It aims on encouraging running and cycling by competitive motivation when activities are done in group, and challenges when exercising alone. When a participant success the challenge, he earns a "badge" for their "trophy case." Endomondo [12] is a mobile app that tracks physical activity by monitoring duration, distance and speed. It motivates users by providing audio feedback, pep talks from friends and user's friends' activities and statistics. Flowie is an application that target older adults [13]. In Flowie, the performance of a senior, collected with a pedometer, is translated by the expression of a small animated flower in a touch-screen photo frame. Ubifit Garden [14] and Fish'n'steps [15] are two other applications that

use persuasive technology to support healthy behavior via pedometer. Ubifit Garden uses a floral garden wallpaper, in a mobile application, that flourish and blooms as the person performs activities. Move2Play [16] and Healthopia [17] are mobile applications that promote a healthier lifestyle and motivates to participate in regular physical activity using wearable and mobile sensors. Many of the existing systems lack context-awareness when proposing physical activities. They also don't consider the profile of the person and his health state. There is also no flexibility when asking a person to do behavior nor customization.

3 Methodology: Personalization and Customization of the Behavior Change Strategy

We argue that targeting better motivation of senior and successful change of their behavior requires that a persuasion technique that take into consideration, in addition to the Captology elements, several factors in relation with the older adult's life such as his health state, his environment, his preferred activities and his tendencies. Therefore, a pre-persuasion step is required to form the senior's profile. The user profile is composed of a personal profile (demographic data, preferred activities and hobbies, social relationships, etc.) and a health profile (physical and mental state). We mainly used the Health Utilities Index Mark 3 (HUI3) [18], a generic health profiles and preference-based systems for measuring health status, reporting health-related quality of life, and producing utility scores, to model the health profile.

The user profile (personal and health) is then used as an entry to our persuasive strategy in conjunction with contextual information to help increase the likelihood of behavioral change success. Our persuasion strategy inspired from Fogg's functional triad and Fogg Behavior Model (FBM) uses the received element to convince older adults to adopt a healthy lifestyle and to avoid sedentary. Our approach is presented in Fig. 1 below.

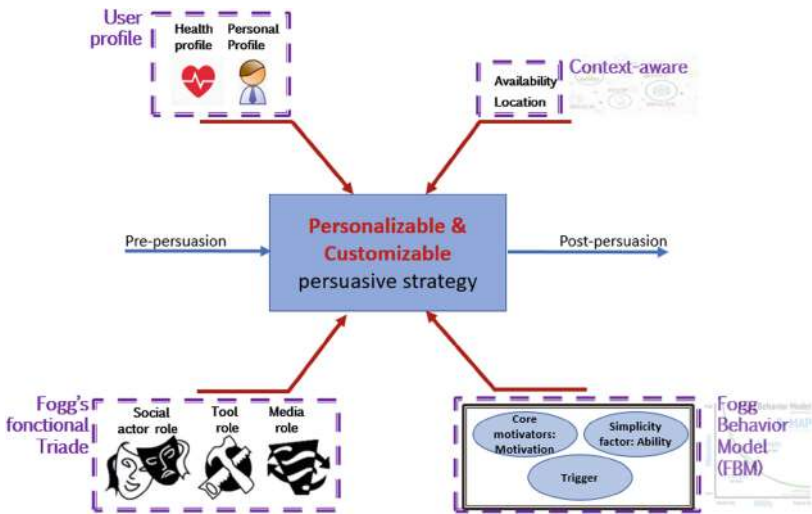


Fig. 1. Customizable persuasion strategy

In our persuasion strategy, we took advantage of Fogg’s functional triad and FBM model to promote physical activity of older adults. The following Table 1 presents each element of Fogg’s functional triad and how it is considered in our system.

Table 1. Adopted behavior change theory

Role	Implementation	Strategy	Examples
Tool	Provide a mobile app that act as a persuasion tool to convince the older adult to change his behavior	Reduction	Simplify the complexity of activities: giving the difficulty of cleaning the house for an older person, we break this activity down into several sub-activities
		Suggestion	Take into consideration the condition of the user when choosing behavior to change: needs, interests, personality, context of use, environment, proximity, availability and adaptability
		Self-monitoring	The older adult receives information on his performance through the mobile app
Media simulation	The mobile app displays sensitive videos showing dangers of a sedentary lifestyle.		
Social actor	The mobile app will act as a social actor	Physical attractiveness	An attractive GUI with several features to attract the user
		Encouraging language	Notifications on the mobile app have to include positive waves and encouraging language
		Social dynamics	Older adults will feel the need for recognition when the mobile app provides social support and serves them well

We also give great importance to social influence that is based on social comparison to other similar persons, also intrinsic motivation through competition, cooperation, and recognition.

In addition, we will put into practice the Fogg’s behavior model (FBM). We implement the pleasure sensation factor to do a physical activity and the anticipation of

hope for a healthy aging. Also, all the 6 factors for maximal ability (time, money, physical effort, brain cycles, social deviance, and non-routine) are considered in our reasoning and persuasion strategy.

4 Proposed Architecture

The connectivity and portability of smartphones makes possible to reach older adults at any time and place using automated notifications. All notifications and encouragement for an older adult are posted on his smartphone via a mobile app. In addition, this app enables collecting information on senior behavior and sent them instantly to a remote decision-making platform via Internet. The platform filters and processes collected data. Additionally, the reasoning of the context and profile, that is based on an ontological model, allow our platform to choose rationally the best persuasion strategy and to propose, at the right time and place, contextualized physical activities based on several criteria such as his personal profile, his health status, his context, his preferred activities, etc. A typical scenario would be sending a notification requesting to do a given activity only if the older adult has the physical and mental capacity to perform it (based on HUI3 utilities) and considering his context (availability and location). Figure 2 shows a simplified presentation of the architecture of our approach.

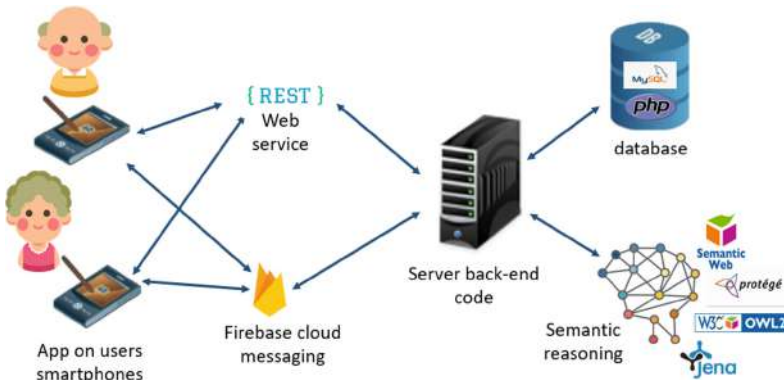


Fig. 2. Overview of the architecture using semantic reasoning

5 Active Senior's First Prototype

Our goal at this stage of the project is to develop a computer system serving as proof of concepts that we have named “Active Senior”. The main objective is to validate the functioning of the first components of our system, i.e., the mobile app, the software modules of the server platform and the communication module.

The server app is connected to a database which contains the data of participants, there login information, the list of activities, to which an older adult can register, and

the list of notifications received by all participants and information whether the activity has been done or not yet by corresponding person. In fact, when receiving a notification to do a behavior on mobile app, an older adult can inform the server that he accepts to do the behavior and he can inform it when the behavior is done. All information about notifications, the deadline for accepting the activity and carrying it out are stored in the database for statistics purpose.

We have defined a new ontology to be able to offer older adults contextualized activities. We have saved our ontology in OWL format which provides a rich vocabulary to add semantics and context and to allow reasoning and inference. Below in Fig. 3 parts of our ontology displayed with OWLViz¹ plugin. For lack of space, we have chosen to present only the three (3) first levels of our ontological model.

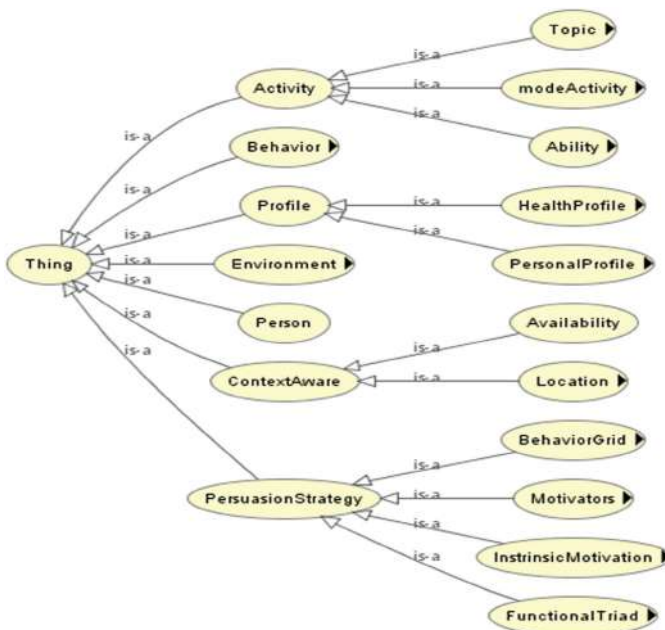


Fig. 3. Part of the class hierarchy of our ontology (with OWLViz plugin)

“Object properties” were defined to describe relationships between two instances of classes (individuals) and “data properties” were defined to describe relationships between instances of classes and their respective values (Fig. 4).

¹ <https://github.com/protegeproject/owlviz>.

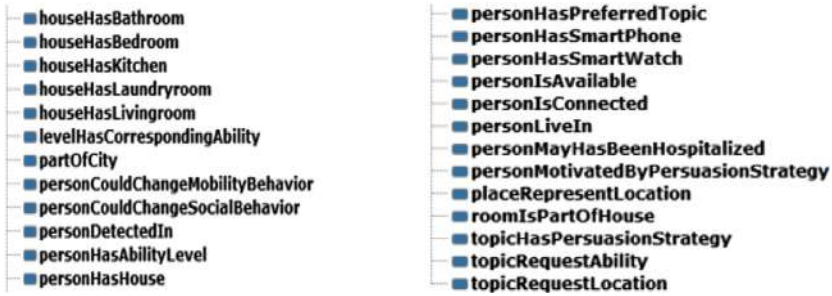


Fig. 4. Examples of defined object properties

Among created “object properties” we cite:

- “personHasPreferredTopic”: allows to link the “Person” class to the “Topic” class. This will therefore make it possible to know the activities in which the older adult is interested.
- “topicHasPersuasionStrategy”: allows to link a “Topic” to a “PersuasionStrategy.”
- “personIsConnected” and “personIsAvailable”: help to guarantee the person’s context-awareness: his current location and his availability.
- “personMotivatedByPersuasionStrategy”: connects each person to the persuasion strategy that most closely matches his profile, state of health and context.

Among created “data properties” we cite: “persuasionStrategyHasDescription” which allows to assign a description to a “persuasionStrategy” and “levelValue” which have a value between 1 and 6 presenting the value of an instance of the class presenting the HUI3 health indicator for a given person. One of the main benefits of building an ontology-based application is the ability to derive additional knowledge about the concepts modeled by using a reasoner. So, to make our persuasion strategy contextual and personalized, we used the “Apache Jena”² reasoning engine. It is an open source Semantic Web Framework for Java that supports OWL. Thereby, we defined rules so that the reasoner can decide if it would be appropriate to ask a senior to do an activity or not.

The exchanges between the server app and the mobile app are done through REST³ (REpresentational State Transfer) web services while the notifications are guaranteed with FCM⁴ (Firebase Cloud Messaging) Google protocol.

² <https://jena.apache.org/>.

³ <https://restfulapi.net/>.

⁴ <https://firebase.google.com/docs/cloud-messaging>.

From the mobile app, each senior chooses one or more activities he is interested in. Persuasion of the older adult is done entirely through the mobile app. Through the mobile app, it is possible to:

- Register a new participant: Using web services, login information is added, in real time, to the database on the server.
- Login to a user account: to receive notifications from the server and to be able to communicate with the database.
- Subscribe to one or more activities (topics) by checking in a list the preferred activities. However, it is possible, at any time, to unsubscribe from an activity (by unchecking it in the list). By clicking on the “Save” button, the information is sent in real time to the server and the database is then updated with the user’s new choices. Then, he will no longer receive notifications to do the unchecked activity.
- Receive notifications: When it’s time to do an already chosen activity, the senior receives a notification on his smartphone asking him to do it. We use the self-monitoring technique that we find in several behavior change theories [4]. Indeed, this method empowers the older adult to reach objectives set in advance. While being convinced of the usefulness of the activity to be carried out, the person will make his effort to complete it (Fig. 5).

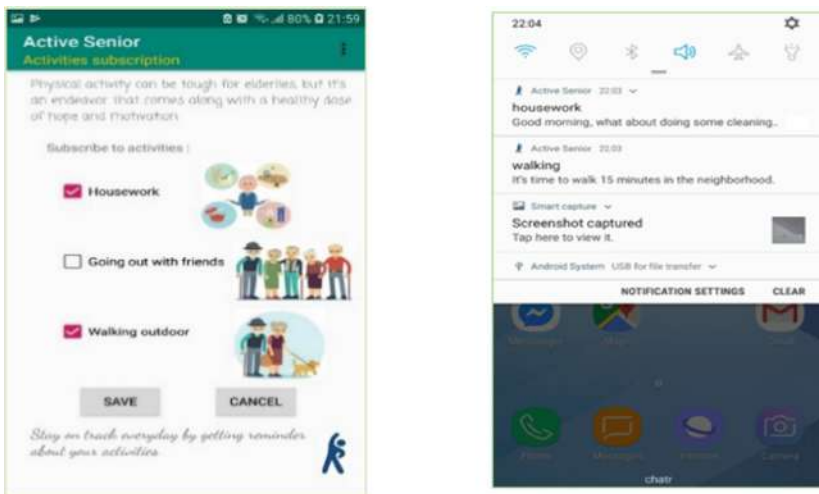


Fig. 5. Subscribing/unsubscribing to activities (topics) and receiving notifications

Our mobile application displays all notifications received by the user and which are incomplete. For each notification, it shows the date and time of its reception, the name of the activity and its description, and 2 buttons:

- Button “Accept”: allows the user to acknowledge receipt and acceptance of the notification. By clicking on this button, the date and time are saved in the database.
- Button “Done”: when the senior complete the requested activity, he clicks on “Done” button. The date and time are sent to the database.

The data of the activities carried out by an older adult are saved in the server database for statistical purposes and to periodically encourage participants whose results will experience an evolution. This will motivate seniors to maintain their effort and to try to achieve better performance (Fig. 6).



Fig. 6. List of notifications received by a senior

6 Validation

To do a first validation of our approach, we propose a textbook case with a limited number of participants and activities. It is an important step that allows us to test the effectiveness and efficiency of our persuasive approach and our decision-making platform before deploying it on a larger scale.

We have defined three topics (preferred activities): “housework,” “walking outdoor” and “going out with friends”. For each topic we have established some expressions based on Fogg’s motivators such as “encouraging language”, “hope anticipation” and “fear anticipation”. For instance, a notification to do housework that uses a hope anticipation motivator may contains the text “A clean and organized home is a beautiful home. It eliminates the risk of developing allergies and asthma; it also reduces stress and it is extremely vital to your mental health”. A fear anticipation motivator in a notification to walk outdoor can be done with the text “Sedentary lifestyle can lead to difficulties in performing the activities of daily living, there’s greater risk of heart disease, diabetes and depression.” An encouraging language motivator in a notification to go out with friends can be “An outing is scheduled tonight by your kind friends. It will be a good opportunity to relax, exchange stories and forget everyday worries”.

We have also created the profiles of three older adults: “JohnDoe”, “JohnWalker” and “JohnGoe”. Each profile contains the physical and health status of the person, his concerns, his environment, his availability, and his location. “JohnDoe” is subscribed to “housework” activity, “JohnWalker” is subscribed to “walking outdoor” activity and “JohnGoe” is subscribed to “going out with friends” activity.

The ontology allows to personalize and customize the persuasive strategy according to the older adult's profile. In Fig. 7 below, we have some Individuals defined in the ontology for the participating older adults and "Property assertions" used for "JohnGoe".

Using the ontology, it is possible to generate new knowledge using inference rules. In fact, inference rules allow to decide the best moment to trigger a behavior.

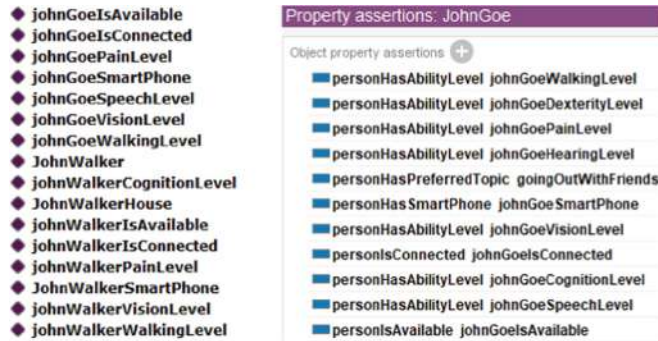


Fig. 7. Some older adults' individuals and property assertions from the ontology

Here is an example of a used rule written in Jena syntax:

```
[Rule1:
(?u pre:personHasPreferredTopic ?t)
(?t pre:topicRequestAbility ?a)
(?u pre:personHasAbilityLevel ?cl)
(?cl pre:levelHasCorrespondingAbility ?a)
(?cl pre:levelValue ?v) lessThan(?v, 3)
(?t pre:topicRequestLocation ?loc)
(?u pre:personDetectedIn ?h) (?h pre:placeRepresentLocation ?loc)
(?t pre:topicHasPersuasionStrategy ?s)
-> (?u pre:personMotivatedByPersuasionStrategy ?s)]
```

Using this rule, the person is motivated by the persuasion strategy only if the following conditions are valid:

- The older adult has a favorite topic and the topic has a persuasion strategy.
- The chosen topic requires one or more health capacities among the 8 elements of HUI3 health status (Vision, Hearing, Speech, Ambulation, Dexterity, Emotion, Cognition, Pain).
- For each state of health, the person has a level between 1 and 6. When the value is 1, it means that he has no health problems for the state of health.
- It is not possible to allow the older adult to do the activity if the value of the health level is > 3 because it could present a risk to his safety and health.
- We also check if the topic requests a location and if the person is this location.

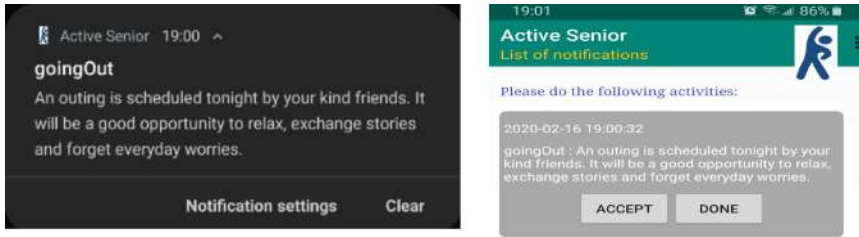


Fig. 8. Received notification by JohnGoe

Our persuasion strategy is therefore personalized in the sense that it respects abilities, habits, choices, health situation, context, etc. of the person being followed.

Figure 8 below show a notification received by JohnGoe whose profile meets the conditions of the ontology rule mentioned above.

7 Conclusion

Persuasive technologies have shown a lot of potentials to influence the behavior and attitudes of individuals. In this paper, we adopted Fogg's persuasive techniques to promote physical activity of older adults. To change the behavior of an older adult, we defined a realistic persuasion strategy which considers senior's profile, his environment and his context. To make our persuasion strategy customizable and contextualizable, we defined an ontology and used rules to deduce new knowledges in order to choose the right moment and place to request the execution of an activity. As first validation of our approach, we developed a first prototype of "Active Senior" to test the used concepts. The first results seem to be promising.

To be successful, new behavior must be maintained and preserved as several older adults may adopt the new proposed behavior for a limited period and they give up after a certain time. This can be explained by the fact that preserving a behavior or attitude requires a lot of effort, energy and time, etc.

In future work, our work will be validated with real volunteer subjects who will be asked to use the mobile app to promote their physical activities. Selection criteria will be set in order to choose subjects with different profiles (physical capacity, habits, social situation, health status, environment, etc.). This will allow us to validate the proposed solution with different profiles.

References

1. W. H. O. (WHO), World Report on Ageing and Health, Geneva (2015)
2. Bandura, A.: Social Foundations of Thought and Action. Englewood Cliffs, NJ (1986)
3. Bandura, A.: Social cognitive theory: an agentic perspective. *Annu. Rev. Psychol.* **52**(1), 1–26 (2001)

4. Fogg, B.J.: Persuasive technology: using computers to change what we think and do, vol. 2002, December 2002
5. Fogg, B.: A behavior model for persuasive design. In: Proceedings of the 4th International Conference on Persuasive Technology - Persuasive 2009, p. 1 (2009)
6. Oinas-Kukkonen, H., Harjumaa, M.: Persuasive systems design: key issues, process model, and system features. *Commun. Assoc. Inf. Syst.* **24**(1), 485–500 (2009)
7. Oinas-Kukkonen, H.: Behavior change support systems: a research model and agenda. In: Proceedings of the 5th International Conference on Persuasive Technology, pp. 4–14 (2010)
8. Fogg, B.J., Hreha, J.: Behavior wizard: a method for matching target behaviors with solutions. In: International Conference on Persuasive Technology, pp. 117–131 (2010)
9. Middelweerd, A., Mollee, J.S., van der Wal, C.N., Brug, J., Te Velde, S.J.: Apps to promote physical activity among adults: a review and content analysis. *Int. J. Behav. Nutr. Phys. Act.* **11**(1), 97 (2014)
10. Stragier, J., Mechant, P.: Mobile fitness apps for promoting physical activity on Twitter: the# RunKeeper case. In: *Etmaal van de Communicatiewetenschap* (2013)
11. West, L.R.: Strava: challenge yourself to greater heights in physical activity/cycling and running. *Br. J. Sport. Med.* **49**(15), 1024 (2015)
12. Endomondo. <https://www.endomondo.com/>. Accessed 10 Feb 2020
13. Albaina, I.M., Visser, T., Van Der Mast, C.A.P.G., Vastenburg, M.H.: Flowie: a persuasive virtual coach to motivate elderly individuals to walk. In: 2009 3rd International Conference on Pervasive Computing Technology Healthc (2009)
14. Consolvo, S., et al.: Activity sensing in the wild: a field trial of ubifit garden. In: Proceedings of the SIGCHI Conference on Human Factors in Computing Systems, pp. 1797–1806 (2008)
15. Lin, J.J., Mamykina, L., Lindtner, S., Delajoux, G., Strub, H.B.: Fish‘N’Steps: encouraging physical activity with an interactive computer game. In: Proceedings of the 8th International Conference on Ubiquitous Computing, pp. 261–278 (2006)
16. Bielik, P., Tomlein, M., Krátky, P., Mitrik, Š., Barla, M., Bieliková, M.: Move2Play: an innovative approach to encouraging people to be more physically active. In: Proceedings of the 2nd ACM SIGHIT International Health Informatics Symposium, pp. 61–70 (2012)
17. Min, C., Yoo, C., Lee, Y., Song, J.: Healthopia: towards your well-being in everyday life. In: Proceedings of the 4th International Symposium on Applied Sciences in Biomedical and Communication Technologies, p. 108 (2011)
18. John Horsman, G.W.T., Furlong, W.J., Feeny, D.I.: The Health Utilities Index (HUI®): concepts, measurement properties and applications. *Health Qual. Life Outcomes* (2003)

Open Access This chapter is licensed under the terms of the Creative Commons Attribution 4.0 International License (<http://creativecommons.org/licenses/by/4.0/>), which permits use, sharing, adaptation, distribution and reproduction in any medium or format, as long as you give appropriate credit to the original author(s) and the source, provide a link to the Creative Commons license and indicate if changes were made.

The images or other third party material in this chapter are included in the chapter’s Creative Commons license, unless indicated otherwise in a credit line to the material. If material is not included in the chapter’s Creative Commons license and your intended use is not permitted by statutory regulation or exceeds the permitted use, you will need to obtain permission directly from the copyright holder.





Baseline Modelling and Composite Representation of Unobtrusively (IoT) Sensed Behaviour Changes Related to Urban Physical Well-Being

Vladimir Urošević¹(✉), Marina Andrić¹, and José A. Pagán²

¹ Belit d.o.o. Beograd, Trg Nikole Pašića 9, 11000 Belgrade, Serbia
vladimir.urosevic@belit.co.rs

² The New York Academy of Medicine, 1216 Fifth Avenue, New York
NY 10029, USA

Abstract. We present the grounding approach, deployment and preliminary validation of the elementary devised model of physical well-being in urban environments, summarizing the heterogeneous personal Big Data (on physical activity/exercise, walking, cardio-respiratory fitness, quality of sleep and related lifestyle and health habits and status, continuously collected for over a year mainly through wearable IoT devices and survey instruments in 7 global testbed cities) into 5 composite domain indicators/indexes convenient for interpretation and use in predictive public health and preventive interventions. The approach is based on systematized comprehensive domain knowledge implemented through range/threshold-based rules from institutional and study recommendations, combined with statistical methods, and will serve as a representative and performance benchmark for evolution and evaluation of more complex and advanced well-being models for the aimed predictive analytics (incorporating machine learning methods) in subsequent development underway.

Keywords: Behaviour recognition · Wearable devices · Unobtrusive sensing · Well-being · Vital health parameters · Data labelling · Composite index modelling

1 Introduction

The urban public health, well-being monitoring, and prevention are recently being transformed from reactive to a predictive and eventually long-term risk mitigating systems, through a number of research initiatives and projects, such as the ongoing PULSE Project (Participative Urban Living in Sustainable Environments, funded from the EU Horizon 2020 programme) focusing on the chronic metabolic and respiratory diseases (such as type 2 diabetes and asthma) affected or exacerbated by the preventable or modifiable environmental and lifestyle factors, and well-being/resilience. A major challenge in the Project is the modelling and assessment/prediction of citizen well-being from the collected and processed Big Data of unprecedented variety and from highly heterogeneous sources (health and vital activity personal data obtained

through wearable devices and other sensing technologies, geo-located online surveys, open/public smart city datasets...), on individual and collective (population/cluster) levels. Overall well-being and its main domains (vitality, supportive relationships, stress levels...) are all significant factors affecting the onset and exacerbation of the stated chronic diseases which are becoming more and more widespread and progressing in urban environments, and overall resilience of citizens and urban communities is increasingly important against other pertaining global and sustainability challenges, like climate change.

The proposed and deployed elementary statistical model presented in this paper is to be the basis for interpretation and contextualization of changes to well-being, and a performance benchmark for evaluation and comparison of more complex and advanced well-being models of the aimed predictive analytics and final intelligent system (incorporating machine learning methods) in subsequent development, supporting the PULSE PHOs (Public Health Observatories established for the relevant policy making and execution in smart cities).

2 Conceptual Background and Approach

The activity and vital/health parameters data measured mostly unobtrusively by wearable devices (wristbands, smartwatches) have particular significance for behaviour analysis and change recognition in PULSE, as these are the input data streams with highest volume, acquisition “velocity”, and temporal resolution/granularity of all the various data collected in the Project, and therefore practically the most (and only) suitable data comprising the sufficiently continuous and non-sparse time series over months, to properly derive or construct the behavioural patterns and analyze behaviour changes. Recent studies performed by the stated major wearable device manufacturers over billions of records of temporal measurements data [1, 2], as well as the experiences from projects like the just concluded City4Age (www.city4ageproject.eu) [3, 4], show the significance and general predictive ability of the measured main vital/health and activity parameters (walking, climbing stairs, physical activity/exercise, heart rate data, consumed calories...) for overall health and physiological/physical well-being assessment. The additional complementary socio-demographic, health, lifestyle/habits and environmental data in less frequent temporal resolution, ingested from the open/public datasets or manual “obtrusive” inputs, are combined to cross-check, adjust and improve integrity of the recognized behaviour changes derived from the main time-series data acquired through the wearable devices.

We adopt a combined knowledge- and data-driven approach in detection and characterization of relevant behaviours that denote significant variations in well-being, with multi-level hierarchical model topology and range/threshold based computational rules as basic primary formal knowledge structures, and statistical analytics as baseline (and performant) data-driven detection methods.

The complexity of human behaviours is commonly represented through multi-level hierarchical structured models, decomposed to more granular “units” like activities and action events [5, 6], with multiple variables from behavioural, physiological and environmental domains of well-being known to additionally increase complexity and

dimensionality [7]. There are other contending approaches, like the monitoring and analysis of individual well-being or behavioural domain indicators or determinants independently in parallel, without hierarchical structuring and substantial synthesis into fewer higher-level composite factors or score(s) [8]. Most, including the adopted and followed approach works (like [9]), are comprehensively covered or referenced in the *Encyclopedia of Quality of Life and Well-Being Research* (Springer 2014) that summarizes recent research works related to well-being and quality of life in spanned various research and policy-making/implementation fields. Main advantages of a few composite synthetic indicators/factors over a battery of multiple separate indicators, namely:

- ability to summarize complex and multi-dimensional real-life phenomena or domains (like well-being),
- easier for interpretation and comparison among (socio-demographic, geospatial/regional...) groups or population clusters,
- more effective for comprehending overall trends, particularly when a number of the underlying indicators denote opposing-trend changes,

are of crucial significance in usage and context settings of the PULSE project, with over 60 indicators formalized in the initial knowledge-based well-being model topology from the systematization of collected data, and with

- visible set of indicators to various stakeholders (policy makers, researchers, general public) needing to be minimal without omitting important underlying information,
- and collaboration, communication and comparison of complex dimensions by various stakeholders needing to be most straightforward, facilitated and effective.

We therefore propose two complementary approaches for synthesis of the composite well-being indicators composed from underlying streamed IoT-sourced time-series data in the context of PULSE. The indicators summarize multi-dimensional aspects of citizen well-being and enable the assessment of individual and synthesized collective urban well-being over time. The notion is illustrated through analysis within the scope of four representative and characteristic key summary indicators of citizen health and fitness, derived from activity and vital/health parameters measured, as stated, using wearable sensing devices: motility, physical activity, sleep quality and cardio-respiratory health/fitness (Fig. 1).

In the first approach, daily and intra-daily underlying measurements (Table 1) are used to estimate levels of adherence to rule- and range-based recommendations matured from institutional knowledge of relevant authorities and population-significant studies in the field, accumulated for over decades in the stated four example domains of motility, physical activity, sleep quality and cardio-respiratory fitness [8, 10, 11].

The complementary data-driven statistical approach is predicated on standard scores that denote the number of standard deviations that a given measurement deviates from the sample mean. This approach allows comparison of individual scores to the corresponding norm groups stratified by common socio-demographic parameters (age, gender...), when considered conditionally independent nodes in the complete model topology. It also allows to place a score for any individual and variable with respect to alternative descriptive statistic or measure of central tendency (variable median,

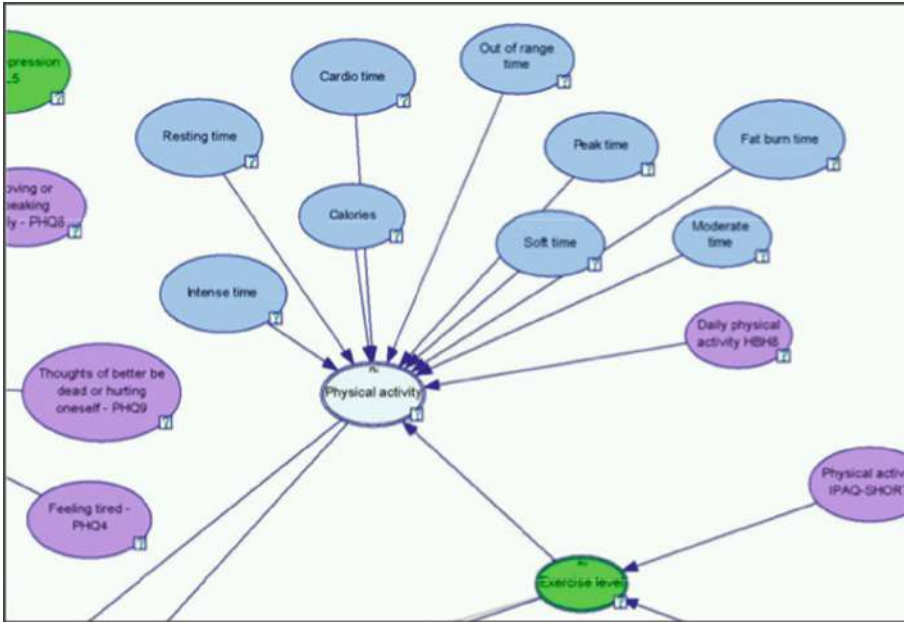


Fig. 1. Excerpt from the hierarchical network structure topology of the initial knowledge-based PULSE well-being model (*blue-coloured nodes* are variables measured by wearable sensing devices, and *magenta-coloured* are reported/input through online app. questionnaires) (Color figure online)

geometric mean, standard deviation or error), so that more accurate or optimal comparison for specific variable distribution can be made.

3 Citizen Activity and Vital/Health Parameters Data

The data are collected by several types of health and fitness wearable tracker devices manufactured by Fitbit, Garmin and ASUS, monitoring physical and walking activity, sleep and heart/cardio parameters, for over 300 recruited citizens participating in the study in 7 global testbed cities (Barcelona, Birmingham, New York, Paris, Pavia(Italy), Singapore, and Keelung/Taipei), supplied with wearable tracker devices by the Project.

Physical activity level as a single measure is mainly expressed in terms of time spent and calories burned while performing light/soft, moderate, and intense/vigorous physical activity. Walking activity is captured with walked steps, distance, speed, and climbed stairs/floors measurements. Heart rate measures capture time spent in different target heart rate zones (like peak, cardio, fat burn), resting and maximal heart rate (hr_{max}), and some still experimental measures like systolic and diastolic blood pressure, measured by the newest recently released devices such as ASUS VivoWatch BP, but not yet acquired in significant volume sufficient for analysis. The peak heart rate zone by default definition ranges from 85 to 100% of person's maximum heart rate (hr_{max}),

the cardio zone ranges from 70 to 84% of hr_{max} , and the fat burn zone ranges from 50 to 69% of hr_{max} . Sleep quality/hygiene measures mainly capture time spent in defined phases of sleep. All the processed measures are listed in Table 1, collected or aggregated with a default daily periodicity, except the ones in gray-shaded rows which are acquired in higher intra-daily temporal resolution, mostly once in every 15 min or up to once in a minute, depending on the variable.

Table 1. List of variables measured by the used wearable devices, with descriptions and *units of measure* (SI base units in square brackets where applicable, like [s]-seconds, or [m]-meters)

Measured variable	Description [unit]
still_calories	amount of calories burned while being still
total_calories	total amount of calories burned (default in a day)
walk_steps	number of walked steps
walk_distance	walked distance [m]
stairs_floor_changes_up	number of floors traversed in climbing stairs up
elevation	vertical distance [m] traversed in climbing stairs
still_time	time [s] spent being still
physicalactivity_soft_time	time [s] spent performing light/"soft" physical activities like relaxed walking/strolling or standing up and moving around in the home, workplace or community
physicalactivity_moderate_time	time [s] spent performing moderate physical activities like swift walking, dancing, gardening
physicalactivity_intense_time	time [s] spent performing intense/vigorous physical activities like running, fast cycling or swimming, tennis, jumping rope
physicalactivity_calories	amount of calories burned while performing physical activities
heartrate_cardio_time	time [s] duration of the heart rate being within the defined "cardio" target range
heartrate_peak_time	time [s] duration of the heart rate being within the defined "peak" target range
heartrate_resting	resting heart rate
heartrate_avg	average heart rate
heartrate_max	maximal heart rate
sleep_time	total time [s] spent in all phases of sleep
sleep_efficiency	calculated score derived from sleep_time, sleep_asleep_time and sleep_wake_time
sleep_deep_count	number of times falling into deep sleep
sleep_deep_time	total time [s] spent in deep sleep
sleep_light_count	number of times falling into light sleep
sleep_light_time	total time [s] spent in light sleep
sleep_rem_count	number of times falling into REM sleep stage
sleep_rem_time	total time [s] spent in REM sleep stage
sleep_wake_count	number of times waking up
sleep_wake_time	total time [s] spent in waking up
sleep_awake_time	total time [s] spent awake during sleep
sleep_awake_count	number of times awakening during sleep
sleep_restless_time	total time [s] spent being restless during sleep
sleep_restless_count	number of times getting restless during sleep
sleep_asleep_time	total time [s] spent being fully asleep
sleep_asleep_count	number of times falling fully asleep

In addition to stated behavioral time-series data, an extensive set of personal socio-demographic, profile (age, gender, ethnicity, educational and marital status, employment status and occupational environment...), as well as health state, risk factors and habits, lifestyle, neighbourhood and quality of life assessment, and other relevant behavioural data are manually input/submitted on each citizen participating in the study via online forms, composed from adapted relevant survey/assessment instruments for each specific field, like Framingham, EuroQoL-5, IPAQ-SF. These data are geo-localized to the residence location of each responding citizen for the purposes of analytics of collective/community well-being, and are collected from a greater number of recruited respondents, but just in rare cases in more than one iteration over time due to the high number and scope of covered variables, and therefore suitable for a broad but mainly static “snapshot” assessment of current well-being state rather than for behaviour change model and analytics. Incorporating both these static and IoT-sensed temporal data into a fully comprehensive predictive well-being model is an ongoing task in progress throughout the end of the Project, with results to be presented in other upcoming publications.

4 Derivation of Domain/Dimension Indices

4.1 Physical Activity/Exercise

Physical activity in our first approach stated above in Sect. 2 can be discretized using several common baseline categorizations related or derived from the above mentioned relevant institutional/governmental and professional expert guidelines for the urban population groups. The example approach taken in the recent health survey of England from 2016 [12] compared well-being and mental health of adults in different socio-demographically stratified population groups by physical activity, among others. The activity level categories used in the analysis were the following:

- *Meets aerobic guidelines*: At least 150 min moderately intensive physical activity or 75 min vigorous activity per week or an equivalent combination of these
- *Asserted activity*: 60 to 149 min moderate activity or 30–74 min vigorous activity per week or an equivalent combination of these
- *Low activity*: 30 to 59 min moderate activity or 15 to 29 min vigorous activity per week or an equivalent combination of these
- *Inactive*: Less than 30 min moderate activity or less than 15 min vigorous activity per week or an equivalent combination of these,

and the corresponding linear scaled scoring function denotes “*Meets aerobic guidelines*” with a score of 4, “*Certain activity*” - 3, “*Low activity*” - 2, and “*Inactive*” with 1. This baseline scoring scale, besides sufficient granularity and robustness exhibited in referenced comprehensive studies, is also convenient for

- mapping to the defined activity level categories used as input parameters for the consensus models for prediction of risk of Type 2 Diabetes (T2D) and asthma onset and exacerbation, developed for the PULSE project [13, 17]

- quantification of longer-term and/or periodic activity level behaviours directly from categorized daily or incidental activity level values as measured and acquired from the wearable tracker devices through relevant APIs (*light/soft*, *moderate*, and *vigorous/intense* activity).

4.2 Specific Walking Activity

Similarly, the authors in [14] and [15] demonstrate the following referent threshold ranges of the number of daily walked steps to be used for classification of walking activity in healthy adults, and the corresponding scoring function linearly assigning the following 1–5 integer scores to the classification categories: *highly active* (12,500 or more steps/day) – 5, *active* (10,000–12,499 steps/day) – 4, *somewhat active* (7,500–9,999 steps/day) – 3, *lowly active* (5,000–7,499 steps/day) – 2, and *sedentary* (under 5,000 steps/day) – 1.

4.3 Cardiovascular Fitness - VO₂max

VO₂max is the metric denoting the maximum amount of oxygen that an individual can use during intense exercise. It is widely and commonly used as an indicator of cardiorespiratory fitness.

A simple generic estimate of VO₂max of an individual can be obtained using their maximum and resting heart rates in the following formula, published in [16]:

$$VO_{2\max} \approx \frac{hr_{\max}}{hr_{\text{rest}}} * 15.3 \text{ mL}/(\text{kg} * \text{min}) \quad (1)$$

Where hr_{\max} can be crudely estimated as $220 - \text{age of the person}$.

A relatively standard convenient and meaningful categorization of VO₂max for Western European and USA populations can be on a scale from 1 - *very low*, through 2 - *low*, 3 - *fair*, 4 - *moderate*, 5 - *good*, and 6 - *very good*, to maximal 7 - *elite*, depending of the individual's gender and age, with common categorization for males and females aged 6 to 75 published by Shvartz & Reibold in [11].

4.4 Quality of Sleep

Total average sleep duration in 24 h is a straightforward direct metric for assessing the quality of sleep in terms of longer-term stable behaviour across complete populations. The US National Sleep Foundation recently provided the following referent expert sleep duration recommendations (in terms of recommended (or not) threshold values for both oversleep and undersleep), categorized by precise granular age ranges [10]:

These recommendations categorize possible output sleep duration times as either *recommended*, *may be appropriate*, or *not recommended*, and the optimal *recommended* duration is 7–9 h for majority of the populations.

Table 2. Detailed US National Sleep Foundation recommended threshold values and ranges for sleep duration per age category

Category <i>age</i>	Recommended	Considered appropriate	Not recommended
Newborns <i>0–3 months</i>	14 to 17 h	11 to 13 h 18 to 19 h	Less than 11 h More than 19 h
Infants <i>4–11 months</i>	12 to 15 h	10 to 11 h 16 to 18 h	Less than 10 h More than 18 h
Toddlers <i>1–2 years</i>	11 to 14 h	9 to 10 h 15 to 16 h	Less than 9 h More than 16 h
Preschoolers <i>3–5 years</i>	10 to 13 h	8 to 9 h 14 h	Less than 8 h More than 14 h
School-aged Children <i>6–13 years</i>	9 to 11 h	7 to 8 h 12 h	Less than 7 h More than 12 h
Teenagers <i>14–17 years</i>	8 to 10 h	7 h 11 h	Less than 7 h More than 11 h
Young Adults <i>18–25 years</i>	7 to 9 h	6 h 10 to 11 h	Less than 6 h More than 11 h
Adults <i>26–64 years</i>	7 to 9 h	6 h 10 h	Less than 6 h More than 10 h
Older Adults <i>65 years and over</i>	7 to 8 h	5 to 6 h 9 h	Less than 5 h More than 9 h

Additionally, relevant recent findings like the extensive meta-analysis performed by the American Diabetes Association to assess the dose-response relationship between sleep duration and risk of type 2 diabetes [18], have concluded that the lowest type 2 diabetes risk is for the average overnight sleep duration from 7 to under 9 h per day, and that both shorter and longer sleep durations than this optimum range denote up to 1.5 times increased risk (and up to 2 times increased cardiac conditions risk shown in the related studies [21], also relevant in the Project). We therefore slightly alter the *maybe appropriate* category from the otherwise adopted recommendations from Table 2 above to *mildly risky*, reflecting the importance of stated health risks in PULSE, and the effect of common or periodically repeated behaviour patterns over months or years to the exasperation of the risks. This categorization will also consequently be communicated on the data visualizations and public health/prevention interventions and campaigns deployed and administered through relevant PULSE system applications and modules (PHO Dashboards, PulsAIR gamified mobile app.) towards the citizens and urban communities, and the resulting function scores assigned to the categories are therefore: **1** for *not recommended*, **1.75** for *mildly risky*, and **2** for *recommended*, inversely proportional to the pessimistically estimated risks increase brought by shorter durations. Complex eventual relations of detailed specific measured sleep parameters to well-being will be explored by more advanced methods in other subsequent work.

4.5 The Composite Physical Well-Being Indicator

From several existing elementary statistical approaches for aggregating the underlying dimensional indices and constructing the summary composite indicator value, we consider the weighted geometric mean of the four constituting dimensional indices as most adequate and appropriate for this specific well-being problematics:

$$WB_{ph} = \sqrt[4]{I_w^{Wt_w} * I_p^{Wt_p} * I_s^{Wt_s} * I_c^{Wt_c}}, \quad (2)$$

where summary dimensional indices denoted by the scoring function values are: I_w – walking activity index, I_p – physical activity/exercise index, I_s – sleep duration index, I_c – cardio-respiratory fitness index (through $VO_2\max$), and Wt_w , Wt_p , Wt_s , and Wt_c are respective weight factors, derived from expert assessments and rank data from relevant previous studies and experience, and assigned to adjust the relative importance and contribution of each of the indices to the resulting composite indicator value, per compositing methods outlined in [19] and [9], or for derivation of composite UN Human Development Index (HDI). As all 4 constituting indices are directly proportional to the resulting composite indicator (i.e. the higher the activity levels or cardio-respiratory fitness scores, the higher the well-being), and low value of either of the four is significant for decreased overall composite (although there is some correlation between the indices - e.g. decrease in cardio-respiratory fitness in most cases causes decreased activity levels as well), the geometric mean is adequate for its sensitivity to low values of each individual constituting index, and ability to combine values on completely different scales without normalization required. Initially assigned values of weight factors are 0.9 for I_w , 1 for I_p , and 1.05 for I_s and I_c , taking into account the importance of specific indices for respiratory disease and T2D risk, volatility of the collected data by now, and known overestimation of some measured variable values (like number of walked steps, $VO_2\max$ estimate, or recognized sessions of cycling and some other exercise types) by the predominantly used wearable devices - Fitbit Charge 2 [20]. The weight factors are set as configuration parameters in the model, so they can be changed to fine-tune the composition according to the data insights acquired over time or the results of the validation described in Sect. 5 below.

Time series of the values of the composite indicator are formed from weekly and monthly aggregations of underlying daily and intra-daily measurements into the 4 constituting index values. Method for computing those values from the measured values of variables listed in Table 1 above is as developed and introduced in [22] for synthesis of indicators and geriatric factors from the same source IoT data, based in this case on univariate normalization of relative changes (quantified in standard scores, as stated above in the “Approach” Sect. 2) of acquired Big temporal Data during the complete study period, and then multivariate weighted linear aggregation of obtained normalized indicators and descriptive statistics into higher-level composite factors, to capture weekly and monthly behavioural patterns and trends, less susceptible to influence of outliers and occasional notably deviating values.

5 Preliminary Validation of the Composite Index and Conclusion

Validation metric is the correlation with specific corresponding summary measure(s) of current well-being, self-reported by the respondent citizens through web and mobile app. questionnaires as mentioned above. They can be summarized from two relevant subset questionnaires: 1) European Social Survey (ESS), and 2) EuroQoL-5D (EQ5) survey instrument, both standardized (with minor adaptations) and common for measuring well-being in multiple continuous and/or repeated relevant Europe-wide and national-level studies, and robust to some degree against extreme fully subjective bias.

15 statements of the ESS questionnaire broadly cover social and most of the other aspects of personal and community well-being that the respondent rates on a 5-degree Likert scale (*Strongly agree*-4, *Agree*-3, *Neither agree nor disagree*-2, *Disagree*-1, *Strongly disagree*-0), the total possible questionnaire score thus ranging from 0, denoting the lowest/worst well-being, to 60 representing the optimum.

EQ5 instrument is focused on physical and mental health status and daily life activities measured in 5 dimensions (mobility, self-care, usual activities, pain/discomfort and anxiety/depression), also self-rated on a 5-degree scale from perceived worst to best like in ESS. Last question asks for assessment of the respondent's overall health state (*hsa*) on the current day, on the scale from 0 (worst) to 100 (best imaginable), also mapped to a number ranged from 1 to 5 by the formula $1 + 4 * hsa/100$ for the purpose of this evaluation. Total cumulative EQ5 score thus ranges from 6 to 30.

Figure 2 below shows the correlation scatter plot of ESS scores and composite well-being indices for 97 respondents of which 12 filled EES questionnaire twice, two filled it three times, and the rest only once during the observed period of 11 months.

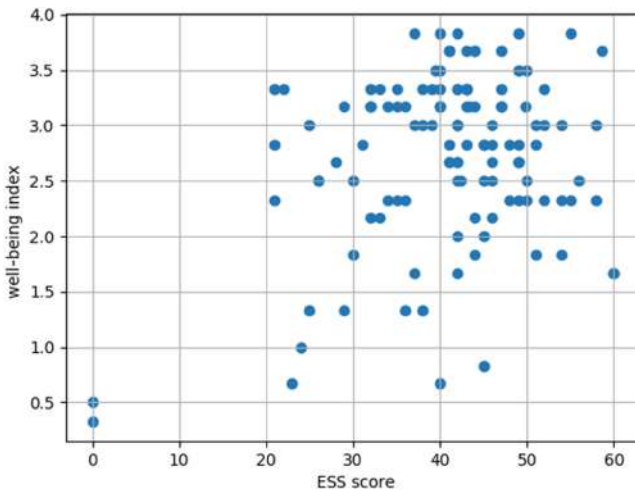


Fig. 2. Scatter plot of composite well-being index vs. cumulative ESS score values

Figure 3 shows the relationship between the composite well-being indices and the obtained EQ5 scores of 107 respondents, 3 of which filled the questionnaire three times, 20 filled it twice, and the rest once during the observed data collection period.

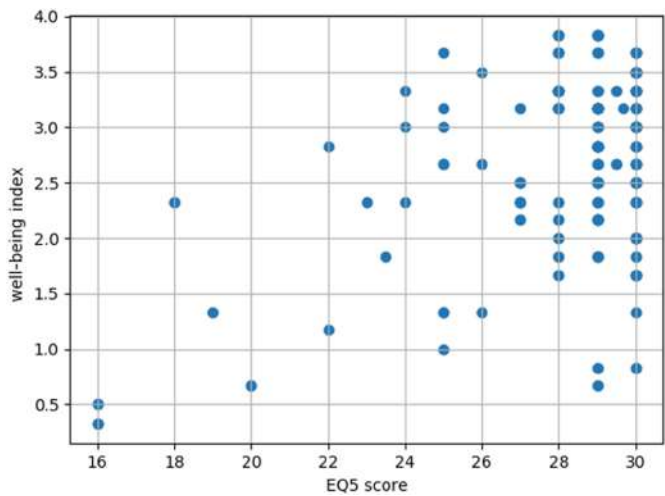


Fig. 3. Scatter plot of composite well-being index vs. cumulative EQ5 score values

The analysis reveals a medium positive correlation of 0.424 (with the p-value of approx. 3.7×10^{-7}) between our constructed composite index and cumulative EQ5 scores. The composite indicator and its constituting domain indices can therefore be considered promising for their intended purpose of basic representation of the urban physical well-being aspects modelled from a variety of heterogeneous underlying activity and health/vital parameters measured by IoT wearable devices, summarized in 4 main dimensional and one overall derived score convenient for comparisons, interpretation and presentation to the end-users, particularly in the required shortest most concise manner and form, such as through a mobile app. UI or intervention messages.

As almost half of the questions in EQ5 are very remotely or not at all related to the physical well-being aspects summarized by the composite indicator, the correlation is expected to increase when the ongoing work in incorporating social and other well-being aspects fully in the model is completed.

Found small positive correlation of 0.287 (p-value 0.001) between the composite indicator and cumulative scores of ESS questionnaire (in which most of the questions are not related to physical well-being) additionally points to the significance of this composite indicator to the overall well-being. The work also continues on the cleaning and pre-processing the data collected on the remaining monitored citizens, incorporation of machine learning methods in the model and exploration and modelling of the influence of detailed sleep and cardiac parameters, as well as of the sensed ambiental data, on the main well-being domains.

Acknowledgment. This work has received funding from the European Union's Horizon 2020 research and innovation programme under the grant agreement No. 727816 (PULSE). The performed research studies have all been granted ethical approval from the relevant IRB authority in each PULSE pilot testbed city (Ethics Committee of the Parc de Salut Mar hospital in Barcelona, through NHS Health Research Authority IRAS (Integrated Research Application System) in Birmingham, New York Academy of Medicine IRB in New York City, etc.), resulting from comprehensive multimonthly evaluation processes. The inclusion and exclusion methods and criteria for recruiting citizens have been specified in relevant previous publications of the Project, such as in Section 2.2.1. *Participation Criteria* in [23].

References

1. <https://www.businesswire.com/news/home/20180214005548/en/>. Accessed Feb 2020
2. <https://www.digitaltrends.com/health-fitness/fitbit-resting-heart-rate-study>. Accessed Feb 2020
3. Abril-Jiménez, P., Rojo Lacal, J., de los Ríos Pérez, S., Páramo, M., Montalvá Colomer, J. B., Arredondo Waldmeyer, M.T.: Ageing-friendly cities for assessing older adults' decline: IoT-based system for continuous monitoring of frailty risks using smart city infrastructure. *Aging Clin. Exp. Res.* **32**(4), 663–671 (2019). <https://doi.org/10.1007/s40520-019-01238-y>
4. Almeida, A., Mulero, R., Rametta, P., Urošević, V., Andrić, M., Patrono, L.: A critical analysis of an IoT-aware AAL system for elderly monitoring. *Future Gener. Comput. Syst.* **97**, 598–619 (2019). <https://doi.org/10.1016/j.future.2019.03.019>
5. Díaz Rodríguez, N.: Semantic and fuzzy modelling for human behaviour recognition in smart spaces. In: *Studies on the Semantic Web*, vol. 23. IOS Press Amsterdam (2016)
6. Azkune, G., Almeida, A.: A scalable hybrid activity recognition approach for intelligent environments. In: *Journal of LaTeX Class Files*, vol. 14, no. 8 (2015)
7. Kolarz, P., Angelis, J., Krčál, A., Simmonds, P., Traag, V., Wain, M.: Comparative impact study of the European social survey (ESS) european research infrastructure consortium (ERIC). Final Report. ESS-SUSTAIN Project (H2020 funded), Technopolis Group (2017)
8. Bagnall, A., South, J., Mitchell, B., Pilkington, G., Newton, Rob., Di Martino, S.: Systematic scoping review of indicators of community wellbeing in the UK. "What Works" Centre for Wellbeing (2017). <https://doi.org/10.13140/rg.2.2.21762.17604>
9. Land, K.C.: Composite index construction. In: Michalos, A.C. (eds.) *Encyclopedia of Quality of Life and Well-Being Research*. Springer, Dordrecht (2014). https://doi.org/10.1007/978-94-007-0753-5_3317
10. Hirshkowitz, M., Whiton, K., Albert, S.M., Alessi, C., Bruni, O., Ohayon, M.: National sleep foundation's sleep time duration recommendations: methodology and results summary. *Sleep Health* **1**, 40–43 (2015)
11. Shvartz, E., Reibold, R.: Aerobic fitness norms for males and females aged 6 to 75 years: a review. *Aviat. Space Environ. Med.* **61**(1), 3–11 (1990)
12. Morris, S., Earl, K., Neave, A.: Health survey for England 2016: well-being and mental health. NHS Digital Health and Social Care Information Centre and the UK Office for National Statistics (2017). ISBN 978-1-78734-099-2
13. Di Camillo, B., et al.: HAPT2D: high accuracy of prediction of T2D with a model combining basic and advanced data depending on availability. *Eur. J. Endocrinol.* **178**(4), 331–341 (2018)
14. Tudor-Locke, C., Bassett, D.: How many steps/day are enough? *Sports Med.* **1**, 1–8 (2004)

15. Tudor-Locke, C., Craig, C.L., Brown, W.J., Clemes, S.A., Cocker, K.D., Schmi, M.D.: How many steps/day are enough? For adults. *Int. J. Behav. Nutr. Phys. Act.* **8**, 79 (2011)
16. Uth, N., Sorensen, H., Overgaard, K., Pedersen, P.: Estimation of VO₂max from the ratio between HRmax and HRrest - the heart rate ratio method. *Eur. J. Appl. Physiol.* **91**(1), 111–115 (2004). <https://doi.org/10.1007/s00421-003-0988-y>
17. Sambo, F., et al.: A Bayesian Network analysis of the probabilistic relations between risk factors in the predisposition to type 2 diabetes. In: *Conference Proceedings IEEE Engineering Medicine Biology Society*, pp. 2119–2122 (2015). <https://doi.org/10.1109/embc.2015.7318807>
18. Shan Z., et al.: Sleep duration and risk of type 2 diabetes: a meta-analysis of prospective studies. *Diabetes Care* **38**(3), 529–537 (2015). <https://doi.org/10.2337/dc14-2073>
19. Smith, L., Smith, H., Case, J., Harwell, L., Summers, J., Wade, C.: Indicators and methods for constructing a US human well-being index (HWBI) for ecosystem services research. US Environmental Protection Agency, Report #EPA/600/R-12/023 (2012)
20. Freeberg, K.A., Baughman, B.R., Vickey, T., Sullivan, J.A., Sawyer, B.J.: Assessing the ability of the fitbit charge 2 to accurately predict VO₂max. *mHealth* **5**, 39 (2019). <https://doi.org/10.21037/mhealth.2019.09.07>
21. Li, W., et al.: Sleep duration and risk of stroke events and stroke mortality: a systematic review and meta-analysis of prospective cohort studies. *Int. J. Cardiol.* **223**, 870–876 (2016). <https://doi.org/10.1016/j.ijcard.2016.08.302>
22. Ricevuti, G., Venturini, L., Copelli, S., Mercalli, F., Nicolardi, G.: Data driven MCI and frailty prevention: geriatric modelling in the City4Age project. In: *IEEE 3rd International Forum on Research and Technologies for Society and Industry (RTSI)*, Modena, pp. 1–6 (2017)
23. Ottaviano, M., et al.: Empowering citizens through perceptual sensing of urban environmental and health data following a participative citizen science approach. *Sensors* **19**(13), 2940 (2019)

Open Access This chapter is licensed under the terms of the Creative Commons Attribution 4.0 International License (<http://creativecommons.org/licenses/by/4.0/>), which permits use, sharing, adaptation, distribution and reproduction in any medium or format, as long as you give appropriate credit to the original author(s) and the source, provide a link to the Creative Commons license and indicate if changes were made.

The images or other third party material in this chapter are included in the chapter's Creative Commons license, unless indicated otherwise in a credit line to the material. If material is not included in the chapter's Creative Commons license and your intended use is not permitted by statutory regulation or exceeds the permitted use, you will need to obtain permission directly from the copyright holder.



Wellbeing Technology



Automatic Daily Activity Schedule Planning for Simulating Smart House with Elderly People Living Alone

Can Jiang^{1(✉)} and Akira Mita²

¹ Graduate School of Science and Technology, Keio University, 3-14-1 Hiyoshi,
Kohoku-ku, Yokohama, Kanagawa, Japan
canjiang@keio.jp

² Department of System Design Engineering, Keio University, 3-14-1 Hiyoshi,
Kohoku-ku, Yokohama, Kanagawa, Japan
Mita@keio.jp

Abstract. A simulation tool that supports developers to build scenarios automatically in multiple simulation platforms is proposed. As an essential part of this simulator, this study proposed an activity schedule generator to mimic the daily life of elderly people living alone. This generator outperforms existing methods of activity schedule planning in three aspects: 1) it is adaptive to the layout of a simulated smart house; 2) there is no unspecified time in the timeline of generated schedules; and 3) it generates stable, but not tedious schedules for a number of days. A real-time location data generator is proposed to convert generated schedules to simulated real-time location data of the resident, and a proposed interface converts these simulated location data to simulated records of virtual passive infrared (PIR) sensors, which can be used to optimize placement of PIR sensors in a smart house.

Keywords: Elderly people living alone · Smart home simulator · Activity of daily living · Motivation · Automatic scenario generation

1 Introduction

The elderly population is increasing worldwide. An estimated 617.1 million people are aged 65 and over in 2015, and this number is projected to increase to 1 billion in 2030, and 1.6 billion in 2050 [1]. More than 20% of men and 40% of women aged 65 and older chose an independent lifestyle in many countries [2]. Pimouguet et al. [3] indicated living alone shortened life expectancy by 0.6 years for elderly people. Elderly individuals living alone would benefit from specialized care, but a shortage in the global workforce of aged-care workers [4] has made this difficult.

Under these conditions, smart houses with a sensor network and domestic robots have been built to address the aged-care worker shortage. The sensor networks provide real-time health monitoring [5] and a means of detecting emergencies [6], while mobile domestic robots provide location-based support [7] and services [8] for residents. To ensure the effectiveness of the sensor networks and robots, real test beds were built to conduct experiments for collecting data. However, building a test bed is expensive, and

simulations are necessary for smart house developers to test and verify their ideas before building a real one.

Developers typically conduct simulations using the following three steps. (1) Manually create a simulation scenario by first building a house and resident body models and defining the activity schedules and movement routes of the virtual resident or controlling the virtual resident manually. (2) Place virtual sensors, devices, or robots to record data and/or operation performances. (3) Analyze recorded data or operation performances and evaluate simulation design. As a typical simulation constructed in step (1) requires a lot of time, developers can only prepare a limited number of scenarios. Moreover, the developers may use multiple simulators for different purposes, e.g., using CST Microwave Studio to test the communication of a wireless sensor network, OpenSHS [9] to collect virtual sensor records for sensor arrangement optimization, and Stage [10] to plan the operation policies of mobile robots. When the developers use another simulator, they must repeat steps (1) even if they use the same simulation scenario.

We propose a simulation tool that provides diverse simulation scenarios and can support smart house developers to complete step (1) automatically in multiple simulation platforms [11]. This simulator consists of generators and interfaces as show in Fig. 1. The proposed generators produce diverse information such as indoor spatial attributes and resident travel patterns. This information is used to create a scenario that can run on different simulation platforms through various interfaces. We proposed a spatial attribute generator [12] and travel pattern generator [11], and used two interfaces [11] to transfer the data generated by them to models and virtual sensor records of the simulators.

As an essential part of our simulator, we propose an activity schedule generator. With generated travel patterns, these schedules are converted to simulated real-time location data, which can be used in simulations with interfaces. The rest of this paper is organized as follows. In Sect. 2, we review related work of daily activity schedule generation. Section 3 describes the methodology to generate activity schedules. Section 4 details the performance of this generator. Section 5 introduces how the generated data can be used in simulations.

2 Related Works

A number of scholars generated daily activity schedules as intermediate results to generate sensor records in a virtual smart house, which are essential for simulations.

Renoux et al. [13] generated activity schedules with a constraint-based planning method. The constraints include that the start time and duration of each activity are over reasonable intervals, and a number of activities need to be performed within certain time intervals before their corresponding activities, e.g., preparing lunch for 0 to 5 min before having lunch.

Bouchard et al. [14] generated activity schedules using behavior trees (BTs) as intermediate results to generate the simulated evolution of signal strength between RFID readers and tags. However, designing BTs is complicate, and the authors only showed an example of generating the schedule for making coffee or tea.

Alshammari et al. [9] replicated and modified schedules originally designed by humans. The methods of modification include combining two samples of original schedules and changing the start and end time of activities. The activity schedules correspond to virtual binary sensor records, thus, a large number of records are generated simultaneously. This method is simple, but generated schedules may have high similarity.

Mshali et al. [15] generated long-term activity schedules using a Markov model, and five transition matrices associated to different periods of a day were designed. The authors also proposed an adaptive and context-aware algorithm for monitoring the daily activities of elderly and dependent persons, and generated schedules were used to test the algorithm in simulations.

Lee et al. [16] generated activity schedules with a motivation-driven method. A motivation value (MV) represents the desire of a virtual agent to perform a class of activities with the agent performing an activity when its corresponding MV reaches its threshold. Motivations are classified by levels; if two MVs reach their thresholds at the same time, the agent will perform the activity that corresponds to the higher-level motivation. This method has sufficient potential for improvement if the mechanism of evolution of the MVs is designed carefully.

3 Activity Schedule Generation

3.1 Problem Statement

To build our activity schedule generator module, we need to improve upon the methods mentioned in Sect. 2 by addressing the following issues. 1) The list of activities that can be performed by a virtual resident is determined by the layout of simulated house, e.g., the resident can only watch TV if a TV is in the house. The above methods are for a determined layout with a fixed activity list. As our simulator contributes to provide diverse simulation scenarios by producing diverse layouts, we need a method that can process dynamic activity lists. 2) The above methods generate schedules whose timelines include unspecified times between the end time of an activity and the start time of the next one. Where the resident has been and what he/she has done during the unspecified time are undetermined, thus, generated sensors records did not cover entire days. 3) Most of the above methods generated schedules for one day or less, but long-term activity schedules are required for our simulation.

We developed a motivation-driven method on the basis of that presented in the reviewed study [16] to build our activity schedule generator. An MV represent a resident's desire to perform an activity sequence (AS). While performing the activity is dependent on its MV reaching its threshold in [16], in our method, the MVs are used to determine the probability distribution (P) of sampling the next AS. The evolution of the MVs is adaptive to the input indoor spatial data and resident's profile. The input data represent a layout that determines what AS can be performed, thus, this adaptive evolution mechanism addresses issue 1). The profile represents a resident's tendencies to activities, which is quantified by durations (D), periods (T) and frequencies (f) of an AS. We need to design an evolution mechanism and initialize the MVs carefully to

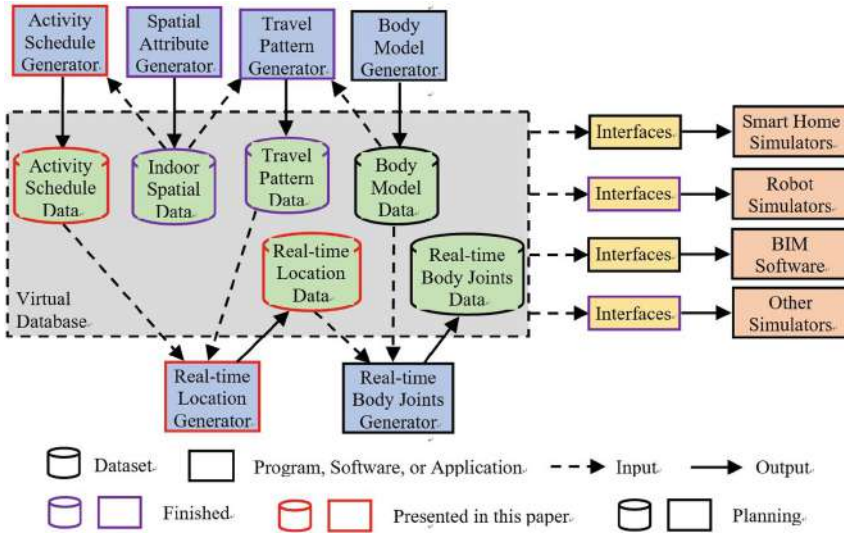


Fig. 1. General framework for building the simulation tool [11].

generate stable, but not tedious, activity schedules in the long term that will address issue 3). We can address issue 2) by taking into account more activities. The studies mentioned in Sect. 2 took into account a limited number of activities, implying that these activities occupy the entire timeline, which is unrealistic.

3.2 Model of AS, MV, Resident Profile, and P

Mapping the Relationship Between AS and MV. A resident performs activities on the basis of motivation, in which MVs quantify the degree of motivation. When an MV is high, the resident may perform a sequence of activities to satisfy the motivation, e.g., if the value of hunger motivation is high, he/she will cook and eat.

We determined that a resident has 13 motivations at most, which correspond to 13 MV_i - AS_i pairs: MV_1 : wash and brush teeth \Rightarrow sleep (at night) \Rightarrow wash and brush teeth, MV_2 : sleep (at noon), MV_3 : take food \Rightarrow cook \Rightarrow take tableware \Rightarrow eat, MV_4 : take a bath \Rightarrow get dressed \Rightarrow put clothes in wash machine, MV_5 : get dressed \Rightarrow go out \Rightarrow get dressed, MV_6 : go to toilet (short duration), MV_7 : go to toilet (long duration), MV_8 : watch TV, MV_9 : read, MV_{10} : clean, MV_{11} : take clothes out of washing machine, MV_{12} : wander, and MV_{13} : relax. An AS consists of one or more activities, and activities in the AS are performed in order without lag to satisfy the corresponding motivation and decrease the corresponding MV_i . MV_i determines the possibility of performing i th AS, P_i .

AS and MV Are Adaptive to the Layout. The actual composition of an AS is also adaptive to the layout like the evolution of MVs. An activity in an AS will be omitted if its corresponding places are not in the layouts. The mapping relationship of all activities

and places is shown in Table 1, e.g., if the kitchen stove, refrigerator, and cupboard are not in the house, AS_3 will omit the procedure take food \Rightarrow cook \Rightarrow take tableware, which implies the resident eats food prepared by someone out of the house in this case. If all activities of an AS can not be performed because of the layout, its MV_i will always be 0.

Resident's Personal Profile. To keep generated schedules diverse and reasonable, parameters corresponding to the evolution of MVs should depend on the resident's profile. The profile represents a resident's tendencies to satisfy different motivations, which is determined by sampling D , T , and f of an AS performed over reasonable intervals. Di means the duration of the resident performing the i th AS in a period (T_i), e.g., D_8 means how long the resident performed the activity "watch TV" per day on average if $T_8 = 1$ day. T_i and f_i mean the period and frequency of performing the i th AS, respectively, e.g., T_{12} means how many days between two instances of the resident's wandering and f_6 means how many times the resident performed the activity "go to toilet (short duration)" per day on average, where $T_i \times f_i = 1$.

Mechanism of MVs Evolution. MVs quantify the motivations to perform activities, MV_i usually decreases when the i th AS is performed, increases when other ASs are performed, and remains unchanged in special cases. The values of D , T , and f determine the speed of the increase and decrease of MVs. The rules below show the evolution of MVs, where Rules 1.1) and 1.2) indicate the situations when MV_i remains unchanged, 2.1) to 2.4) show the mechanism of MVs increasing, and 3.1) to 3.4) show the mechanism of them decreasing.

Rule 1.1) MV_i is always 0 if i th AS can not be performed.

Rule 1.2) $MV_{13} = 1.02 \text{Norm_MV}$ in any case, where Norm_MV is a constant.

Note: MV_{13} corresponds to relax. This rule means the resident is performing the activity "relax" when all other MVs are low. Setting MV_{13} as a constant keeps MVs stable in the long term.

Rule 2.1) Ways of MVs increasing include linear and step functional increasing.

Rule 2.2) If MV_i is not fixed and $i \neq 7$ or 11, MV_i increases linearly when the i th AS is not performed. The increment is determined by Eq. (1),

$$MV_i(t + \Delta t) = \begin{cases} MV_i(t) + \omega_i \Delta t + \varepsilon, & \text{if the resident is not sleeping.} \\ MV_i(t) + 0.1\omega_i \Delta t + \varepsilon, & \text{if the resident is sleeping, and } i = 3 \text{ or } 6. \\ MV_i(t) + \varepsilon, & \text{if the resident is sleeping, and } i \neq 3 \text{ and } 6. \end{cases} \quad (1)$$

where ω_i is an increasing rate and ε is random noise.

Note: When the resident is sleeping, the increasing rates of the MVs of "eat" and "go to toilet (short duration)" decrease to 10%, rates of other MVs decrease to 0.

Table 1. Mapping relationship between activities and places.

Activity	Place
Sleep (at night)	Bed
Sleep (at noon)	
Relax	
Wash and brush teeth	Bathroom
Take a bath	
Take food	Refrigerator
Take tableware	Cupboard
Take food	Kitchen stove
Take tableware	
Cook	
Eat	Dining table-chair set
Put clothes in washing machine	Washing machine
Take clothes out of washing machine	
Go to toilet (short duration)	Toilet
Got to toilet (long duration)	
Watch TV	Sofa-TV set
Relax	
Relax	Writing desk-chair set
Read	
Get dressed	Wardrobe
Eat	Entrance
Go out	
Clean	Trash bin
Wander	None

Rule 2.3) Following the principle that MV_i should be generally unchanged after one period in an ideal case, ω_i can be determined by D , T , and f .

Note: e.g., for the 8th AS, watching TV, assuming that the resident watches TV for 4 h (D_8), and sleeps 8 h ($D_1 + D_2$) per day ($T_8 = 24$ h), ω_8 is determined by Eq. (2),

$$\omega_8 = \frac{\text{Norm_MV}}{[T_8 - (D_1 + D_2) - D_8]}. \quad (2)$$

which means ω_8 should increase by Norm_MV in the remaining 12 h, while it decreases by Norm_MV during the 4 h (D_8).

Rule 2.4) MV_i increases step by step if $i = 7$ or 11. For the 7th AS, “going to toilet (long duration)”, MV_7 increases by $\text{Norm_MV}/(3 \times T_7)$ 2.5 h after the resident starts eating. For the 11th AS, “taking clothes out of the washing machine”, MV_{11} increases by Norm_MV 1 h after the resident puts their clothe into the washing machine.

Rule 3.1) MV_i will decrease if the i th AS has been performed except if $i = 13$.

Rule 3.2) The decrease of MV_i depends on the T_i and actual duration, AT . It is defined by Eq. (3) except if the AS is eating breakfast, the decrease is $(2AT/3T_i) \times \text{Norm_MV}$.

$$MV_i(t + AT) = MV_i(t) - \frac{AT}{T_i} \text{Norm_MV}. \quad (3)$$

Rule 3.3) AT is related to T_i , AT is sampled from $[0.97T_i, 1.03T_i]$ for $i = 1$, from $[0.4T_i, 0.9T_i]$ for $i = 5$, from $[0.3T_i, 0.7T_i]$ for $i = 8$ or 9 , and from $[0.95T_i, 1.05T_i]$ for other cases.

Rule 3.4) The resident may perform the activities “eat” and “go to toilet” outside. When he/she is going out, if MV_3 , MV_6 or MV_7 reach Norm_MV , and there is sufficient time to perform the corresponding AS, this MV decreases as the AS is performed.

Initialization of MVs. MVs should be initialized before evolution, which can be achieved by determining when each AS will be performed for first time. The time when the i th AS is first performed is approximately equal to the time when MV_i first reaches Norm_MV . We sample the initial time from 9:30 PM of one day to 1:00 AM of the next day, and the resident is going to sleep. MV_0 thus is Norm_MV , as D_i and ω_i is known, other initial MVs can be calculated with Eq. (1), e.g., assuming that $D_1 = 8$ h, and the resident will eat breakfast 1 h after waking up, initial MV_3 is calculated by Eq. (4).

$$MV_3 = \text{Norm_MV} - 0.1\omega_3 \times 8 \text{ h} - \omega_3 \times 1 \text{ h}. \quad (4)$$

To keep the generated schedule stable in the long term, we need to avoid two MVs whose ASs require long durations to reach Norm_MV at the same time.

Relationship Between MV and P. The possibility of performing the i th AS depends on the motivation value, MV_i , as shown in Eq. (5)

$$P_i = \frac{\exp[\max(0, MV_i - 0.98\text{Norm_MV})]}{\sum_{j=1}^{13} \exp[\max(0, MV_j - 0.98\text{Norm_MV})]}. \quad (5)$$

3.3 Implementation

We wrote a Python3 program to achieve activity schedule generation. A sample of the indoor spatial attribute data (*Spatial_data*) and total generation duration (*Total_Dur*) were input into the program, and it returns a resident’s daily activity schedule during the *Total_Dur*. The pseudocode of the program is shown below, where constants, variables, and variable vectors are in regular, italic, and bold italic styles, respectively.

```

program Schedule_Generation(Spatial_data, Total_Dur):
1 AS_canbe_perform := Process_Input(Spatial_data)
2 T, D, f := Generate_Resident_Profile()
3  $\omega$  := Calculate_Increase_rate(T, D, f)
4 MV, Init_time := Initialize_MVs&time(T, D, f)
5 Current_ASnum, time := 1, Init_time
6 ASnum_list, time_list := [], []
7 while time < Init_time + Total_Dur do:
8   AT := Determine_actual_duration(Current_ASnum, T)
9   MV := Update_MV(Current_ASnum, time, MV,  $\omega$ , T, AT)
10  time := time + AT
11  Next_ASnum = Sample_next_ActSeq(MV)
12  If Next_ASnum != Current_ASnum do:
13    ASnum_list.append(Next_ASnum)
14    time_list.append(time)
15    Current_ASnum := Next_ASnum
16  Activity_Schedule = Post_Process(ASnum_list, time_list, Spatial_data)
17 return Activity_Schedule

```

The program first processes the input spatial attribute data, analyzes the layout, and determines what ASs can be performed in the house in Line 1. The resident's profile is determined by sampling **D**, **T**, and **f** in Line 2. ω is calculated in Line 3 in accordance with Rule 2.3). The original **MV** and the start time of the schedule generation are determined in Line 4. In Line 5, we assume the resident performs AS₁ at the beginning of the generation, and the variable *Time* records the current time. Two lists are created in Line 6, **ASnum_list** and **time_list**, which will record the number of all performed ASs and their start times chronologically, respectively. From Lines 7 to 15, the program determines the **AT** of performing each AS with Rule 3.3), updates **MV** using the other rules, samples the next performed AS with Eq. (5), and stores the number of performed ASs and their start times in **ASnum_list** and **time_list**, respectively. The program converts these two lists into an activity schedule in Line 17. The schedule indicates the start times of all activities performed.

4 Performance of the Generator

We input indoor spatial data generated by the spatial attribute generator into the activity schedule generator, which then produces diverse activity schedule data. For example, a sample of spatial data whose layout is shown in Fig. 2 is input into the generator. As the places “desk” and “washing machine” do not exist in the house, AS₉ (read) and AS₁₁ (take clothes) can not be performed. The activity schedule generator then determines the resident's profiles and generates their corresponding schedules. Two example schedules are shown in Fig. 3. Figure 3a) shows a schedule for a resident who sleeps around noon, goes out, watches TV, and takes a bath every day, while Fig. 3b)

shows a schedule for who does not sleep around noon, watches TV, and takes a bath every day, but only goes out every four days.

We also tested the performance of our generator on PC with an Intel^(R) core^(TM) i7-8550U @1.80-GHz CPU. The generator ran 100 times in 3.987 s.

Additional generated schedules are available via this website [17].

5 Using Generated Activity Schedules for Simulation

Smart house are often equipped with passive infrared (PIR) sensors. When residents are in the detection range of one, it turns on, otherwise, it remains off. Each PIR sensor has a unique ID number which can be recorded when the sensor turns on or off. By placing several PIR sensors in the house and analyzing their records, a resident's movement trajectories can be acquired, which can be used to determine whether they contain wandering travel patterns associated with dementia [18].

In the simulation, the PIR sensor records were generated from simulated real-time location data. We built a generator that could convert an activity schedule, a sample of indoor spatial data, and several samples of travel pattern data into a sample of real-time location data. We developed an interface to convert the real-time location data into virtual PIR sensor records, which can be used to optimize the placement of the PIR sensors in a smart house.

Examples of the performance of the real-time location data generator and the interface are shown in figures and tables. Figure 2 shows a sample of spatial data. Table 2 shows part of an activity schedule. The travel pattern data are shown in Fig. 4. The above data are input into the generator to produce the real-time location data. Figure 4 also shows the positions of the five PIR sensors located in the virtual house. Their coordinates are [100, 0], [300, -150], [500, -200], [550, 50] and [850, 0]. The interface converts the real-time location data into the records of PIR sensors, which is shown in Table 3.

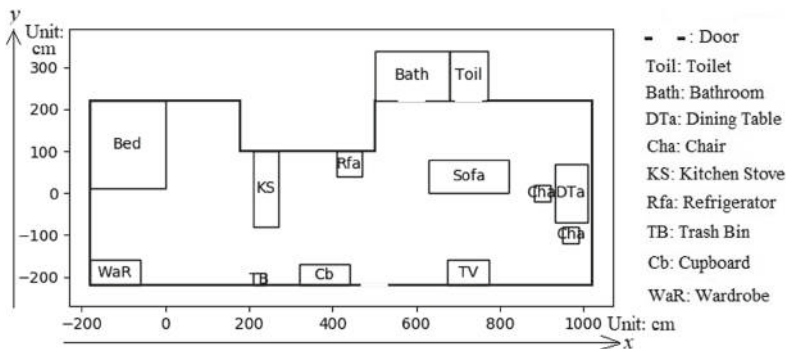


Fig. 2. Layout of input indoor spatial data.

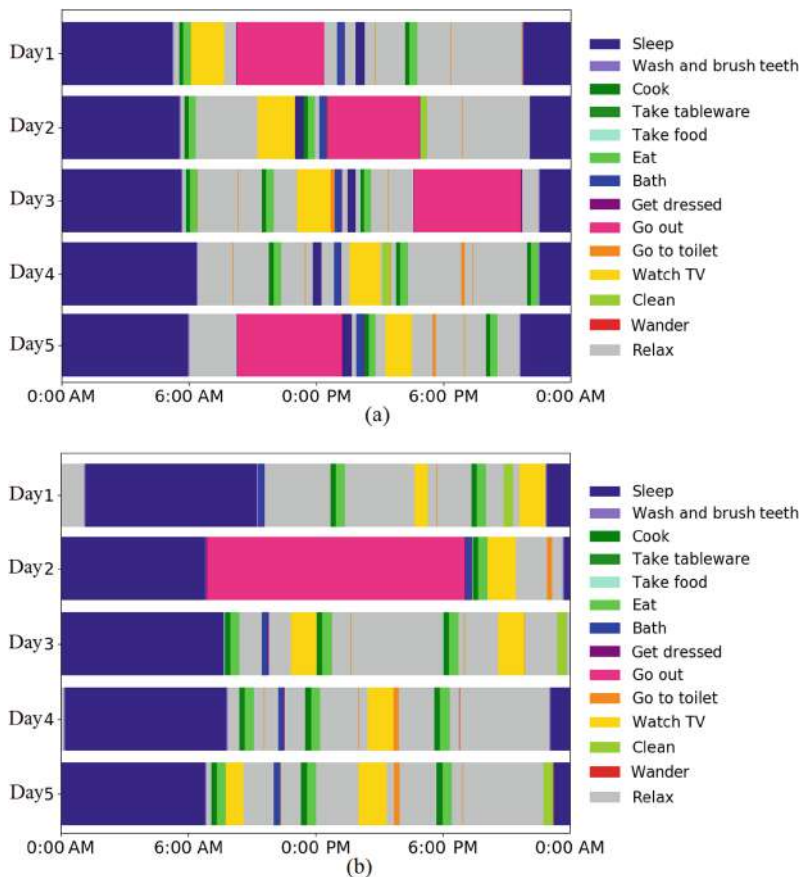


Fig. 3. Generated activity schedules.

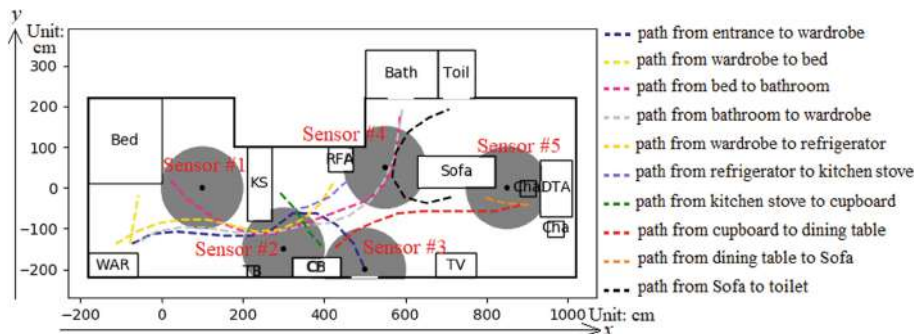


Fig. 4. Layout of input indoor spatial data with PIR sensors and travel pattern data.

Table 2. Part of the activity schedule shown in Fig. 3(a).

Activity	Start time	Activity	Start time
Go out	5d AM 8 h 17 m 7 s	Cook	5d PM 2 h 17 m 56 s
Get dressed	5d PM 1 h 13 m 59 s	Take tableware	5d PM 2 h 28 m 44 s
Sleep	5d PM 1 h 16 m 12 s	Eat	5d PM 2 h 29 m 46 s
Relax	5d PM 1 h 40 m 0 s	Relax	5d PM 2 h 49 m 20 s
Bath	5d PM 1 h 54 m 36 s	Watch TV	5d PM 3 h 15 m 1 s
Get dressed	5d PM 2 h 15 m 10 s	Go to toilet	5d PM 4 h 30 m 33 s
Take food	5d PM 2 h 17 m 18 s		

Table 3. Simulated records of virtual PIR sensors.

Time		Time	
5d PM 1 h 13 m 45 s 9	#3 ON	5d PM 2 h 17 m 7 s 5	#1 ON
5d PM 1 h 13 m 47 s 8	#3 OFF	5d PM 2 h 17 m 9 s 7	#1 OFF
5d PM 1 h 13 m 50 s 2	#2 ON	5d PM 2 h 17 m 10 s 9	#2 ON
5d PM 1 h 13 m 53 s 4	#2 OFF	5d PM 2 h 17 m 14 s 0	#2 OFF
5d PM 1 h 54 m 19 s 5	#1 ON	5d PM 2 h 17 m 50 s 5	#4 ON
5d PM 1 h 54 m 22 s 9	#1 OFF	5d PM 2 h 17 m 50 s 6	#4 OFF
5d PM 1 h 54 m 24 s 2	#2 ON	5d PM 2 h 17 m 53 s 6	#2 ON
5d PM 1 h 54 m 27 s 5	#2 OFF	5d PM 2 h 28 m 38 s 5	#2 OFF
5d PM 1 h 54 m 30 s 2	#4 ON	5d PM 2 h 28 m 39 s 7	#2 ON
5d PM 1 h 54 m 34 s 4	#4 OFF	5d PM 2 h 29 m 34 s 5	#2 OFF
5d PM 2 h 14 m 52 s 3	#4 ON	5d PM 2 h 29 m 34 s 5	#3 ON
5d PM 2 h 14 m 56 s 4	#4 OFF	5d PM 2 h 29 m 36 s 1	#3 OFF
5d PM 2 h 14 m 59 s 1	#2 ON	5d PM 2 h 29 m 41 s 9	#5 ON
5d PM 2 h 15 m 2 s 5	#2 OFF	5d PM 3 h 30 m 21 s 7	#5 OFF
5d PM 2 h 15 m 4 s 4	#1 ON	5d PM 3 h 30 m 23 s 8	#4 ON
5d PM 2 h 15 m 5 s 1	#1 OFF	5d PM 3 h 30 m 27 s 7	#4 OFF

6 Conclusion

Smart houses with a sensor network and domestic robots were built to take care elderly people living alone. Many simulation tools have been proposed to help smart house developers test and verify their designs, but it takes time and effort to build a simulation scenario, and developers need to repeat scenario-generation procedures if they want to use multiple simulators. To address these issues, we proposed a simulation tool that provides diverse simulation scenarios and enables developers to build scenarios automatically in multiple simulation platforms [11].

In this paper, we proposed an activity schedule generator that is an essential part of our simulator. With an improved motivation-driven method, the generator produces diverse daily activity schedules to mimic the daily lives of residents living alone. It outperforms existing generators in three aspects: 1) it is adaptive to the layout of a

simulated smart house; 2) there is no unspecified time in the timeline of generated schedules; and 3) it generates stable, but not tedious schedules for a number of days.

A generated schedule includes a list of activities and their start time. The list of activities determines all starts and ends of indoor walking paths with spatial attributes of a virtual house, the travel pattern generator then generates all paths. The generated paths determine simulated real-time locations of a resident with the list of start time.

The real-time locations can be converted to records of virtual sensors with interfaces, and these records can be used to optimize designs of smart house. For example, we convert the real-time locations to records of virtual PIR sensors, and the records are useful for optimizing placement of these sensors.

Acknowledgments. This research was partially supported by a grant from the Japan Society for the Promotion of Science (JSPS KAKENHI 18H00968) and a scholarship of Mizuho International Foundation.

References

1. He, W., Goodkind, D., Smith, P.K.: *An Aging World: 2015: International Population Reports*, U.S. Census Bureau (2016)
2. Reher, D., Requena, M.: Living alone in later life: a global perspective. *Popul. Dev. Rev.* **44**(3), 427–454 (2018)
3. Pimouguet, C., et al.: Impact of living alone on institutionalization and mortality: a population-based longitudinal study. *Eur. J. Public Health* **26**(1), 182–187 (2016)
4. Simoens, S., Villeneuve, M., Hurst, J.: *Tackling nurse shortages in OECD countries: Technology Report*, Organisation for Economic Co-operation and Development (2005)
5. Vuong, N.K., Chan, S., Lau, C.T., Chan, S.Y., Yap, P.L., Chen, A.S.: Preliminary results of using inertial sensors to detect dementia-related wandering patterns. In: *Proceedings of 37th International Conference on Engineering in Medicine and Biology Society (EMBC2015)*, Milan, pp. 3703–3706 (2015)
6. Das, B., Cook, D.J., Krishnan, N.C., Schmitter-Edgecombe, M.: One-class classification-based real-time activity error detection in smart homes. *IEEE. JSTSP* **10**(5), 914–923 (2016)
7. Do, H.M., Pham, M., Sheng, W., Yang, D., Liu, M.: RiSH: a robot-integrated smart home for elderly care. *Rob. Auton. Syst.* **101**, 74–92 (2018)
8. Fischinger, D., et al.: Hobbit, a care robot supporting independent living at home: first prototype and lessons learned. *Rob. Auton. Syst.* **75**(A), 60–78 (2016)
9. Alshammari, N., Alshammari, T., Sedky, M., Champion, J., Bauer, C.: OpenSHS: open smart home simulator. *Sensors* **17**, 1003 (2017)
10. Vaughan, R.: Massively multi-robot simulation in stage. *Swarm Intell.* **2**, 189–208 (2008)
11. Jiang, C., Mita, A.: Automatic spatial attribute and travel pattern generation for simulating living spaces for elderly individuals living alone. *Build. Environ.* **176**, 106776 (2020). <https://doi.org/10.1016/j.buildenv.2020.106776>
12. Jiang, C., Mita, A.: Automatic floorplan generation of living space for simulating a life of an elderly resident supported by a mobile robot. In: *Proceedings of 36th International Symposium on Automation and Robotics in Construction (ISARC 2019)*, Banff, pp. 688–695 (2019)

13. Renoux, J., Klügl, F.: Simulating daily activities in a smart home for data generation. In: Proceedings of Conference on Winter Simulation (WSC2018), Gothenburg, pp. 798–809 (2018)
14. Bouchard, B., Gaboury, S., Bouchard, K., Francillette, Y.: Modeling human activities using behaviour trees in smart homes. In: Proceedings of 11th Conference on Pervasive Technologies Related to Assistive Environments (PETRA), Corfu, pp. 67–74 (2018)
15. Mshali, H., Lemlouma, T., Magoni, D.: Context-aware adaptive framework for e-health monitoring. In: IEEE International Conference on Data Science and Data Intensive Systems, Sydney (2015)
16. Lee, W., et al.: Automatic agent generation for IoT-based smart house simulator. *Neurocomputing* **209**, 14–24 (2016)
17. <https://github.com/Idontwan/Activity-Schedule-Generator/tree/master/Schedules>
18. Gochoo, M., Tan, T., Velusamy, V., Liu, S., Bayanduuren, D., Huang, S.: Device-free non-privacy invasive classification of elderly travel patterns in a smart house using PIR sensors and DCNN. *IEEE Sens. J.* **18**(1), 390–400 (2018). <https://doi.org/10.1109/JSEN.2017.2771287>

Open Access This chapter is licensed under the terms of the Creative Commons Attribution 4.0 International License (<http://creativecommons.org/licenses/by/4.0/>), which permits use, sharing, adaptation, distribution and reproduction in any medium or format, as long as you give appropriate credit to the original author(s) and the source, provide a link to the Creative Commons license and indicate if changes were made.

The images or other third party material in this chapter are included in the chapter's Creative Commons license, unless indicated otherwise in a credit line to the material. If material is not included in the chapter's Creative Commons license and your intended use is not permitted by statutory regulation or exceeds the permitted use, you will need to obtain permission directly from the copyright holder.





A Novel On-Wrist Fall Detection System Using Supervised Dictionary Learning Technique

Farah Othmen^{1,2,3(✉)}, Mouna Baklouti^{2,3(✉)}, André Eugenio Lazzaretti^{4(✉)},
Marwa Jmal^{3(✉)}, and Mohamed Abid^{2(✉)}

¹ Ecole Polytechnique de Tunisie, Université de Carthage, La Marsa, Tunisia
`farah.othmen@ept.rnu.tn`

² Telnet Innovation Labs, Telnet Holding, Ariana, Tunisia
`mouna.baklouti@enis.tn`, `med.abid@enis.tn`

³ CES Lab, National School of Engineers of Sfax, University of Sfax, Sfax, Tunisia
`Marwa.Jmal@groupe-telnet.net`

⁴ Federal University of Technology, Paraná (UTFPR), Curitiba, Brazil
`lazzaretti@utfpr.edu.br`

Abstract. Wrist-based fall detection system provides a very comfortable and multi-modal healthcare solution, especially for elderly risking falls. However, the wrist location presents a very challenging and unstable spot to distinguish falls among other daily activities. In this paper, we propose a Supervised Dictionary Learning approach for wrist-based fall detection. Three Dictionary learning algorithms for classification are invoked in this study, namely SRC, FDDL, and LRSDL. To extract the best descriptive representation of the signal data we followed different preprocessing scenarios based on accelerometer, gyroscope, and magnetometer. A considerable overall performance was obtained by the SRC algorithms reaching respectively 99.8%, 100%, and 96.6% of accuracy, sensitivity, and specificity using raw data provided by a triaxial accelerometer, accordingly overthrowing previously proposed methods for wrist placement.

Keywords: Fall detection · Supervised Dictionary Learning · Machine learning · Wrist-based wearable · Signal processing

1 Introduction

The elderly population rate has witnessed dramatic growth over the last decades and is projected to be still increasing throughout the upcoming years to reach 35% by the year 2050, and thus, jointly increasing the population dependency

This research and innovation work is supported by MOBIDOC grants from the EU and National Agency for the Promotion of Scientific Research under the AMORI project and in collaboration with Telnet Innovation Labs.

© The Author(s) 2020

M. Jmaïel et al. (Eds.): ICOST 2020, LNCS 12157, pp. 184–196, 2020.

https://doi.org/10.1007/978-3-030-51517-1_15

rate [17]. Falling is one of the most crucial health risks faced by this fragile population, classified as a disease in the International Classification of Diseases [27]. According to [16], the risk of falling varies from 30% for elderly over 65 to 50% for those over 85 each year.

Wearable fall detection systems have captivated much interest in later years literature as they can fit easily into smart wearable accessories like wristbands assuring anywhere-anytime accessibility and comfortable use compared to other existing solutions, i.e the vision and ambient-based [22]. Commonly, state-of-the-art methods for wearable fall detectors are either threshold-based or machine learning-based, for which the latter received superior interest recently [29]. Abstracting an optimal combination between extracted features and classifiers, while enhancing system reliability, has been extensively researched in most related works [19, 23]. However, classification performance can degrade substantially, as hand-crafted features may be very specific to the sensor, device placement, or dataset [2, 8].

Dictionary learning approaches (DLA) have gained a lot of enthusiasm in image processing including sparse representation based classification algorithm for face recognition [30], as it has shown robustness especially for a limited number of channels and samples, thus reducing the need to select the best feature combination and classifier for the application. Therefore, DLA has been recently emerged into the biomedical signal processing field, of which some associated works have been proposed mainly for Electroencephalography (EEG) and electrocardiogram (ECG) signal classification [3, 13].

In the same direction, we propose in this paper a novel on-wrist fall detection system based on Supervised Dictionary Learning (SDL), to autonomously generate optimal features selection that best represents acquired data. Indeed, the work presented here extends previous study [19] that implemented a movement decomposition method to extract features (direction components and body orientation) and machine learning algorithms for fall detection based on wrist wearable device. For evaluation purposes, three SDL and sparse representations algorithms with different experimental situations will be assessed throughout this paper, besides comparing it with previous related works. In this context, multiple sensors and features combinations in different experimental arrangements will be used. To the extent of our knowledge, such a dictionary-based approach is still underexplored in the related literature, so it is the main contribution of this work.

The remainder of this paper is organized as follows. Section 2 presents the main theoretical background behind our study. A detailed description of our proposed method is provided in Sect. 3. Section 4 illustrates the obtained results and compares them with prior works. Conclusion and future related work are provided in Sect. 5.

2 Theoretical Background and Related Work

2.1 Wearable Fall Detection System

Wearable-based fall detection systems illustrate all on-body attached garment devices that usually embed inertial measurement units (IMU) to inspect the body's motions, positions, and rotation movements in the space [22]. Commonly, inertial sensors such as accelerometers, gyroscopes, and magnetometers are the most used for fall detection to discriminate and notify the occurrence of a fall event as soon as possible [15]. It mostly presents an ideal solution for indoor and outdoor monitoring, especially with the emergence of nowadays advances in wearable technologies like a pendant, band, and glasses to make it more comfortable and tolerable to be wear.

Most of the analysis methods being employed in wearable fall detection are grounded on threshold and machine learning algorithms [10]. Threshold-based approaches usually compare the sensor's acquired data (or extracted features) with a predefined threshold(s) and a fall is detected when the predefined value is exceeded [26]. However, these algorithms are practically unreliable as fall is often confused with other activities like jumping. Additionally, a huge amount of soft falls are likely to be unidentified, due to their low threshold [6]. To enhance the accuracy limitation of the threshold algorithms, the literature proposed various machine learning-based solutions through classification algorithms like SVM, ANN, KNN, etc [1, 23]. These algorithms are more efficient as they can globe a greater number of fall types, yet very dependent of the on-body placement. Thus, machine-learning algorithms have shown impressive practical results when placed in steady body location (near gravity point of the body) such as waist and chest-worn. Otherwise, they are less efficient especially when placed in extremities such as wrist, requiring further investigations to improve the performance in those cases, mainly because wrist-based solutions are the most comfortable from a user point of view and less associated to the stigma of using a medical device [12, 18, 19].

2.2 Dictionary Learning for Classification

Sparse Representation and Supervised Dictionary Learning Characteristics. DLA has received a lot of interest as a representation learning paradigm by achieving state-of-the-art performance in many practical fields in computer vision such as information retrieval, image restoration, and classification [5].

It has been observed that DLA intends to learn a dictionary directly from the training samples by generating the space where the given signal could be represented properly to provide improved processing and better results in fitted to the problem domain. In DLA models, given a set $\mathbf{X} = [\mathbf{x}_1, \dots, \mathbf{x}_m]$ of m samples, the objective is to generate a dictionary \mathbf{D} which maps a high and sparse dimensional representation denoted \mathbf{A} for each input sample. Generally,

one can obtain this by solving an optimization problem defined by the following equation:

$$\min_{\mathbf{D}, \mathbf{A}} \sum_{i=1}^m \left(\frac{1}{2} \|\mathbf{x}_i - \mathbf{D}\mathbf{a}_i\|_2^2 + \lambda_1 \|\mathbf{a}_i\|_1 \right), \quad (1)$$

where, λ_1 defines the regularization parameter that affects the number of nonzero coefficients.

To cover classification tasks, many techniques have been proposed in the literature [5]. The latter, exploit the label information in the learning of either the dictionary atoms, the coefficients of the sparse vector, or both. Based on [21], both extra restraint function $f_A(\cdot)$ and $f_D(\cdot)$ are added to Eq. (1) that satisfies:

$$\min_{\mathbf{D}, \mathbf{A}} \left\{ \sum_{i=1}^m \left(\frac{1}{2} \|\mathbf{x}_i - \mathbf{D}\mathbf{a}_i\|_2^2 + \lambda_1 \|\mathbf{a}_i\|_q \right) + \lambda_2 f_A(\mathbf{A}) + \lambda_3 f_D(\mathbf{D}) \right\}, \quad (2)$$

where, $f_A(\cdot)$ could be a logistic function, a linear classifier, a label consistency term, a low-rank constraint, or the Fisher discrimination criterion. As for $f_D(\cdot)$ is to force the incoherence of the dictionary for different classes. Hence, it is possible to jointly learn the dictionary and classification model, which attempt to optimize the learned dictionary for classification tasks [9]. λ_2 and λ_3 are two scalar parameter corresponding respectively to the associated function [5].

Assuming that SDL methods and sparse representation differ in the way they exploit class labels, we will detail three of the most popular SDL algorithms, namely, the SRC, FDDL, and LRSDL.

Sparse Representation-Based Classification (SRC). SRC was first proposed by Wright et al. in their work [28] with robust face recognition approach, and have accordingly proved its effectiveness for low to moderate amount of data based problems [5]. This approach aims to concatenate the training data from different classes into a single dictionary and uses class-specific residue for the recognition. Thus, the test samples are represented as a linear combination of just the training samples corresponding to the same class. Literally, no actual training is performed in his method, since the integrity of the training samples are used in the dictionary and the sparse representation is extracted and classified over the testing phase following two main stage process:

1. The SRC algorithm computes the sparse coefficient \mathbf{a} of the test sample \mathbf{x}_{test} via the *Lasso* equation as:

$$\min_{\mathbf{a}} \left\{ \frac{1}{2} \|\mathbf{x}_{test} - \mathbf{D}\mathbf{a}\|_2^2 + \lambda_1 \|\mathbf{a}\|_1 \right\}, \quad (3)$$

Assuming that $\mathbf{D} = \mathbf{X}_{train}$.

2. Class label of each test sample is assigned while maintaining a minimum residual error of the classes according to:

$$Label(\mathbf{x}_{test}) = \min_i r_i(\mathbf{x}_{test}), \quad (4)$$

where, $r_i = \|\mathbf{x}_{test} - \mathbf{D}\sigma_i(\mathbf{a})\|_2^2$, σ_i is the selective function of the coefficient vector associated to the class i .

Fisher Discrimination Dictionary Learning (FDDL). In [31], Yang et al. proposed an SDL method that learns class-specific structured dictionary while managing its discriminability through adding a Fisher criterion. Thus, the learned dictionary $\mathbf{D} = [\mathbf{D}_1, \mathbf{D}_2, \dots, \mathbf{D}_m]$, where \mathbf{D}_i is a sub-dictionary corresponding to the class i , powerfully represents the inter-class similarity and the intra-class variance. To describe FDDL more formally, suppose $\mathbf{X} = [\mathbf{X}_1, \mathbf{X}_2, \dots, \mathbf{X}_c]$, such as the training samples are grouped according to the classes they belong and c is the total number of classes. The overall objective function of FDDL is written as shown by Eq. (5):

$$\min_{\mathbf{D}, \mathbf{A}} \{r(\mathbf{X}, \mathbf{D}, \mathbf{A}) + \lambda_1 \|\mathbf{A}\|_1 + \lambda_2 f(\mathbf{A})\}, \quad (5)$$

where, $\mathbf{A} = [\mathbf{A}_1, \mathbf{A}_2, \dots, \mathbf{A}_c]$ regroups the sparse representation of each training sample over \mathbf{D} ; $r(\mathbf{X}, \mathbf{D}, \mathbf{A})$ is the Fisher fidelity term; $f(\mathbf{A})$ defines the discrimination constraint.

2.3 Low-Rank Shared Dictionary (LRSDL)

Vu et al. proposed an SDL framework in their works [24, 25], that aims to enhance the capability of capturing shared features of the FDDL approach. The LRSDL approach intent to simultaneously learn sub-dictionaries with discriminative and shared features of each class, as different classes often share common patterns. Accordingly, the main focus of the LRSDL is the shared part in which two intuitive constraints are added to the corresponding objective function. The first one is the low-rank structure constraint, that allows the shared dictionary to contain some discriminative features. As for the second, the sparse coefficients corresponding to the shared dictionary should be very similar.

3 Proposed Dictionary Learning Method

Considering that the wrist-worn devices are the most comfortable body location for the patient [18], they are yet very unstable for the IMU [32]. Since arms are usually very moving parts of the body, many hand movements, i.e clapping, rising, and releasing hands, may present similar motion patterns compared with fall movements. Thus, these movement similarities may present a bottleneck for the feature extraction task as it may become very specific to the collected data and the selected sensors.

To overcome this issue while bearing in mind the system reliability, we propose a fall detection approach based on the dictionary learning algorithms for classification. Therefore, different SDL classification algorithms will be evaluated and compared through their prediction performances with previous on-wrist solutions presented in the literature. The pipeline of the designed architecture is illustrated by Fig. 1. In this section, we will describe the main phases presented in the illustration, namely the preprocessing, the training, and the test phases.

3.1 Dataset

The data set has been collected throughout de Quadros et al. study [19]. In fact, the signal acquisition was done by the use of three main triaxial IMU sensors, i.e, accelerometer, gyroscope, and magnetometer which are embedded in the GY-80 IMU model device. To acquire and register data signals from the latter sensors, an Arduino Uno was integrated with the IMU device into a wrist-worn band at the non-dominant hand. The raw sensors data were obtained in a 100 Hz sampling rate and 4 g, 500 degrees/sec, and 0.88 Gs for the accelerometer, gyroscope, and magnetometer respectively.

In order to make the data set more generalized and accurate, twenty-two volunteers with different ages, heights, and weights were engaged in this experimental protocol. Each one performs two main event categories, namely, fall incidents and Activities of Daily Living (ADL). The recorded fall incident covers forward to fall, backward fall, right-side fall, left-side fall, fall after rotating the waist clockwise, and fall after rotating the waist counterclockwise. The ADL's performed activities enclose walking, clapping hands, moving an object, tying shoes and sitting on a chair. The average duration of the recorded activities is 9.2s, assuming that each one starts with a resting arm (resting state) followed by a few steps before the activity's performance.

For the sake of removing any external influence that affects the accelerometer [6], the accelerometer data was preprocessed with a low pass filter with a window size of 40 and a subtraction of a fixed value equal to 1 g to eliminate the gravity-related information.

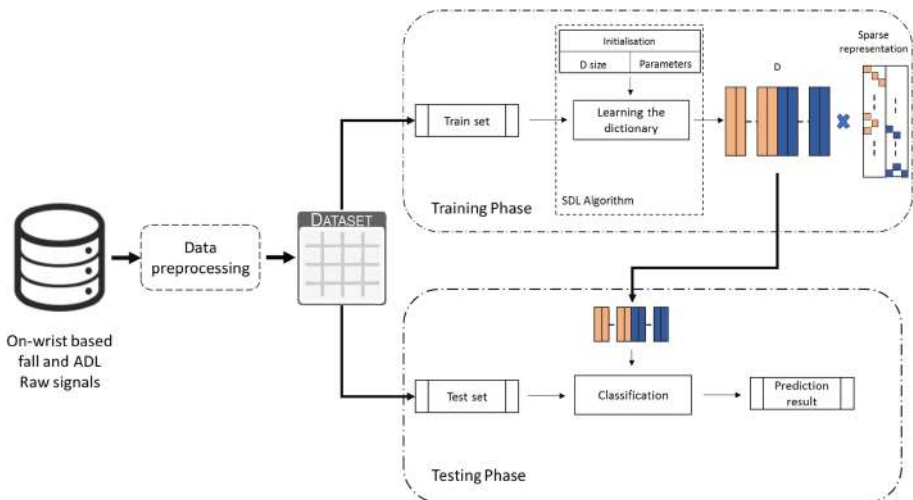


Fig. 1. Pipeline overview of the proposed SDL-based fall detection system.

3.2 Data Preprocessing

Most of the proposed wearable fall detection relies, mainly, on the data preprocessing phase, including feature extraction and feature selection, as it plays a critical role in defining an accurate fall detector [14]. In this sense, one of the faced challenges for this placement is extracting relevant features that better describe raw data and discriminate ADL events from a fall event, especially for overlapped and similar data. Finding significant attributes that better illustrate the raw data has always been a challenge depending on the device's on-body position. For instance, most on-wrist solution presented in the literature depends mainly on accelerometer [4, 11, 20, 34], while some others fuses it with other sensors like gyroscope [7, 32, 33], gyroscope and magnetometer [19], or heart rate sensor [14].

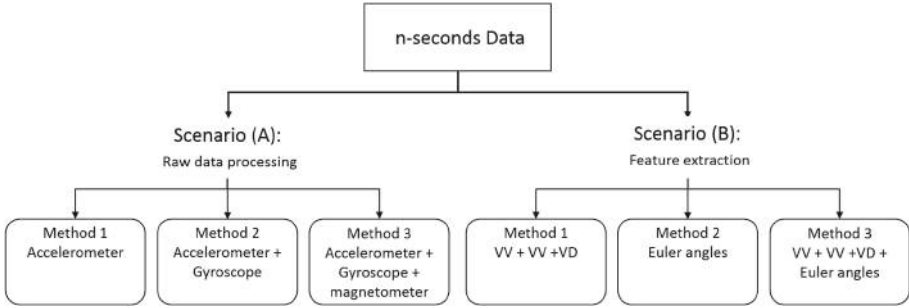


Fig. 2. Proposed scenarios for data preprocessing.

This work implements SDL for classification approaches in a wrist-based fall detection system with the aim of benefiting of its capacity to generate more discriminative features using sparse representation. For this purpose, we consider two scenarios as demonstrated in Fig. 2. In scenario (A), the system will process a time window of raw data, where we will test the effect of each sensor in the system efficiency by adding one sensor at a time. The second scenario (B) experiments extracted features, as we will adopt the movement decomposition-based feature extraction method used in [19]. We will only acknowledge the vertical component of the movement and the orientation decomposition as it reached the best results in the latter work. We denote VA, VV, and VD respectively as Vertical Acceleration, Vertical Velocity, and Vertical Displacement. The Euler angles present the spacial orientation features, i.e. yaw, pitch, and roll.

3.3 Dictionary Learning for Fall Detection

As being a branch of Machine Learning, the classification based on SDL involves two main phases, namely the training and the testing phases. In the training phase, the goal of the SDL algorithm is to map the low dimensional training

data to a high and sparse dimensional representation using a learned dictionary \mathbf{D} , to make a more discriminated pattern and easier to be distinguished. In this paper, we consider three SDL algorithms, SRC, FDDL, and LRSDDL, that we previously detailed in Sect. 2.2.

Considering the test phase, the testing sample can be classified by directly coding it over the obtained \mathbf{D} . Generally, the sparse code is then used as a feature descriptor of the data in order to calculate the reconstruction error associated to each class. The prediction is accorded to the class with the least error following the formula expressed by Eq. (4). However, the SDL performance is directly affected by the dictionary size. To abstract each SDL's higher performance we will inspect the impact of the Dictionary size into the system's accuracy.

4 Experimental Validation

4.1 Performance Metrics

This study is evaluated in terms of three common metrics, namely, Accuracy (AC), Sensitivity (SE), and Specificity (SP). AC represents the overall true detection, SE represents the ability to detect authentic falls among all detected falls, and SP represents the capacity to detect real ADL in all the detected ADL.

4.2 Experimental Configuration

In our experimental analysis, we assume that a 4-s time window is sufficient to extract a fall or an ADL event. We consider that the collected data set is subdivided such as 75% of the data (nearly 300 samples for each class) is for the training phase and 25% for the test phase. From our experiments, the SDL algorithms' hyper-parameters are set based on the best-achieved performances for our dataset using random training features. Thus, we initiate them as follows: SRC: $\lambda = 0.01$; FDDL: $\lambda_1 = \lambda_2 = 0.001$; LRSDDL: $\lambda_1 = 0.001$, $\lambda_2 = 0.01$, $\eta = 0.02$. Throughout this study, the size of the dictionary \mathbf{D} for the FDDL and the LRSDDL algorithm will vary between 50 and 300 atoms per class depending on the experiment.

4.3 Experimental Result

In this study, we followed two main experimentation scheme to validate the high sensitivity and efficiency of our proposed method. Firstly, we fix the Dictionary size in order to assess the SDL classification performance behavior compared with each outline of both scenarios showcased in Fig. 2. Secondly, we evaluate the best performance of the previous experiment with multiple \mathbf{D} sizes for the FDDL and LRSDDL algorithms to exhibit for each the best-fitted size to our proposed system.

Table 1. Performance comparison for different methods of raw data scenario.

Algorithm	SRC			FDDL			LRSDL		
	AC	SE	SP	AC	SE	SP	AC	SE	SP
Acc	99.8	100	99.6	98.0	98.0	98.0	97.4	97.9	96.9
Acc, Gyr	90.6	90.6	90.6	90.6	93.8	87.5	90.1	93.8	86.5
Acc, Gyr, Mag	97.4	96.9	97.9	96.4	96.9	95.8	97.4	96.9	97.9

Table 2. Performance comparison for different methods of feature extraction scenario.

Algorithm	SRC			FDDL			LRSDL		
	AC	SE	SP	AC	SE	SP	AC	SE	SP
VA, VV, VD	96.4	97.9	94.8	95.9	99.0	92.7	95.8	99.0	92.7
Euler	99.5	99.0	100	98.4	100	96.9	98.4	100	96.88
(+Euler)	96.9	96.9	96.9	95.8	96.9	94.8	96.4	95.8	96.9

1st Experiment. The SRC algorithm generates a dictionary \mathbf{D} with the size of the training samples, we set a \mathbf{D} size of 300 atoms per class.

Table 1 and Table 2 exhibit respectively the performance of the tested SDL algorithms under Scenario (A) and Scenario (B). In Table 1, an impressive performance is achieved by the SRC algorithm using a single triaxial accelerometer raw data. Even though joining the gyroscope has significantly decreased efficiency, it has proved its convenience when fused with the magnetometer. Table 2 shows that the extracted spacial orientation angles present a better accuracy compared with it when fused with a vertical movement component. Overall, the SRC has reached the best accuracy of 99.8% compared to FDDL and LRSDL when processed with a raw data accelerometer.

2nd Experiment. In order to inspect the best performance of both SDL algorithms, i.e FDDL and LRSDL, we vary the \mathbf{D} size in the range of $[50, \dots, 300]$ atoms per class. As illustrated in Fig. 3, the change in SDL performance depends roughly on the patterns of the input set. Consequently, the LRSDL has reached the best accuracy of 99.5%, when processed with Euler angles an input data and \mathbf{D} presents a total of 400 atoms.

Table 3. Comparison of performance for related on-wrist fall detectors.

	[34], 2014	[7], 2014	[14], 2016	[19], 2018	[11], 2018	[20], 2019	[32], 2019	[33], 2019	Our work
Accuracy	93.75	NA	92.9	99.0	95.47	98.1	98.36	99.86	99.8
Sensitivity	83.33	95.0	80.95	100	83.33	98.1	95.1	99.93	100
Specificity	95.4	96.7	98.35	97.9	95.96	98.1	100	99.8	99.6

We listed in Table 3 a full synthesis of performances, in terms of sensitivity, specificity, and accuracy of prior works related to the on-wrist fall detection system. Zheng et al. [33] achieved the best accuracy performance of 99.86% with the use of an accelerometer and gyroscope using the Convolution Neural Network (CNN) architecture, yet very close with the one accomplished with our proposed study using a single sensor adopting a simpler algorithm SRC. Moreover, our work reached the maximum sensitivity of 100% likewise the one obtained by de Quadros et al. [19] resulting in a maximum ability to distinguish real falls, thereafter a more reliable system.

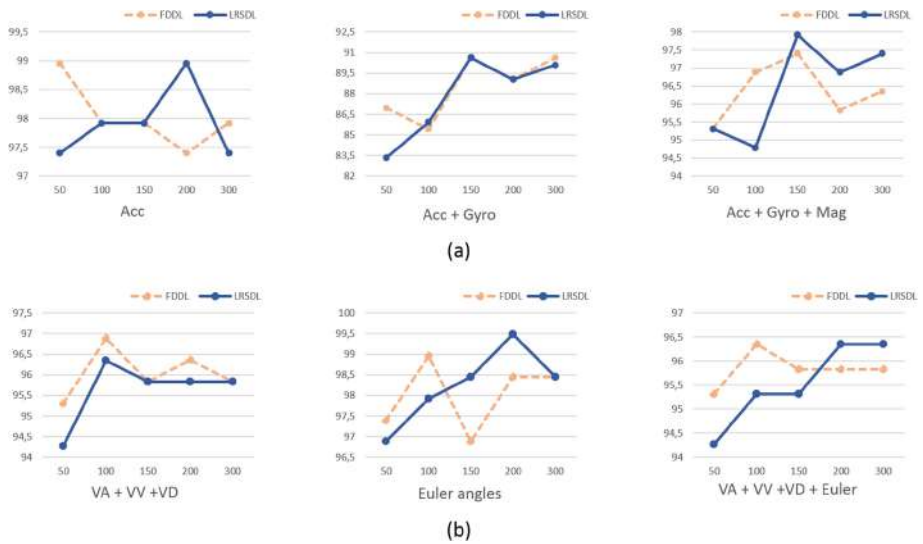


Fig. 3. Performance of the FDDL and LRSDL for different D size, (a) Scenario A, (b) Scenario B.

5 Conclusion

In this work, we introduced a new classification method, Dictionary Learning, for a wrist-based fall detection system. Thus, our contribution mainly lies in applying the Supervised Dictionary Learning approach into an on-wrist fall detection system as it has not been explored yet in literature. We explored three main SDL algorithms, namely SRC, FDDL, and LRSDL with different experiments in order to abstract the best performer and compares it to those reported in previous related work. The SRC has proved its efficiency reaching respectively 99.8%, 100%, and 96.6% of accuracy, sensitivity, and specificity. Indeed, our proposed method has proven the best capacity to classify real falls correctly and the higher accuracy with just one accelerometer mounted. This solution is energy

efficient compared with the one presenting similar accuracy thanks to its simpler algorithm complexity compared with the CNN architecture.

Thorough experimentation will be conducted in future work, we expect an additional improvement of results even further. As being a popular representation based paradigm, we plan next to test the performance of the SDL on jointly learn a frame-like representation of further complex patterns like cepstral representations and classification parameters in order to enhance the system's reliability.

In our future related work, we will study a further advantage of the DLA benefits by testing its robustness in regards to noisy signals. For this proposal, we will be combining a Signal-to-Noise Ratio (SNR) to the raw signal and compare its performance behavior with traditional machine learning models.

References

1. Ansari, M., Mahmood, N., Nadeem, A., Mehmood, A., Rizwan, K.: Fall detection system for the elderly based on the classification of shimmer sensor prototype data. *Healthc. Inform. Res.* **23**, 147–158 (2017)
2. Aziz, O., Musngi, M., Park, E.J., Mori, G., Robinovitch, S.N.: A comparison of accuracy of fall detection algorithms (threshold-based vs. machine learning) using waist-mounted tri-axial accelerometer signals from a comprehensive set of falls and non-fall trials. *Med. Biol. Eng. Comput.* **55**(1), 45–55 (2016). <https://doi.org/10.1007/s11517-016-1504-y>
3. Ceylan, R.: The effect of feature extraction based on dictionary learning on ECG signal classification. *Int. J. Intell. Syst. Appl. Eng.* **1**, 40–46 (2018)
4. Degen, T., Jaeckel, H., Rufer, M., Wyss, S.: SPEEDY: a fall detector in a wrist watch. In: *Seventh IEEE International Symposium on Wearable Computers 2003, Proceedings*, pp. 184–187, October 2003
5. Gangeh, M., Farahat, A., Ghodsi, A., Kamel, M.S.: Supervised dictionary learning and sparse representation-a review, February 2015
6. Genoud, D., Cuendet, V., Torrent, J.: Soft fall detection using machine learning in wearable devices. In: *2016 IEEE 30th International Conference on Advanced Information Networking and Applications (AINA)*, pp. 501–505 (2016)
7. Hsieh, S., Chen, C., Wu, S., Yue, T.: A wrist -worn fall detection system using accelerometers and gyroscopes. In: *Proceedings of the 11th IEEE International Conference on Networking, Sensing and Control*, pp. 518–523, April 2014
8. Igual, R., Medrano, C., Plaza, I.: A comparison of public datasets for acceleration-based fall detection. *Med. Eng. Phys.* **37**, 870–878 (2015)
9. Jiang, Z., Lin, Z., Davis, L.S.: Learning a discriminative dictionary for sparse coding via label consistent K-SVD, pp. 1697–1704, June 2011
10. Khel, M.A.B., Ali, M.: Technical analysis of fall detection techniques. In: *2019 2nd International Conference on Advancements in Computational Sciences (ICACS)*, pp. 1–8 (2019)
11. Khojasteh, S.B., Villar, J.R., Chira, C., González, V.M., De la Cal, E.: Improving fall detection using an on-wrist wearable accelerometer. *Sensors* **18**(5), 1350 (2018)
12. Krupitzer, C., Szttyler, T., Edinger, J., Breitbach, M., Stuckenschmidt, H., Becker, C.: Beyond position-awareness-extending a self-adaptive fall detection system. *Pervasive Mob. Comput.* **58**, 101026 (2019)

13. Mo, H., Luo, C., Jan, G.E.: EEG classification based on sparse representation. In: 2017 International Joint Conference on Neural Networks (IJCNN), pp. 59–62, May 2017
14. Nho, Y., Lim, J.G., Kim, D., Kwon, D.: User-adaptive fall detection for patients using wristband. In: 2016 IEEE/RSJ International Conference on Intelligent Robots and Systems (IROS), pp. 480–486, October 2016
15. Noury, N., et al.: Fall detection - principles and methods. In: 2007 29th Annual International Conference of the IEEE Engineering in Medicine and Biology Society, pp. 1663–1666, August 2007
16. World Health Organization: WHO Global Report on Falls Prevention in Older Age. NIH Publication, Bethesda (2008)
17. World Health Organization of Aging, U.N.I.: Global Health and Ageing. NIH Publication, Bethesda (2011)
18. Ozdemir, A.: An analysis on sensor locations of the human body for wearable fall detection devices: principles and practice. *Sensors* **16**, 1161 (2016)
19. de Quadros, T., Lazzaretti, A.E., Schneider, F.K.: A movement decomposition and machine learning-based fall detection system using wrist wearable device. *IEEE Sens. J.* **18**, 5082–5089 (2018)
20. Urresty Sanchez, J.A., Muñoz, D.M.: Fall detection using accelerometer on the user's wrist and artificial neural networks. In: Costa-Felix, R., Machado, J.C., Alvarenga, A.V. (eds.) XXVI Brazilian Congress on Biomedical Engineering. IP, vol. 70/1, pp. 641–647. Springer, Singapore (2019). https://doi.org/10.1007/978-981-13-2119-1_98
21. Suo, Y., Dao, M., Srinivas, U., Monga, V., Tran, T.D.: Structured dictionary learning for classification (2014)
22. Vallabh, P., Malekian, R.: Fall detection monitoring systems: a comprehensive review. *J. Ambient Intell. Humaniz. Comput.* **9**(6), 1809–1833 (2017). <https://doi.org/10.1007/s12652-017-0592-3>
23. Vallabh, P., Malekian, R., Ye, N., Capeska Bogatinoska, D.: Fall detection using machine learning algorithms, September 2016. <https://doi.org/10.1109/SOFTCOM.2016.7772142>
24. Vu, T.H., Monga, V.: Learning a low-rank shared dictionary for object classification, pp. 4428–4432, September 2016
25. Vu, T., Monga, V.: Fast low-rank shared dictionary learning for image classification. *IEEE Trans. Image Process.* **26**, 5160–5175 (2016)
26. Wang, F.T., Chan, H.L., Hsu, M.H., Lin, C.K., Chao, P.K., Chang, Y.J.: Threshold-based fall detection using a hybrid of tri-axial accelerometer and gyroscope. *Physiol. Meas.* **39**, 105002 (2018)
27. World Health Organization: ICD-11 for mortality and morbidity statistics (version 04/2019). <http://icd.who.int/browse11/l-m/en#/id.who.int/icd/entity/134290789>. Accessed 09 Nov 2019
28. Wright, J., Yang, A.Y., Ganesh, A., Sastry, S.S., Ma, Y.: Robust face recognition via sparse representation. *IEEE Trans. Pattern Anal. Mach. Intell.* **31**(2), 210–227 (2009)
29. Xu, T., Zhou, Y., Zhu, J.: New advances and challenges of fall detection systems: a survey. *Appl. Sci.* **8**, 418 (2018)
30. Xu, Y., Li, Z., Yang, J., Zhang, D.: A survey of dictionary learning algorithms for face recognition. *IEEE Access* **5**, 8502–8514 (2017)
31. Yang, M., Zhang, L., Feng, X., Zhang, D.: Fisher discrimination dictionary learning for sparse representation, pp. 543–550, November 2011

32. Zhang, H., Alrifai, M., Zhou, K., Hu, H.: A novel fuzzy logic algorithm for accurate fall detection of smart wristband. *Trans. Inst. Meas. Control* **42**, 786–794 (2019). <https://doi.org/10.1177/0142331219881578>
33. Zheng, G., Zhang, H., Zhou, K., Hu, H.: Using machine learning techniques to optimize fall detection algorithms in smart wristband. In: 2019 25th International Conference on Automation and Computing (ICAC), pp. 1–6, September 2019
34. Zhou, C., et al.: A low-power, wireless, wrist-worn device for long time heart rate monitoring and fall detection. In: 2014 International Conference on Orange Technologies, pp. 33–36, September 2014

Open Access This chapter is licensed under the terms of the Creative Commons Attribution 4.0 International License (<http://creativecommons.org/licenses/by/4.0/>), which permits use, sharing, adaptation, distribution and reproduction in any medium or format, as long as you give appropriate credit to the original author(s) and the source, provide a link to the Creative Commons license and indicate if changes were made.

The images or other third party material in this chapter are included in the chapter's Creative Commons license, unless indicated otherwise in a credit line to the material. If material is not included in the chapter's Creative Commons license and your intended use is not permitted by statutory regulation or exceeds the permitted use, you will need to obtain permission directly from the copyright holder.





Combined Machine Learning and Semantic Modelling for Situation Awareness and Healthcare Decision Support

Amira Henaïen¹(✉) , Hadda Ben Elhadj²(✉), and Lamia Chaari Fourati²

¹ King Khalid University, Abha, Kingdom of Saudi Arabia
aheniaen@kku.edu.sa

² Laboratory of Technology and Smart Systems (LT2S), LR16CRNS01, Digital
Research Center of Sfax, Sfax, Tunisia
Hadda.Ibnelhadj@ESTI.rnu.tn, lamia.chaari@enis.rnu.tn

Abstract. The average of global life expectancy at birth was 72 years in 2016 [1], however, the global *healthy* life expectancy at birth was only 63.3 years in the same year, 2016 [2]. Living a long life is not any more as challenging as assuring active and associated life [25]. We propose in this paper an IoT based holistic remote health monitoring system for chronically ill and elderly patients. It supports smart clinical decision help and prediction. The patient heterogeneous vital signs and contexts gathered from wore and surrounding sensors are semantically simplified and modeled via a validated ontology composed by FOAF (Friend of a Friend), SSN (Semantic Sensors Network)/SOSA (Sensor, Observation, Sample and Actuator) and ICNP (International Classification Nursing Practices) ontologies. The reasoner engine is based on a scalable set of inference rules cohesively integrated with a ML (Machine Learning) algorithm to ensure predictive analytic and preventive personalized health services. Experimental results prove the efficiency of the proposed system.

Keywords: Active and assisted living · Ontologies · ML · Health monitoring · Preventive personalized health services

1 Introduction

Information revolution and wireless mobile technology growth have made a considerable contribution to the expansion and empowering of E-health services. In fact, smart remote and mobile healthcare applications are making an enormous shift in the health and social care workforce efficiency as well as patients' well-being. The main target of such applications is leveraging IoT, ML and Semantic Web technologies to ensure opportunities that enable people to be and do what they value throughout their lives despite illness. The headline goal of E-health is promoting elderly independence and sustaining cognitive and physical capability via multidisciplinary and user-friendly technology. [6] is one of the earliest

studies that has highlighted the importance of the development of a powerful healthcare system. The study conclude that an integrated multidisciplinary infrastructure allowing interoperability and scalability is crucial. From that stage to nowadays, innovations in Information and Communication Technologies have radically changed healthcare services, created several manners for collecting and managing data effectively and provided several solutions to e-healthcare challenges [11]. The health sector is nowadays in its knowledge age: data, information, and knowledge are used in real time to support effective integration of prevention, treatment, and recovery services across healthcare services. Computers are not only used to provide health services but also to improve health itself through the management of the knowledge base and the automatic support of decisions. Therefore, healthcare applications are now exchanging and performing not only an enormous volume of data but also an important quantity of information and a large knowledge base Fig. 2. Thus, the semantic interoperability is becoming a crucial feature that is hard to imagine a healthcare or clinical system architecture without it [15]. The IoT ontologies appear as a suitable alternative to exchange knowledge per providing the required semantics to augment the data contained in the information model, and that to support service management operations [32]. Ontological models are becoming commonly used models in healthcare systems providing a flexible approach to integrate data and share meaning and able to assist inferring meaning [24,33]. Often ontology-based systems are using rule-based decision support system in order to assure an active and assisted monitors of patients [33]. However, a majority of those systems are not performing an automatic updates of the knowledge base. Hence, we propose in this paper a semantic-based healthcare monitoring system with seamless integration of many intricate existing knowledge, ontologies and ML technologies. It is a dynamic rule-based system, which infers information and medical recommendations based on the interaction of IoT input captured data, subjective and objective knowledge and a dynamic rule base updates by a ML algorithm based rules generator. The main contribution of this work is a combinations of semantic rules reasoning and ML reasoning to provide a new ubiquitous context awareness situation framework for healthcare monitoring systems. Those two highly modern and very powerful tools: semantic rules based reasoning and ML based reasoning, should provide complementary and supportive roles in the collection and processing of data, identification of clinical situations and automated decision making for supporting medical activities.

Paper Organization: The structure of this paper is as follows: Sect. 2 briefly introduces the related works and background. Section 3 outlines our methodology. Section 4 describes in details our proposed system. Section 5 presents context and situation awareness ontological modelling. Section 6 focuses on the knowledge and reasoning component engine. Section 7 evaluates the proposed system. Concluding remarks and perspectives are presented in Sect. 8.

2 Background and Related Works

Adoption of EHR¹ has increased almost 9 times since 2008 [12]. This huge amount of data circling in clinical information systems has formed new challenges as: semantic interoperability, standardization, automatic medical discovery, knowledge reuse, preventive personalized health services, etc. Aligned with this list of challenges, our work is based on three key concepts: Ontologies, Semantic Rules and ML; presented in the sequel:

Ontologies Based Semantic Healthcare Modelling: The conceptual model ontology is encouraging knowledge reuse and simplify problem solving in various fields. Healthcare applications are one of the systems that benefit from using ontologies: drug recommendations discovery [8], clinical support decisions [31], home personalized care to chronic patients [20], healthcare monitoring [33], etc. In Ontologies engineering, integration of ontologies is a useful process that consists on the combination of two or more standard validate ontologies from different disciplines in the aim to create a new multi-disciplinary ontology [23].

Semantic Rules Healthcare Reasoning: Semantic web and its technologies are providing efficient solutions in the information and system integration in any distributed information system environments including eHealth systems for which information integration and knowledge discovery are highly recommended [7]. The combination of Semantic Web Rules with Ontology are becoming a mature technology [14]. It use widespread in healthcare and clinical systems. A semantic rules are used in reasoning based approach for dieting and exercising management for diabetics [9]. OWL ontologies and SWRL are combined to integrate reasoning for decision support in alerting system [21].

ML Techniques for Healthcare: The high dimensional features and the availability of high quality software made the ML techniques widely used in all fields [4]. It refers to a set of algorithms used to extract useful knowledge or to learn by searching for interesting patterns in a large volumes of previously collected data. The use of ML algorithms in medicine is a hot research topic: disease progression [36,37], diagnosis prediction [5,19,35], and so on. However, those technologies are not mature enough and researchers are still working in the different possibilities and manners to integrate ML algorithms in healthcare systems [29]. One of the combination that appears successful and promising is the combination of ML techniques and ontologies [18,26,28].

3 Proposed Methodology

Our main goal is the integration of the ML Techniques in a combined ontology semantic modelling and semantic rules based reasoning healthcare framework for

¹ Electronic Health Records.

chronically ill and elderly patients. Our framework is build up in three keys stage: ontology for semantic modelling and representation, semantic rules for reasoning and machine learning techniques for learning; detailed in the following:

Semantic Representation and Ontological Modelling: The aim of this step is to find the best practices in semantic representation for holistic remote health monitoring system that is characterized by a large set of terminologies. Ontology modelling is one of the best choices, and as discussed before, the combination of different standard and valid ontologies is one of the recommended practice to build up an integrated multidisciplinary ontology.

Semantic Rules Reasoning Based Prediction: This step consists in the definition of primary knowledge base: a prediction based set of semantic rules. It exists two categories of rules: objectives and subjective. Objective knowledge contains medical rules defined in general medicine textbooks. Subjective knowledge is defined about the patient profile and context such as prior medical history, genetic diseases, personal lifestyle, etc.

Machine Learning Based Healthcare Reasoning: The outcome of this step is the best ML algorithm able to give the efficient support to the risk assessment system by providing the best and accurate new medical rules, detailed later in the Algorithm 1.

3.1 Information Life Cycle

In this subsection, we explain the information life cycle in our system: from a data, to an information, then finally a knowledge. The schema of Fig. 1 represents the different steps starting from the collection of data, passing by the different information uses in real-time ubiquitous healthcare monitoring, finally generating of knowledge. We have two main types of data sources: received data from smart devices and entered data by users (medical staff basically). All the data is collected and prepared to be analysed. The first step of the data preparation consists on highlighting the outliers and missing values: any abnormal value could be an alert. Then, in data selection, only contextual and health attributes are selected that are related to the environment or the health situation of a patient. un-selected data will be temporary removed from the data. Different transformations are required, viz, String to Nominal, Unify Date Format. The data mining step is our main contribution because it is not only processed using data mining techniques but also it is based on inferring meaning applied using a set of rules which consists on the subjective knowledge. In a first step, the inferring meaning is used in real-time by the system to determinate the current health situation of the patient, instantaneous alert, healthcare risk assessment and anomalous detection. Each applied rule is registered in the subjective knowledge. This knowledge base is able to grow in terms of number of rules. This

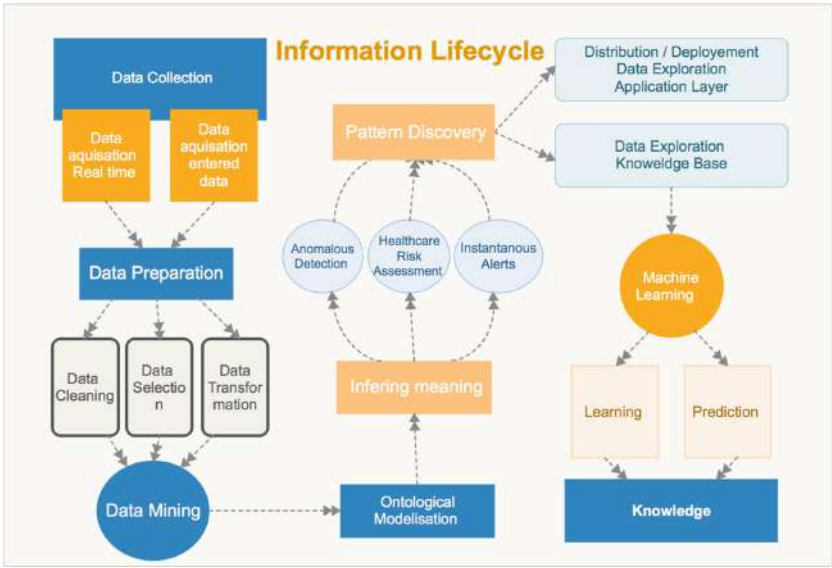


Fig. 1. The life cycle of information: data, information, knowledge

growth is assisted by a ML engine. The new learned rules will be dynamically and automatically provided to the objective knowledge. The system should allow the updates of the ML algorithm manually and the updates of the subjective knowledge automatically.

4 Detailed System Description

The main functionalities of the system are summarized in the following:

- Electronic Health Record:** is the basic functionality in our system since its the main way of the data collection. It is a systematic recording of contextual and environmental signs adequate to a multimodal, continuous and real-time user interactions.
- Alerts for Instantaneous Rescue:** is the main functionality of our system which consists in providing a help support system for elderly persons with chronic diseases. It awareness users about risks and emergency situations for an early and preventive health care.
- Reasoning for Clinical Decision Support:** is the major contribution of our system providing all necessary techniques that ensure predictive analytic and preventive personalized health services for a better clinical support system.

Ubiquitous Monitoring and Patient Tracking: is an optional functionalities provide an instantly monitoring and tracking that may be used for the already mentioned functionalities.

Patient Reminder: is an optional but highly recommended functionality. It is hard to imagine a healthcare system that is not providing a patient reminder about medical appointment, daily medical operations, etc. Aligned with the list of proposed functionalities, Fig. 2 is the generic architecture for a combined ML and ontology based situation awareness framework for clinical monitoring and healthcare decision supporting. The main contribution in this architecture is the dynamic updates of its knowledge base in its objective and subjective parts. Our system is a multi modal user interaction application, i.e. different smart devices are available in the patient's environment or in the patient's body. The data is collected from different devices like: body sensors worn by the user, ambient sensors surrounding the user or smart devices, as phone, tablet, etc. Body sensors are used to capture the health profile of the patient, viz, vital signs, motion, location, etc. Ambient sensor reflect an image of the patient's environment, viz, ambient temperature, lightness, existence of a caregiver, etc. Smart devices are basically used to allow the communication between the user and the system and between users, viz sending an alert to user about a patient's situation, monitoring a patient, etc. The architecture of the proposed system is layered and detailed in the following:

Active and Assisted Living Sensors Layer: contains all smart devices including the set of wearable and nearable sensors related directly to the user, his body and his environment. Its role is collecting data for a complete holistic health profile for each patient: health data, ambient data, location, motion, personal information, etc.

Networking and Communication Layer: a set of networking device allowing the communication between the different physical elements and the connection of those elements to the internet. **Ontological model based Data Layer:** it contains the set of the collected (current and previous) data and the ontology used in this system.

Multi-modal Interactions Application Layer: is the implementation of all the functionalities of the system providing all the services for ubiquitous and continuous medical monitoring and supporting the multi-modal interaction.

Semantic Rules Based Knowledge Layer: it is composed by the objective and the subjective knowledge. It is playing a fundamental role in our system since it contains the prediction component, i.e. prevention and detection of emergency cases and alert management.

ML Based Reasoning Layer: it is the layer performing the main contribution of our system which is the learning of new predictive and preventive medical or technical rules.

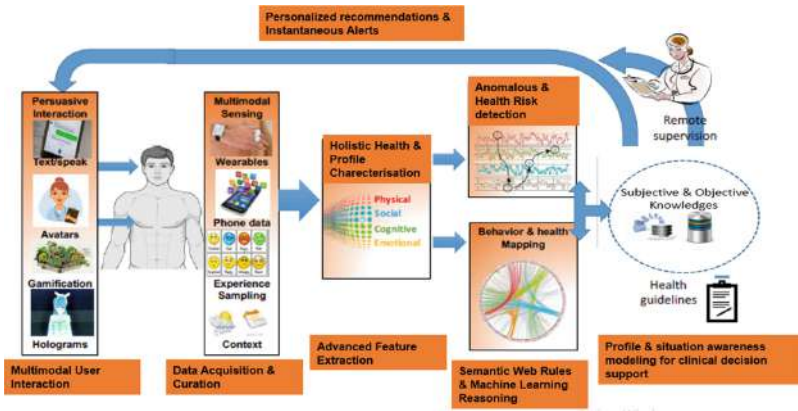


Fig. 2. Proposed architecture.

5 Context and Situation Awareness Modelling

Our ontology, Fig. 3, is composed from different valid and standard ontologies: ICNP, SSN/SOAS and FOAF. ICNP includes terminologies from the nurses' statements. And no doubt, nursing science has a significant contribution in healthcare services since nurses' statements are the early and important step in systematizing and prioritizing healthcare services [10]. In the following, we differentiate predefined classes and properties from ours by prefixing each one of them by the name of its original ontology. As One of the main classes in our application, we consider *icnp : Patient* representing the patient, *icnp : VitalSign* representing its vital signs and *icnp : Result* representing all results of any diagnosis (measurement of vital sign, measurement from blood test, etc). The W3C, SSN is one of the popular ontologies in describing sensors. It describes the sensors capabilities, actuators observation and all the related concepts [3, 27]. SOSA is the lightweight core of SSN that provide general purpose specification model for interaction between sensors. SOSA is an extension of the SSN ontology in semantic web community by providing a flexible framework and easy to use vocabulary [16]. The class *sosa : Observation* represents any estimation or calculation of a value of a property of a feature of interest. FOAF declares the person profile in different fields such as health, finance, law, etc. [17]. It has four main categories of information: basic, personal, online accounts and personal documents and images. Those standard and valid ontologies are integrated together: merged, mapped and extended in order to provide the final ontology. In the following, some example of the mentioned operations: **Merging**: in our case this

operation has poorly affect our ontology since, it is only linking class with the same name which are not many in the three ontologies. The outcome of this operation a set of equivalent axioms defining equivalence between components having the same name as the entity Person. **Mapping:** we are using FOAF to present the personal profile of users. However, the ontology ICNP has an entity called Individual presenting the health profile of a user as height, weight. So, a merging operation has been performed between the entities FOAF: person and ICNP: individual. **Extending:** The entity Platform from SSN gathers all the entities as sensors, actuators, other platforms hosted in the same platform. We created the property has Platform to link each user to his sensors.

6 Knowledge and Reasoning Engine

The knowledge component is defining: general medicine domain and context data using a set of semantic rules SWRL [14] in an abstract manner. So, the semantic rules based knowledge engine will be basically applying such medical knowledge to prevent and detect emergency cases. However, the reasoning techniques will be able to learn dynamically from the previous facts, i.e. previous applied rules, and provide new SWRL rules. The proposed system will allow a self-learning about new relations instances of cause & effect relations between data. Causes are the health situation represented by a set of signs and symptoms. Effects are the medical situation of a patient, viz, emergency case, disease, diagnosis, etc.

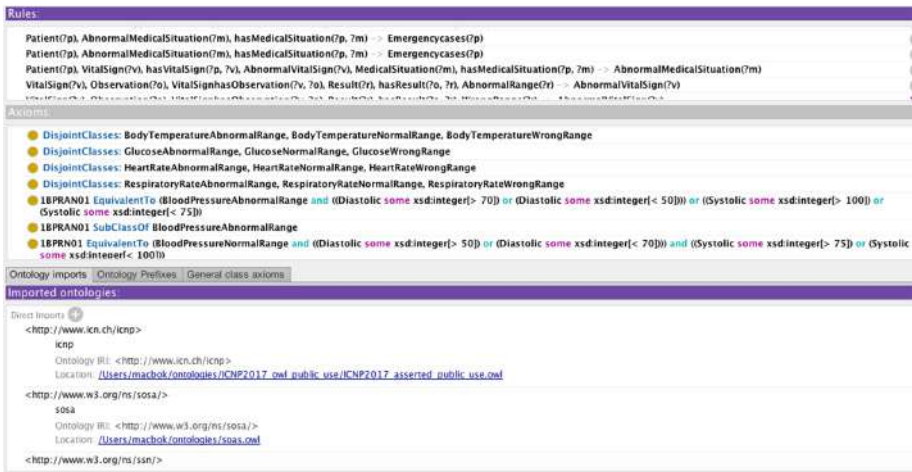


Fig. 3. Ontology overview

6.1 Semantic Rules Knowledge

Reasoner Engine (RE) applies the knowledge into the collected data in the order to determinate new facts about the current patient's situation in real-time way. RE will be in continuous search of causes which are any changes in the medical situation (signs and symptoms of each patient). Our preliminary set of SWRL is only containing a basic set of medical rules allowing to detect few emergency cases as: less blood pressure, height temperature, etc. To resume any abnormal value for a vital sign, we define the following SWRL² rule (*GM*): $icnp : VitalSign(?v) \wedge sosa : Observation(?o) \wedge VitalSignhasObservation(?v, ?o) \wedge icnp : Result(?r) \wedge sosa : hasResult(?o, ?r) \wedge AbnormalRange(?r) \rightarrow AbnormalVitalSign(?v)$. The rule is defining abnormal vital signs as the following: for a vital sign $?v$ and its observation $?o$, if the result $?r$ of the observation $?o$ is a value in an abnormal range, then $?v$ is an abnormal vital sign. $VitalSignhasObservation(?v, ?o)$ and $sosa : hasResult(?o, ?r)$ are expressing the relation between a vital sign and its observation and between an observation and its result. The class $AbnormalRange(?r)$ is representing abnormal ranges.

6.2 Learning and Prediction Reasoning

ML Engine (MLE) learns from previous patient's detected alarms to produce new reasoning rules in different steps from the Algorithm 1. The MLE is based on the Fast Decision Tree (FDT) Learning Algorithm [34]. Decision Tree (DT) Learning Algorithms are known because of their simplicity, comprehensibility, absence of parameters, and ability to handle mixed-type data. In addition, FDT is a well-known adapted version of DT that scales up well to large data sets with large number of attributes as a healthcare data set.

Algorithm 1. Compose Fast Decision Tree Learning Algorithm and Semantic rules reasoning based Healthcare System

Data: Medical Data set

Result: Medical Inference Rules

forall *patients* **do**

 Load data

 Apply preprocessing techniques

 Apply transformation techniques

 Classify per types of alarms using Fast Decision Tree Learner

 Learn new rules from generated tree

² We recommend [14] for further information about SWRL notation. The symbol ? is proceeding names of variables and \wedge is the logical And.

7 Performance Evaluation and Results

In order to prove the feasibility of the proposed approach and to evaluate its performance, we have tested the general process previously proposed in Algorithm 1 to an electronic health recorded data set from [22,30]. This data is considered as preliminary data set. The different proposed steps have been realised with WEKA [13]. An example of new rule is the detection of a low level of SpO2-Oxygen Saturation- that is used to continuously monitor the oxygenation status of critically ill patients. Actually the SpO2 measurement provides: Pleth waveform (visual indication of patient's pulse), Oxygen saturation of arterial blood (SpO2) in percent, Pulse rate (derived from Pleth wave), Perfusion indicator (Perf)- numerical value for the pulsatile portion of the measured signal caused by arterial pulsation. Only a medical staff is able to read and to interpret such result, then to detect an emergency case. The result of Algorithm 1 applied to data from one patient allow the definition of the following new rule: Perf < 0.5 and AWW < 3749.05 and AWF < 10.4 and NBP (Sys) < 105 is an emergency case with alarm labelled SpO2 LOW PERF, Fig. 4. Then, the different instances of non normal range of the following signs: Perf, AWW, AWF et NBP will be updated. For example, the following axioms will be defined (or update if it exists previously): **Axiom 1** *PerfAN SubClassOf PerfAbnormalRange* and **Axiom 2** *PerfAN EquivalentTo PerfAbnormalRange and some xsd : real[< 0.5]*. Then, the rule GM will be applicable to determinate a new alert.

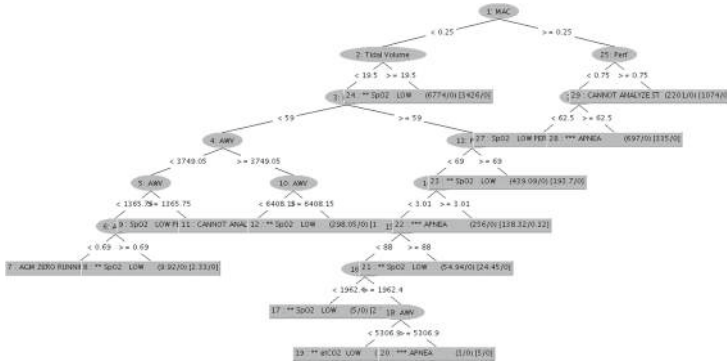


Fig. 4. Example of Weka result

8 Conclusions

This paper presents a combined semantic rules reasoning and Fast Decision Tree Learner algorithm for a predictive, preventive and personalized medical framework. The main idea consists in a knowledge and reasoning engine able to apply SWRL medical rules on collected data to generate alerts and able to create new general medicine rules based in previous detected alerts. As a continuation

of this work, we are aiming to develop a prototype of the proposed system and test it on a larger samples of data collected from an elderly population with chronic diseases.

References

1. World Health Organization. https://www.who.int/gho/mortality_burden_disease/life_tables/situation_trends/en/
2. World Health Organization. https://www.who.int/gho/mortality_burden_disease/life_tables/hale/en/
3. Alamri, A.: Ontology middleware for integration of IoT healthcare information systems in EHR systems. *Computers* **7**(4), 51 (2018). <https://doi.org/10.3390/computers7040051>
4. Baltrušaitis, T., Ahuja, C., Morency, L.P.: Multimodal machine learning: a survey and taxonomy. arXiv preprint [arXiv:1705.09406](https://arxiv.org/abs/1705.09406) (2017)
5. Choi, E., et al.: Multi-layer representation learning for medical concepts. In: Proceedings of the 22nd ACM SIGKDD International Conference on Knowledge Discovery and Data Mining, pp. 1495–1504 (2016)
6. Detmer, D.E.: Building the national health information infrastructure for personal health, health care services, public health, and research. *BMC Med. Inform. Decis. Mak.* **3**(1), 1 (2003)
7. Dogdu, E.: Semantic web in ehealth, January 2009. <https://doi.org/10.1145/1566445.1566542>
8. Doulaverakis, C., Nikolaidis, G., Kleontas, A., Kompatsiaris, I.: GalenOWL: ontology-based drug recommendations discovery. *Biomed. Semant.* **3**, 1–9 (2012)
9. Faiz, I., Mukhtar, H., Qamar, A., Khan, S.: A semantic rules & reasoning based approach for diet and exercise management for diabetics, pp. 94–99, January 2015. <https://doi.org/10.1109/ICET.2014.7021023>
10. Félix, N.D.d.C., Ramos, N.d.M., Nascimento, M.N.R., Moreira, T.M.M., de Oliveira, C.J.: Nursing diagnoses from ICNP® for people with metabolic syndrome. *Rev. Bras. Enferm.* **71**(suppl 1), 467–474 (2018). <https://doi.org/10.1590/0034-7167-2017-0125>
11. Haluza, D., Jungwirth, D.: ICT and the future of healthcare: aspects of pervasive health monitoring. *Inform. Health Soc. Care* **43**(1), 1–11 (2018)
12. Henry, J., Pylypchuk, Y., Searcy, T., Patel, V.: Adoption of electronic health record systems among us non-federal acute care hospitals: 2008–2015. *ONC Data Brief* **35**, 1–9 (2016)
13. Holmes, G., Donkin, A., Witten, I.H.: WEKA: a machine learning workbench. In: Proceedings of ANZIIS 1994-Australian New Zealand Intelligent Information Systems Conference, pp. 357–361. IEEE (1994)
14. Horrocks, I., Patel-Schneider, P.F., Boley, H., Tabet, S., Grosz, B., Dean, M.: SWRL. <https://www.w3.org/Submission/SWRL/>
15. Iroju, O., Soriyan, A., Gambo, I., Olaleke, J.: Interoperability in healthcare: benefits, challenges and resolutions. *Int. J. Innov. Appl. Stud.* **3**(1), 262–270 (2013)
16. Janowicz, K., Haller, A., Cox, S.J.D., Le, D.: Web semantics : science, services and agents on the world wide web SOSA: a lightweight ontology for sensors, observations, samples, and actuators. *Web Semant. Sci. Serv. Agents World Wide Web* **56**, 1–10 (2019). <https://doi.org/10.1016/j.websem.2018.06.003>

17. Kalemi, E., Martiri, E.: FOAF-academic ontology. In: 2011 Third International Conference on Intelligent Networking and Collaborative Systems, pp. 440–445 (2011). <https://doi.org/10.1109/INCoS.2011.94>
18. Kassahun, Y., et al.: Automatic classification of epilepsy types using ontology-based and genetics-based machine learning. *Artif. Intell. Med.* **61**(2), 79–88 (2014). <https://doi.org/10.1016/j.artmed.2014.03.001>. <http://www.sciencedirect.com/science/article/pii/S0933365714000207>
19. Kourou, K., Exarchos, T.P., Exarchos, K.P., Karamouzis, M.V., Fotiadis, D.I.: Machine learning applications in cancer prognosis and prediction. *Comput. Struct. Biotech. J.* **13**, 8–17 (2015)
20. Lasier, N., Alesanco, A., Guillén, S., García, J.: A three stage ontology-driven solution to provide personalized care to chronic patients at home. *J. Biomed. Inform.* **46**(3), 516–529 (2013). <https://doi.org/10.1016/j.jbi.2013.03.006>
21. Lezcano, L., Sicilia, M.A., Rodríguez-Solano, C.: Integrating reasoning and clinical archetypes using OWL ontologies and SWRL rules. *J. Biomed. Inform.* **44**(2), 343–353 (2011)
22. Liu, D., Görges, M., Jenkins, S.A.: University of Queensland vital signs dataset: development of an accessible repository of anesthesia patient monitoring data for research. *Anesth. Analg.* **114**, 584–589 (2012)
23. Liu, J., Li, Y., Tian, X., Sangaiah, A.K., Wang, J.: Towards semantic sensor data: an ontology approach. *Sensors (Switzerland)* **19**(5), 1–21 (2019). <https://doi.org/10.3390/s19051193>
24. Liyanage, H., Krause, P., de Lusignan, S.: Using ontologies to improve semantic interoperability in health data. *BMJ Health Care Inform.* **22**(2), 309–315 (2015). <https://doi.org/10.14236/jhi.v22i2.159>. <https://informatics.bmj.com/content/22/2/309>
25. Marcelino, I., Laza, R., Domingues, P., Gómez-Meire, S., Fdez-Riverola, F., Pereira, A.: Active and assisted living ecosystem for the elderly. *Sensors* **18**(4), 1246 (2018)
26. Martin, H., Tsymbal, A., Zillner, S.: Medical ontologies for machine learning and decision support. US Patent 7,899,764, 1 March 2011
27. Nachabe, L., Girod-genet, M., Hassan, B.E.: Unified data model for wireless sensor network. *IEEE Sens. J.* **15**(7), 3657–3667 (2015). <https://doi.org/10.1109/JSEN.2015.2393951>
28. Ongena, F., et al.: A probabilistic ontology-based platform for self-learning context-aware healthcare applications. *Expert Syst. Appl.* **40**(18), 7629–7646 (2013). <https://doi.org/10.1016/j.eswa.2013.07.038>. <http://www.sciencedirect.com/science/article/pii/S0957417413005174>
29. Puri, C.A., Gomadam, K., Jain, P., Yeh, P.Z., Verma, K.: Multiple ontologies in healthcare information technology: motivations and recommendation for ontology mapping and alignment. In: ICBO (2011)
30. The University of Queensland: The University of Queensland vital signs dataset. <http://dx.doi.org/10.100/6914/>
31. Riaño, D., et al.: An ontology-based personalization of health-care knowledge to support clinical decisions for chronically ill patients. *J. Biomed. Inform.* **45**(3), 429–446 (2012). <https://doi.org/10.1016/j.jbi.2011.12.008>
32. Serrano, M., Barnaghi, P., Carrez, F., Cousin, P., Vermesan, O., Friess, P.: Internet of Things IoT semantic interoperability: research challenges, best practices, recommendations and next steps. European Research Cluster on the Internet of Things, Technical report, IERC (2015)

33. Sondes, T., Ben Elhadj, H., Chaari, L.: An ontology-based healthcare monitoring system in the internet of things. In: 2019 15th International Wireless Communications & Mobile Computing Conference (IWCMC), pp. 319–324. IEEE (2019)
34. Su, J., Zhang, H.: A fast decision tree learning algorithm. In: AAAI, vol. 6, pp. 500–505 (2006)
35. Suo, Q., et al.: A multi-task framework for monitoring health conditions via attention-based recurrent neural networks. In: AMIA Annual Symposium Proceedings, vol. 2017, p. 1665. American Medical Informatics Association (2017)
36. Wang, X., Sontag, D., Wang, F.: Unsupervised learning of disease progression models. In: Proceedings of the 20th ACM SIGKDD International Conference on Knowledge Discovery and Data Mining, KDD 2014, pp. 85–94. Association for Computing Machinery, New York (2014). <https://doi.org/10.1145/2623330.2623754>
37. Xiao, H., Gao, J., Vu, L., Turaga, D.S.: Learning temporal state of diabetes patients via combining behavioral and demographic data. In: Proceedings of the 23rd ACM SIGKDD International Conference on Knowledge Discovery and Data Mining, KDD 2017, pp. 2081–2089. Association for Computing Machinery, New York (2017). <https://doi.org/10.1145/3097983.3098100>

Open Access This chapter is licensed under the terms of the Creative Commons Attribution 4.0 International License (<http://creativecommons.org/licenses/by/4.0/>), which permits use, sharing, adaptation, distribution and reproduction in any medium or format, as long as you give appropriate credit to the original author(s) and the source, provide a link to the Creative Commons license and indicate if changes were made.

The images or other third party material in this chapter are included in the chapter's Creative Commons license, unless indicated otherwise in a credit line to the material. If material is not included in the chapter's Creative Commons license and your intended use is not permitted by statutory regulation or exceeds the permitted use, you will need to obtain permission directly from the copyright holder.





Improving Access and Mental Health for Youth Through Virtual Models of Care

Cheryl Forchuk^{1,2(✉)}, Sandra Fisman³, Jeffrey P. Reiss^{1,2},
Kerry Collins⁴, Julie Eichstedt⁴, Abraham Rudnick^{5,6},
Wanrudee Isaranuwachai⁷, Jeffrey S. Hoch⁸, Xianbin Wang²,
Daniel Lizotte², Shona Macpherson⁴, and Richard Booth^{1,2}

¹ Lawson Health Research Institute, London, ON, Canada
cforchuk@uwo.ca

² Western University, London, ON, Canada

³ St. Joseph's Health Care, London, ON, Canada

⁴ London Health Sciences Centre, London, ON, Canada

⁵ Department of Psychiatry and School of Occupational Therapy,
Dalhousie University Halifax, Halifax, NS, Canada

⁶ Nova Scotia Operational Stress Injury Clinic, Nova Scotia Health Authority,
Halifax, NS, Canada

⁷ St. Michael's Hospital, Toronto, ON, Canada

⁸ Division of Health Policy and Management, Department of Public Health
Sciences, University of California Davis, Davis, CA, USA

Abstract. The overall objective of this research is to evaluate the use of a mobile health smartphone application (app) to improve the mental health of youth between the ages of 14–25 years, with symptoms of anxiety/depression. This project includes 115 youth who are accessing outpatient mental health services at one of three hospitals and two community agencies. The youth and care providers are using eHealth technology to enhance care. The technology uses mobile questionnaires to help promote self-assessment and track changes to support the plan of care. The technology also allows secure virtual treatment visits that youth can participate in through mobile devices. This longitudinal study uses participatory action research with mixed methods. The majority of participants identified themselves as Caucasian (66.9%). Expectedly, the demographics revealed that Anxiety Disorders and Mood Disorders were highly prevalent within the sample (71.9% and 67.5% respectively). Findings from the qualitative summary established that both staff and youth found the software and platform beneficial.

Keywords: Smart technology · Youth · Mental health · eHealth

1 Introduction

In Canada, the total cost of treatment, care and support services for mental health problems exceeds 42.3 billion Canadian dollars per year [1], with mental health services for young people being the second highest youth healthcare expenditure after injuries [2]. Although 70% of mental health problems develop during childhood and adolescence [3], only a quarter of the 10–20% of Canadian youth affected by mental

illness will receive mental health services [4]. Suicide is the second leading cause of death among Canadian youth, accounting for 24% of the deaths among individuals aged 15–24 [4]. Research on the integrated use of information technologies has shown strong improvements in the accessibility, quality, and efficiency of health and mental healthcare services [5]. Mobile technologies, in particular, appear to be a promising avenue due to the ubiquitous and portable nature of mobile devices. Smart phones have been successfully used to complement the treatment of a wide range of illnesses such as schizophrenia [6], bipolar disorder [7], and social phobia [8].

This ongoing study is integrating a mobile technology solution into routine care for youth who have symptoms of anxiety and depression. This technology is expected to: 1) promote healthcare outcomes, community inclusion and quality of life; and 2) reduce healthcare system costs by preventing hospitalization and reducing the need for outpatient visits. This report focuses on baseline data and the initial set of focus group data with youth and their care providers.

2 Materials and Methods

Study Design

This participatory action research project utilized a pre-post, mixed methods design. This paper reports on the baseline data from interviews and the initial focus groups after the youth had been using the application for less than 3 months.

Semi-structured interviews are being conducted at baseline, 6, and 12 months respectively. Focus groups will be held with youth and separate groups with care providers. A standardized evaluation framework will be instituted to facilitate systematic effectiveness, economic, ethical, and policy analyses [9]. The primary outcome measure for effectiveness is the Community Integration Questionnaire – Revised.

Participants

This two-year project will recruit 125 youth participants and have recruited 115 youth (ages 14–25) from the caseloads of 46 mental healthcare providers in London and Woodstock, Ontario, Canada who are receiving hospital-based or community agency-based outpatient care.

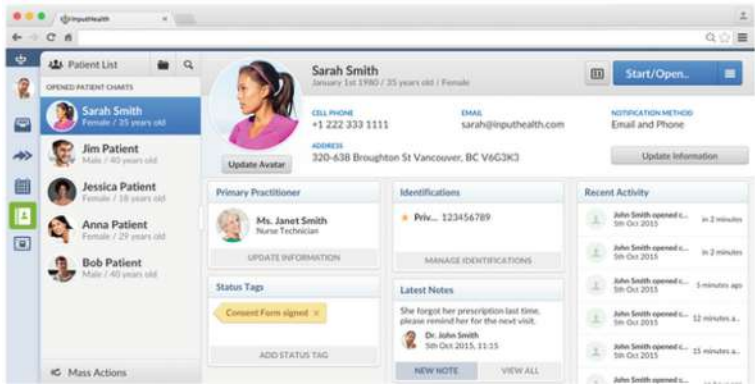
Additional inclusion criteria for participants to participate in the study include:

1. Must be on a caseload of a participating staff or care provider.
2. Able to understand English to the degree necessary to participate.
3. Have symptoms of anxiety or depression.
4. Youth must be 14–25 years old.

Intervention

The study, called Youth Telemedicine and Patient-Reported Outcome Measurement (TELEPROM-Y), allows participants synchronous and asynchronous communication with their staff/care provider team through the Collaborative Health Record (CHR). The CHR integrates the workflow of the full spectrum of healthcare providers, while also having embedded patient engagement functionality. These functionalities include the ability to: book appointments online; track quality of health and health outcome scores using mobile devices; access tailored educational content pertaining to their mental health;

and engage in both synchronous (e.g. video-conferencing) and asynchronous (e.g. secure messaging) virtual visits with their healthcare providers. Youth participants used a smartphone application (app) to connect to the CHR. The intervention is designed to facilitate better care and engagement between the patient and their care team.



Collaborative Health Record (CHR)



TELEPROM-Y app

Measures

Measures included a demographic questionnaire, the Community Integration Questionnaire [10], Lehman's Quality of Life [11], EQ-5D, health and social services utilization, and Likert scales assessing perception of technology, a researcher-developed questionnaire that inquires about participants' attitudes and opinions of the smartphone provided, provided data plan, and the CHR. Common qualitative items included feedback from participants on what they do and do not like about the technology, as well as suggestions for improvement on ethical principles such as autonomy, privacy and beneficence. A thematic analysis [12] using an ethnographic [13] method of analysis will be used to observe the broader social and cultural contexts surrounding individual experiences as well as the impact on staff/care providers and how the intervention influenced their practice.

3 Results

Data Analysis

At present, a total of 115 participants have been recruited into the study (see Table 1). There was a wide range of ages among the participants on enrollment from 14 to 25. The majority of participants identified themselves as Caucasian (66.9%) as shown in Table 1. Expectedly, the demographics revealed that Anxiety Disorders and Mood Disorders were highly prevalent within the sample (71.9% and 67.5% respectively). Of this sub-population of the sample who reported prior psychiatric admissions, the mean number of days since their most recent hospitalization was 68. The Perception of Smart Technology found that a lot of the youth participants were not using the CHR, nor had they even downloaded it. The individuals who had used it found that it improved their healthcare. See Figs. 1 and 2 (Table 2).

Table 1. Demographics (N = 115)

Age (mean)	19.57 yrs
<i>Sex</i>	
Female	63 (55.3%)
Male	51 (44.7%)
Other	1 (0.9%)
<i>Ethnicity</i>	
Caucasian	77 (66.9%)
Indigenous	12 (10.4%)
Black	6 (5.2%)
Asian	2 (1.7%)
Latin American	2 (1.7%)
Arab	1 (0.8%)
Other	5 (4.3%)
Missing	6 (5.2%)
<i>Psychiatric diagnosis</i>	
Anxiety disorder	82 (71.9%)
Mood disorder	77 (67.5%)
Disorder of childhood/adolescence	42 (36.8%)
Personality disorder	17 (14.9%)
Psychotic disorder	14 (12.3%)
Substance-related disorder	13 (11.4%)
Developmental handicap	7 (6.1%)
Other	24 (21.0%)
<i>Previous psychiatric hospitalization?</i>	
Yes	71 (62.3%)
No	43 (37.7%)
Missing	1 (0.9%)
<i>Age at first psychiatric hospitalization (mean) (n = 71)</i>	15
<i>Estimated total number of psychiatric hospitalizations (mean) (n = 70)</i>	5.9

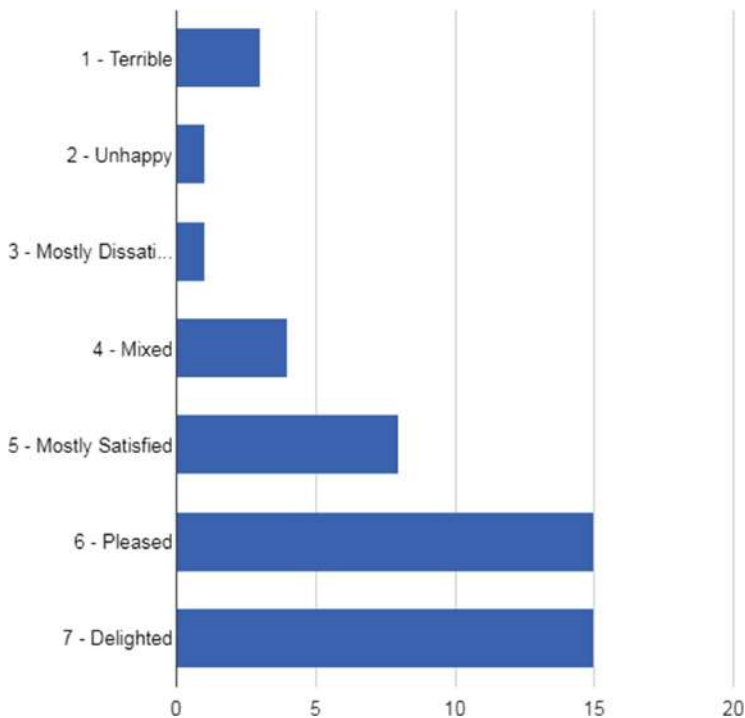
Table 2. Community Integration (N = 115)

<i>Approximately how many times a month do you usually visit friends or relatives?</i>	
Never	14 (12.3%)
1–4 times	50 (43.9%)
5 or more	50 (43.9%)
Missing	1 (0.9%)
<i>When you participate in leisure activities do you usually do this alone or with others?</i>	
Mostly alone	25 (21.9%)
Mostly with friends who have mental health challenges	22 (19.3%)
Mostly with family members	11 (9.6%)
Mostly with friends who do not have mental health challenges	18 (15.8%)
With a combination of family and friends	38 (33.3%)
Missing	1 (0.9%)
<i>How often do you travel outside the home?</i>	
Almost every day	85 (74.6%)
Almost every week	25 (21.9%)
Seldom/never (less than once per week)	4 (3.5%)
Missing	1 (0.9%)
<i>How often do you write to people for social contact using the Internet (e.g., Facebook)?</i>	
Every day/most days	83 (72.2%)
Almost every week	21 (18.3%)
Seldom/never	11 (9.6%)
<i>How often do you make social contact with people by talking or text messaging using your phone?</i>	
Every day/most days	80 (70.2%)
Almost every week	14 (12.3%)
Seldom/never	20 (17.5%)
Missing	1 (0.9%)

Initial Focus Groups

A staff focus group and 2 youth focus groups have been completed prior to 3 months of implementation.

Youth described the advantages of both the app as well as having a phone. For the application itself, youth identified increased communication with their care provider, primarily through the messaging function. They also appreciated having the availability of information on phone including safety plan, the ability to set up appointments and, reminders related to wellness plan, as well as medication prompts. They enjoyed using



Counts/frequency: 1 - Terrible (3, 6.4%), 2 - Unhappy (1, 2.1%), 3 - Mostly Dissatisfied (1, 2.1%), 4 - Mixed (4, 8.5%), 5 - Mostly Satisfied (8, 17.0%), 6 - Pleased (15, 31.9%), 7 - Delighted (15, 31.9%)

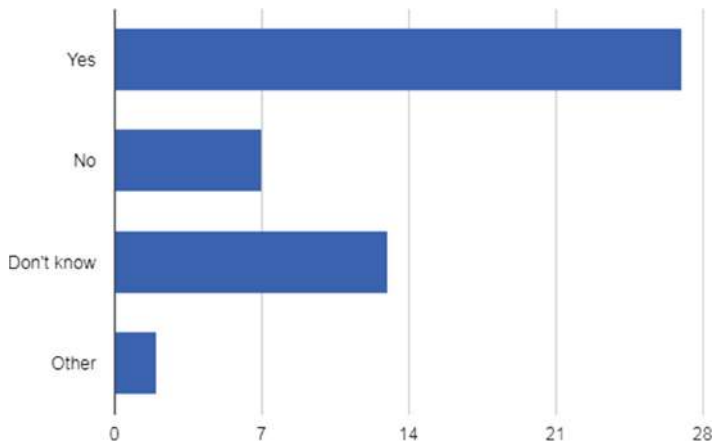
Fig. 1. How do you feel about connecting with your care provider using your smartphone?

a paperless format for things such as completing forms on-line that were sent by the care provider. Examples of comments include:

I liked doing the little survey thing. Cause like when I'm bored and or like on a bus or something and I think, need to stop focusing on people, like, probably not staring at me but staring at me. I'll go on it. It gives me something to do so, and like it's helpful to so. I'll do like the surveys and questionnaires that pop-up ...

Well I mean just yesterday, I was able talk to Dr.(Name), who scheduled an a, an appointment for Friday, which I found really helpful because I wouldn't know how to contact her otherwise

The youth also described areas for improvement. They described that they initially had to take time to figure out the functions. There were several complaints about the cumbersome log-in process. Although they identified that they understood the log-in privacy concerns they thought it could still be streamlined. Some examples of quotes include:



Counts/frequency: Yes (27, 55.1%), No (7, 14.3%), Don't know (13, 26.5%), Other (2, 4.1%)

Fig. 2. Has the use of the Smartphone and CHR for personal health information improved your healthcare?

At first it was confusing, but then figured it out. I don't know, like I don't know exactly how it's confusing but like, it was like, it, it was new, ...

Yeah randomly it signed me out the other day like it was signed in for like a good few weeks now and I was like thank you. And then it just randomly signed out and I was like damn. I remember my stuff but it's just annoying how you would put it in every single time but like I know that's for like confidentiality and like some people can't go on it. But, kinda sucks sometimes.

The other major theme related to the importance of having a phone. Many of the youth in the study were experiencing poverty and twenty (17.5%) reported being homeless. The phones themselves helped youth feel comfortable and connected to other people. They reported the advantage of having a phone at all. Some examples of quotes include:

When I didn't have a phone like I just hate going places and not knowing where I'm going, or like I don't know, my anxiety's really bad.

Then, the phones helped me to not only help myself, but to help others in like emergent situations... which I had to do a couple weeks ago and had I not gone to the study, like I wouldn't have been able to help them so it's helped in a lot of ways.

Staff identified similar issues using the app in particular the ability to securely message their clients frequently. Specifically, staff identified the advantages were the ability to send questionnaires and to set appointments using the app. They discussed that sometimes youth felt more comfortable to first raise uncomfortable topics by phone/messaging and this resulted in strengthening the relationship between the youth and care provider and empowering the youth. Staff supporters also identified the importance of their clients having a phone at all.

Some examples of quotes include:

Yeah I use messaging, especially one time um one of my youth didn't have any minutes on their phone so we actually were a couple times messaging through the site
I think a good one for me is the mood Qnaire and the medication one. Um, because a lot of my youth, their mood fluctuates either in a single day – when I see them in the morning they could be doing amazing and then by the afternoon they're just doing horrible. So, I can send them one of those and then kind of see like maybe what a trend is and figure out the trend and then that way I can better support them as well
So that they do make it to their appointments on time, and at their like right day. I'm able to text them ahead of time to remind them
So, they don't want to like give away things in person like if its ... going to cause them to cry. It ... allows them to be more vulnerable
If anything it's increased the relationships and made them like stronger and better

For improvements they noted the app had a medical look to it that was not inviting to youth:

It does, like I feel like if I'm a 23-year-old and I'm just looking and it's this nice bright blue and white, but...it's just reminds me of a doctor's office and a lot of our youth may be triggered by doctor's offices, or have had really bad experiences...

They also noted that they do not spend much time on their computer so they really need a phone app themselves for the provider version.

4 Discussion

The demographic findings from the baseline interviews were characterized by a wide age range (14–25 years) with a comorbidity of psychiatric illnesses. There were 62.3% of participants who stated that they had been admitted to a hospital for psychiatric reason. When asked the estimate total number of psychiatric admissions, the average number of hospitalizations among youth who did report a hospitalization was 5.9 times.

With regards to community integration the sample appeared to be socially isolated as only 43.9% visiting friends or relatives at least weekly. The majority of the sample used social media on most days.

Based on the preliminary findings, we report that the use of smart technology was successfully deployed to a range of youth with symptoms of depression or anxiety. Both staff and youth identified strengths of both having the application as well as having a phone. The ability to communicate more easily was noted as a particular strength that has the potential to improve access to care and support the therapeutic relationship. As previously noted in the literature, smartphones have been found to be successful in assisting individuals with bipolar disorder [6], and social phobia [7]. It is anticipated that the TELEPROM-Y project will be able to provide greater assistance to individuals with mental illness through enhanced access to resources and supports, as well as further opportunities for communication with care providers. Moreover, the use of smartphones may represent a more convenient approach to mental healthcare as opposed to in-person appointments or printed resources (i.e. brochures, information sheets) that are easily lost or damaged. As described in the preliminary focus groups of this study, some individuals may not wish to visit a healthcare provider's office due to

previous negative experiences. Some participants voiced that they like receiving care from the comfort of their own environment using the CHR app. This can also negate any potential missed appointments or concerns going unchecked, therefore providing early intervention and prevention.

From the perspective of care providers, the CHR also allows for greater monitoring of clients for early intervention and prevention. By using the app to complete the questionnaires in real time the care providers can be alerted to any potential mental healthcare crises that may have otherwise been unreported or unacknowledged. This approach could allow mental healthcare providers to see and communicate with more individuals in one day. By improving this connectivity with care providers, participants in this study can overcome barriers to care such as lack of money or transportation to attend appointments, and difficulty accessing much-needed services. In Canada alone, 64% of street-involved youth have reported difficulty accessing services [14].

A challenge for this project was encouraging hospital health care providers to adopt this technological approach. Although a number of hospital care providers embraced the technology and efficiency of the software available, others were skeptical. Due to the personal nature of the data being collected, some were concerned about the participants' privacy. Through the CHR is fully compliant with jurisdictional standards of practice, professional standards and guidelines, some care providers still did not want to participate in the study, so our team recruited from community agencies.

Another unanticipated expense was the amount of smartphones and data plans needed. In our proposal we anticipated purchasing 40 smartphones and 40 data plans but since a lot of the youth participants are living in poverty and/or homeless, an additional 55 had to be provided with a smartphone and 73 with a data plan to participate.

This study was limited by not being controlled other than by the pre/post-intervention design; future research could benefit from a comparison with a similar cohort of participants who do not receive the intervention during the study period, perhaps as part of a waiting list that could later receive the intervention.

5 Conclusion

The implications of this study could be far-reaching. This intervention may provide a more efficient approach that enhances connectivity with care services. Further, this intervention could represent a more efficient approach to mental healthcare by providing participants with greater opportunities to seek additional support and resources. We further anticipate that these extra supports will result in greater community integration among participants, which in turn could improve quality of life.

Acknowledgments. We would like to acknowledge St. Joseph's Health Care, the London Health Sciences, Woodstock General Hospital, Youth Opportunities Unlimited, WAYS Mental Health Support for facilitating the research environment. We would like to thank the participants and staff/care providers for their voluntary participation. In addition, we appreciate the commitment of the research assistants for data collection and auditing to make sure the quality of research is assured. Finally, we would also like to acknowledge the granting agency Ontario Centre for Excellence for making the funding available.

Conflicts of Interest. The authors declare no conflict of interest.

Reference

1. Mental Health Commission of Canada: Making the Case for Investing in Mental Health in Canada (2013). <http://www.mentalhealthcommission.ca/English/node/5020>
2. Mental Health Commission of Canada: Strengthening the Case for Investing in Canada's Mental Health System: Economic Considerations. Mental Health Commission of Canada (2017)
3. Gill, P.J., Saunders, N., Gandhi, S., et al.: Emergency department as a first contact for mental health problems in children and youth. *J. Am. Acad. Child Adolesc. Psychiatry*. **56**(6), 475–482 (2017). e4pmid:28545752
4. Canadian Mental Health Association: Fast Facts about Mental Illness (2016). <http://www.cmha.ca/media/fast-facts-aboutmental-illness/#.VsosVjbSI3g>
5. E-Mental Health in Canada: Transforming the Mental Health, January 2014. https://www.researchgate.net/publication/275210722_E-Mental_Health_in_Canada_Transforming_the_Mental_Health_System_Using_Technology
6. Ben-Zeev, D., Kaiser, S.M., Brenner, C.J., Begale, M., Duffecy, J., Mohr, D.C.: Development and usability testing of FOCUS: a smartphone system for self-management of schizophrenia. *Psychiatric Rehabil. J.* **36**(4), 289–296 (2013). <https://doi.org/10.1037/prj0000019>
7. Nicholas, J., Larsen, M.E., Proudfoot, J., Christensen, H.: Mobile apps for bipolar disorder: a systematic review of features and content quality. *J. Med. Internet Res.* **17**(8), e198 (2015). <https://doi.org/10.2196/jmir.4581>
8. Dagö, J., et al.: Cognitive behavior therapy versus interpersonal psychotherapy for social anxiety disorder delivered via smartphone and computer: a randomized controlled trial. *J. Anxiety Disord.* **28**, 410–417 (2014). <https://doi.org/10.1016/j.janxdis.02.003>
9. Forchuk, C., Reiss, J.P., O'Regan, T., Ethridge, P., Donelle, L., Rudnick, A.: Client perceptions of the mental health engagement network: a qualitative analysis of an electronic personal health record. *BMC Psychiatry* **15**, 250 (2015). <https://doi.org/10.1186/s12888-015-0614-7>
10. Wilier, B., Ottenbacher, K.J., Coad, M.L.: The community integration questionnaire a comparative examination. *Am. J. Phys. Med. Rehabil.* **73**(2), 103–111 (1994). <https://doi.org/10.1097/00002060-199404000-00006>
11. Lehman, A.: A quality of life interview for the chronically mentally ill. *Eval. Program Plann.* **11**, 51–62 (1988). [https://doi.org/10.1016/0149-7189\(88\)90033-X](https://doi.org/10.1016/0149-7189(88)90033-X)
12. Alhojailan, M.I.: Thematic analysis: a critical review of its process and evaluation. In: WEI International European Academic Conference, pp. 8–21 (2012). <https://www.westeastinstitute.com/wp-content/uploads/2012/10/ZG12-191-Mohammed-Ibrahim-Alhojailan-Full-Paper.pdf>

13. Leininger, M.M.: Ethnography and ethnonursing: models and modes of qualitative data analysis. In: Leininger, M.M. (ed.) *Qualitative Research Methods in Nursing*, pp. 33–71. Grune and Stratton, Orlando (1987). <https://doi.org/10.1177/160940691201100306>. https://www.researchgate.net/publication/277198481_Ethnonursing_A_Qualitative_Research_Method_for_Studying_Culturally_Competent_Care_Across_Disciplines
14. Barker, B., Kerr, T., Nguyen, P., Wood, E., DeBeck, K.: Barriers to Health & Social Services for Street-Involved Youth in a Canadian Setting. *J. Public Health Policy* **36**(3), 350–363 (2015). <https://doi.org/10.1057/jphp.2015.8>. <https://www.ncbi.nlm.nih.gov/pmc/articles/PMC4515178/>

Open Access This chapter is licensed under the terms of the Creative Commons Attribution 4.0 International License (<http://creativecommons.org/licenses/by/4.0/>), which permits use, sharing, adaptation, distribution and reproduction in any medium or format, as long as you give appropriate credit to the original author(s) and the source, provide a link to the Creative Commons license and indicate if changes were made.

The images or other third party material in this chapter are included in the chapter's Creative Commons license, unless indicated otherwise in a credit line to the material. If material is not included in the chapter's Creative Commons license and your intended use is not permitted by statutory regulation or exceeds the permitted use, you will need to obtain permission directly from the copyright holder.

